Universidade de Lisboa
Faculdade de Ciências da Universidade de Lisboa
Departamento de Biologia Vegetal

IRON HOMEOSTASIS IN IMMUNE MONONUCLEAR CELLS: A POTENTIAL ROLE IN ATHEROGENESIS

Liliana Alves da Silva Marques

Doutoramento em Biologia - Biologia Molecular
2014

Universidade de Lisboa
Faculdade de Ciências da Universidade de Lisboa
Departamento de Biologia Vegetal

IRON HOMEOSTASIS IN IMMUNE MONONUCLEAR CELLS: A POTENTIAL ROLE IN ATHEROGENESIS

Liliana Alves da Silva Marques

Tese orientada pela Doutora Luciana Maria Gonçalves da Costa, Doutor François Canonne-Hergaux e Prof. Doutora Rita Maria Pulido Garcia Zilhão, especialmente elaborada para a obtenção de grau de Doutor em Biologia, especialidade em Biologia Molecular

2014

“Do not go where the path may lead,
Go instead where there is no path
And leave a trail.”

Ralph Waldo Emerson

Agradecimentos

A minha jornada na ciência e na Investigação durante os últimos anos não teria sido a mesma sem cada uma das pessoas que fizeram parte da minha vida e a marcaram para melhor! Apenas a vida me dará a oportunidade para agradecer a cada uma delas da melhor maneira possível, mas eu vou aproveitar a oportunidade para vos agradecer aqui também, no início deste manuscrito que resume todo o trabalho durante estes últimos anos.

Em primeiro lugar, eu gostaria de agradecer à Fundação para a Ciência e a Tecnologia for financiar o meu projeto de doutoramento bem como agradecer a todas as instituições e respetivas equipas/departamentos por me terem recebido e providenciado todas as condições necessárias para que eu pudesse desenvolver o meu trabalho: Grupo de Imunologia Molecular e Celular do Departamento de Promoção da Saúde e Prevenção de Doenças Não Transmissíveis, Instituto Nacional de Saúde Doutor Ricardo Jorge, I.P (INSA, Lisboa; Portugal); Departamento de Biologia Vegetal, Faculdade de Ciências da Universidade de Lisboa (FCUL, Lisboa, Portugal); Équipe 34 do Institut de Chimie et Substance Naturelles (ICSN, Gif-sur-Yvette, França); Équipe Génétique et Régulation du Métabolisme du Fer do Centre de Physiopathologie de Toulouse-Purpan (CPTP, Toulouse, França). Em particular, gostaria de agradecer ao Doutor Jean-claude Drapier no ICSN, Doutora Marie-Paule Roth e Doutora Hélène Chopin at CPTP por me terem recebido nas suas equipas e respetivos laboratórios durante as minhas estadias profissionais em França.

Gostaria de agradecer aos meus orientadores Doutora Luciana Costa (INSA, Lisboa, Portugal), Doutor François Canonne-Hergaux (ICSN em Gif-sur-Yvette até 2011, CPTP em Toulouse de 2011 até à atualidade, França) e Prof. Doutora Rita Zilhão (FCUL, Lisboa, Portugal) por todo o apoio e orientação ao longo de todos estes anos. Em especial, gostaria de agradecer a constante disponibilidade da Prof. Rita para me ajudar a todos os níveis sempre que precisei da sua ajuda e também pelo seu entusiasmo contagiante em todos os nossos encontros! E um agradecimento muito especial para a Luciana e para o François que foram não só meus orientadores, mas também se tornaram meus amigos durante estes anos. Eles partilharam comigo não só a sua visão da Ciência com tudo o que isso acarreta de bom e menos bom, mas partilharam também a sua sincera amizade. Posso dizer que acima de tudo o que foi o nosso caminho conjunto da Ciência e na Vida com todas as suas alegrias e dificuldades, são muitos os momentos e conversas que guardarei com carinho no meu coração!

Gostaria de agradecer à Doutora Anne Negre-Salvayre (Inserm/UPS UMR 1048-I2MC, Toulouse, França) pela sua colaboração durante os últimos meses em Toulouse. A sua preciosa partilha de conhecimento, recursos e inclusive de

reagentes foi essencial para uma parte fulcral do trabalho aqui apresentado, pelo que eu gostaria de expressar a minha profunda gratidão pela sua constante disponibilidade e apoio.

Gostaria também de agradecer, sem qualquer ordem específica, a todos os colegas com quem partilhei a vida no laboratório: Vânia, Tânia, Rita, João, Alexandra G., Arminda, Bárbara, Flávia, Inês S., Helena, Inês C., Catarina C., Sara, Sónia, Ana M., Ana Margarida M., Ana Isabel, Catarina A, Cláudia B., Ângela C, Bruno S., Rute, Paulo, Bruno A., Nuno, Fátima, Sofia N., Alexandra W., Anne, Sérgio, Ioana, Cendrine, Nora, Sahar, Cristina, Lorenne, Aurélie, e Céline.

Um grande obrigada ao João por me ter ajudado a dar os "primeiros passos" no laboratório e por me ter iniciado na cultura celular e por convencer de como a proteína é tão importante, tudo isto sempre acompanhado de boa música! Um grande obrigada às minhas queridas amigas Vânia, Tânia, Rita, Bárbara, Ana, Flávia e Arminda por todo o apoio sempre que precisei de um ombro amigo para chorar, um abraço para celebrar ou apenas uma mente brilhante que me ajudasse a perceber o que fazer nas minhas experiências! Um grande obrigada à Alex, Anne, Lorenne, Céline e Aurélie por me terem recebido tão bem e me terem ensinado e ajudado sempre que eu "caí" nos seus laboratórios em Gif-Sur-Yvette e em Toulouse! E um grande obrigada à Nora, Sahar e Cristina por me fazerem sentir em casa durante a minha estadia em Toulouse!

Um obrigada muito especial à Vânia, à Tânia e à Nora! Vânia, tu tens sido uma presença constante na minha vida, em todos os altos e baixos e em todas as minhas frustrações de trabalho (e pessoais) sem te queixares e sempre com o teu melhor sorriso e o abraço mais forte! Foste tantas vezes a pessoa com quem eu discuti o meu trabalho, a pessoa que me animava nos dias menos bons ou que simplesmente lidava com o meu (ocasional) mau humor. Tu sabes o quão especial tens sido na minha vida, por isso obrigada pela tua amizade, pelo teu apoio incondicional durante todos estes anos e por me dares a conhecer o Carnaval de Torres Vedras todos os anos! Tânia, nós demorámos algum tempo até entrarmos na vida uma da outra, mas convidar-te para ires connosco a Londres foi das melhores ideias que eu e a Vânia tivémos já que foi assim que demos os primeiros passos para nos tornarmos grandes amigas e, sem saber, para nos tornarmos família! E como não mencionar que és ainda a minha melhor parceira de dança e coreografias?! Obrigada pela tua amizade e por fazeres parte da minha vida! E Nora, tu entraste na minha vida recentemente, mas foste a minha salvação em Toulouse! Obrigada por todos os dias, noites, fins-de-semana partilhados, por todos os almoços e jantares improvisados no lab (os nossos inesquecíveis noodles picantes!), as nossas longas caminhadas de regresso a casa pela noite dentro quando já não haviam

transportes, os nossos preciosos e raros momentos de lazer, as nossas eternas conversas filosóficas sobre a vida e, acima de tudo, obrigada por partilhares comigo estes meses difíceis no final dos nossos doutoramentos e por me teres dado força para aguentar e seguir em frente! Nunca me irei esquecer da tua citação de Winston Churchill “Se estás a passar no inferno, continua a andar”. E é tão verdade!

Um grande obrigada às minhas “meninas” Filipa, Raquel,Sílvia, Taia e Rita por fazerem parte da minha vida durante todos estes anos e pela bonita amizade que partilhamos. Foi na vossa companhia que descobri e partilhei a minha paixão pela Ciência! E ainda hoje, sempre que nos encontramos, toda a distância física que nos separa desaparece e é como se nunca nos tivéssemos separado e ainda andassemos pelos corredores da universidade todos os dias! E agora com os novos membros da nossa “família” que vieram para nos roubar os nossos corações e sorrisos: a Caterina e o Simão!

E para a minha verdadeira família: a minha mãe, o meu pai e o meu irmão... não há palavras para vos agradecer ou para descrever o quão importantes vocês são na minha vida! Vocês os três são a razão pela qual, por mais difícil que por vezes possa ser, eu me levanto todos os dias e coloco o meu melhor sorriso para iniciar o novo dia! Foi o vosso amor que fez de mim quem eu sou hoje e que continua a guiar-me a todos os níveis! E foi a vossa força que me ajudou em todos os momentos difíceis da minha vida! Cada um de vocês tem um papel único e incomparável na minha vida! Obrigada a todos por me terem recebido na vossa família e casa pois eu não consigo imaginar a minha vida sem vocês ou uma melhor família a quem pertencer! Amo-vos com todo o meu coração!

E finalmente, eu dedico este trabalho à minha avó Ângela de quem eu tenho tantas saudades e que me perguntava durante todos estes anos quando é que eu terminaria os meus estudos para poder finalmente começar a minha própria família! Avó, eu não sei o que a vida me reserva, mas aqui estou eu a terminar o meu doutoramento e prestes a iniciar um novo e desconhecido capítulo da minha vida, e espero sinceramente que te faça sentir orgulhosa de mim onde quer que estejas!

Acknowledgements

My journey in Science and in Research over the last years would have not been the same without every single person who took part of my life and marked it for better! Only life will give me the opportunity to thank each one of you in the best possible way, but I will take the chance to thank you here, at the very beginning of this manuscript that sums up all the work of these last years.

In the first place, I would like to thank Fundação para a Ciência e a Tecnologia for funding my PhD work and to thank all the different institutions and respective teams/departments which received me and provided all the conditions necessary so that I could perform my research work: Grupo de Imunologia Molecular e Celular at Departamento de Promoção da Saúde e Prevenção de Doenças Não Transmissíveis, Instituto Nacional de Saúde Doutor Ricardo Jorge, I.P (INSA, Lisbon; Portugal); Departamento de Biologia Vegetal at Faculdade de Ciências da Universidade de Lisboa (FCUL, Lisbon, Portugal); Équipe 34 at Institut de Chimie et Substance Naturelles (ICSN, Gif-sur-Yvette, France); Équipe Génétique et Régulation du Métabolisme du Fer at Centre de Physiopathologie de Toulouse-Purpan (CPTP, Toulouse, France). In particular, I would like to thank Doctor Jean-Claude Drapier at ICSN, Doctor Marie-Paule Roth and Doctor Hélène Chopin at CPTP for having received me in their teams and respective laboratories during my periods of work in France.

I would like to thank my supervisors Doctor Luciana Costa (INSA, Lisbon, Portugal), Doctor François Canonne-Hergaux (ICSN at Gif-sur-Yvette until 2011, CPTP in Toulouse from 2011 until today, France) and Prof. Doctor Rita Zilhão (FCUL, Lisbon, Portugal), for all the support and guidance through all these years. A sincere thank you to Prof. Rita for her constant availability to help me at all levels whenever I needed her assistance and for her contagious enthusiasm during all our meetings! A special thank you to Luciana and to François who were not only my supervisors, but who also became close friends during these years. They shared with me not only their view of Science with all the good and bad that comes with it, but also their sincere friendship. I can say that above all that was our joint path in Science and Life with all the joys and difficulties, there were many moments and many conversations that marked me as I am today and which I will cherish in my heart!

I would like to thank Doctor Anne Negre-Salvayre (Inserm/UPS UMR 1048-I2MC, Toulouse, France) for all her cooperation during the last months of my stay in Toulouse. Her precious share of knowledge, resources and even reagents was essential for a vital part of my work, so I would like to express my sincere gratitude for her constant availability and support.

I would also like to thank, with no particular order, to all the colleagues with whom I shared my life in the lab: Vânia, Tânia, Rita, João, Alexandra G., Arminda, Bárbara, Flávia, Inês S., Helena, Inês C., Catarina C., Sara, Sónia, Ana M., Ana Margarida M., Ana Isabel, Catarina A, Cláudia B., Ângela C, Bruno S., Rute, Paulo, Bruno A., Nuno, Fátima, Sofia N., Alexandra W., Anne, Sérgio, Ioana, Cendrine, Nora, Sahar, Cristina, Lorenne, Aurélie, e Céline.

A big thank you to João who helped me giving my first steps in the lab and who taught me about cell culture and how protein is so important, all this always at the sound of great music! A big thank you to my dear friends Vânia, Tânia, Rita, Bárbara, Ana, Flávia, and Arminda for being there whenever I needed a shoulder to cry on, a hug to celebrate or a cleaver mind to help me figure out what to do next in my experiments! A big thank you to Alex, Anne, Lorenne, Céline and Aurélie for welcoming me so well, teaching me and helping me out whenever I “fell” in their labs at Gif-sur-Yvette and Toulouse! And a big thank you to Nora, Sahar and Cristina for making me feel like home during my stay in Toulouse!

A special thank you to Vânia, Tânia and Nora! Vânia, you’ve been there for me during all these years, in all the ups and downs and all my lab (and life) frustrations without complaining and always with your best smile and strongest hug! You were so many times the person with whom I discussed my work, the person who would cheer me up in a bad day or just handle my (occasional) bad mood. You know how special you have been and continue to be in my life, so thank you for your friendship, for your support all these years and for taking me to Carnival at Torres Vedras every year! Tânia, we took some time to get into each other’s lives, but I’m glad we had the idea to invite you to come to London as that was the first step for us to become close friends and, without a clue, for us to become family! And how could I not to mention that you are also my best choreography dance partner?! Thank you for your friendship and for being part of my life! And Nora, we met recently, but you were my salvation in Toulouse! Thank you for all the days, nights, weekends, for our improvised lunches and dinners at the lab (oh our unforgetable instant spicy noodles!), our long walks home late at night, our precious and so rare relaxing moments, our eternal philosophical discussions about life and, above all, thank you for sharing with me these difficult months at the very end of our PhD’s and for giving me the strength to hold on and just do it! I will never forget your quote on Winston Churchill: “If you’re going through hell, keep going”. And it is so true!

And a big thank you to my girls Filipa, Raquel, Sílvia, Taia, and Rita for being in my life all these years and for the beautiful friendship that we share! It was in your company that I discovered and shared my passion for Science! And even today, whenever we meet, all the distance disappears and it feels like we were never apart and as if we were still walking through the university corridors

everyday! And now with the newest members of our “family” who came to steal our smiles and hearts: Caterina and Simão!

And to my true family: my mother, my father and my brother… there aren’t enough words to thank you or to describe how important you are in my life! The three of you are the reason why, no matter how hard it might be, I will always wake up every day and put up my best smile to face the new day! It was your love that made me who I am today and that keep guiding me in every possible way! And it was your strength that ultimately helped me in all the difficult moments of my life! Each one of you plays a unique and incomparable role in my life! Thank you all for having received me in your family and in your home as I can’t imagine my life without you or a better family to belong to! Love you all with all my heart!

And finally, I dedicate this work to my grandmother Ângela who I miss so much and who kept asking me during all these years when would I finish my studies so that I could finally start my own family! I don’t know what life has reserved for me, but here I am finally finishing my PhD and about to start writing a new and unknown chapter of my life, and sincerely hoping that I can make you proud of me wherever you are!

Resumo

A aterosclerose (AT) é uma doença inflamatória caracterizada pela formação de lesões designadas “placas ateroscleróticas” na parede de vasos sanguíneos. A formação destas lesões tem início na disfunção endotelial decorrente da ação de vários fatores de risco e que resulta na acumulação e modificação de partículas de lipoproteína de baixa densidade (LDL) (nomeadamente LDL oxidado (oxLDL)). A acumulação subendotelial de oxLDL promove a ativação das células endoteliais e o consequente recrutamento de células imunitárias, incluindo monócitos e linfócitos do sangue periférico. Os monócitos infiltrados diferenciam-se em macrófagos que, por ingestão de oxLDL, acumulam lípidos no seu interior e se diferenciam nas chamadas “células esponjosas” (do inglês “*foam cells*”), que são características das placas ateroscleróticas.

Vários autores observaram a acumulação de ferro em placas ateroscleróticas, frequentemente associada a “células esponjosas” derivadas de macrófagos. Em 1981, Sullivan propôs a chamada “hipótese do ferro” na qual o nível de ferro armazenado no organismo poderia constituir um fator de risco no desenvolvimento e progressão da AT. De acordo com esta hipótese, a reduzida frequência de desenvolvimento de AT em doentes com hemocromatose hereditária – caracterizados por macrófagos deficientes em ferro apesar da elevada sobrecarga de ferro sistémica – sugere que a retenção de ferro no macrófago promovida pela hepcidina (Hepc) poderá constituir um mecanismo pró-aterogénico crucial na possível associação do ferro à aterogénese. De facto, estudos recentes indicam que a Hepc pode desempenhar um papel pró-aterogénico e que a promoção da saída de ferro mediada pela ferroportina-1 (Fpn1) poderá constituir um mecanismo de resistência do macrófago à diferenciação em “células esponjosas”. Por outro lado, e apesar do seu potencial papel como ferroxidase envolvida na saída de ferro em macrófagos, a ceruloplasmina (Cp) é também capaz de oxidar outros substratos tais como as partículas de LDL. Adicionalmente, visto que a sua expressão é fortemente induzida em condições pró-inflamatórias, a Cp tem sido proposta como um potencial fator pró-aterogénico. Neste contexto, o principal objetivo do presente estudo foi clarificar a regulação da expressão de proteínas envolvidas no metabolismo do ferro nas células imunitárias que infiltram as placas ateroscleróticas, com particular interesse na proteína exportadora de ferro Fpn1 e na Cp como sua potencial parceira neste processo.

Numa primeira fase, o objetivo do estudo foi caracterizar a expressão das duas isoformas da Cp em linfócitos, monócitos e macrófagos bem como avaliar o seu potencial envolvimento como ferroxidase na saída de ferro no macrófago mediada pela Fpn1. Os resultados obtidos demostraram que, para além da isoforma solúvel da Cp (sCp) já descrita em outros estudos, os linfócitos,

monócitos e macrófagos expressam também uma isoforma membranar desta proteína. A diminuição da expressão da Cp membranar após o tratamento com PIPLC – uma enzima que corta especificamente proteínas com âncoras GPI – demonstrou que pelo menos parte da Cp associada à membrana corresponde à isoforma GPI-Cp nestas células. Adicionalmente, os resultados obtidos pelo nosso grupo de investigação permitiram concluir que a regulação da expressão da Cp em células imunitárias varia de acordo com o tipo de célula, com o seu estado de ativação e inclusivé com o tipo de isoforma. De facto, neste estudo observou-se que condições de stress oxidativo promoveram a diminuição do nível de mRNA de ambas as isoformas da *Cp*, ao passo que condições pró-inflamatórias induziram o aumento significativo e exclusivo do nível de mRNA da isoforma solúvel (sCp). A expressão da Cp nas células imunitárias que se encontram envolvidas na formação e desenvolvimento das placas ateroscleróticas (monócitos/macrófagos e linfócitos) pode constituir uma fonte de Cp na placa e, consequentemente, um mecanismo adicional para a oxidação de partículas de LDL em condições pró-inflamatórias, o que é corroborado pela co-localização da Cp e oxLDL anteriormente descrita em áreas pró-ateroscleróticas na parede do vaso. Efetivamente, a hipótese da Cp constituir um fator pró-aterogénico é apoiada por vários estudos que observaram uma associação entre o elevado nível de Cp sérica e o risco de desenvolvimento da AT.

Contudo, a expressão da Cp em células imunitárias pode estar também associada ao efluxo de ferro nestas células. Estudos recentes demonstraram que após estimulação com ferro, a expressão de Fpn1 em macrófagos aumenta significativamente em macrófagos, sendo recrutada para a membrana plasmática, onde se encontra enriquecida em microdomínios denominados de "jangadas lipídicas" (do inglês "*lipid rafts*"). Neste estudo, o padrão pontilhado da distribuição da Cp observado à superfície celular de monócitos, macrófagos e hepatócitos imortalizados (HepG2) é indicativo de que esta proteína se encontra concentrada em domínios membranares. Os resultados obtidos confirmaram que parte da Cp expressa em macrófagos bem como em células HepG2 se encontra localizada nas "jangadas lipídicas" e demonstraram ainda uma co-localização parcial entre a GPI-Cp e a Fpn1 em macrófagos estimulados com uma elevada concentração de ferro, o que sugere que a Cp poderá participar como ferroxidase no efluxo de ferro mediado pela Fpn1. Contudo, dado o caráter parcial da co-localização da GPI-Cp e Fpn1, é possível que a sCp ou uma outra ferroxidase possam estar também envolvidas no transporte de ferro pela Fpn1 em macrófagos estimulados com sobrecarga de ferro. Um estudo recente sugere que a proteína precursora do péptido β-amilóide (APP) poderá estar envolvida no efluxo de ferro mediado pela Fpn1 em neurónios, o que é corroborado pela acumulação de ferro nestas células em ratinhos *App*$^{-/-}$. Os resultados aqui apresentados confirmaram a expressão da APP em macrófagos e demonstraram que condições de elevada

concentração de ferro promovem o aumento da expressão da APP bem como a sua co-localização com a Fpn1 nas “jangadas lipídicas”. Estes resultados estão de acordo com a hipótese de que a APP possa colaborar com a Fpn1 no efluxo de ferro em macrófagos estimulados com sobrecarga de ferro. Deste modo, é proposto um modelo no qual ambas as isoformas da Cp bem como a APP poderão estar envolvidas no efluxo de ferro mediado pela Fpn1 em macrófagos, podendo apresentar papéis sobrepostos mas também complementares.

Numa segunda fase, propusemo-nos a clarificar o efeito da presença das partículas de oxLDL na expressão de algumas proteínas-chave no metabolismo do ferro em macrófagos. Os nossos resultados demonstraram que a estimulação de macrófagos com oxLDL levou à polarização do fenótipo Mox descrito por Kadl *et al*, bem como à acumulação intracelular de lípidos. A análise da expressão génica revelou que a exposição às partículas de oxLDL promoveu o aumento significativo da transcrição da heme oxigenase-1 (HO-1, gene *Hmox1*) e da *Fpn1.* Este aumento da transcrição de *Hmox1 e Fpn1* não foi observado na presença de partículas de LDL nativo ou acetilado, o que sugere que este efeito é específico da modificação oxidativa das partículas de LDL. Tratamento de macrófagos *Nrf2*$^{-/-}$ e *Nrf2*$^{+/+}$ com oxLDL mostrou que o aumento do nível de mRNA da *Hmox1* e da *Fpn1* induzido por oxLDL é mediado, pelo menos em parte, pelo fator de transcrição Nrf2. A exposição dos macrófagos a oxLDL conduziu ainda ao aumento significativo da transcrição da *Hamp1* (gene da Hepc), interleucina-6 (IL-6, gene *Il6*) e da cadeia pesada da ferritina (H-Ft, gene *Fth1*), bem como a diminuição significativa da transcrição de ambas as isoformas da *Cp.* Contudo, e ao contrário do observado na HO-1, o aumento significativo do nível de mRNA da *Fpn1* induzido por oxLDL não foi traduzido num aumento significativo a nível proteico. Este resultado sugere que a síntese da Fpn1 se encontra limitada no fenótipo Mox, provavelmente através de um mecanismo de regulação pós-transcricional influenciado pelo nível intracelular de ferro. Estes resultados sugerem ainda que, apesar da forte indução da transcrição da *Fpn1*, o efluxo de ferro nos macrófagos Mox se mantém provavelmente residual devido ao nível proteico basal da Fpn1. Contudo, como uma consequência a longo prazo da redução da transcrição da *Cp* e/ou do aumento da *Il6* e *Hamp1*, é possível que o efluxo de ferro possa estar diminuído nos macrófagos Mox.

Por outro lado, a estimulação simultânea de macrófagos com oxLDL (ativador do fenótipo Mox) e com lipopolissacarídeo combinado com interferão-γ (LPS/IFNγ, ativadores do fenótipo M1) induziram a diferenciação de um fenótipo misto entre Mox e M1 (Mox/M1), o que demonstrou que o fenótipo Mox não é predominante sobre o fenótipo M1 nestas condições. Os macrófagos Mox/M1 apresentaram acumulação intracelular de lípidos à semelhança dos macrófagos Mox, sendo caracterizados por um aumento significativo da

transcrição da *Hmox1, Il6, Fth1* e *Cp* (especificamente a isoforma sCp) e por uma diminuição significativa da transcrição da *Fpn1* à semelhança dos macrófagos M1. Estes resultados sugerem que macrófagos expostos a um ambiente rico em oxLDL e em condições pró-inflamatórias como LPS/IFNγ promovem a acumulação intracelular de lípidos e de ferro em conjunto com o aumento da produção de sCp e de citocinas pró-inflamatórias tais como a IL-6, provavelmente contribuindo para a oxidação das partículas de LDL e para a inflamação local, o que poderá ter um papel pró-aterogénico.

De acordo com estudos recentes, é o aumento de expressão de Fpn1 que desencadeia um mecanismo que conduz ao transporte reverso de colesterol e consequente resistência ao desenvolvimento de "células esponjosas". Deste modo, podemos assumir que a expressão basal (Mox) ou diminuída de Fpn1 (M1, Mox/M1) não confere proteção contra a formação das "células esponjosas", o que é apoiado pelos resultados de elevada acumulação intracelular de lípidos observada em macrófagos Mox e Mox/M1.

Concluindo, os resultados apresentados neste estudo estão de acordo com a "hipótese do ferro" proposta por Sullivan e indicam potenciais mecanismos quer para a acumulação de ferro em macrófagos, quer para a oxidação de LDL, ambos favorecendo a diferenciação de "células esponjosas" nas placas ateroscleróticas, o que contribui para o desenvolvimento e instabilidade das lesões e consequentemente para a progressão da AT.

Palavras-chave

Ferro, aterosclerose, ceruloplasmina, ferroportina-1, proteína precursora do péptido β-amilóide, células imunitárias

Abstract

Atherosclerosis is an inflammatory disease characterized by the formation of vessel wall plaques, initiated by oxidized LDL (oxLDL) accumulation and infiltration of immune cells. Iron accumulation in atherosclerotic plaques was proposed to constitute a risk factor in atherogenesis and immune cells could contribute to this risk. Herein, we studied the iron homeostasis of lymphocytes, monocytes and macrophages in a context of atherogenic conditions. Particularly, we investigated the expression and regulation of the iron exporter ferroportin-1 (Fpn1) and its potential functional partner ceruloplasmin (Cp).

We demonstrated that lymphocytes, monocytes and macrophages express both a soluble Cp and a membrane GPI-Cp. Through oxidation of LDL, Cp expressed by immune cells could contribute to the reported association between high Cp levels and increased cardiovascular risk. We showed that GPI-Cp partially co-localizes with Fpn1 in lipid rafts of iron-treated macrophages and could participate in Fpn1-mediated iron export. However, we proposed that besides Cp, the β-amyloid precursor protein (APP) could be a functional partner of Fpn1 in macrophages that needs to be further studied.

The effect of oxLDL on the iron homeostasis was investigated in macrophages. Despite oxLDL-driven Nrf2 activation and increased heme oxygenase-1 expression, Mox macrophages were not protected from foam cell formation like Mhem/M(Hb) macrophages, showing lipid accumulation, basal levels of Fpn1 at cell surface along with upregulation of interleukine-6 and hepcidin. Simultaneous exposure to oxLDL and LPS/IFNγ induced a Mox/M1 phenotype closer to M1 than Mox, with increased interleukine-6 and H-ferritin expression along with decreased Fpn1 expression. Our results suggest that macrophages exposed to a microenvironment rich in oxLDL and pro-inflammatory cytokines are prone to accumulate both lipids and iron while secreting high levels of pro-inflammatory cytokines and Cp, which will further promote the local inflammation and LDL oxidation. In summary, our results support the “iron hypothesis” in atherogenesis proposed by Sullivan.

Keywords

Iron, atherosclerosis, ceruloplasmin, ferroportin-1, β-amyloid precursor protein, immune cells.

Abbreviations

ABCA1	ATP-binding cassette, subfamily A1
ABCG1	ATP-binding cassette, subfamily G1
acLDL	Acetylated LDL
Apo-Tf	Apo-transferrin (iron-free)
APP	β-amyloid precursor protein
App/APP	Murine/human gene for β-amyloid precursor protein
Arg-1	Arginase-1
ATF1	Activating transcription factor 1
ATH	Atherosclerosis
BMDM	Bone marrow derived macrophages
BMP6	Bone morphogenetic protein 6
BSA	Bovine serum albumin
Cav-1	Caveolin-1
CD163	Receptor for complex hemoglobin:haptoglobin
CD91	Receptor for complex heme:hemopexin
cDNA	Complementary DNA
CO	Carbon monoxide
Cp	Ceruloplasmin
Cp/CP	Murine/human gene for ceruloplasmin
Dcytb	Duodenal cytochrome b
DHFR	Dihydrofolate reductase
DMT1	Divalent metal transporter 1
DRM	Detergent resistant membrane
EC	Endothelial cell
EDTA	Ethylenediaminetetraacetic acid
EP	Erythrophagocytosis

FBS	Fetal bovine serum
Fe^{2+}	Ferrous iron (reduced form)
Fe^{3+}	Ferric iron (oxidized form)
Flot-1	Flotillin-1
FLVCR	Feline leukemia virus subgroup C receptor
Fpn1	Ferroportin-1
Fpn1/FPN1	Murine/human ferroportin-1 gene, also known as *Slc40a1/SLC40A1*
Ft	Ferritin
Fth1/FTH1	Murine/human ferritin gene
GST	Glutathione-S-transferase
GPI-Cp	Membrane glycosylphosphatidylinositol-anchored ceruloplasmin
Hamp1/HAMP	Murine/human gene for hepcidin
Hb	Hemoglobin
HBSS	Hank's balanced salt solution
HCP-1	Heme carrier protein 1
Hepc	Hepcidin
Heph	Hephaestin
HFE	Hereditary hemochromatosis protein
H-Ft	Heavy chain-ferritin
HH	Hereditary hemochromatosis
HIF	Hypoxia inducible factor
Hmox1/HMOX1	Murine/human gene for heme oxygenase-1
HO-1	Heme oxygenase-1
Holo-Tf	Holo-transferrin (iron-loaded)
Hp	Haptoglobin
Hprtl/HPRT	Murine/human gene for hypoxanthine guanine phosphoribosyltransferase
Hpx	Hemopexin

HRE	Hypoxia responsive element
HRG1	Heme responsive gene 1
HRP	Horseradish peroxidase
huPBL	Human peripheral blood lymphocytes
huPBMC	Human peripheral blood mononuclear cells
huPBMn	Human peripheral blood monocytes
IFNγ	Interferon-γ
IL	Interleukine
Il6	Murine gene for interleukine-6
iNOS	Inducible nitric oxide synthase
IRE	Iron responsive element
IRP	Iron regulatory protein
LCCM	L929-condicioned culture medium
Lcn2	Lipocalin 2
LDL	Low density lipoprotein
Lf	Lactoferrin
L-Ft	Light chain-ferritin
LIP	Labile iron pool
LPS	lipopolysaccharide
LXR	Liver X receptor
M(Hb)	Hemoglobin-activated macrophage phenotype
M1	Classically activated macrophage phenotype
M2	Alternatively activated macrophage phenotype
M4	CXCL4-activated macrophage phenotype
Mhem/HA-mac	Heme-activated macrophage phenotype, previously known as HA-mac (hemorrhage associated-macrophage)
Mox	Oxidized phospholipids-activated macrophages phenotype
MPO	Myeloperoxidase

MR	Mannose receptor, also known as CD206
mRNA	Messenger RNA
MTT	Methyl thiazolyl tetrazolium
NDRM	Non-detergent resistant membrane
NK cell	Natural killer cell
nLDL	Native low density lipoprotein
Nrf2	NFE2-related factor 2 (transcription factor)
NTBI	Non-transferrin bound iron
O/N	Overnight
oxLDL	Oxidized low density lipoprotein
P/S	Penicillin-streptomycin
PBS	Phosphate-buffered saline
PCBP1	Poly (rC)-binding protein 1
PCR	Polymerase chain reaction
PI	Protease inhibitor
PMA	Phorbol myristate acetate
PMSF	Phenylmethylsulfonyl fluoride
qPCR	Quantitative polymerase chain reaction
R/T	Room temperature
RT	Reverse transcription
RT-PCR	Reverse transcription-polymerase chain reaction
RNS	Reactive nitrogen species
ROS	Reactive oxygen species
sCp	Soluble isoform of ceruloplasmin
SMAD	Small mothers of decapentaplegic (transcription factor)
SMC	Smooth muscle cell
TAM	Tumor-associated macrophage phenotype
TB	Terrific broth

Tf	Transferrin
TfR1	Transferrin receptor 1
TfR2	Transferrin receptor 2
TGF-β	Transforming growth factor β
Tim2	T cell immunoglobulin-domain and mucin-domain-2
TLR4	Toll-like receptor 4
TNFα	Tumor necrosis factor α
VD	Vascular diseases
VEGF	Vascular endothelial growth factor
Vegf	Murine gene for vascular endothelial growth factor
Zp	Zyklopen

Table of Contents

Figures

Tables

I. General Introduction

1. Iron

1.1. Iron: a micronutrient essential to life

Iron is one of the most abundant elements on Earth, constituting approximately 5% of its crust and almost entirely its nucleus. It is a metal commonly used in our society, but few know that iron is a trace element essential for most living organisms. It is a functional component of oxygen-carrying proteins, cytochromes, DNA polymerase, and enzymes involved in electron transfer. However, given its high chemical reactivity, iron can be very toxic by generating free radicals through the Fenton reactions and contributing to oxidative stress and cell damage [1]. The challenge for most organisms is to acquire adequate iron supply and simultaneously avoid its toxicity. Thus, highly regulated mechanisms were developed by complex organisms in order to control iron absorption, its distribution and storage in cells and tissues [2].

Iron is a transition metal that exists in two reversible redox states: reduced ferrous (Fe^{2+}) and oxidized ferric (Fe^{3+}) iron. Under an oxygen-rich atmosphere, the most stable form of iron commonly found in nature is Fe^{3+}, which is insoluble and thus poorly available for human and animal intake. In our diet, iron can be found in the form of heme (meat, poultry, and fish) or non-heme iron (mostly found in cereals and some vegetables), this latter one corresponding to the major source of dietary iron for humans (90%) [3]. However, despite being the most predominant source of iron, non-heme iron has low absorption efficiency. In fact, human populations with a predominantly vegetarian diet are commonly associated with high prevalence of iron deficiency [4].

The iron content in human body is 3-4 g, with iron daily losses of approximately 1-2 mg in adults (0.1% of total iron) that must be replaced by dietary iron in order to maintain iron balance. Apart from menstruation in adult women, iron losses occur predominately through desquamation of epithelial cells at the intestine and skin as well as through minor bleedings. There is no efficient iron excretion and thus the losses of iron cannot significantly increase in response to excessive iron intake and storage.

The major portion of human iron content (70%) is contained in erythroid precursors and mature erythrocytes as key component of hemoglobin (Hb), 20% is stored as ferritin (Ft) and hemosiderin in hepatocytes (liver) and in tissue macrophages (kupffer cells in the liver, splenic and bone marrow macrophages) while 10% is found in myoglobin in muscles cells or used by several iron-dependent enzymes in several tissues [5]. The major destination of iron in human body is the bone marrow, where erythroid precursor cells incorporate iron atoms into heme during Hb synthesis. The liver has first access to dietary nutrients and can readily uptake iron for storage in hepatocytes. Tissue macrophages are

responsible for elimination of senescent erythrocytes and recycling of Hb-associated iron. The lifespan of human erythrocytes is 120 days, meaning that every day about 0,8% of all erythrocytes are recycled by macrophages. The recycling of heme is an essential process as the erythropoietic daily needs are about 20 mg/day, of which only 1-2 mg are daily absorbed (Figure I.1) [5,6].

Despite large flows of iron in the plasma compartment, iron circulates mostly associated to transferrin (Tf) and its concentration is maintained in the range of 10-30 µM under normal homeostatic conditions. Low plasma iron concentration restricts iron uptake by erythroid precursors, limiting Hb synthesis and oxygen-transport, causing anemia. On the other hand, high plasma iron concentration that exceeds Tf binding capacity will lead firstly to iron accumulation at the liver and secondary iron accumulation in other tissues. However, excessive iron accumulation potentiates cell and tissue damage possibly by iron-mediated generation of reactive oxygen species (ROS) [1]. Thus, a tight control must be kept between dietary iron absorption, iron recycling and iron losses in order to prevent iron homeostasis disorders.

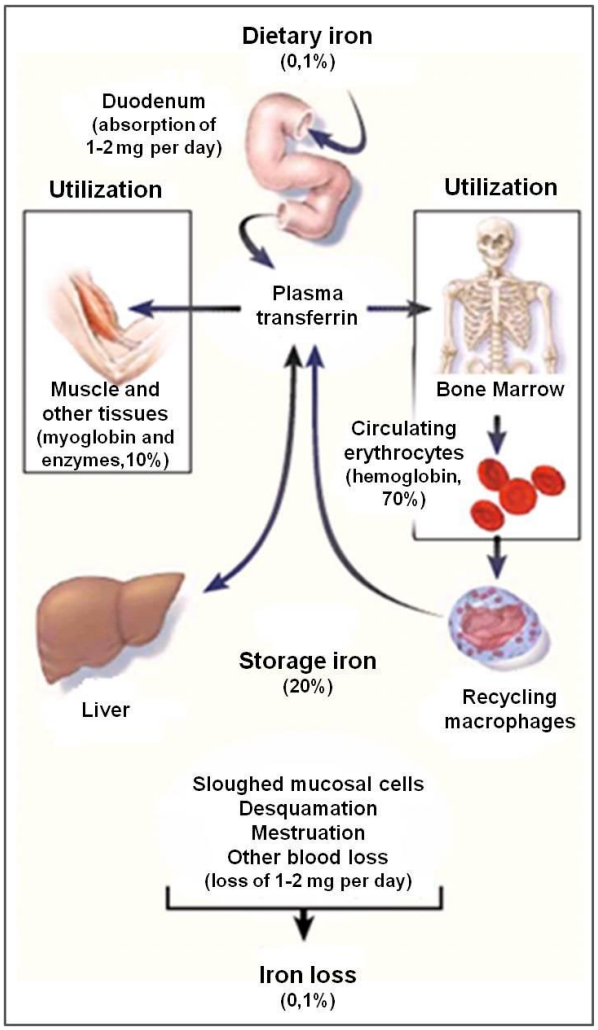

Figure I.1 - Distribution of iron in adults. In a balanced state, the human body has 3-4 g of total iron with a daily iron intake and loss of 1-2 mg (0,1%). Iron is absorbed at the duodenal enterocytes, being then loaded onto the plasma iron carrier Tf. Tf delivers iron to most cells/tissues, with bone marrow being the major destination for Hb synthesis at erythroid precursors and mature erythrocytes, followed by muscles fibers for myoglobin synthesis and other tissues. Excess of iron in circulation can be stored in Ft molecules in hepatocytes (liver) or at tissue macrophages as result of iron recycling from senescent erythrocytes. Without an efficient iron excretion mechanism, the regular daily iron loss is modest and occurs mainly by blood loss (menstruation and others) and by desquamation of epithelial and intestine mucosal cells. Image adapted from the original published at NC Andrews [5].

1.2. Iron metabolism: absorption, transport, storage and recycling

1.2.1. The intestinal iron absorption

The absence of an efficient mechanism for iron excretion makes the control of iron absorption extremely important for insuring iron homeostasis. In mammals, the absorption occurs at the intestinal mucosa level, on the proximal portion of the duodenum, and it is an extremely controlled process that is modulated in agreement with the changes in body iron stores, tissue hypoxia and erythropoietic demand for iron. In that portion of the duodenum, polarized cells named enterocytes are organized on fingerlike villi that protrude into the intestinal lumen to maximize absorptive surface area. Duodenal enterocytes are the cells responsible for iron absorption, migrate from the crypt toward the tip of the villus (maturation axis) as they become polarized during their maturation process. Each absorptive enterocyte is a polarized cell with a microvillous brush border at the apical membrane that faces the intestinal lumen where cellular iron uptake takes place. Subsequently, iron is either stored in Ft molecules or transferred across the cell to the basolateral membrane where it is exported into plasma. Ft iron will be shed along with the senescent enterocytes (short life cycle of 2-3 days) and eliminated through the gastrointestinal tract [5-7].

Iron absorption is a complex process that involves many proteins for the iron uptake at the apical membrane (importers), transport across the cytoplasm (chaperones), storage (Ft), transport across the basolateral membrane (exporter) and change of redox state of iron associated with import (reductase) and export (oxidase) activity.

Routes of iron import at the apical membrane of enterocytes vary according to the type of iron source: inorganic iron, heme and Ft (Figure I.2).

1.2.1.1. Inorganic iron apical uptake

Non-heme iron, also referred as inorganic iron, corresponds to Fe^{3+} and is transported by the divalent metal transporter 1 (DMT1, originally named Nramp2) localized at the apical membrane of enterocytes [8,9]. This transporter is not exclusive to iron, but animal models as well as human patients carrying mutations in DMT1 showed severe microcytic anemia evidencing the key role of this protein as the main iron importer involved in iron absorption[10,11]. DMT1 transports only divalent metals, meaning that Fe^{3+} ions must be reduced to Fe^{2+} prior to transport by DMT1 at the apical membrane. Although there is some controversy on the topic [12,13], so far such reduction has been attributed to the duodenal cytochrome b (Dcytb) which is also expressed at the apical membrane of enterocytes, and that may use ascorbic acid as a co-factor for

Fe^{3+} reduction [14]. Both DMT1 and Dcytb show increased expression at the apical membrane of enterocytes under iron deficiency and hypoxia conditions [9,14,15]. Some work suggests that DMT1 expression in enterocytes could also be downregulated by the master regulator of iron metabolism Hepcidin (Hepc) in conditions of iron overload [16] (see section 1.3.2.1).

1.2.1.2. Heme apical uptake

Two heme transporters have been reported in mammalian cells: heme carrier protein 1 (HCP-1, potential heme importer localized at the apical membrane of enterocytes) and heme responsive gene 1 (HRG1, potential heme exporter localized at the basolateral membrane and/or endosome membrane in polarized cells) [17-19]. The mechanisms underlying heme absorption are not very clear, but it is believed that heme is imported at the apical membrane either by HCP-1 or through receptor-induced endocytosis, with HRG1 possibly exporting heme out of the endosome into the cytoplasm. Once in the cytoplasm, heme could be catabolized by heme oxygenase-1 (HO-1, also known as HMOX1), generating free iron that would join the intracellular labile iron pool (LIP) [18,20].

1.2.1.3. Ferritin apical uptake

Dietary Ft has also been shown to be absorbed at intestinal level by a yet unknown, but independent mechanism from the ones involved in duodenal uptake of heme and inorganic iron [21], constituting another source of iron absorbed by enterocytes.

1.2.1.4. The basolateral iron export

After uptake in the enterocytes, intracellular iron can then be either incorporated into Ft molecules for storage or carried to basolateral membrane. At that site, ferroportin-1 (Fpn1, also known as SLC40A1), which is the only known iron exporter in mammals, transports iron to plasma in cooperation with the membrane multicopper oxidase hephaestin (Heph) [22-25]. The involvement of the circulating plasma multicopper oxidase ceruloplasmin (Cp) in such process was also reported under conditions of bleeding-induced acute anemia [26]. In addition, it was recently proposed the existence of a third unidentified soluble ferroxidase expressed in enterocytes [27].

Fpn1 expression at the basolateral membrane of enterocytes is also induced by iron deficiency and hypoxia, being downregulated by post-translational mechanisms involving Hepc under systemic iron overload conditions as well as inflammation and infection, blocking iron absorption [28]. In addition to export of iron by Fpn1, intracellular heme in the enterocytes can be also exported at the basolateral membrane by HRG1, entering the plasma

where it forms complexes with other macromolecules such as hemopexin (Hpx)[18].

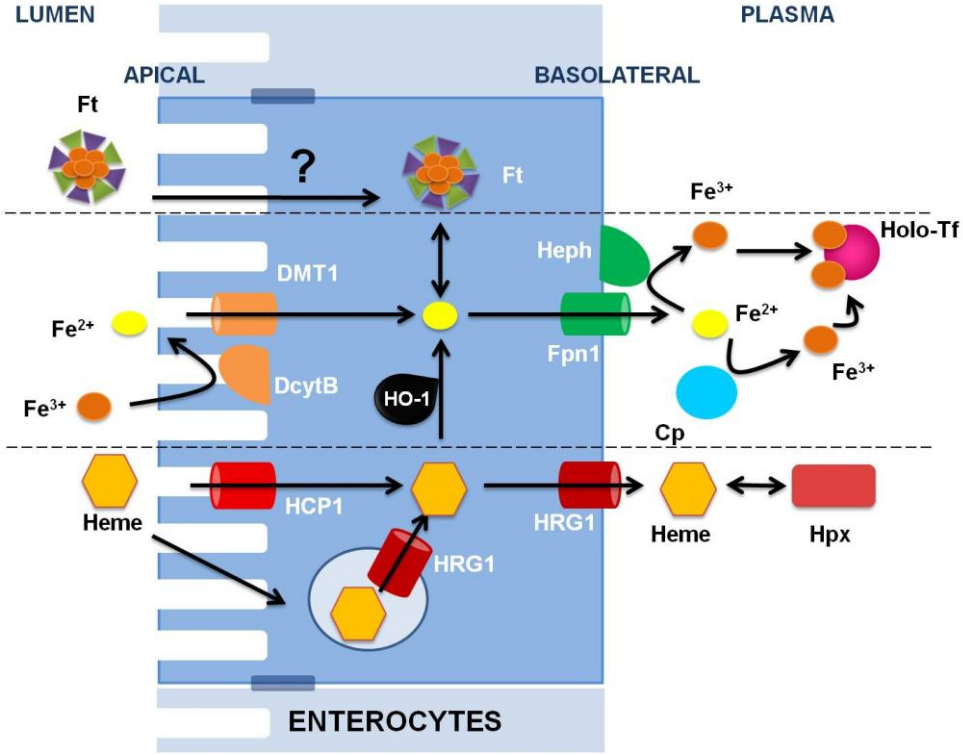

Figure I.2 - Schematic illustration of the different pathways for iron intestinal absorption. The enterocyte is a polarized cell, presenting microvillosities at the apical membrane that contacts the intestinal lumen and a smooth side at the basolateral membrane which contacts with the plasma. Iron can be absorbed in various forms: inorganic iron (Fe^{3+}) through DMT1 coupled with the reductase Dcytb; heme through HCP1 and/or endocytosis followed by export to the cytoplasm and at the basolateral membrane through HRG1; iron associated with Ft through a yet undisclosed mechanism. Depending on the body iron requirement, the absorbed iron can be stored in Ft molecules or exported to the plasma through the iron exporter Fpn1 coupled with the oxidase Heph and circulating Cp. The free iron can then be transported by Tf in plasma while heme circulates associated with Hpx.

1.2.2. Iron distribution and general cellular uptake

Once in plasma and given its high redox reactivity, iron circulates mostly associated with other molecules and subsequently enters cells through different mechanisms (Figure I.3), of which some are exclusive of specific cells/tissues.

1.2.2.1. The transferrin cycle

Under physiological conditions, Fe^{3+} in plasma circulates mostly associated with Tf, corresponding to approximately 30% of total circulating Tf. This protein is considered to be the main plasma iron carrier with high affinity to Fe^{3+} and it is mostly secreted by liver hepatocytes. Tf can circulate dissociated from iron as apo-transferrin (apo-Tf, iron dissociated Tf) or associated to one Fe^{3+} atom (monoferric Tf) or two atoms of Fe^{3+} (diferric Tf), both designated as holo-transferrin (holo-Tf, iron associated Tf) [29]. Cells can uptake holo-Tf through

a Tf specific receptor denominated Tf receptor 1 (TfR1), which is expressed in most cells, with variable degree of expression according to the cell iron requirements [30]. One important destination for circulating holo-Tf is the bone marrow, where erythroid precursors express high levels of TfR1, importing most of plasma holo-Tf for incorporation into heme during Hb synthesis [31].

All cells, including erythroid precursors, uptake holo-Tf complexes through an endocytosis process known as “Tf cycle”. Diferric-Tf has higher affinity to TfR1 than monoferric Tf, favoring the maximum uptake of iron per TfR1 molecule. After holo-Tf binding to TfR1, an endocytosis process is triggered and a clatherin vesicle is formed containing the complex TfR1-Tf. Acidification (low pH) inside the vesicle favors conformational changes in Tf that lead to the release of the iron atoms [32]. Free Fe^{3+} atoms are then reduced into Fe^{2+} by a reductase (STEAP3 in erythroid precursors, macrophages and hepatocytes) and then transported out of the vesicle into the cytoplasm by DMT1 [33]. Apo-Tf then returns to the cell surface, completing its cycle as it is released for iron reload in plasma while TfR1 remains at cell surface. One molecule of TfR1 can perform up to 100-200 endocytosis cycles during its lifespan.

1.2.2.2. Non-transferrin bound iron uptake

Under systemic iron overload conditions in which the plasma iron level exceeds the iron-binding capacity of Tf (Tf saturation), a significant amount of free Fe^{3+}, usually referred as non-Tf bound iron (NTBI), may circulate in plasma usually complexed with citrate, acetate and albumin molecules [34]. Despite its association with these carriers, NTBI can easily participate in Fenton reactions and subsequent formation of ROS [1,34]. NTBI can be absorbed by hepatocytes in the liver and other cells through the transport activity of DMT1 coupled with a reductase.

1.2.2.3. Heme and hemoglobin uptake

Free heme can also be taken up by cells, in particular hepatocytes and tissue macrophages [35,36]. However, as a consequence of intravascular hemolysis of erythrocytes, free heme and Hb also circulate in plasma and are usually associated with other macromolecules such as Hpx and haptoglobin (Hp), respectively. The complexes heme-Hpx and Hb-Hp will be recognized and internalized through CD91 and CD163 receptor-mediated endocytosis in macrophages and hepatocytes, protecting the organism and the cells against the toxic effect of heme and Hb [37-39].

1.2.2.4. Ferritin uptake

Recently, Ft was reported to deliver iron to cells and that the iron delivery was significantly higher when heavy chain-Ft (H-Ft) was used compared with

light chain-Ft (L-Ft), which suggests that the mechanism of Ft uptake preferably binds H-Ft and not L-Ft [40]. T cell immunoglobulin-domain and mucin-domain-2 (Tim-2) is an H-Ft specific receptor expressed in immune and non-immune cells. H-Ft was shown to be taken up by Tim-2 through a pathway distinct from that of Tf cycle, followed by iron delivery at the cytoplasm confirming that Ft uptake may constitute an efficient way of iron delivery to the cells [41]. Additionally, besides Tf, TfR1 was recently reported to also specifically binding to H-Ft, which could constitute an alternative receptor for Ft uptake [21,42].

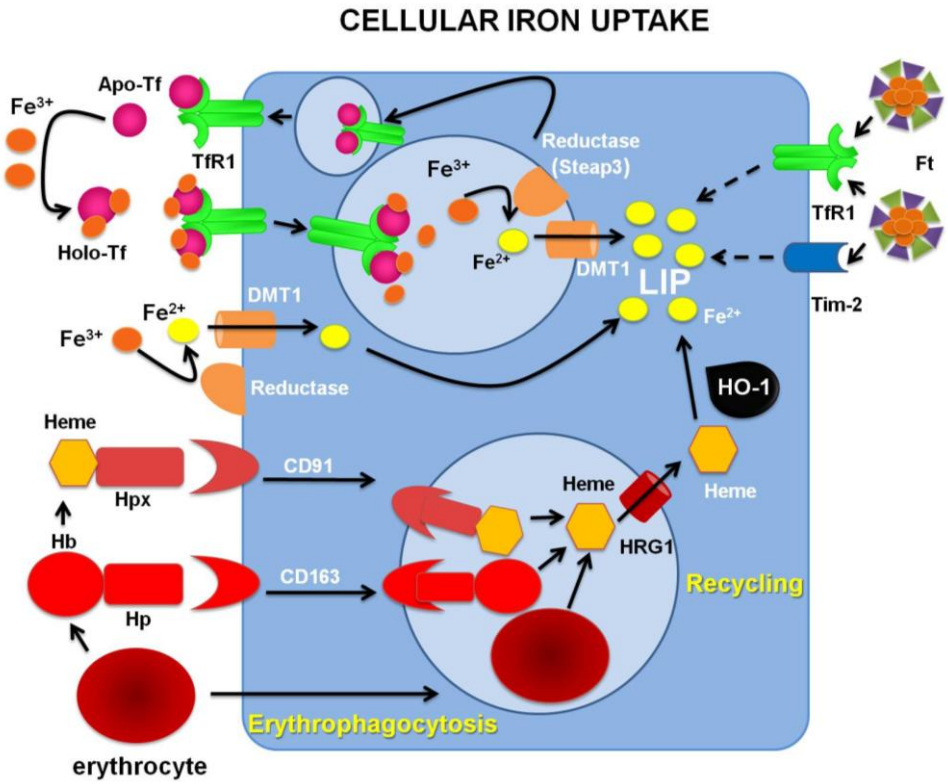

Figure I.3 - Scheme illustrating the different pathways for cellular iron uptake from circulation. Most cells uptake circulating iron through the Tf cycle, in which the holo-Tf binds to TfR1 and the complexes TfR1-Tf are endocytosed, releasing the iron from Tf. Dissociated iron is then pumped by DMT1 into the cytoplasm where it joins the LIP. Free **Fe^{3+}** may circulate in conditions of iron overload, in which it is mostly uptaken by hepatocytes through DMT1 coupled with a reductase. Another source of iron mostly used by macrophages and hepatocytes is heme, which can circulate: 1) associated with Hpx (heme:Hpx); 2) incorporated in circulating Hb molecules that may result from hemolysis and are mostly associated with Hp (Hb:Hp); 3) incorporated in Hb molecules inside erythrocytes. While heme-Hpx and Hb-Hp can be uptaken through receptor-mediated endocytosis, senescent erythrocytes can be phagocytosed exclusively by macrophages. In all three cases, the resulting heme iron is then likely pumped by HRG1 into the cytoplasm, where HO-1 catabolizes heme, releasing the Fe^{3+} atoms that will join the LIP. Ft was also reported to be uptaken by some cells through an independent mechanism involving Tim-2 and/or TfR1 as receptors.

1.2.3. Cellular iron trafficking, storage and mobilization

Once in the cytoplasm and independently of its uptake mechanism, free intracellular iron will enter the LIP, which consists of iron complexed with low affinity ligands and is therefore highly reactive. The LIP is kept at its minimum, corresponding to about 5% of total cellular iron and, given its reactivity, it is considered to be a good marker for cell iron-derived oxidative stress [34]. Once in the LIP, iron can be used for different purposes (Figure I.4):

- Directed towards the mitochondria for heme synthesis in specific cells;
- Used by iron and heme-dependent enzymes;
- Stored associated with Ft or hemosiderin molecules;
- Exported outside of the cells by the transporter Fpn1 in collaboration with an oxidase.

1.2.3.1. Intracellular iron trafficking

Given the high reactivity and toxicity of iron, its intracellular transport is thought to be mediated by metallochaperones that would safely deliver iron to be incorporated in iron-depending enzymes, heme synthesis, iron storage or export. However, little is currently known about iron chaperones apart from some likely candidates. For instance, poly (rC)-binding protein 1 (PCBP1) was recently identified as a chaperone that delivers iron to Ft [43]. The authors showed that PCBP1 bound to Ft *in vivo* and *in vitro,* also facilitating iron loading into Ft *in vitro*. PCBP1 and its homologue PCBP2 play a role in iron delivery to the iron-dependent prolyl hydroxylases that are involved in the regulation of hypoxia transcription factors [44], suggesting that PCBPs proteins may be involved in iron delivery to other cytosolic proteins besides Ft. Another protein with possible iron chaperone function is frataxin, which binds and transfer iron atoms and was shown to play an important role in the assembly of iron-sulfur complexes at the mitochondria [45].

1.2.3.2. Intracellular iron storage

Whenever cellular iron exceeds its iron requirement, the excessive iron is stored in a bioavailable form as Ft, which protects cells from potentially toxic iron reactions [1]. Ft is the main molecule involved in iron storage and is composed of a total of twenty-four subunits of H-Ft and L-Ft, with a variable ratio of H-Ft and L-Ft. This protein has high affinity to Fe^{3+} atoms, being capable to oxidize Fe^{2+} atoms into Fe^{3+} (activity associated to H-Ft) and to bind up to 4000-4500 iron atoms per molecule [46]. Ft expression is controlled by intracellular iron levels as well as by inflammatory conditions [47]. Hemosiderin, a product of Ft degradation, is also a form of iron storage in cells commonly found in conditions of iron overload [46].

1.2.3.3. Intracellular iron mobilization

In condition of high body iron demand, iron can be mobilized from the LIP and iron storage molecules such as Ft, in order to be exported from the cytoplasm of cells into the plasma through the activity of the iron transporter Fpn1. Indeed, low level of systemic iron or increased erythropoietic demand is thought to induce Ft degradation by lysosomal proteolysis and release of stored iron [48,49]. Iron is then exported from the cells and loaded onto Tf molecules, entering circulation for distribution throughout the organism.

In addition to free iron export by Fpn1, secretion of iron-loaded Ft from cells (particularly from macrophages) has been described [50]. Besides holo-Tf, circulating iron-loaded Ft could be more important in iron homeostasis than expected as discussed recently [41,42,50].

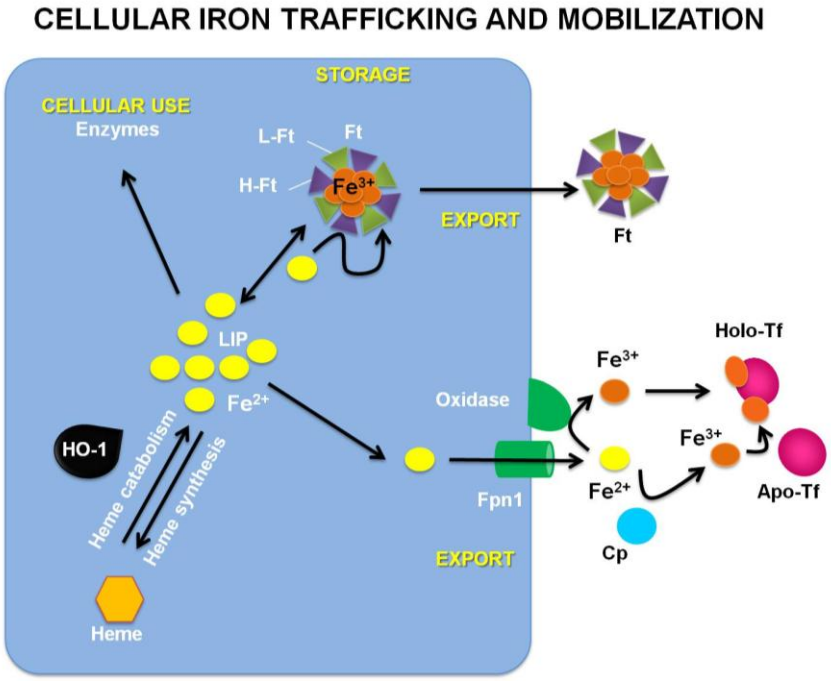

Figure I.4 - Intracellular iron trafficking pathways and its mobilization. Once inside the cell, according to the cell type and under conditions of low body iron demands, the iron can be stored in Ft, consumed in the activity of enzymes and in synthesis of heme to be used in enzymes (hepatocytes), Hb (erythrocytes) and myoglobin (muscle cells). In conditions of high body iron demand, the Ft in iron stores such as macrophages and hepatocytes can be degraded and the released iron can be exported through Fpn1 coupled with a membrane oxidase and/or circulating Cp, entering circulation. In addition, macrophages and hepatocytes were also shown to secrete Ft to plasma.

The oxidase Cp, and in particular its secreted soluble isoform, has been reported to be the ferroxidase associated with Fpn1 export of iron in both hepatocytes and macrophages [51]. However, its role is not completely understood and depending of the cell types, other oxidases associated to the membrane or secreted to the circulation could also be important. This topic on Fpn1 ferroxidase partners will be further discussed in section 1.4.3.

1.2.4. Specialized cellular iron trafficking

1.2.4.1. The erythroid precursors and heme metabolism

Erythroid precursors have a strong requirement for iron in order to produce an important amount of heme and Hb, uptaking iron from the circulation mostly via the Tf cycle (Figure I.5). Therefore these cells express high level of TfR1 and DMT1. In addition, erythroid precursors can also express the heme exporter feline leukemia virus subgroup C receptor (FLVCR), which appears to be vital for erythrocyte maturation and survival. Export of heme by erythroid cells likely corresponds to an intracellular iron homeostasis regulatory mechanism in order to protect these cells from the toxicity of high intracellular heme concentration [52]. In addition, it was recently reported that erythroid cells express HO-1 and that its expression is upregulated during erythroid differentiation having an immediate impact on heme and Hb levels, which points to an important role of HO-1 on the tight control of the regulatory heme pool at appropriate levels during the different stages of erythroid differentiation [53].

1.2.4.2. The hepatocytes and iron storage

One of the main human cells involved in iron storage is the hepatocyte in the liver (Figure I.5). Hepatocytes express high levels of TfR1 and Ft, both proteins being regulated through a post-transcriptional mechanism according to intracellular iron levels. In addition to iron uptake through Tf cycle, hepatocytes express DMT1 and avidly uptake circulating NTBI in conditions of iron overload, storing it mostly associated to Ft molecules in the cytoplasm. The hepatocytes can also uptake the complex heme-Hpx from circulation as well as to synthesize heme [36,54] in order incorporated in heme-containing enzymes such as the cytochrome P-450. Heme can also be degraded in hepatocytes and the derived iron stored in Ft molecules. Interestingly, despite Fpn1 expression, hepatocytes clearly favor the storage of iron even in conditions of high intracellular iron content [55], which may explain why the liver is the main organ for iron storage and is also the first target for iron toxicity in disorders involving iron overload.

Nonetheless, under conditions of high body iron demand, the stored iron in hepatocytes can be mobilized by degradation of Ft and iron export through Fpn1 in association with a ferroxidase, likely Cp. In addition, hepatocytes also secrete a form of Ft to plasma circulation that is usually more enriched in L-Ft chains than intracellular Ft [56,57]. Despite its unclear function, the level of circulating Ft is proportional to intracellular Ft levels in iron store cells and is thus considered as a plasma marker for body iron store level [56]. In addition, although minor than intracellular Ft, the iron content of circulating Ft is significant and also proportional to the body iron store level [58]. Ft is also an acute phase protein with its levels being upregulated by inflammation and infection [47].

1.2.4.3. The macrophages and iron recycling

Erythropoietic daily requirements are approximately 20-22 mg, but only 1-2 mg of iron is absorbed in the duodenum during this period, which would be clearly insufficient. Thus, macrophages have developed specialized iron uptake and recycling mechanisms in order to fulfill the organism needs.

Indeed, most of the daily iron requirement in mammals is provided by a highly efficient recycling of Hb-derived iron from senescent erythrocytes through a process denominated erythrophagocytosis (EP) [31]. This specific process of EP occurs at a rate of $5x10^6$ erythrocytes per second [59] in macrophages mostly concentrated in the liver (Kupffer cells), spleen and bone marrow [60]. As they reach the terminal age (120 days in humans), erythrocytes undergo modifications at cell surface that are specifically recognized by tissue macrophages, leading to their phagocytosis [59]. After engulfment, inside the erythophagosome, heme is released from erythrocyte-Hb by proteolytic activity and likely transported outside the erythrophagosome into the cytoplasm by the heme transporter HRG1 [61,62]. Indeed, HRG1 was reported as being expressed at the erythrophagosome membrane, while HO-1 is located outside the erythrophagosome, either at the cytoplasm or associated to the cytosolic side of the erythrophagosome membrane. On the other hand, DMT1 is perfectly co-localized with TfR1 and not with erythrophagosomal membrane marker, which supports the proposal that heme is transported by HRG1 through the erythrophagosomal membrane into the cytoplasm [61,62], where it is then catabolized by HO-1, leading to the release of iron, carbon monoxide (CO), and biliverdin/bilirubin [59]. The precise cytosolic compartment where HO-1 activity takes place is still under investigation. Additionally, in some conditions like intravascular hemolysis, macrophages can also directly uptake Hb and the complexes Hb-Hp and heme-Hpx through CD163- and CD91-mediated endocytosis, respectively [35]. After endocytosis, heme is likely transported by HRG1 to the cytoplasm for subsequent catabolism by HO-1 and iron release.

Once in the cytoplasm, free iron enters the LIP in the macrophage and can be either incorporated into Ft for iron storage or exported by Fpn1 in cooperation with a ferroxidase according to the body iron demand [31].The macrophage ferroxidase involved on iron efflux is not completely identified, but Cp has been proposed. Patients with aceruloplasminemia, that do not produce Cp, present strong iron accumulation in the liver in both hepatocytes and Kupffer cells (resident liver macrophages), among other organs [51,63]. In addition to Fpn1 iron export, a recent study suggests that circulating Ft is derived primarily from macrophages, and not from hepatocytes, through a non-classical secretory pathway constituting an additional and Fpn1-independent pathway for macrophage iron export [50]. The heme exporter FLVCR was also reported to be expressed at macrophage plasma membrane, showing that heme can also be

exported by macrophages in a mechanism that is Hpx-dependent and that constitute another mechanism of macrophage iron export [52,64].

Summing up, macrophages recycle iron mainly from senescent erythrocytes, but also from other sources such as circulating Hb or heme, and can store it or export iron in different physiological forms: free Fe^{3+}, Ft, and heme (Figure I.5).

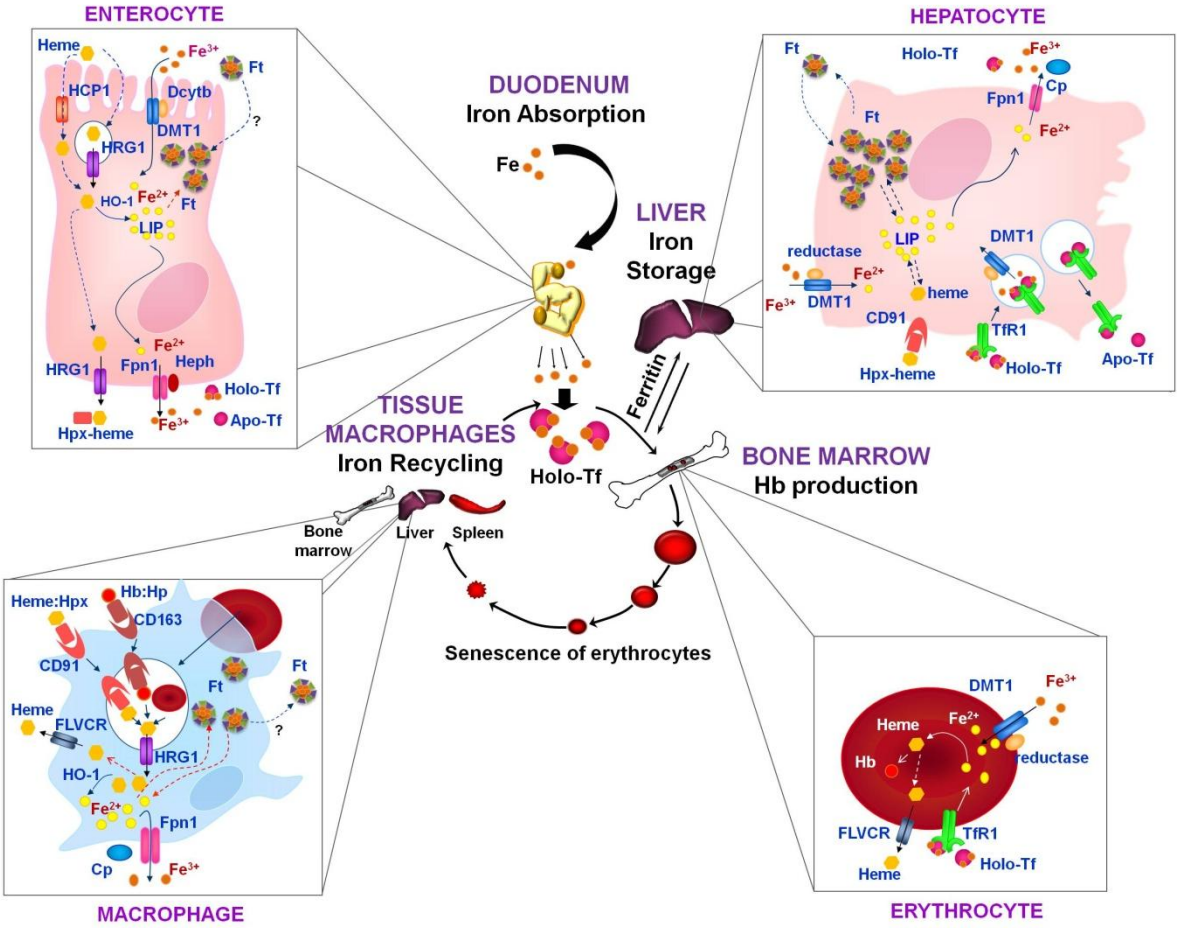

Figure I.5 - Overview of iron metabolism in the human body and in the different organs/cells. The central portion of the figure depicts the flow of iron throughout the human body, from intestinal absorption to blood circulation associated with Tf (holo-Tf) which delivers iron throughout the body, including its major site of utilization - the bone marrow - where it is incorporated into Hb during erythrocytes maturation process. As erythrocytes become senescent, they are phagocytosed by tissue macrophages located at the spleen, liver (Kupffer cells) and bone marrow. Macrophages recycle the iron contained in Hb, storing it in Ft molecules or releasing it back to the circulation via Fpn1. In addition, both erythroid precursors and macrophages express the heme exporter FLVCR and are therefore capable of exporting heme to circulation. Together with tissue macrophages, the hepatocytes in the liver are the main cells of iron storage in Ft molecules. In conditions of systemic iron deficiency, Ft molecules in hepatocytes and macrophages are degraded and the iron is released and exported by Fpn1 back to blood circulation, re-starting the cycle.

1.3. Iron homeostasis: cellular and systemic regulation

The main mechanism developed for controlling iron homeostasis in mammals is based on a strict control of dietary iron absorption as well as controlling the availability of stored and recycled iron accordingly to the body iron demand [5,6]. Regulation of iron homeostasis occurs at two different but interconnected levels: cellular and systemic iron homeostasis. Iron homeostasis is maintained by the regulation of the expression of the proteins involved in cellular iron uptake, storage and export in agreement with the levels of intracellular iron levels. These regulatory mechanisms occur at both transcriptional and post-transcriptional level and are modulated by anemia hypoxia, iron deficiency, iron overload and inflammation.

1.3.1. Cellular iron homeostasis

1.3.1.1. Hypoxia and iron metabolism genes

Under conditions of low oxygen (hypoxia) and low iron level (iron deficiency), hypoxia inducible factors (HIFs) are induced, affecting the transcription of many genes involved in iron metabolism. Under these conditions, the transcription of HIF-1α and HIF-2α subunits is upregulated along with protein stabilization. Indeed, HIF-1α and HIF-2α proteins are targets of ubiquitination and proteosomal degradation triggered by iron-depending enzymes. For this reason, besides transcription upregulation triggered by hypoxia, low intracellular iron levels also prevent HIF-1α and HIF-2α degradation, stabilizing these subunits that, together with the constitutively expressed HIF-1β and HIF-2β, originate the heterodimers HIF-1 and HIF-2. HIFs are transcription factors that bind to specific hypoxia-response elements (HRE) and promote transcriptional induction or suppression depending on the gene target. HIFs have been reported to suppress Hepc transcription while inducing transcription of several genes such as Tf, TfR1, Fpn1, DMT1, Dcytb, HO-1, and Cp among others, clearly promoting iron cellular uptake as well as iron export [31,65]. From a systemic point of view, the regulation of these proteins in hypoxic conditions could correspond to increased iron absorption at intestinal level as well as mobilization from iron stores in order to increase systemic iron levels in response to erythropoietic iron demand.

1.3.1.2. Cytokines and iron metabolism genes

Another transcriptional regulatory mechanism of iron cellular homeostasis is controlled by cytokines such as interferon -γ (IFNγ), tumor necrosis factor-α (TNFα) and interleukins (IL), namely IL-1β, IL-2, IL-6. These cytokines have been reported to bind to specific receptors, triggering specific signaling cascades that will lead to either induced or repressed transcription of cytokines-

regulated genes in a cytokine and gene specific manner. As an example, IL-6 and IL-1 induce Ft and Cp among others genes in hepatocytes and monocytes/macrophages, while combined IFNγ and lipopolysaccharide (LPS) induce HO-1, Cp, Ft and downregulate Fpn1 and TfR1 transcription in monocytes [31,66]. Noteworthy, the master regulator of iron homeostasis Hepc is transcriptionally upregulated by pro-inflammatory cytokines such as IL-6 [67].

1.3.1.3. The IRE/IRP system

The post-transcriptional regulation of iron metabolism genes is considered to be major mechanism underlying the maintenance of cellular iron homeostasis. Indeed, a post-transcriptional regulation is a faster, easier and more efficient way of controlling protein expression than a transcriptional one [6]. The main cellular post-transcriptional iron regulation system is the IRP/IRE regulatory network.

This system comprises two RNA binding proteins named iron regulatory protein 1 and 2 (IRP1 and IRP2) and *cis*-regulatory RNA elements named iron responsive elements (IREs) to which IRP1 and IRP2 bind specifically. The IREs are stable RNA hairpins with a characteristic secondary structure that exist in the untranslated regions (5'-UTR or 3'-UTR) of mRNA of some genes involved in iron metabolism. The position of IREs at the 5'-UTR or at 3'-UTR of a specific mRNA leads to opposite effects on translation. Binding of both IRPs to IRE on 5'-UTR interferes with the recruitment of the small ribosomal subunit to the mRNA, thereby blocking the translation of mRNA. On the other hand, IRPs binding to IRE at the 3'-UTR blocks the activity of endonucleases, protecting the mRNA from degradation (stabilization) and promoting its translation.

i. <u>Iron and IRPs activity</u>

Iron levels modulate the binding of IRP1 and IRP2 to the IRE, leading to the post-transcriptional regulation of IRE-containing mRNAs expression [68]. IRP1 is a protein presenting two different and mutually exclusive activities: one as aconitase and the other as a RNA binding protein. This protein contains an iron-sulfur cluster that is responsible for the aconitase activity and that requires the binding of iron atoms to be active. In iron-deficient conditions, the iron-sulfur cluster is not formed, leading to the absence of IRP aconitase activity as well as to the exhibition of a conformation that allows IRP1 to bind to the IREs, promoting (3'-UTR IRE) or blocking (5'-UTR IRE) the IRE-containing mRNAs translation. On the other hand, under iron-replete conditions, the iron-sulfur cluster is formed and IRP1 undergoes conformational changes that lead to the release of this protein from the IRE and to the gain of aconitase activity, thus counteracting the previous effect of IRP1 on the translation of IRE-containing mRNAs.

Unlike IRP1, IRP2 does not present any aconitase activity and acts as a RNA binding protein only. This protein is rapidly targeted for proteosomal degradation by an iron-dependent mechanism involving ubiquitination. Under iron-deficient conditions, this degradation mechanism is prevented and IRP2 accumulates in the cytosol and binds to IRE, blocking or promoting the translation of the respective mRNA depending on the UTR position of the IRE. In the presence of iron-replete conditions, the degradation mechanism is triggered, IRP2 is degraded and its effect on IRE-containing mRNAs translation is prevented [69,70].

ii. Iron genes and the IRE/IRP system

Many proteins involved in iron metabolism present IREs on its mRNA 3'-UTR (TfR1, DMT1) and 5'-UTR (H-Ft, L-Ft, and Fpn1 among others) and a typical model for this IRP/IRE regulatory network is the TfR1/Ft post-transcriptional regulation by intracellular iron levels [70]. Through the IRP/IRE regulation network, low intracellular iron promotes translation of DMT1 and TfR1 (iron uptake) and blocks translation of proteins involved in iron storage (Ft), utilization (ALAS2 involved in heme synthesis, among others) and export (Fpn1) while high intracellular iron induce the opposite regulation of these proteins (Figure I.6). IRPs were also reported as being regulated by other stimuli besides iron, but currently the available data are contradictory and the mechanisms involved are still not completely understood.

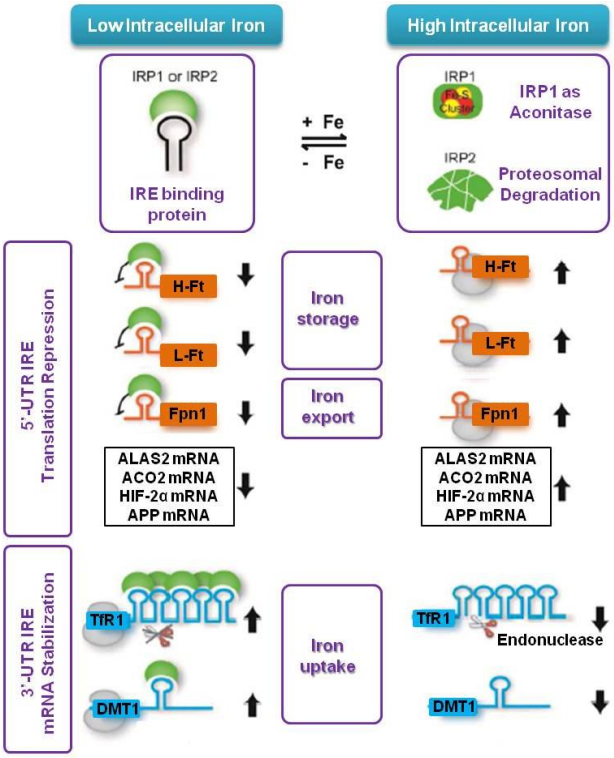

Figure I.6 - IRP/IRE Regulatory Network. IRP1 and IRP2 bind to IRE in iron-deficient conditions (- Fe), mediating the repression of the translation of mRNAs with 5'-UTR IRE (Ft, Fpn1, ALAS2, ACO2, HIF2α, APP) or mRNA stabilization and translation of mRNAs with 3'-UTR IRE (TfR1, DMT1). In iron overload conditions (+Fe), IRP1 binds to iron, releasing the IRE and gaining aconitase activity while IRP2 is targeted for proteosomal degradation. In both cases, once dissociated from the IRPs, the target mRNAs will be either translated (5'-UTR IRE) or targeted for degradation (3'-UTR). ALAS2: erythroid- specific delta-aminolevulinate synthase; ACO2: aconitase-2; HIF-2α: hypoxia inducible factor 2 alpha; APP: β-amyloid precursor protein. Image adapted from the book Iron Metabolism (2012) InTech [70].

1.3.2. Systemic iron homeostasis: the hepcidin/ferroportin-1 axis

Systemic iron homeostasis results from the balance between iron absorption, recycling and mobilization and it is regulated by four major factors: systemic iron status (stores regulator), iron demand for erythropoiesis (erythropoietic regulator), hypoxia and inflammation (inflammatory regulator). Over the last decade, evidence showed that regulation of systemic iron homeostasis in response to all these factors is mostly orchestrated by the iron-regulatory hormone Hepc and its cellular target Fpn1 [71].

1.3.2.1. Mechanisms of hepcidin action

Hepc is a small peptide that is mostly produced and secreted by hepatocytes (liver), but also in a lesser extent in other organs/cells such as the kidney [72], heart [73], lymphocytes [74], monocytes [75], and macrophages [76]. Nonetheless, a recent study suggests that the hepatocyte constitutes the predominant reservoir for systemic Hepc and that the production of Hepc by other tissues is unable to compensate the lack of Hepc production by the liver[77].

Hepc is synthesized as an 84-amino acid (aa) pre-propeptide that is processed into 60-aa prohepcidin by removal of the signal peptide. The mature and biologically active Hepc comprises 25-aa and results from removal of the pro-region by the pro-hormone convertase furin [78]. Hepc is a negative regulator of iron homeostasis that blocks iron flow from enterocytes, hepatocytes, and macrophages, impairing iron absorption and mobilization from iron stores, thus leading to decreased plasma iron availability [79]. To date, Fpn1 is the only known target for Hepc and it was demonstrated that Hepc promotes Fpn1 internalization and degradation through an ubiquitination process, blocking iron export [28,80]. This Hepc-dependent downregulation of Fpn1 has been reported in cell lines overexpressing Fpn1 [80] as well as in primary hepatocytes [55], macrophages [76], monocytes [75], and lymphocytes [74].

However, this mechanism of Hepc-induced internalization of Fpn1 in enterocytes is still in debate. On one hand, *in vivo* expression of duodenal Fpn1 is upregulated in mouse models of Hepc downregulation or downregulated in models of Hepc overexpression, suggesting that Fpn1 could be the target of Hepc also in enterocytes [81-84]. On the other hand, Fpn1 was reported to be resistant to Hepc in intestinal cells and DMT1 was proposed to be the direct target of Hepc by these cells being downregulated [85]. Moreover, it was recently shown that Hepc induces DMT1 degradation shortly after treatment with physiological concentrations of Hepc in both duodenal segments (*ex vivo*) and intestinal cell line while Fpn1 expression remains unaffected at that time point [16].

1.3.2.2. Regulation of hepcidin expression

Hepc regulation occurs at the transcriptional level, being upregulated by inflammation/infection and by high iron status, while increased erythropoietic demand, hypoxia, anemia and low iron status suppress Hepc expression (Figure I.7).

i. Hepcidin regulation by iron

Hepc is regulated by plasma iron levels as well as by the intracellular iron level in stores. This regulatory mechanism involves a negative feedback loop, in which increased iron concentration at both plasma and iron stores induce Hepc expression by hepatocytes and its release into circulation, blocking iron absorption and iron release from stores (liver and recycling macrophages). This mechanism modulates Hepc expression at transcription level since its mRNA level usually correlates with the level of Hepc peptide at both plasma and urine [31,86].

Human genetic iron disorders such as Hereditary Hemochromatosis (HH) and iron-refractory iron deficiency anemia as well as murine knockout models presenting impaired iron homeostasis were vital to identify key proteins involved in the modulation of Hepc expression by iron. In addition to the basal transcriptional level promoted by the liver-enriched transcription factor C/EBPα [87], the iron-dependent upregulation of Hepc transcription is promoted by the small mothers of decapentaplegic (SMAD) transcription factors 1, 5 and 8 and its mediator SMAD4. This SMAD signaling pathway is controlled by two known parallel and likely interconnected pathways: 1) bone morphogenetic protein 6 (BMP6), BMP receptor and its co-receptor hemojuvelin that control the SMAD signaling cascade; 2) TfR1, Tf receptor 2 (TfR2) and hereditary hemachromatosis protein (HFE) that are presumed to act as a complex sensor for holo-Tf level (extracellular iron), triggering the SMAD signaling cascade [31,88].

ii. Hepcidin regulation by erythropoiesis and hypoxia/anemia

Low iron status also promotes erythropoiesis impairment, which will lead to the low production of mature erythrocytes (anemia) and subsequent impaired oxygen transport in tissues (hypoxia). Therefore, increased erythropoietic demand is often the result of hypoxia/anemia, suppressing Hepc and subsequently promoting iron absorption and mobilization from stores (hepatocytes and tissue macrophages), all resulting in a greater supply of iron for Hb synthesis.

The regulation of Hepc by erythropoietic factors is the regulatory mechanism currently less understood. Besides the known dominance of erythropoietic iron demand (erythropoietic regulator) over the body iron status

(stores regulator), leading to Hepc suppression independently of the iron stores status, the exact molecules involved in this regulation are not fully characterized. These molecules/factors are believed to be produced at the level of the bone marrow and enter plasma circulation to reach liver and inhibit Hepc production. To this date, some molecules have been proposed: erythropoietin, growth differentiation factor 15, twisted gastrulation protein homologue 1 [47], and recently erythroferron [89], all of them upregulated by increased erythropoietic demand.

On the other hand, some studies suggest that Hepc suppression in the hepatocytes is not directly mediated by anemia, but by tissue hypoxia-derived erythropoietic demand [90], possibly mediated by Hepc transcriptional regulation through HIFs [65].

iii. Hepcidin regulation by inflammation/infection

Almost every bacterial pathogen requires iron for multiplication. As a consequence, natural selection has favored mechanisms that induce iron sequestration under inflammatory/infectious conditions and Hepc is believed to play a key role in this process. During inflammation and infection, IL-6 is highly upregulated along with other cytokines, and was shown to upregulate Hepc transcription through the STAT3 signaling pathway [67]. Besides IL-6, activin B was shown to have an unexpected, but crucial role in the induction of Hepc in inflammatory conditions [91].

As a result of Hepc upregulation, Fpn1 internalization leads to impaired iron efflux, blocking its absorption while promoting cellular iron retention in iron stores. This iron sequestration will rapidly lead to decreased plasma iron levels (hypoferremia), limiting iron availability to pathogens, but also to Hb synthesis [92,93]. Diseases characterized by a chronic inflammation lead to impaired erythropoiesis due the limited iron availability, developing the so-called anemia of inflammation or anemia of chronic disease [94].

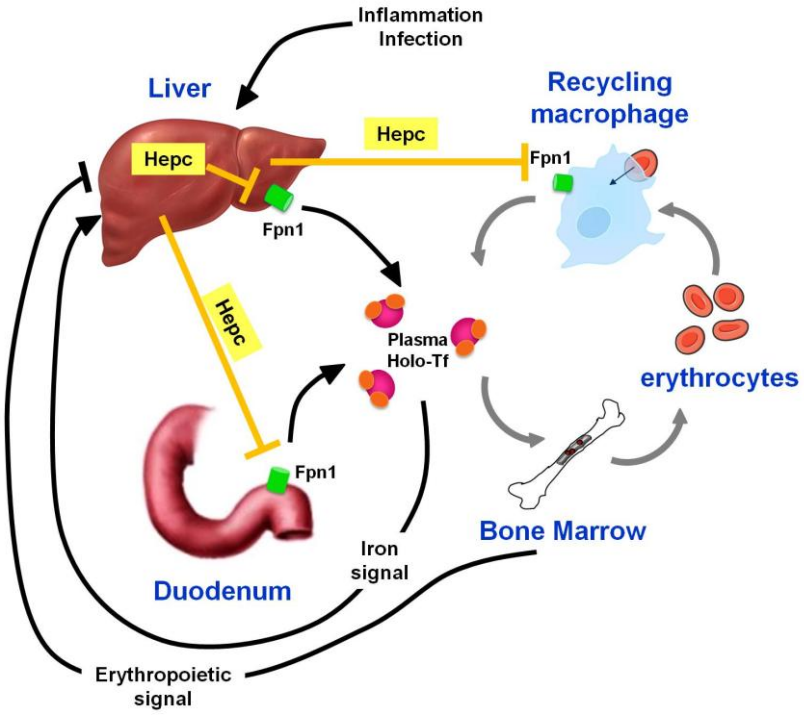

Figure I.7 - Systemic regulation of iron metabolism by hepcidin. Circulating Hepc is mostly produced by the liver (hepatocytes), being induced by iron overload or by inflammation/infection while suppressed by high erythropoietic demand (iron deficiency, anemia, hypoxia). The upregulated Hepc is secreted into circulation, reaching different tissues and promoting Fpn1 downregulation, which leads to impaired iron export from stores (recycling macrophages in liver, spleen and bone marrow as well as hepatocytes in the liver) and from intestine (enterocytes), resulting in decreased systemic iron levels. On the contrary, suppressed Hepc synthesis favors iron intestinal absorption and mobilization from stores, increasing circulating iron levels in order to respond to the high erythropoietic demand.

1.4. The iron exporter ferroportin-1: the cellular target of hepcidin

Fpn1 is the sole iron exporter identified in mammals [24,95,96], being highly expressed at the plasma membrane of duodenal enterocytes (basolateral membrane), macrophages and hepatocytes, where it contributes to iron absorption and mobilization from stores [55,97]. Mutants with complete lack of Fpn1 in zebrafish and mammals were shown to be embryonic lethal, unless rescued with iron injections [96]. The surviving newborns presented severe iron deficiency and were unable to absorb dietary iron [96], showing the extreme importance of this transporter in iron metabolism and homeostasis [98].

Fpn1 has an approximate molecular weight of 62 kDa, but it varies according to the cell/tissue due to post-translational modifications such as glycosilation. For instance, Fpn1 in murine duodenum, spleen and liver presents a molecular weight of 70, 65 and 63 kDa, respectively whereas Fpn1 presents a molecular weight of 65 kDa in murine macrophages differentiated *in vitro* [99].

The topology of Fpn1 is not fully defined, but the current model proposes that this protein has twelve transmembrane domains, with both N-terminal and C-terminal extremities in an intracellular position [100]. As a transporter, Fpn1 has been proposed to act as a monomer [100-102] as well as a dimer [103]. Although this topic is still under debate, the dominant inheritance of Fpn1 mutations in genetic disorders such as the negative effect of Fpn1 mutations in HH type 4 (also known as “ferroportin disease”) suggests that Fpn1 acts as a dimer. However, there are other possible explanations for the dominant effect such as haploid insufficiency or a multimeric structure of Fpn1 [104,105]. Fpn1 mutations can be classified as class I or “gain-of-function” which cause Fpn1 resistance to Hepc-dependent internalization, or as class II or “loss-of-function” which affect the transporter activity of Fpn1 [106].

Fpn1 expression is regulated at multiple levels: transcriptional, post-transcriptional, translational and post-translational in response to different stimuli and mechanisms.

1.4.1. Regulation of ferroportin-1 mRNA expression

At transcriptional level, *Fpn1* is upregulated in response to heme [107] and to hypoxia [65]. Upregulation of *Fpn1* by hypoxia is mediated HIF-2α [108], while heme upregulates *Fpn1* transcription through a dual mechanism. Heme binds to the transcriptional repressor Bach1, dissociating it from the small Maf proteins at the MARE/ARE sequence motif upstream of *Fpn1* promoter, triggering Bach1 ubiquitination and degradation. Simultaneously, heme stabilizes the transcription factor NFE2-related factor 2 (Nrf2), promoting its accumulation in the nucleus. Nrf2 dimerizes with the small Maf proteins at the MARE/ARE, forming a complex that promotes *Fpn1* transcription [109]. Noteworthy, the protoporphyrin ring of heme devoid of iron is capable of triggering *Fpn1* transcription to a less extent than heme, but not Fpn1 translation which is dependent on the presence of iron [107,109].

Pro-inflammatory cytokines such as IFNγ and TLR4-activation by LPS as well as by pathogens (*P. aeruginosa*) induce severe downregulation of *Fpn1* mRNA [110-112]. Remarkably, *Fpn1* downregulation by LPS *in vivo* was reported to occur also through an Hepc-independent mechanism that remains to be clarified [113]. However, recent publications report opposite regulation of *Fpn1* induced by infection [114,115], which adds some controversy to the transcriptional regulation of *Fpn1* by infection.

Additionally, a novel mechanism of post-transcriptional downregulation of *Fpn1* mRNA level was reported in response to iron deficiency through a specific micro-RNA (miR-485-3p) [116].

1.4.2. Regulation of ferroportin-1 protein expression

At translational level, *Fpn1* mRNA presents an IRE element on its 5'-UTR sequence to which IRP protein binds, blocking its translation. Only in the presence of iron, IRP dissociates from *Fpn1* mRNA unblocking its translation. Noteworthy, Zhang *et al* reported a novel *Fpn1* transcript lacking the 5'-UTR IRE, being expressed exclusively in the duodenum and erythroid precursors [117].

Post-translational regulation of Fpn1 occurs mainly through an Hepc-dependent mechanism in which Hepc binds to Fpn1 at cell surface inducing its internalization and degradation in response to inflammation, infection or iron overload [28]. Auriac *et al* reported that Fpn1 is localized in lipid raft microdomains in murine macrophages and demonstrated that this feature is essential for Hepc-mediated endocytosis and subsequent Fpn1 degradation in these cells[118].

Another mechanism controlling Fpn1 level at cell surface was reported in murine macrophages, in which Fpn1 in mostly localized in intracellular vesicles under basal conditions, being enriched at cell surface upon iron stimulation [119]. Additionally, de Domenico *et al* and other authors reported that Fpn1 stability at cell surface during iron export was dependent on the activity of a ferroxidase (Cp) that converted Fe^{2+} into Fe^{3+}, preventing Fpn1 internalization and degradation [120-122].

However, it is worth mentioning that de Domenico – which is one of the researchers whose recent publications focused mostly of Fpn1 and significantly contributed to the current knowledge on this protein – was recently subject of an investigation of research misconduct carried by the University of Utah. As stated by the Salt Lake Tribune, the conducted investigation concluded that significant errors were found in ten of the eleven publications by de Domenico which were subject of analysis and recommended that those publications should be either corrected or retracted. Therefore, any publication by de Domenico in the iron metabolism area should be considered cautiously and its reproducibility by other groups should be evaluated. In summary, it is important to re-evaluate and confirm the knowledge on the axis Hepc/Fpn1/ferroxidases to which de Domenico significantly contributed over the last years [123].

1.4.3. Ferroportin-1 partners for iron export

To date, four proteins were reported to have ferroxidase activity and/or to promote iron export in mammalian cells: Heph, Cp, zyklopen (Zp), and β-amyloid precursor protein (APP).

Heph, Cp and Zp are multicopper oxidases and were shown to oxidize Fe^{2+} into Fe^{3+} in addition to oxidation of organic substracts, promoting iron efflux in different cells/tissues [124].

Heph is a transmembrane oxidase firstly identified in the sex-linked anemia (*sla*) mice bearing a mutation in *Heph* gene. These animals presented a microcytic hypochromic anemia which resulted from impaired iron export from enterocytes to the plasma due to impaired Heph activity [25]. Heph main role in iron metabolism appears to be mostly linked to intestinal iron absorption, but its expression was also reported other tissues/organ [125-127], indicating that Heph may also act as ferroxidase outside of the intestine.

Recently, Zp was identified as a transmembrane multicopper oxidase as Heph, being highly expressed at the placenta [128]. Zp expression was also detected in the murine embryo (brain, bladder, eye and brown fat) as well as in the adult mice (brain, kidney, testes and retina) [128]. An unidentified ferroxidase referred to as a Cp homolog was previously reported in BeWO cells, a placental choriocarcinoma cell line, likely corresponding to Zp [129,130]. This ferroxidase is downregulated by copper deficiency as observed for Zp [128,129], and its downregulation was associated with iron accumulation in these cells, suggesting that Zp ferroxidase activity might be involved in iron export from the placental cells to the fetus circulation [129].

Cp was first isolated from the plasma by Holmberg and Laurell and was literally named as the “blue substance from plasma” [131]. Cp ferroxidase activity combined with its abundant level in plasma lead to the recognition of Cp as an important anti-oxidant plasma component, preventing Fe^{2+} participation in Fenton reactions and subsequent formation of ROS [132,133]. Unlike Heph and Zp, Cp is not a transmembrane multicopper oxidase and can be expressed either as a soluble protein secreted to extracellular milieu (sCp) or as a membrane protein anchored to cell surface by a glycosylphosphatidylinositol (GPI) motif [134-136]. Interestingly, while hepatocytes express and secrete high levels of sCp, GPI-anchored Cp (GPI-Cp) was never reported in the liver and it was shown that this isoform corresponds to the predominant form of Cp expressed in the brain, where it plays a crucial role in iron homeostasis and anti-oxidant defense in the central nervous system [134,137]. The ferroxidase activity of both Cp isoforms was previously reported to be essential to Fpn1 iron export in different cells/tissues. Impaired Cp expression in $Cp^{-/-}$ mice and aceruloplasminemia patients is associated with iron accumulation in different tissues/organs, in particular liver (hepatocytes and Kupffer cells), spleen (macrophages), brain (astrocytes and neurons), β-cells in the pancreas, and retina [138].

APP is the precursor of β-amyloid peptide, which is linked to the development of Alzheimer disease. Recently, Duce *et al* reported that the E2 domain in APP presents ferroxidase activity [139]. In this study, APP was shown to co-localize with Fpn1 in neurons, where its ferroxidase activity was essential for Fpn1 iron export. Accordingly, $APP^{-/-}$ mice showed brain iron accumulation mostly associated with neocortical and hippocampal neurons, but also in other

organs such as the liver (hepatocytes) and kidney [139]. However, posterior publications by another research group question APP ferroxidase activity and report that APP E2 domain has no such activity [140,141]. In agreement, another research group recently showed that sAPP (a soluble form that results from APP cleavage) modulates iron efflux from brain microvascular endothelial cells by promoting Fpn1 stabilization levels at cell surface, but does not promote iron oxidation [142]. In conclusion, while APP putative ferroxidase activity is still unsure, its interaction with Fpn1 and the subsequent effect on iron efflux has been reported by different groups and in different cells, reinforcing its involvement in iron metabolism.

2. Iron and the Immune System

2.1. Crosstalk between immune cells and iron

2.1.1. The immune system

Immune system is composed by a network of cells, tissues, and organs that protects the body (host) against infections caused by pathogens like bacteria, virus, and parasites by preventing and limiting their entry and their growth inside the body. It can be divided in two interactive systems: the innate immunity and the adaptive immunity. The innate immunity mobilizes a response against invading pathogens, toxin or allergen by distinguishing self from non-self. It is the first line of defense, being activated rapidly and responding in a stereotypic manner against any threath. It is mostly composed of cells of myeloid origin including neutrophils, monocytes/macrophages, and natural killer (NK) cells, involving the release of cytokines, chemokines, ROS and reactive nitrogen species (RNS).

On the other hand, adaptive immunity is involved in the elimination of pathogens during the late phase of infection and it consists on a targetted response against a specific antigen. The key cell of adaptative immunity is the lymphocyte, which can be classified in several subtypes, including the two major subpopulations B and T lymphocytes. The response of this type of immunity depends mostly on the activation, proliferation and differentiation of antigen specific B and T lymphocytes that will be involved in antibody- and cell-mediated response against the recognized antigen. The antigen receptors result from a very complex DNA rearragement that recognize a wide range of potential antigens [143].

2.1.2. Links between iron homeostasis and immunity

The interaction between the immune system and iron homeostasis has been studied for decades. Multiple evidences support this complex interaction, varying from limiting the bioavailability of iron to invader pathogens (“nutritional immunity”) to the effect of iron deficiency or overload on the host immune response. Indeed, the key process of iron recycling that is vital for erythropoiesis is performed by an immune cell: the macrophage. It is also at the macrophage level that a major part of iron sequestration takes place during infection.

Infection and inflammatory processes affect iron homeostasis and, conversively, the disruption of iron homeostasis affects the immune system and its capacity to protect the body against pathogens [144].

2.1.2.1. Iron deficiency effect on the immune system

Iron deficiency was reported to be associated with suppressed immunity that may predispose the body to infection, affecting both innate and adaptive immunity. Some of the iron-deficiency effects on the immune system include: reduced neutrophil function by affecting the activity of iron-dependent enzymes such as myeloperoxidase and possibly impaired intracellular bactericidal activity; impaired NK cell activity; decreased T lymphocyte counts; impaired cytokines production by lymphocytes and macrophages; defective T lymphocyte-induced proliferative response; decreased production of macrophage migration inhibition factor [144-146].

2.1.2.2. Iron overload effect on the immune system

Iron overload compromises the function of many immune cells. For instance, in iron overload conditions as observed in thalassemia patients that suffer from severe anemia and blood transfusion-dependent iron overload, there is an increased susceptibility to infection that has been associated with iron accumulation in tissue macrophages along with defective immune function. These patients present decreased NK cells activity as well as defective chemotaxis and phagocytosis by neutrophils and macrophages [147,148]. On the other hand, in HH type I (mutations in *Hfe* gene) patients, iron depletion from macrophages despite systemic iron overload seems to protect against infection by intracellular pathogens such as *Mycobacterium tuberculosis* [149]. However, patients with HH type I present increased susceptibility to infection by *Yersinia enterecolitica* and *Vibrio vulcanicus* (extracellular pathogens) that proliferate systemically, taking advantage of the systemic iron overload condition in HH [150,151]. It was also reported that HH type I patients present impaired cytokine response (low TNFα and IL-6) that has been associated with impaired Toll-like receptor 4 (TLR4) signaling and is corrected by treatment with iron or Hepc [152]. This suggests that the low intracellular iron concentration in HFE-deficient macrophages is at the origin of TLR4 signaling impairment. Also, HH patients show decreased $CD8^+$ T lymphocytes numbers, both in peripheral blood and infiltrated in the liver. The cytotoxic activity of $CD8^+$ T lymphocytes is also compromised and an inverse correlation was found between the $CD8^+$ T lymphocytes counts and the severity of iron overload in HH [153-157]. Altogether, these data support the intrinsic dependence between the immune system and iron homeostasis in such a way that impairment in one of these systems is reflected in the other's function and balance.

2.2. Iron and Infection

Iron is an essential element for pathogen growth, in particular bacteria and parasites. In fact, a significant part of bacteria's genome codify genes involved in iron handling, clearly showing how iron is essential for their survival. As a consequence, as both host and pathogen compete for access to iron, the resistance to infection will rely in part on the outcome of this competition and will determine the regulation of mammalian iron homeostasis under inflammatory and infectious conditions. As described before, Fpn1 is downregulated at both mRNA and protein level by inflammatory and infection-related conditions. Indeed, pro-inflammatory cytokines such as IL-6 as well as LPS itself (TLR4 activation) upregulate Hepc production and secretion by the liver, promoting Fpn1 internalization and degradation. Downregulation of Fpn1 at cell surface leads to iron retention in the iron stores (hepatocytes and macrophages) and block of the iron absorption, reaching hypoferremia within hours after infectious or inflammatory stimuli [158].

The expression of acute phase proteins such as Tf, Ft, and Cp at the liver is upregulated by pro-inflammatory cytokines, favoring iron storage as well as promoting iron loading onto Tf through the ferroxidase activity of circulating Cp. Indeed, in normal conditions, Tf saturation is usually maintained close to 30-40% so that no iron remains free in circulation not only to protect against iron toxicity, but also as a first line of defense against infection [159]. Another acute phase protein that plays an important role scavenging serum iron is lactoferrin (Lf). Lf is a host glycoprotein that, like Tf, binds to iron with high affinity. It is highly concentrated in mucosal secretions, being also secreted by the liver as an acute phase protein and also a component of neutrophils granules, being released at site of infection. Noteworthy, unlike Tf, Lf still binds iron with high affinity at acidic pH, constituting an advantage for the host at the site of infection [160,161].

Some pathogens cause hemolysis as a strategy to promote iron availability in the form of Hb and heme. The upregulation of both Hp and Hpx as acute phase proteins is also very important for sequestering any circulating Hb and heme, again insuring that no form of iron is available in circulation for pathogen growth [162,163]. This mechanism of iron sequestration by the host is such a vital tool against infection that, under conditions of prolonged infection or inflammation, the host still favors this strategy of iron withhold despite severe limitation of erythropoiesis. The overall cost of such strategy is the development of the so-called anemia of inflammation or anemia of chronic disease [158,164].

In face of such battle for iron, pathogens also evolved by developing escape strategies to compete for iron. The expression and release of siderophores and hemophores that bind free iron and heme with high affinity,

constitute an important iron uptake strategy by the pathogens [165]. Given the ability of siderophores to scavenge iron so efficiently, it is not surprising that the host also evolved mechanisms to overcome siderophores synthesis by the pathogen. Lipocalin-2 (Lcn2), also known as siderocalin, is an acute phase protein expressed mostly by neutrophils able to bind to bacterial siderophores, sequestering them and making them unavailable to the pathogen [166]. Therefore, the host responds to infection by upregulating Lcn2 expression via TLR signaling in order to sequester bacterial siderophores and thus limit microbial access to iron.

Besides all these strategies to restrain the growth of pathogens, the innate immune response through professional phagocytes such as neutrophils and macrophages constitute the first line of defense to eliminate these invaders. In addition, Hepc production by neutrophils, macrophages, monocytes and lymphocytes in response to inflammatory/infectious stimuli could be of extreme importance to secure local iron withhold in these cells at site of infection, particularly in macrophages as iron store cells [74,75,112].

2.3. Macrophages, iron and immunity

The macrophage is a key cell of innate immunity that plays also a crucial role in the maintenance of iron homeostasis. Interestingly, several polarized macrophage phenotypes have been described under the influence of different microenvironments [167]. Among those polarized phenotypes, two particular ones were associated with opposite inflammatory conditions: M1 and M2 macrophages. M1 phenotype corresponds to the classically activated macrophages, presenting a pro-inflammatory phenotype while M2 phenotype corresponds to alternatively activated macrophages, presenting an anti-inflammatory phenotype. Until now, the best tool to distinguish between these two phenotypes has been the cytokine profile of expression, with M1 being IL-12^{high} IL-10^{low} whereas M2 are IL-12^{low} IL-10^{high} among others. Interestingly, gene expression profiles are strikingly polarized in these two macrophage phenotypes, with over 60% of genes associated with iron metabolism being differentially expressed between human M1 and M2 macrophages [111,168] (Figure I.8).

2.3.1. Inflammatory macrophages M1

M1 macrophages are classically activated by IFNγ, TNFα and bacterial products (like LPS), being characterized by high expression of inducible nitric oxide synthase (iNOS), pro-inflammatory cytokines (IL-1β, TNFα, IL-6, IL-12) and chemokines (CXCL9, CXCL10, CXCL11) as well as low expression of the anti-inflammatory cytokine IL-10, arginase-1 (Arg-1), CD163, and mannose receptor (MR, also known as CD206) [111,169].

M1 macrophages are potent effector cells with enhanced microbicidal capacity, producing great amount of ROS and RNS along with high expression of apoptosis genes, altogether increasing their killing capacity. They also recruit other immune cells by expression of chemokines, in particular monocytes and lymphocytes (T and NK cells), promoting their activation, proliferation and killing capacity [169]. Pro-inflammatory cytokines and TLR4-activation induce Fpn1 downregulation in monocytes and macrophages both transcriptionally (TLR4-activation) and post-translationally by autocrine Hepc upregulation and secretion, promoting iron retention in such infectious and pro-inflammatory conditions [75,111,112,170]. Interestingly, increased intracellular iron has also been reported to induce expression of pro-inflammatory cytokines in macrophages lacking Fpn1, likely through NF-κB activation by iron [171,172].

Hb-Hp, heme-Hpx and holo-Tf uptake in M1 macrophages is impaired by downregulation of CD163, CD91 and TfR1, respectively. M1 macrophages also promote storage of intracellular iron through upregulation of Ft [111,168,173,174]. DMT1 expression in M1 macrophages is controversial, with some authors reporting upregulated DMT1 in response to LPS alone [175] or combined with IFNγ [176], while others reported that DMT1 is significantly upregulated in M2 macrophages when compared with M1 macrophages [177]. In infected macrophages, the expression of Nramp1 at the phagolysosomal membrane, exporting iron out of this compartment containing the pathogen, is crucial for overcoming intracellular infection [178].

In addition, the multicopper oxidase Cp is also highly induced and secreted by M1 macrophages. Cp is an acute phase protein mostly associated with its anti-oxidant role in oxidizing Fe^{2+} into Fe^{3+}, promoting extracellular iron loading in Tf and Lf locally produced by immune cells [111]. Noteworthy, macrophage-derived Cp was reported to be crucial for protection against inflammation and tissue injury in *Cp*$^{-/-}$ mice [179]. Interestingly, M1 macrophages also express high levels of copper importers (SLC31A2 and CTR1), supporting the high expression of Cp as well as the known copper bactericidal properties [169,180].

Previous studies on HO-1 expression in M1 macrophages have reported contradictory results, with some authors reporting LPS-dependent upregulation of HO-1 while others showed downregulation in M1 macrophages [111,170,181-183]. However, M1 macrophages have been associated with increased erythophagocytic activity which would support a role for HO-1 upregulation in this polarized phenotype [170,184].

2.3.2. Alternatively activated macrophages M2

Alternatively activated macrophages (M2) correspond to a polarized phenotype of macrophages driven by immune stimuli including IL-4, IL13, transforming growth factor β (TGF-β) and glucocorticoids. M2 macrophages express high levels of the anti-inflammatory cytokine IL-10, Arg-1, CD163, MR as well as low levels of iNOS and pro-inflammatory cytokines (IL-1β, TNFα, IL-6, IL-12) [168,169].

M2 macrophages are characteristic of the resolution phase of inflammation in which the pathogens have already been cleared, dampening pro-inflammatory cytokine levels, secreting components of the extracellular matrix (fibrinogen, fibronectin) and promoting tissue repair at the site of infection/injury [169]. M2 macrophages express high levels of scavenger receptors, which will contribute to clearing surrounding tissue of cell debris. Amongst these scavenger receptors, CD163 and CD91 promote uptake of Hb-Hp and heme-Hpx that may exist at the site of infection/injury as a result of hemolysis often associated with these conditions [111,168,174]. As a consequence, M2 macrophages express a cell machinery of proteins involved in Hb and heme recycling, namely high HO-1 and Fpn1. One particularity of M2 macrophages is the low expression of Ft and high expression of Fpn1, suggesting that these macrophages promote iron recycling for clearing the site of infection/injury, but mostly for supplying iron to the surrounding cells and tissues, promoting collagen synthesis, fibroblast proliferation and tissue repair [111,168]. Indeed, it has been shown that switch from M1 to M2 phenotype is essential for muscle regeneration, a condition in which high levels of iron are essential for building new and functional myofibers [185]. In addition, the intracellular iron content of M1 macrophages may also affect the switch into M2 phenotype, thereby compromising the healing of the injured sites [184].

Interestingly, extracellular medium of M2 macrophages was reported to promote proliferation of tumor cells, supporting their role in the promotion of injury repair [111]. Curiously, tumor associated macrophages (TAM) present a M2-like phenotype, supporting the hypothesis that TAM, like M2, may be involved in iron supply to tumor cells, promoting their survival and proliferation [186]. In fact, it was shown that Fpn1 levels in breast cancer cells were inversely correlated with tumor malignancy, showing how Fpn1 levels and consequent iron retention in cancer cells is vital for their proliferation and could constitute a therapeutical target in cancer research [187]. Accordingly, another study confirmed an “iron retention” profile in breast cancer epithelial cells with increased Hepc, TfR1 and lower H-Ft expression when compared with non-cancerous mastectomy samples, which is compatible with the high proliferation status of cancer cells. Moreover, both lymphocytes and macrophages in cancerous mastectomy samples presented an “iron-donor” profile with high Fpn1 and H-Ft expression

along with an activation profile characterized by increased Hepc and TfR1. The “iron-donor” profile by lymphocytes and macrophages support the potential role of immune cells in supplying iron essential for the proliferation of the tumor cells [188].

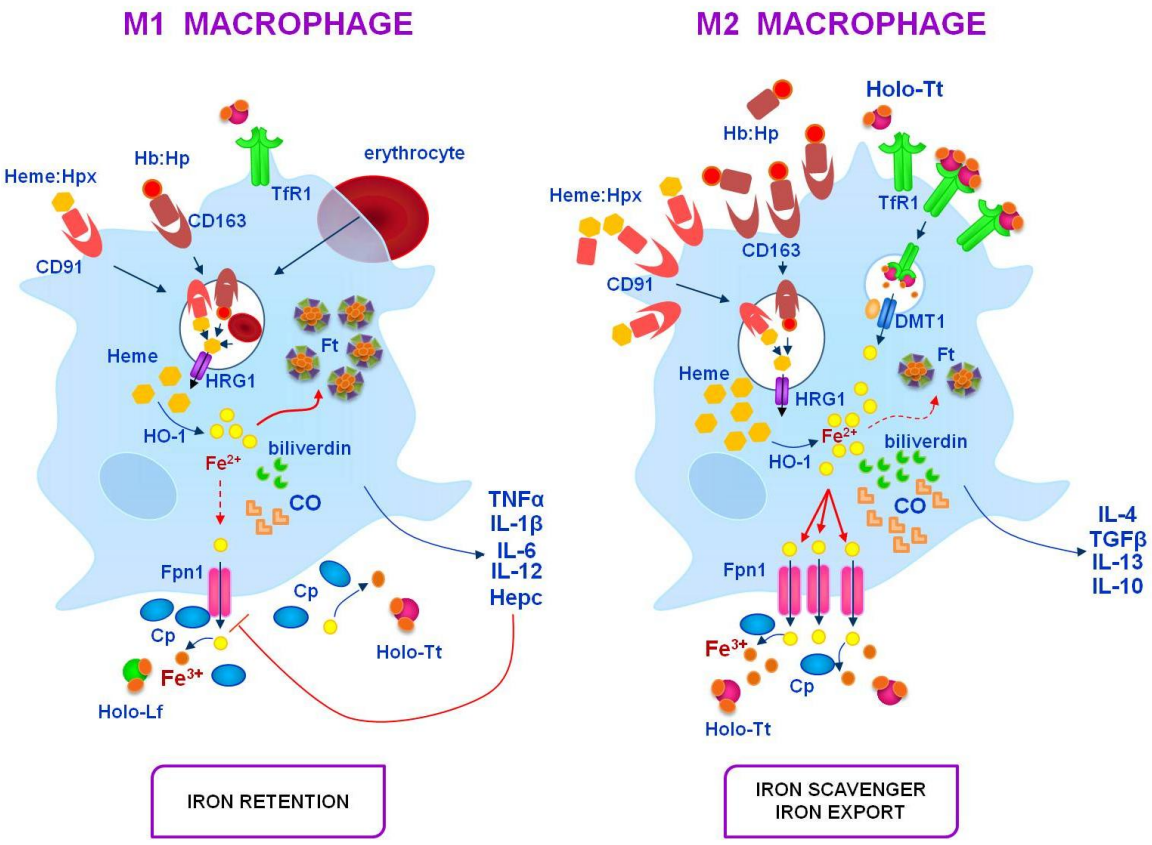

Figure I.8 - Iron metabolism in polarized macrophages M1 and M2. M1 macrophages express low TfR1, CD163 and CD91 limiting the uptake of iron sources. These cells also present increased phagocytic capacity for both pathogens and damaged erythrocytes at the local. Secretion of Hepc by M1 macrophages in response to infection/inflammation leads to low levels of Fpn1 at cell surface, promoting the iron retention and storage in Ft, in a clear strategy for promotion of pathogen iron starvation. M1 macrophages are also characterized by expression of pro-inflammatory cytokines and chemokines for recruitment of other immune cells. On the other hand, M2 macrophages are characterized by expression of anti-inflammatory cytokines and high expression of CD163 and CD91, promoting uptake of Hb and heme, subsequent iron recycling through HO-1 activity and export by Fpn1 to the extracellular medium. Iron supply by M2 macrophages is crucial for matrix remodeling and tissue repair at the resolution phase of inflammation, but has also been associated with promotion of tumor cells proliferation.

2.4. Lymphocytes and iron

Over the decades, the immune system was described as a complex network orchestrated only for protection of the organism from external threats (pathogens) and for self and non-self (transformed cells) recognition. However, in 1978, close observation of lymphocyte trafficking and positioning within tissue lead Professor Maria de Sousa to postulate that the immune system could also play an important role in the surveillance of iron toxicity in the organism [74,189]. The author proposed that lymphocytes could be recruited to sites of high iron concentration by sensing a gradient of iron-proteins such as Ft, Lf and Tf. By expressing receptors for these iron-carrier proteins at their cell surface, circulating T lymphocytes would sense the iron-carrier proteins gradient and migrate towards the site of iron deposition, where they would contribute to iron detoxification [189,190].

Despite the fact that, since 1978, many studies showed the close interaction between the immune system and iron homeostasis, the mechanism by which the lymphocytes could monitor and protect against local iron toxicity remains unclear. However, some pieces of the puzzle may already have been found:

1) activated lymphocytes present high levels of TfR1 for efficient holo-Tf uptake that is crucial for DNA synthesis and cell division, both important steps for lymphocyte proliferation [191];
2) both activated and non-activated lymphocytes synthesize Ft with high content of H-chains [192].

It is therefore pertinent to propose that lymphocytes could constitute a “mobile” iron compartment that would be recruited towards sites of high iron deposition, where these cells could store iron in the form of Ft while consuming it during active proliferation, explaining also the high number of lymphocytes found at sites of high iron deposition. On the other hand, one can hypothesize that as a potential mobile iron store compartment, lymphocytes could also be recruited to sites with high iron demand where they could supply iron, in a similar manner as polarized M2 macrophages during tissue repair.

Attesting the relevance of iron metabolism in lymphocytes, Pinto *et al* reported that human lymphocytes express basal levels of endogenous Hepc in all lymphocytes subpopulations, with $CD4^+$ and $CD19^+$ cells expressing the highest mRNA levels of human Hepc gene (*HAMP)* [74]. In these studies, upon treatment of human lymphocytes with high concentration of holo-Tf or iron citrate (NTBI), *HAMP* transcription was significantly upregulated in a mechanism that was neither HFE/TfR2-dependent nor BMP6-dependent. Analysis of cytokine expression profile showed that treatment with holo-Tf specifically upregulated TNFα and that TNFα silencing would impair *HAMP*

mRNA upregulation by holo-Tf. In addition, the author reported that *HAMP* transcriptional upregulation mediated the internalization of overexpressed GFP-Fpn1 in these cells, impairing iron export and promoting cellular iron retention. Since iron is extremely important for activated lymphocytes proliferation, the effect of cell activation on transcription of *HAMP* was tested. As expected, lymphocyte activation upregulated IL-2, IFNγ, TNFα and Hepc. It was also demonstrated that Hepc upregulation in activated lymphocytes is crucial for cell proliferation, probably by promoting intracellular iron retention to be used for DNA synthesis and cell division, both intrinsic steps of T cell proliferation. Altogether, the demonstration of endogenous expression of Hepc by lymphocytes and its vital role for lymphocyte proliferation upon activation gain particular interest in the context of inflammation/infection [74].

In inflammatory conditions, M1 polarized macrophages also secrete autocrine Hepc as well as TNFα, thereby contributing to local Hepc levels as well as promoting Hepc expression by lymphocytes and subsequent iron retention and storage in both cell types along with lymphocyte proliferation. In fact, H-Ft was shown to be upregulated by TNFα, which suggest that in addition to macrophages, lymphocytes could also uptake and store iron by synthesizing H-Ft [193]. Finally, recent data by the same research group show that, like hepatocytes, T lymphocytes can uptake and accumulate NTBI (in particular iron citrate), giving further support to this hypothesis [194]. The finding of an “iron-donor” profile in lymphocytes as well as macrophages present in cancerous mastectomy samples also support the role of lymphocytes as a mobile iron storage compartment that could provide iron to the surrounding cells/tissues [188].

Overall, although *in vivo* studies are necessary to further understand the relevance of lymphocyte-derived Hepc, these findings give further support to the possible role of lymphocytes in the surveillance of iron toxicity as postulated in 1978 by De Sousa.

3. Atherosclerosis: an inflammatory disease with infiltration of immune cells, lipids and iron accumulation

3.1. Atherosclerosis and cardiovascular disease

A study conducted by the World Health Organization reported that vascular diseases (VD) are the main cause of death worldwide from 2000-2012, particularly in industrialized countries [195]. VD refer to the clinical manifestations of coronary heart disease, cerebrovascular disease and peripheral artery disease, all of which frequently have atherosclerosis (ATH) as the underlying pathology [196]. Today, ATH is considered a chronic inflammatory condition resulting from interaction between modified lipoproteins, infiltrated immune cells and the components of the arterial wall, all leading to the development of complex lesions that protrude into the arterial lumen. These lesions or atherosclerotic plaques constitute the hallmark of ATH and, although advanced complex plaques may compromise or block the blood flow, it is often the rupture of such plaques and subsequent formation of thrombus or cloths that are responsible for the occurrence of acute vascular events such as myocardial infarction and stroke.

Among the several identified genetic and environmental risk factors associated with ATH, elevated levels of serum cholesterol are unique in being sufficient to drive the development of ATH in the absence of other risk factors. Indeed, the animal models commonly used to study ATH have defects on key proteins of lipid metabolism leading to hypercholesterolemia phenotype and accelerated ATH development [197]. However, ATH is no longer considered a simple lipid-laden disorder and the role of inflammation in this pathology has been widely acknowledged by the scientific community [198]. Interestingly, many individuals suffering from cardiovascular acute events present regular cholesterol levels, clearly pointing to other mechanisms in atherogenesis that are unrelated to cholesterol plasma level [199]. The discovery of statins as a pharmacological tool to decrease the circulating cholesterol levels created the false expectation that ATH would soon be a treatable pathology. Nonetheless, VD continue to be the main cause of death worldwide [195] despite the efficacy of statins on lowering cholesterol levels. Understanding other key factors involved in atherogenesis is therefore essential for discovering alternative and efficient therapeutic targets to control this pathology.

3.2. Atherogenesis

The artery wall is composed of three organized layers: tunica intima, tunica media and tunica adventitia. The intima layer corresponds to a single layer of endothelial cells (EC) on top of the internal elastic lamina. The media layer is delimited by the internal elastic lamina and the external elastic lamina, being composed of vascular smooth muscle cells (SMC) embedded in interstitial extracellular matrix. The adventitia is the most external layer of the blood vessel and is composed of connective tissue, fibroblasts and perivascular nerves. In large vessels, the adventitia layer is characterized by a dynamic microvasculature (*vasa vasorum*) that maintains the media layer and presents an additional source for leukocyte infiltration.

Atherosclerotic lesions can present different degrees of complexity, but in general they are composed of cells (immune cells, ECs and SMCs), extracellular matrix, lipids and debris. In 1977, Ross *et al* proposed the "response-to-injury" model of atherogenesis that has been refined and developed ever since [200]. Today, the current model proposes that atherosclerotic lesions arise from the inflammatory response to focal endothelial injury.

3.2.1. Endothelial dysfunction

Several VD risk factors such as high blood pressure, smoking, elevated cholesterol and glucose levels favor the occurrence of endothelial dysfunction often associated with sites of turbulent blood flow where shear stress is increased. The endothelial dysfunction leads to ROS production and increased permeability, promoting the retention of lipoproteins such as low density lipoprotein (LDL) between the intima and the media layer. Once in the sub-endothelial region, LDL undergoes enzymatic and non-enzymatic modifications such as oxidation, lipolysis, proteolysis and aggregation, giving origin to the so-called modified LDL [201].

3.2.2. Immune cells recruitment and formation of fatty streaks

Accumulation of modified LDL is a key event in ECs activation, inducing the expression of adhesion molecules and chemokines that recruit immune cells to the site of lesion, in particular monocytes and T lymphocytes [202]. Once in the lesion, the release of cytokines (TNFα, IFNγ) and growth factors (macrophage-colony stimulating factor, M-CSF) cause monocytes to differentiate into macrophages and to mature into active macrophages, which release pro-inflammatory cytokines and ROS species. Such event will amplify the inflammatory and oxidative microenvironment at the lesion in a vicious cycle of lipoprotein oxidation and local inflammation. During the maturation process, the

expression of scavenger receptors is upregulated, promoting the uptake of modified LDL by the macrophage. Accumulation of cholesteryl esters in the cytoplasm of macrophages will lead to the differentiation of lipid-laden cells denominated foam cells [203]. In addition to macrophages, SMC were also reported to uptake and accumulate lipids, contributing to the total amount of foam cells within the atherosclerotic plaque [204,205]. Subendothelial accumulation of foam cells results in the formation of lesions denominated as “fatty streaks” that are considered the onset of ATH. These lesions are small and may or not progress into larger and complex atheromatous plaques.

3.2.3. Formation of atheromathous plaques

During the progression into a more complex lesion, fatty streaks develop a necrotic core and a fibrous cap. The excessive lipid uptake by foam cells ultimately leads to cell death and release of their cytoplasmic content to the extracellular medium, promoting the formation of a necrotic core rich in lipids and cell debris at the center of the lesion, whereas the infiltration of monocytes and T lymphocytes continues to take place mostly at the shoulder region. As the lesion grows larger and more complex, the increased production of inflammatory cytokines such as IFNγ induces apoptosis of macrophages, contributing to the necrotic core development [206,207]. At this point, the atheromathous plaque is denominated as “atheroma”.

Production of growth factors and cytokines by degranulated platelets, ECs, macrophages, SMCs, and foam cells promotes the de-differentiation and proliferation of SMCs. In addition, the release of matrix metalloproteinases and IFNγ by macrophages and foam cells induces the downregulation of matrix production by SMCs, which further contributes to the degradation of the extracellular matrix while facilitates the migration of the SMCs from the media to the intima layers and subsequent formation of the fibrous cap [208]. The lesions presenting a defined fibrous cap overlaying the necrotic core are denominated as “fibroatheroma”.

As the lesions become more advanced and complex, some typical features may be observed, including development of intraplaque microvessels and calcifications. Indeed, the development of microvessels and intraplaque hemorrhage has been associated with accelerated atherogenesis as it allows for infiltration of leukocytes and erythrocytes, promoting the pro-inflammatory environment in the plaque. Occurrence of fissures or rupture, hematoma and thrombosis in fibroatheroma plaques give origin to the so-called “complicated lesions” [205].

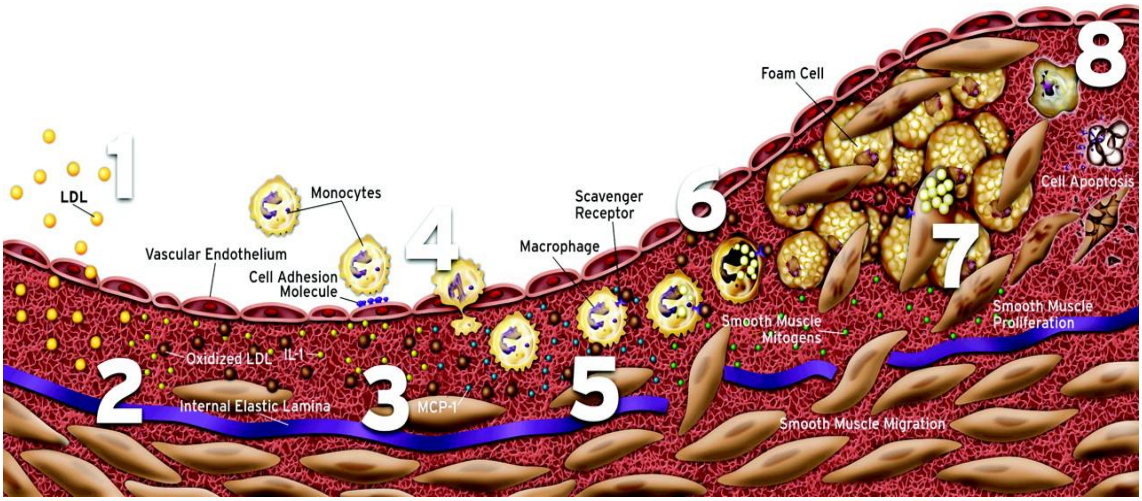

Figure I.9 - The development of an atherosclerotic plaque. The subendothelial accumulation of LDL and its modification (step 1 and 2) trigger the activation of ECs, which results in the release of cytokines and growth factors as well as induction of adhesion molecules (step 3), favoring the infiltration of monocytes to the site of lesion (step 4). Intralesional monocytes differentiate into macrophages (step 5) which, along with SMCs, will uptake and accumulate the modified LDL, forming the so-called foam cells (step 6). Foam cell accumulation and death by necrosis along with SMC proliferation result in a lesion with a necrotic core and fibrous cap, leading to the formation of the fibroatheroma (steps 7 and 8). Image originally published in Faxon *et al* (2004) [209].

3.2.4. Stable and unstable atheromathous plaques

According to its composition, the atherosclerotic lesion can be classified as a stable or unstable plaque, this latter one being more prone to rupture. A plaque with a small necrotic core, reduced number of inflammatory cells and thick fibrous cap is considered to be a stable plaque. On the other hand, a plaque with a large necrotic core, high number of inflammatory cells and a thin fibrous cap is considered to be unstable and likely to rupture, particularly at the shoulder regions where the inflammation is concentrated. Rupture of a plaque leads to the formation of a thrombus, which may occlude the artery lumen and cause acute cardiovascular events such as myocardial infarction or stroke [206,210]. Nonetheless, the rupture of a plaque does not necessarily lead to the occlusion of the artery and the plaque may heal by regeneration or scarring. However, the cost of the rupture is the enlargement of the plaque due to the thrombus formation, narrowing the blood vessel (stenosis). Indeed, the growth of atherosclerotic plaques appears to occur in bursts, probably associated with repeated events of plaque rupture and healing that are often associated with a greater incidence of fatal acute vascular events [211] (Figure I.10).

The rupture of the plaque is associated with increased apoptosis of SMCs, reduced production and increased degradation of extracellular matrix leading to the thinning of the fibrous cap. Also, the apoptosis of macrophages in addition to the apoptosis of foam cells increase the size of the necrotic core, inducing pressure on the fibrous cap as it becomes thinner [206]. Another cause for plaque

rupture is the formation of microvessels within the plaque and subsequent intraplaque hemorrhage, which can potentiate its instability through the infiltration of more leukocytes as well as erythrocytes [212].

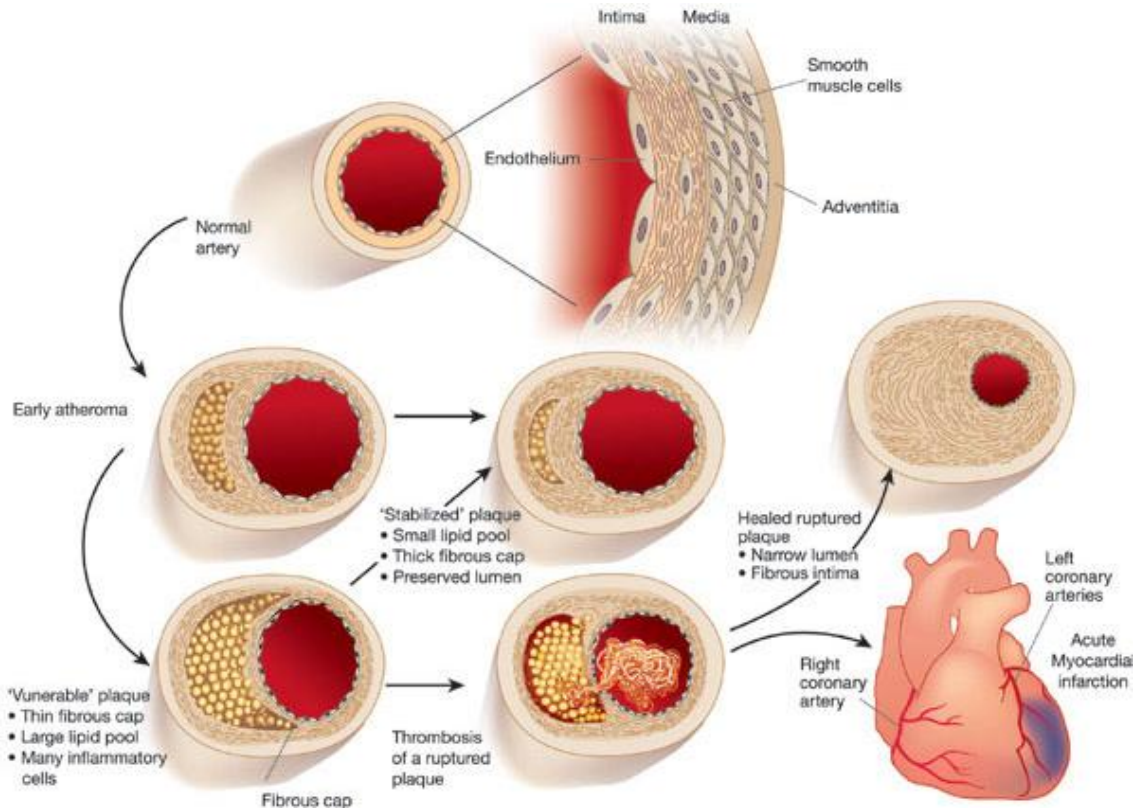

Figure I.10 - Atheroma plaque progression and stability. During atherogenesis, the sub-intimal accumulation of modified LDL triggers the infiltration of immune cells and differentiation of foam cells. The progressive accumulation of these cells and their subsequent death by necrosis leads to the formation of a necrotic core and a fibrous cap in the lesion (atheroma). The atheroma may evolve into a stable lesion with a small necrotic core and thick fibrous cap, or into a vulnerable plaque prone to rupture due to the large necrotic core and thin fibrous cap. The rupture of a vulnerable plaque leads to the formation of a thrombus, which may occlude the artery and trigger a cardiovascular event such as an acute myocardial infarction. However, if the occlusion is only partial, the plaque may heal at the additional cost of its enlargement, narrowing the lumen of the vessel (stenosis). Image originally published in P. Libby (2002) [213].

3.3. Iron as a potential risk factor in Atherosclerosis

3.3.1. The iron hypothesis

In 1981, Sullivan presented the “iron hypothesis” in which it was proposed that iron could constitute a modifiable risk factor in ATH [214]. This hypothesis suggested an alternative or additional explanation for the gender-associated difference of ischemic heart disease incidence, in which pre-menopausal women presented a significantly lower risk than age-matched men. This same risk of cardiovascular acute events would double in post-menopausal women when compared with pre-menopausal women. Possible explanations associated with the increased cholesterol levels after menopause or associated

with estrogen production as a protective factor were proposed. However, the rise in cholesterol levels in post-menopausal women was not sufficient to explain the doubling of ischemic heart disease incidence observed [214,215]. Also, regarding estrogen as a protective factor, the fact that the women's protection against VD was not observed in surgery-induced post-menopausal woman that preserved their ovaries, argues against this hypothesis. In addition, the hormonal replacement therapy has been associated with increased risk of VD complications, which is contrary to what was expected [216].

As a fundament of his hypothesis, Sullivan noticed that VD corresponded to the main cause of death in industrialized countries, an observation that remains valid to this day. Accordingly, in undeveloped countries where the majority of the population lives in poor conditions, VD associated with ATH were not at the top of the list of death causes. Interestingly, Sullivan pointed out that a condition often associated with the population of such countries is iron deficiency [214]. Pre-menopausal women often present iron deficiency or low levels of body iron stores as a consequence of the blood losses associated with menstruation. On the other hand, men progressively accumulate iron at a higher rate than pre-menopausal women, presenting mean Ft levels of 108-120 µg/L at age of 25 to 44 years old, while women present mean Ft levels of 38 µg/L at the same age. While men present a Ft blood concentration of 139-143 µg/L at age 45-64 years old, this value increases to 60-74 µg/L in women reflecting the increase of body iron stores in women after menopause [217]. Sullivan proposed that higher iron stores would be translated in higher availability of redox-active iron at site of oxidative and/or inflammatory injury, in which iron could play a role at site of atherosclerotic lesions promoting its progression. Accordingly, a state of sustained iron depletion or mild iron deficiency induced by regular phlebotomy could have a protective effect against ATH progression [214,218].

3.3.2. Presence of iron in atherosclerotic lesions

Since its proposal in 1981, the iron hypothesis has been the focus of many studies, supporting a still ongoing controversy. Evidence of the existence of catalytic iron in human atherosclerotic lesions was previously shown by Smith *et al*, who reported lipid peroxidation induced by the iron-rich content of the plaque [219]. Pang *et al* reported that both H-Ft and L-Ft (iron storage) are highly expressed in human atherosclerotic plaques, being induced on both ECs and macrophages at the early onset of the lesion and previous to the occurrence of intralesional hemorrhage often observed in advanced lesions. The same group showed that Ft was also induced in SMC in advanced lesions, where it could be involved in the promotion of cell proliferation. In this study, rabbits fed with high fat diet expressed high Ft levels in early and advanced lesions, but detection of iron deposits by Prussian blue was only observed in advanced lesions [220]. The use of more sensitive techniques such as nuclear microscopy by another group

revealed a significant increase of iron content observed in early atherosclerotic lesions of rabbits placed on a high fat diet [221].

3.3.3. Iron depletion and atherosclerosis

A previous report showed that repeated bleeding of rabbits placed on a high fat diet decreased the iron level accumulated in the lesions and delayed the onset of the disease [221]. In a similar study using high cholesterol-fed rabbits, treatment with an iron chelator induced a decrease in both lesion area and iron content, supporting a role for iron in early stages of ATH [222]. A different strategy was adopted by other researchers, using a murine model presenting a defect in apolipoprotein E (ApoE) which develops hypercholesterolemia independently of a cholesterol-rich diet. Lee *et al* observed a progressive accumulation of iron in lesions on apoE-deficient mice placed on a standard diet. After an iron-restricted diet for three months, a decrease of approximately 30% on circulating Ft was confirmed along with lower level of circulating auto-antibodies against oxidized LDL (oxLDL, the most common form of modified LDL) and increased resistance of isolated lipoproteins towards copper-induced oxidation. Accordingly, a decrease in the area of atheromatous plaques was observed in this iron-restricted group [223]. Altogether, these studies support a protective role of the depletion of body iron stores on the progression of ATH as suggested by Sullivan.

Indeed, Sullivan initially proposed that a possible test to his “iron hypothesis” in ATH would be a randomized prospective study evaluating the risk for developing VD in frequent blood donors in comparison with appropriate controls. Ensuring depletion of body iron stores without causing anemia would be an important condition in such study. Over the last decades, some trials attempted to test the effect of blood donation on the susceptibility to VD, but different study designs lead to opposite conclusions [224-227]. Interestingly, the results from the study which presented the closest experimental design to the one proposed by Sullivan indicated that high-frequency blood donors showed decreased body iron stores, decreased oxidative stress and enhanced vascular function when compared with low-frequency donors. These observations suggest that sustained iron depletion may have a protective effect towards the development of VD [228].

3.3.4. Iron overload and atherosclerosis

Although Sullivan emphasized the importance of testing the effect of sustained iron depletion state on ATH, many other studies focused their investigation on the role of iron overload on ATH progression generating confusing results.

Chronic administration of iron-dextran (which is specifically cleared from circulation by macrophages in the liver, spleen and bone marrow) followed by photochemical carotid artery injury in mice lead to accelerated arterial thrombosis, increased vascular oxidative stress, and impaired vaso-relaxation [229]. Araujo *et al* reported augmented formation of atherosclerotic lesions in rabbits placed on a cholesterol-rich diet combined with iron overload condition through iron-dextran administration [230]. In contrast, a similar study (iron dextran overload) using the same rabbit model by Dabbagh *et al* reported a decrease in the lesion area associated with iron overload rabbits while iron-deficient ones presented a slight increase in the area of lesions [231]. Noteworthy, the different iron status in this study influenced the circulating cholesterol levels, and iron-dextran was proposed to have a hypocholesteromic effect, decreasing the cholesterol levels and likely leading to the observed decrease in the lesions formation [231]. The conflicting results of the multiple studies sustained the controversy around the "iron hypothesis" to this day.

3.3.5. Hepcidin, iron macrophage and atherosclerosis

A common argument often pointed out against the "iron hypothesis" relied on the lack of association between HH and increased susceptibility to ATH development [232,233]. In response to the controversy around HH, a refinement of the "iron hypothesis" was later on presented by Sullivan [234,235]. Inspired by the recent knowledge about Hepc as the master regulator on systemic iron homeostasis, downregulating the iron exporter Fpn1 and blocking both iron absorption and mobilization from hepatocytes and macrophages, Sullivan proposed a possible mechanism in which Hepc could play a role in the progression of ATH. HH is characterized by systemic iron overload as result of disrupted Hepc-Fpn1 axis, causing continuous iron absorption and mobilization from stores. Interestingly, a curious fact about HH patients is that despite the iron overload, these patients present iron-depleted macrophages as a result of inappropriately low level of Hepc (in face of the body iron overload) or Fpn1 gain-of-function mutations. Given the key role of macrophages in ATH and the multiple observations of iron accumulation in macrophages and foam cells at the atherosclerotic plaque, Sullivan proposed that macrophage iron retention could be an essential feature for the progression of lesions in ATH. Indeed, Hepc is upregulated by inflammatory conditions in lymphocytes, monocytes and macrophages, which could promote macrophage iron retention. Noteworthy, iron loading in macrophages was reported to favor cholesterol uptake and accumulation by upregulating scavenger receptor 1 [236]. Hepc-dependent iron retention in intraplaque macrophages could therefore contribute to the formation of foam cells and subsequent progression of the lesion. Accordingly, iron-depleted macrophages typically observed in HH patients could therefore constitute a mechanism of protection against foam cell formation. Additionally, milder inflammatory response and decreased cholesterol levels also associated

with HH condition could contribute to protect against ATH despite systemic iron overload [234]. Interestingly, recent studies by Valenti *et al* showed Hepc levels correlated with the release of IL-6 and MCP-1 as well as with vascular damage in high-risk individuals with metabolic alterations, with exception for those with HH which presented low Hepc levels [237].

Unlike HH, pathologies characterized by chronic macrophage iron retention could show increased susceptibility to ATH. For instance, anemia of inflammation is a condition that presents iron-loaded macrophages as a consequence of Hepc upregulation by inflammatory conditions. Interestingly, Hepc was considered a direct link between anemia of inflammation and the increased risk for ATH development in patients suffering from rheumatoid arthritis [238]. In addition, Saeed *et al* recently reported that pharmacological suppression of Hepc in apoE-deficient mice using a BMP inhibitor decreased macrophage iron content and increased cholesterol efflux. This resulted in reduced foam cell formation and decreased lipid burden and area of atherosclerotic lesions, pointing to an eventual protection against ATH progression by inducing Hepc inhibition [239]. Accordingly, another study suggests that Hepc may constitute a positive regulator of atherosclerotic plaque destabilization by regulating macrophage iron homeostasis. In particular, overexpressed Hepc production at the carotid artery affected the plaque composition, increasing the number of intraplaque macrophages while decreasing SMCs and collagen content. In addition, Hepc overexpression induced iron retention in macrophages, increasing oxidative stress and production of pro-inflammatory cytokines concomitantly to the increase in oxLDL levels in intraplaque macrophages [240].

Altogether, these findings support the “iron hypothesis” and indicate that interaction between Hepc, cellular iron retention (particularly in macrophages) and lipid accumulation are critical for development of foam cells, leading to plaque destabilization. However, a recent study conducted by Kautz *et al* to test the effect of Hepc and iron-loaded macrophages in ATH progression in *ApoE* knockout mice found no association between macrophage iron loading and ATH progression, adding again new controversy to the “old” iron hypothesis.

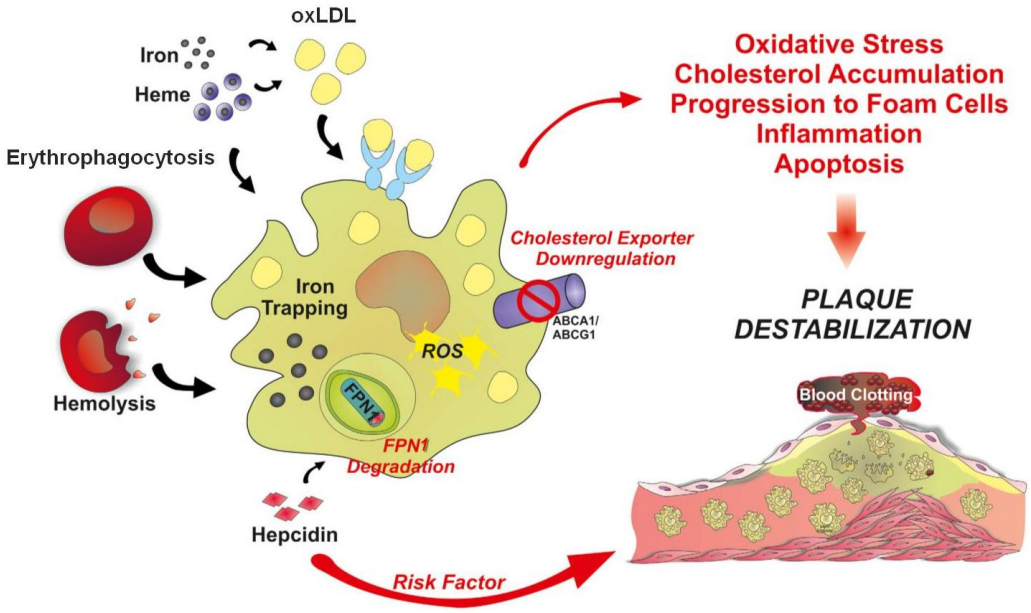

Figure I.11 - Schematic overview of the iron hypothesis. Macrophages can accumulate iron from different sources, including heme (free or associated with Hb) as a result of heme intestinal absorption, hemolysis or erythrophagocytosis. Once stored in the cell, iron can be mobilized to the bloodstream via Fpn1-mediated export according to the body iron demand through a mechanism regulated by Hepc. The "iron hypothesis" proposes that high hepcidin levels may constitute a risk factor for plaque progression and destabilization. The inflammatory conditions associated with atherogenesis may upregulate Hepc levels, leading to Fpn1 internalization and subsequent macrophage iron retention. The iron accumulation in macrophages would increase intracellular ROS levels and ultimately lead to decreased cholesterol efflux, promoting cholesterol accumulation and foam cell formation, inflammation and eventual plaque instability. Image adapted from Vinchi *et al* (2014) [241].

3.3.6. Macrophage polarization, iron and Atherosclerosis

3.3.6.1. M1, M2 and M4 phenotypes

Macrophages can be polarized into different phenotypes according to the surrounding microenvironment (see section 2.3). Indeed, macrophage polarization represents a continuum of functional states that encompasses a broad range of macrophage phenotypes with interchangeable characteristics, in which fully polarized M1 and M2 phenotypes represent two opposite extremes.

During the progression of atherosclerotic lesions, the complex microenvironment within the plaque is reflected in the heterogeneity of macrophages phenotypes. Indeed, M1 and M2 polarized macrophages were reported to co-exist in the atherosclerotic plaque and, although M1 is portrayed as pro-atherogenic due to its pro-inflammatory characteristics and M2 is considered to be anti-atherogenic, both M1 and M2 were shown to uptake lipids and subsequent transformation into foam cells *in vivo* [242,243]. However, besides M1 and M2, a mixed M1/M2 phenotype was also observed along with other polarized macrophage phenotypes in atherosclerotic lesions.

For instance, Gleissner *et al* reported that platelet chemokine CXCL4 polarizes macrophages into a M4 phenotype with some common genes to both M1 (e.g.: IL-6 and TNFα) and M2 (e.g.:CCL18 and CCL22). However, some other genes showed that M4 macrophages constitute a different phenotype. Among those distinct markers are: low expression oxLDL scavenger receptors such as scavenger receptor 1 and CD36, low MR and complete absence of Hb-Hp receptor CD163, low HO-1 and IL-10 expression, and increased levels of cholesterol exporters. Moreover, this newly characterized phenotype was shown to be present in the atherosclerotic plaques and experiments with double knockout mice ApoE and CXCL4-deficiency (*ApoE*$^{-/-}$*Pft4*$^{-/-}$) presented reduced ATH, which indicates that M4 macrophages could have a pro-atherogenic role[244].

3.3.6.2. Hemorrhage-associated macrophages

Boyle *et al* reported a new polarized phenotype distinct from M1 and M2 macrophages. These polarized macrophages were denominated as hemorrhage associated-macrophages (HA-mac) and were first identified in human plaques with fatal coronary thrombosis, where they would localize around the hematoma, being mostly absent in the stable and hemorrhage-free plaques analyzed. HA-mac are distinct from the lipid-laden macrophages, presenting low lipid content, suppressed oxidative stress and decreased expression of myeloperoxidase (MPO) and human leukocyte antigen (HLA-DR), as well as increased expression of CD163, MR, HO-1 and IL-10. This polarized phenotype was differentiated *in vitro* by exposure to oxidized erythrocytes, Hb or heme during seven days, in which HO-1 upregulation was found to be Nrf2-dependent and essential for the polarization of HA-mac [245,246]. Later on, Boyle renamed HA-mac as Mhem macrophages and clarified the underlying regulatory mechanism in which heme triggered the activation of both Nrf2 and ATF-1 and their translocation to the nucleus. HO-1 upregulation was mediated by both activating transcription factor 1 (ATF-1) and Nrf2, while ATF1 alone mediated liver X receptor (LXR) induction (likely LXR-β) and subsequent upregulation of ApoE as well as cholesterol exporter, promoting cholesterol mobilization out of the Mhem macrophage [247].

In a parallel study, Finn *et al* reported a polarized macrophage phenotype denominated as M(Hb) and driven by Hb-Hp during macrophage differentiation, resembling the Mhem phenotype reported above [248]. When comparing M(Hb) with M2 macrophages, similar levels of MR were observed along with higher levels of CD163 and IL-10 in M(Hb) macrophages as observed in Mhem. Finn observed that M(Hb) were localized in the area surrounding intraplaque hemorrhage as previously observed for Mhem macrophages described by Boyle, presenting also upregulated HO-1. A mechanism was reported in which increased Fpn1 levels and subsequent increased iron export in M(Hb)

macrophages resulted in low intracellular iron and ROS. The low oxidative stress activated LXR-α, leading to increased levels of the cholesterol exporters ATP-binding cassette A1 and G1 (ABCA1 and ABCG1), protecting M(Hb) from transformation into foam cells [248]. In another study by the same research group, the atheroprotective effect of M(Hb) was proposed to be dependent on low Hepc production by these cells and subsequent high levels of Fpn1 and low intracellular iron, pointing pharmacological suppression of Hepc as a possible strategy against ATH progression [239].

3.3.6.3. The Mox phenotype

Another polarized macrophage phenotype entitled as Mox was recently reported by Kadl *et al*, differentiated upon exposure to oxidized phospholipids (particularly oxPAPC) [249]. Mox macrophages presented decreased phagocytic capacity of beads and apoptotic thymocytes as well as decreased capacity of promoting monocyte migration when compared with M1 and M2 macrophages. Also, both M1 and M2 macrophages were polarized into Mox phenotype *in vitro* upon exposure to oxPAPC, suggesting that Mox macrophages could constitute a major population in the atherosclerotic plaque. Mox macrophages also presented a distinct pattern of gene expression, in which M1 and M2 markers such as iNOS, TNFα, IL-12, MCP-1 and Arg-1 are not upregulated. Instead, a total of 119 genes analyzed were exclusively upregulated in Mox macrophages, including the ones coding for HO-1, glutathione reductase 1, sulforedoxin-1, thioredoxin reductase, glutathione reductase 1, glutamate-cysteine ligase modifier subunit, thrombospondin, and vascular endothelial growth factor (VEGF). Apart from VEGF, the other genes mentioned above present anti-oxidant or anti-angiogenesis activities. The upregulation of some of these anti-oxidant genes was found to be Nrf2-dependent, including the gene coding for HO-1 among others. Additionally, Kadl *et al* reported that Mox macrophages presented decreased protection against cell death in the absence of Nrf2 or HO-1, revealing the importance of this pathway in the survival of macrophages in such oxidative environment as the one found in atherosclerotic lesions.

Finally, analysis of macrophages isolated from atherosclerotic lesions of *LdlR*$^{-/-}$ mice placed on high-fat diet using flow cytometry technique revealed the presence of 39.2% M1 ($CD86^+$, $HO\text{-}1^-$, MR^-), 34.4% Mox ($CD86^-$, $HO\text{-}1^+$, MR^-), 21.8% M2 ($CD86^-$, $HO\text{-}1^-$, MR^+) and 9.6% Mox/M1 ($CD86^+$, $HO\text{-}1^+$, MR^-) and 2.3% Mox/M2 ($CD86^-$, $HO\text{-}1^+$, MR^+) polarized macrophages, proving the existence of Mox macrophages in atherosclerotic lesions [249]. The observation of the mixed populations Mox/M1 and Mox/M2 suggests that the different populations of M1, M2 and Mox may co-exist within the plaque in spatially distinct microenvironments, in which the mixed populations could be located in the transition of the different microenvironments. Interestingly, the mixed

phenotype Mox/M2 (CD86^{-}, HO-1^{+}, MR^{+}) could also correspond to Mhem/M(Hb) phenotype described before.

Interestingly, in a different study, Seneviratne *et al* reported that Mox macrophages constitute the main macrophage population in the aortic root lesions (36% Mox vs. 5,6% M1 and 0,2% M2). Additionally, the same author used a murine model to test low shear stress into the development of vulnerable plaques, and oscillatory shear stress to induce a stable plaque phenotype in the carotid artery [250]. The results showed that Mox and M2 populations were not significantly different between lesions triggered by either low or oscillatory shear stress, while M1 macrophages were significantly increased in advanced LSS-induced lesions (unstable plaque) [250], which suggests that Mox macrophages constitute a major population during the progression of atherosclerotic plaques, independently from their stability.

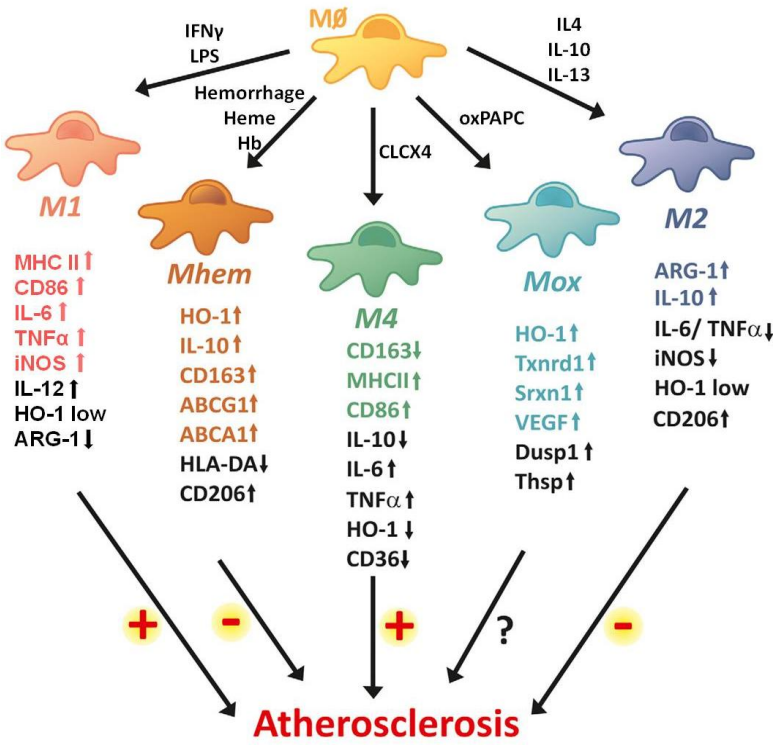

Figure I.12 - Macrophage polarized phenotypes in Atherosclerosis. Macrophages (Mø) present a high plasticity in response to the surrounding microenvironment, in which M1 and M2 macrophages constitute the two extreme phenotypes. M1 macrophages show strong pro-inflammatory properties and are involved in the development and progression of the lesion (+) while M2 macrophages are considered anti-inflammatory and have been reported as anti-atherogenic (-). In addition, several other macrophage phenotypes are observed in the atherosclerotic plaque: Mhem macrophages which are characterized by high levels of HO-1, CD163 and MR (CD206) as well as ABCA1 and ABCG1 (cholesterol exporters), promoting the reverse cholesterol export and considered to be anti-atherogenic; Mox macrophages which present anti-oxidant properties, expressing high levels of anti-oxidant genes such as HO-1, Txnrd1, and Srxn1. However, the potentially athero-protective effect of Mox macrophages needs to be demonstrated; M4 macrophages which differentiate in response to the chemo-attractant CXCL4, showing pro-inflammatory and pro-atherogenic effects and presenting low levels of CD163 and high levels of MHCII and CD86. Illustration adapted from Vinchi *et al* (2014) [241].

3.3.7. Ferroportin-1 and its partners in atherogenesis

Several studies show iron and lipid accumulation co-exist in foam cell macrophages, with exception to Mhem/M(Hb) polarized phenotype in which cells present low intracellular iron and low intracellular lipid content. Both M1 and M2 macrophages have already been characterized concerning the main proteins involved in iron metabolism (section 2.3.1). However, apart from HO-1, expression of iron metabolism proteins in Mox macrophages is poorly described. Concerning the significant proportion of Mox macrophages in atherosclerotic lesions and how iron and lipid metabolisms are interconnected, the characterization of the expression of iron metabolism proteins in this polarized phenotype is highly relevant, with particular interest for the proteins involved in iron export: Fpn1 and its ferroxidase partner(s).

Fpn1 is so far the only iron exporter identified in mammals [24,95,96]. Recent publications point to an important role of macrophage iron retention in the progression of atherosclerotic lesions [184,240,248,251]. Moreover, increased macrophage iron export by Fpn1 was shown to be essential for resistance to foam cell formation [248]. Indeed, Fpn1 expression is downregulated at both mRNA and protein level by pro-inflammatory conditions (M1 phenotype), leading to impaired iron export and progressive iron accumulation in M1 macrophage [28,110,111,252]. In Mox macrophages, the transcription factor Nrf2 is activated in response to oxidized phospholipids [249]. Interestingly, Nrf2 is involved in Fpn1 upregulation in response to heme [109], suggesting that Fpn1 could be upregulated in Mox macrophages. However, oxLDL was also reported to induce the release of pro-inflammatory cytokines [253], which could promote Fpn1 downregulation. Understanding how Fpn1 expression is modulated in response to oxLDL (Mox) is fundamental considering the relevant role of iron retention in the progression of atherosclerotic lesions.

Besides Fpn1 expression, the iron export is also modulated by the expression of the ferroxidase partner interacting with Fpn1. Indeed, lack or impaired ferroxidase activity, in particular Cp, was associated with decreased levels of Fpn1 at cell surface, which suggested that ferroxidase activity could promote Fpn1 stabilization at cell surface [121,122]. Macrophage iron retention in pathological conditions (aceruloplasminemia) or animal models (*Cp*$^{-/-}$ mice), in which Cp expression is impaired or nonexistent, indicates that Cp plays an important role in macrophages iron export [51,63]. Indeed, Sarkar *et al* reported extracellular Cp activity was essential for iron export from macrophage under hypoxic conditions [254]. Interestingly, Cp is an acute phase protein and, as such, its levels are highly upregulated in pro-inflammatory conditions (IFNγ, IL-1β, IL-6, LPS) [136], while Fpn1 is downregulated. However, in addition to its role in cellular iron export, Cp can also oxidize other substracts, including lipoproteins such as LDL [255,256]. Increased levels of circulating Cp have been associated

with increased cardiovascular risk [255,257-259], which could be attributed to its capacity to oxidize circulating LDL. In addition to increased circulating Cp levels, the pro-inflammatory conditions as well as hypoxia found in atherosclerotic plaques could promote Cp expression and subsequently LDL oxidation. Accordingly, co-localization of Cp and oxLDL in the enlarged intima of pro-atherosclerotic areas was previously reported, supporting the hypothesis that Cp local production by immune cells at the site of lesion could be associated with increased LDL oxidation, and thus to increased susceptibility to VD [260]. Noteworthy, in addition to Cp-mediated LDL oxidation, Cp was also reported to enhance SMC- and EC-mediated LDL oxidation by a superoxide-dependent mechanism [261]. Therefore, considering both its role in cellular iron export as well as LDL oxidation, characterization of Cp isoforms expression in lymphocytes, monocytes, and macrophages is necessary to get insight on the role of Cp in atherogenesis.

Another possible partner of Fpn1 is APP, which was reported by Duce *et al* to act as a ferroxidase in neurons [139]. Although its putative ferroxidase activity is currently under discussion [140,141], APP interaction with Fpn1 was demonstrated by McCarthy *et al* which showed that sAPP stabilized Fpn1 at cell surface of brain microvasculature ECs, thereby influencing the iron export in these cells [142]. APP expression in monocytes and macrophages was previously reported [262], which suggests that APP could be one additional partner of Fpn1 in macrophages. Moreover, like Fpn1, APP translation is regulated by the IRE/IRP system and its expression was shown to be upregulated by iron in neural cell lines [263,264]. Increased iron accumulation in the liver (hepatocytes), kidney and brain (neurons) of *App*$^{-/-}$ mice point to an important role of APP in iron metabolism [263]. Interestingly, an association was found between ATH and Alzheimer's disease [265], a pathology in which APP is directly involved. In fact, double knockout mice for ApoE and APP (*ApoE*$^{-/-}$*App*$^{-/-}$) showed increased susceptibility to ATH, developing larger lesions than *ApoE*$^{-/-}$ mice [266]. In this same study, *ApoE*$^{-/-}$*App*$^{-/-}$ mice presented upregulated levels of chemokines, adhesion molecules and pro-inflammatory cytokine IL-6, showing that APP plays a role in protection against ATH [266]. As some of these features have also been associated with increased macrophage iron retention [184,240,251], it is thus possible that APP involvement in Fpn1 stabilization and iron export could be at the origin of the increased ATH susceptibility in *ApoE*$^{-/-}$*App*$^{-/-}$.

Overall, Fpn1, Cp and APP have been individually associated with ATH and are likely involved in iron efflux in macrophages. In addition, Cp capacity of directly oxidizing LDL points to a role of Cp in atherogenesis that goes beyond the iron export. Therefore, understanding the effect of pro-inflammatory and atherogenic conditions on these proteins in immune cells and, in particular, in macrophages is important to bring insight on their role in ATH and to clarify the relationship between iron and ATH.

4. Rationale of the study and objectives

The iron hypothesis on ATH etiology is based on the principle that high stored iron levels could constitute a risk factor in the development and progression of ATH. Characterization of the mechanisms underlying the regulation of iron metabolism in the main immune cells involved in the progression of atherosclerotic lesions is thus necessary to understand the role of iron in atherogenesis.

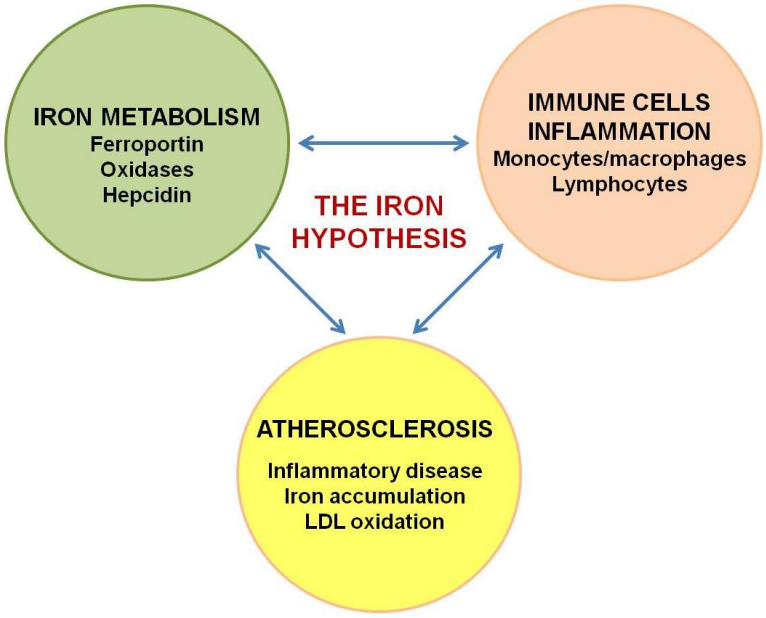

Figure I.13 - Schematic illustration of the interconnection between iron metabolism, immune cells and inflammation on the "iron hypothesis" of atherosclerosis etiology.

In this broad perspective to understand how iron metabolism, immune cells and atherogenesis are interconnected (Figure I.13), we designed three major objectives:

1) *Characterize the expression of Cp isoforms (sCp and GPI-Cp) in lymphocytes, monocytes and macrophages.*

In chapter 1 and 2, we studied the expression of iron metabolism proteins in immune cells that infiltrate the plaque and actively contribute to its progression In this context, we focused of the expression of Cp in immune cells given its potential role as a ferrroxidase partner of Fpn1 in these cells as well as its potential pro-oxidant role in atherogenesis.

2) Investigate the potential ferroxidase(s) interacting with Fpn1 in macrophages.

In chapter 2, we clarified some aspects of iron metabolism concerning the ferroxidase partners of Fpn1 in macrophages.

3) *Study the effect of pro-inflammatory (M1) and/or atherogenic (Mox) context on macrophages iron metabolism, particularly on the regulation of the proteins involved in iron efflux.*

In chapter 3, we characterized the effect of pro-atherogenic conditions on the expression of key iron metabolism proteins in macrophages. In particular, we studied the expression of iron metabolism proteins in the new polarized phenotype Mox. We also investigated the effect of simultaneous challenge with M1 and Mox activators on macrophage polarization as well as on the expression of some iron metabolism proteins.

II. Material and Methods

1. Reagents

1.1. Source of reagents

All chemical reagents and human AB serum were purchased from Sigma-Aldrich, unless stated otherwise. All cell culture media, bovine serum and antibiotics were purchased from Invitrogen (GIBCO BRL). All cytokines were purchased from BD Biosciences. All reagents for Western blot were purchased from Bio-RAD unless stated otherwise. Reagents for In-Cell Western blot were purchased from Li-COR unless stated otherwise. Plasmid containing human GPI-Cp full-length cDNA was a kind gift from Doctor Jonathan Gitlin (Marine Biological Laboratory, Massachusetts, USA). Plasmid containing human Fpn1 full-length cDNA was purchased from ORIGENE. Construction of plasmids containing the sequence of the different epitopes of human Fpn1 for antibody production was carried out as a service by IMAGIF (ICNS, Gir-sur-Yvette, France). All primers used for quantitative transcriptional analysis are indicated in Table 1 while all antibodies used in the different proteomic techniques are indicated in Tables 2, 3 and 4. Native LDL solution was a kind gift from Doctor Anne Negre-Salvayre (Inserm/UPS UMR 1048-I2MC, Toulouse, France). The antibody anti-Hepc was a gift from Doctor Sophie Vaulont (Institut Cochin, Paris, France) [267].

1.2. Preparation of native, oxidized and acetylated LDL

Native LDL (nLDL) solution was extensively dialyzed 20 h at 4ºC against $NaCl_2$ (9 g/L) with several changes of buffer in order to remove the traces of ethylenediaminetetraacetic acid (EDTA). The nLDL solution was then filtered with 0,2 µm filter for sterilization and then quantified and diluted to 1 mg/ml, before being incubated for 24 h at 37ºC in the presence of 10 µM of $CuSO_4$ for preparation of oxLDL. For each experiment, fresh oxLDL solution was prepared and used immediately after completing the 24 h incubation since oxidation is a continuous process that would only be stopped by EDTA addition. Untreated "control" cells were incubated in parallel in the presence of the same concentration of $NaCl_2$ and $CuSO_4$ in culture medium as in oxLDL-treated cells. For preparation of acetylated LDL (acLDL), non-dialyzed nLDL was quantified and diluted to 2 mg/ml and then diluted 1:1 with saturated acetate solution to a final concentration of 1 mg/ml. Then, under mild agitation, anhydrous acetic acid was added (2 µL acid/mg LDL) every 15 min for 1 h at 4ºC. The resulting acLDL was then extensively dialyzed against overnight (O/N) a 4ºC against NaCl2 (9 g/L) with several changes of buffer to remove all traces of acid and EDTA. The solution of acLDL was then filtered for sterility and dosed using BCA, being stored at 4ºC or used directly on cells. Efficiency of both oxLDL and acLDL

treatment was monitored by lipid staining using a specific dye. Oxidation level of oxLDL and nLDL solutions was verified by TBARS determination in collaboration with Doctor Anne Negre-Salvayr's Lab.

1.3. Preparation of plasmids

Large-scale production of recombinant plasmids containing full-length cDNA of human GPI-Cp and human Fpn1 were performed by transformation of competent DH5α *E.coli* (Invitrogen) through thermal shock, followed by plasmid DNA extraction using the PureLink HiPure Plasmid Filter Maxiprep Kit (Invitrogen). Plasmids were then precipitated with absolute ethanol O/N at -20ºC, washed with 70% ethanol, and then resuspended in sterile TE (pH 8.0). Quantitative and qualitative analysis were performed using Nanodrop 1000 (Thermo Scientific) and electrophoretic agarose gel (0,8%) analysis. Presence of GPI-Cp or Fpn1 cDNA cassettes was confirmed by conventional polymerase chain reaction (PCR) using specific primers.

2. Cell culture

2.1. Human peripheral blood cells

Human peripheral blood mononuclear cells (huPBMC) were isolated from either buffy coats or whole blood of healthy blood donors collected at Hospital Reynaldo dos Santos using either Ficoll-Paque (GE Healthcare) or BD vacutainer CPT tubes (BD Biosciences), respectively. Remaining erythrocytes were lysed by incubating the cells in erythrocyte lysis solution (10 mM Tris, 16 mM NH_4Cl, pH 7.4) for 10 min at 37ºC and followed by centrifugation at 400 *g* for 10 min. huPBMC were resuspended in warm RPMI 1640 culture medium and centrifuged at 300 *g* for 15 min to remove most platelets from suspension. huPBMC were then washed in Hank's balanced Salt solution (HBSS) and resuspended in RPMI 1640 culture medium supplemented with GlutaMAX^{TM} I, 25 mM HEPES buffer, 10% fetal bovine serum (FBS) and 1% penicillin-streptomycin (P/S).

For lymphocyte enrichment (huPBL), huPBMC were seeded in T75 culture flasks pre-coated with FBS, followed by 1 h incubation at 37ºC with 5% CO_2 atmosphere. Cells in suspension were collected and washed in phosphate-buffered saline (PBS) solution. For monocyte enrichment (huPBMn), cells adherent to the flask after 1h incubation were washed several times with HBSS (Mg^+Ca^+) and scrapped in PBS-EDTA (2 mM). Cells were then collected by centrifugation and washed in PBS before undergoing cell fixation or lysis according to different protocols. Purity of cell suspension (huPBL > 95%; huPBMn > 87%) was confirmed by flow cytometry using Simultest LeucoGATE (CD45-FITC/CD14-PE) reagent (BD Biosciences).

For human macrophage culture, the adherent huPBMn were washed with warm HBSS (with calcium and magnesium) followed by incubation with RPMI 1640 medium supplemented with 10% FBS, 10% human AB serum, 1% P/S and 50 ng/ml recombinant human M-CSF (R&D Systems). At day 5, medium was removed and adherent cells were washed with warm HBSS to remove any dead cells, followed by addition of new complete medium. Cells remained in culture with medium renewal every 2 days until treatment at day 7/8.

2.2. Murine bone Marrow Derived Macrophages

Murine bone marrow derived macrophages (BMDM) were cultured as described previously [170]. Briefly, bone marrow cells were isolated from femurs of SWISS or C56BL/J6 mice, washed in HBSS and seeded in complete medium (RPMI 1640 supplemented with 10% FBS, 10% L929-condicioned culture medium (LCCM) and 1% P/S) at a concentration of $3x10^5$ cells/ml and incubated at 37ºC with 5% CO_2 atmosphere. Cells were seeded in 100 mm diameter plates for protein extraction (subcellular fractionation and iodixanol gradient), 35 mm diameter plates for RNA extraction, 96-well or 48-well cell culture plates for In-Cell Western blot analysis (LI-COR) or onto circle glass coverslips placed in 24-well cell culture plates for immunofluorescence and Oil Red O staining. At day 4, the medium was removed and adherent cells were washed twice with warm HBSS to remove non-adherent dead cells, followed by addition of new complete medium. Cells remained in culture with daily medium renewal until treatment at day 7/8.

2.3. Cell lines

Human hepatocarcinoma cell lines HepG2 and HuH7 as well as monocytic cell line THP-1 were cultured in RPMI 1640 medium supplemented with 10% FBS and 1% P/S. For THP-1 derived macrophages, cells were treated with phorbol myristate acetate (PMA) at 20 nM for 48h. CHO cells were cultured in advanced DMEM F12 medium supplemented with 10% FBS and 1% P/S. J774A1 were cultured in DMEM medium supplemented with 10% FBS and 1% P/S. All cultures were performed at 37ºC with 5% CO_2 atmosphere. Cells were seeded in 100 mm diameter plates for protein extraction, on 35 mm diameter plates for RNA extraction or onto glass coverslips in 6-well plates for immunofluorescence studies.

2.4. Treatment of cells

HepG2 and J774A1 were treated at 80% confluence (48 h culture), murine BMDM and human macrophages were treated at days 7/8 of culture, human PBL were seeded at $2x10^6$ cells/ml before treatment, THP-1 macrophages were seeded at $8x10^5$ cells/ml and differentiated with 20 nM PMA for 48 h at 37ºC

before treatment. All treatments were performed at 37ºC with 5% CO_2 atmosphere and the specific conditions are described below:

- Iron: cells were treated with Fe-nitrilotriacetate solution (FeNTA, 50-200 µM), apo-Tf (3 mg/ml) or holo-Tf (3 mg/ml) for 18 h in complete medium.

- Cytokines: huPBL cells were treated with recombinant human IFNγ, IL-6, and TNFα (20 ng/ml, 18 h, BD Biosciences) in complete medium. Murine BMDM were treated with LPS /IFNγ (10 ng/ml each, 18 h) for differentiation of M1 macrophages.

- Hepcidin: In general, cells were treated with 700 nM of human hepcidin (Peptides International) for 3 h in complete medium. For two particular experiments, THP-1 cells were treated with 1 µM human Hepc for 4 h while HepG2 cells were treated with 700 nM human Hepc for 18 h in complete medium.

- PIPLC: cells were incubated with 0,5 U/ml enzyme (Invitrogen) for 1 h at 37ºC prior to Cp immunofluorescence staining.

- Anti-Hepc: HepG2 cells were incubated with 0,6 µg/ml anti-Hepc [267] in complete culture medium for 18 h.

- LDL: cells were treated with dialyzed nLDL, dialyzed acLDL or non-dialyzed oxLDL at 50-100 µg/ml during different time points (3,5 h, 7 h, 24 h) in complete medium. Cell viability after incubation with the different LDL solutions for the maximum time point (24 h) was evaluated through a colorimetric assay using methyl thiazolyl tetrazolium (MTT).

In all treatments, control cells (untreated) were incubated with the vehicle solution (water in general, PBS for cytokines, $NaCl_2$ for LDL solutions) used for each treatment.

3. Transfection

Transient transfection of CHO or HuH7 cells with a plasmid containing the human GPI-Cp or human Fpn1 full-length cDNA was performed using Lipofectamine 2000 (Invitrogen) according with the manufacturer's instructions and in the absence of antibiotics. After 6h of incubation with cells at 37ºC, medium containing DNA-lipid complexes was removed and cells were washed with warm medium before addition of new complete medium without antibiotics. Transfected cells were incubated O/N before any protein or RNA extraction. Transfection success was confirmed by semi-quantitative reverse transcription-PCR (RT-PCR) using cDNA of the transfected cells and specific primers against GPI-Cp, Fpn1 and β-actin cDNA.

4. RNA analysis

4.1. RNA extraction

For RNA analysis of adherent cells, TRIzol reagent (Invitrogen) was added directly to cell culture plates after discarding all culture medium, homogenized and stored at -80ºC until RNA extraction. Total RNA was extracted according to manufacturer's instructions, followed by quantitative and qualitative analysis using Nanodrop 1000 (Thermo Scientific) or Nanophotometer P360 (Implen).

4.2. Two step reverse transcription-quantitative PCR

4.2.1. Reverse transcription

Synthesis of cDNA was carried out through a reverse transcription (RT) reaction using 1 µg of total RNA, oligo(dT) primers and MMLV Reverse Transcriptase (Invitrogen) according to the manufacturer's instructions. All cDNA's were diluted 1/8 with water in a total volume of 160 µL. A pool of cDNA was prepared for each experiment mixing equal amount of each diluted cDNA sample and used for preparation of serial dilutions (1/2, 1/4, 1/8, 1/16, 1/32 and 1/64) for calculation of qPCR reaction efficiency.

4.2.2. Quantitative PCR

Quantitative PCR (qPCR) was performed on a LightCycler 480 instrument (Roche Diagnostics) using a mix with 2 µL of diluted cDNA sample or cDNA pool dilutions, 5 µL of LightCycler 480 DNA SYBR Green I Master reaction mix (Roche Diagnostics), specific primers (600 nM) and water up to 10 µL per reaction. The following cycling parameters used were: 5 min at 95°C, followed by 40 cycles of denaturation for 15 sec at 95°C, annealing for 10 sec at 60°C, and extension for 10 sec at 72ºC. Melting curve analysis of amplified products was performed for confirmation of primers specificity. The sequence of all the primers used in qPCR is indicated in Table 1.

Hprt gene coding for hypoxanthine guanine phosphoribosyltransferase was used as reference gene and relative quantification was performed using the ΔΔCt method. [268]. The relative expression ratios were calculated using the formula $2^{-\Delta\Delta Ct}$, in which $\Delta\Delta Ct_{A-B} = (Ct_{gene} - Ct_{Hprt})_B - (Ct_{gene} - Ct_{Hprt})_A$ and A=control group and B = experimental group. All samples were run in duplicate (technical duplicate) and, for each experiment, all conditions were tested in biological duplicates. A set of 3 independent experiments were used for statistical analysis, using paired Student's *t* test on ΔCt values (α=0,05). Comparison of specific gene expression between BMDM $Nrf2^{+/+}$ and $Nrf2^{-/-}$ was performed using two-way repeated measure ANOVA (α=0,05), which allowed also to analyse the interaction between Nrf2 genotype and each *in vitro* treatment on

gene expression. The significant results are presented as: *p-value (p)<0.05, **p<0.01, ***p<0,001 and ****p<0.0001. GraphPad Prism 6 software was used for statistical analysis.

5. Protein analysis

5.1. Preparation of crude membrane and cytosolic extracts

Suspension cells such as huPBL were collected by centrifugation at 400 *g* for 10 min at 4ºC while adherent cells were collected by scrapping in PBS-EDTA (2 mM) on ice and followed by centrifugation in the same conditions. Exceptionally for human macrophages, to avoid cell adherence to tube walls, cells were incubated with PBS-EDTA (5 mM) for 30 min at 4ºC before scrapping and collection by centrifugation at 400 *g* for 10 min at 4ºC. Cell pellets were homogenized in lysis buffer (10 mM Tris-HCl, pH 7; 1 mM $MgCl_2$) supplemented with protease inhibitor cocktail (PI's; Sigma-Aldrich) and phenylmethanesulfonylfluoride (PMSF; Sigma Aldrich). The lysates were centrifuged at 1,200 *g* for 10 min at 4ºC to eliminate nuclei and unbroken cells. The protein extracts (post-nuclear supernatant, PNS) were then ultracentrifuged at 260,000 *g* at 4ºC for 1 h in TLA100.3, TLA 100.4, or TLS55 rotor (Beckman) to separate the crude membrane fractions from the cytosolic proteins. Supernatants corresponding to cytosolic extracts were then collected and membrane pellets were resuspended in TNE buffer (10 mM Tris-HCl, pH 7.0; 100 mM NaCl; 10 mM EDTA) containing PI's and PMSF. All protein extracts (PNS, membrane or cytosolic fractions) were quantified by BCA assay (Piercenet) or Bradford assay (Bio-RAD) and stored at -80°C until use.

5.2. Preparation of protein extracts from culture medium

Culture medium of huPBL suspension was separated from cells by centrifugation at 400 *g* for 10 min at 4ºC, collected in new tubes and then stored at -80ºC until use. For each experimental condition, 4 ml of culture medium was concentrated using Amicon ultra-4 centrifugal filter tubes (Merck Millipore) according to manufactor's instructions. The concentrated sample was then precipitated by addition of 10 volumes of ice-cold 10% trichloroacetic acid in acetone (w/v), followed agitation and precipitation O/N at -20ºC. The precipitated protein was then collected by centrifugation at 15,000 *g* for 15 min at 4ºC, washed once in 100% acetone, and then air-dried after discarding supernatant. The dried protein pellets were then rehydrated using TNE buffer (see section 6.2) supplemented in PI's and PMSF. Culture medium-derived protein extract was quantified by BCA assay (Piercenet) and stored at -80ºC until use.

5.3. Preparation of lipid raft/detergent resistant membrane fractions

Lipid rafts from BMDM and HepG2 cells were isolated as detergent (Triton X-100) resistant membranes (DRM) as described previously [118]. Briefly, cells were washed with cold PBS, scrapped into PBS-EDTA (2 mM), collected by centrifugation 400 *g* for 10 min at 4ºC and incubated for 1 h at 4°C in 600 µL of lysis buffer (150 mM NaCl, 25 mM MES, 5 mM EDTA, pH 6.5, 1% Triton X-100) supplemented with PI's and PMSF. Samples were then homogenized by 20 passages through a 25-gauge needle (5/8-inch). For HepG2, cell lysates were centrifuged at 1,200 *g* for 10 min at 4ºC and the supernatant was recovered. Crude cell lysate (BMDM) or post-nuclear supernatant (HepG2) were adjusted to a final concentration of 40% (w/v) iodixanol (OptiPrep®, Sigma-Aldrich) and the mixture was then layered under a 20-40% discontinuous iodixanol gradient and centrifuged at 260,000 *g* for 16 h at 4°C using an SW 41 Ti Rotor (Beckman Coulter) and no break. After spinning, fractions of 1 ml were collected from the top to the bottom of the gradient tube. Aliquots of each gradient fraction were immediately prepared in Laemmli buffer (equal volume independently of the protein concentration of each gradient fraction) and stored at -20ºC, while the original fractions were stored at -80ºC. Quantification of protein content for all fractions was determinated using Bradford assay. Western blot analysis of these fractions for the known raft proteins caveolin-1 (Cav-1) or Flotillin-1 (Flot-1) and non-raft proteins (TfR1) was performed to identify the fractions enriched in DRM and non-DRM (NDRM) proteins.

5.4. SDS-PAGE and Western blot

All samples were prepared in Laemmli buffer (50 mM Tris, 55 mM SDS, 1 M glycerol, 570 mM β-mercaptoethanol and bromophenol blue) and denaturated for 30 min at room temperature (R/T) or for 5 min at 95ºC depending on the target protein. For Cp detection, serum purified human Cp (Sigma-Aldrich) and extracts of transfected CHO expressing human GPI-Cp cDNA (CHO-GPICp) were used as positive controls. Samples were resolved in 7-12% acrylamide gels according to standard protocols and transferred onto PVDF membrane (Amersham). To control protein loading and transfer, membranes were stained with 0,1% Red Ponceau S for 5 min an R/T. Membranes were then unstained in 0,1% Tween-PBS and blocked O/N at 4ºC or for 1 h at R/T with 5% skim milk in 0,1% Tween-PBS. Each membrane was probed with adequate dilution of primary antibody in blocking solution for 2 h at R/T or O/N at 4ºC. After washing in 0,1% Tween-PBS, blots were incubated in blocking solution for 1 h at R/T containing the respective diluted secondary antibody conjugated with horse radish peroxidase (HRP). Membranes were then washed in 0,1% Tween-PBS and followed by development with either Immobilon Western (Millipore) or ECL Prime (Amersham) Chemiluminescent

HRP substrate reagents. Primary and secondary antibodies used and the respective dilutions are indicated in Tables 2, 3 and 4.

5.5. Quantitative immunofluorescence assay (In-Cell Western blot)

After treatments, BMDM cultured in 48-well or 96-well cell culture plates were fixed with 100% methanol for 15 min at -20°C, washed with PBS, and then permeabilized with Triton X-100 (0.1% in PBS) for 10 min at R/T. Cells were washed in PBS, blocked with Odyssey blocking buffer (LI-COR Bioscience) for 1h at R/T and then incubated O/N at 4°C with specific primary antibody (table 2 and 3) diluted in Odyssey blocking buffer. After 5 washes with 0.5% Tween-PBS, cells were incubated for 1 h at R/T with LI-COR IRDye 800 labeled secondary antibodies (1/800, LI-COR Bioscience) and with Sapphire700 (1/1000, LI-COR Bioscience) and DRAQ5 (1/2000, LI-COR Bioscience) for cell number normalization. Sapphire700 is a non-specific cell stain that accumulates in both nucleus and cytoplasm of fixed cells whereas DRAQ5 is a cell permeable DNA-interactive agent. Finally, cells were washed 5 times with 0.5% Tween-PBS, twice with PBS and dried before the scan of the plate by Odyssey Infrared Imaging System (LI-COR Bioscience). Scans were analyzed and raw data extracted using Odyssey 2.1 software (LI-COR Bioscience). Primary and secondary antibodies used and the respective dilutions are indicated in Tables 2, 3 and 4.

5.6. Immunofluorescence

In general, cells were fixed with 100% methanol for 20 min at -20ºC or with 2-4% formaldehyde in PBS for 20 min at R/T. Fixed cells were stored in PBS at 4ºC until immunostaining. When required, permeabilization of cells was performed by incubation for 10 min at R/T with 0.1% Triton X-100 in PBS. Apart from Cp/Fpn1 co-labeling in BMDM, all cells were blocked for 30 min at R/T with 1% bovine serum albumin (BSA) in PBS (exclusively for Cp single labeling) or with 1% BSA and 10% goat serum in PBS (for all other proteins labeling). Primary antibodies incubations were performed O/N at 4ºC or for 45 min at R/T while incubation with fluorochrome-conjugated antibodies (primary or secondary antibody) was performed for 45 min at R/T in the dark. All washes during the labeling protocol were carried out with 0,5% BSA in PBS. After the final washes, labeled cells were mounted in Vectashield (VectorLab) or Prolong Gold (DAKO) mounting medium with DAPI. Image acquisition were performed either with a confocal microscope (Leica TCS, SPE model) using a 63x oil objective or with a fluorescent microscope (Nikon TE2000E equipped with a Nikon DXM1200F digital camera or Leica DM4000 B) using a 40x or 60x oil objective. Mean fluorescence intensity (MFI) of Cp in huPBL and HepG2 was quantified using the software package Image J (Rasband, W.S., ImageJ, U.S. National Institutes

of Health, Bethesda, Maryland, USA, http://rsb.info.nih.gov/ij/, 1997-2010) and Image-Pro Plus 4.0 (Media Cybernetics). Statistical analysis was performed using paired *t* student test for comparison of Cp expression levels at cell surface on untreated and PIPLC-treated cells. Primary and secondary antibodies used and the respective dilutions are indicated in Tables 2, 3 and 4.

5.6.1. Human peripheral blood cells

All huPBMC, huPBL and huPBMn were fixed in formaldehyde and set to adhere onto sylane coated-slides (Sigma-Aldrich) using Shandon cytospin III (Thermo) before blocking and labeling steps. Cells were blocked for with 1% BSA in PBS, incubated in the dark with sheep anti-human Cp FITC-conjugated (BIOTREND GmbH), followed by washes and mounting. Labeling of the monocyte marker CD14 was performed by blocking in1% BSA and 10% goat serum in PBS solution, followed by incubation with mouse anti-CD14 (Abcam). Cells were then washed, incubated with anti-mouse IgG Cy3-conjugated antibody (Jackson Immunoresearch Laboratories) in the dark, washed and mounted.

5.6.2. HepG2 cells

Cells were grown onto glass coverslips in 6-well plates at 37ºC with 5% CO_2 atmosphere. To observe membrane Cp, cells were blocked with 1% BSA in PBS, probed with sheep anti-human Cp FITC-conjugated (BIOTREND GmbH) for 45 min at R/T in the dark and then fixed with 100% methanol, washed and mounted. For cytosolic Cp labeling, cells were firstly fixed in 100% methanol as described before, permeabilized, blocked and finally probed with sheep anti-human Cp FITC-conjugated (BIOTREND GmbH) for 45 min at R/T in the dark, washed and mounted.

5.6.3. Murine Bone Marrow Derived Macrophages

For single labeling, BMDM were fixed with 100% methanol (for Fpn1/HO-1 staining) or with formaldehyde (for Cp, CD11b and APP staining). Cells were then permeabilized if required, blocked and incubated with primary antibody for 45 min at R/T or O/N at 4ºC. After washes in 0,5% BSA in PBS, cells were incubated with secondary antibody for 45 min at R/T and in the dark, followed by washes and mounting. The following primary and secondary antibodies used for single labeling were: commercial rabbit anti-mouse Fpn1 (Alpha Diagnostics), non-commercial rabbit anti-mouse Fpn1 (antibody developed by Doctor François Canonne-Hergaux [269]), mouse anti-mouse Cp (BD Biosciences), rat anti-CD11b (AbD Serotec), rabbit anti-human HO-1 (Stressgene), mouse APP (Millipore), Alexa^{488} goat anti-rabbit IgG, Alexa^{568} goat anti-mouse IgG, Alexa^{568} goat anti-rat IgG or the Alexa^{488} goat anti-mouse IgG antibodies (Invitrogen).

For Fpn1 and Cp co-labeling, living cells were blocked with 1% BSA in PBS for 5 min at 4ºC and then incubated with mouse anti-mouse Cp (BD Biosciences) for 30 min at 4ºC prior to 100% methanol fixation and permeabilization. After PBS washes, cells were incubated in blocking solution (BSA 1% and 10% heat-inactivated goat serum in PBS) for 30 min at R/T. Incubation with rabbit anti-mouse Fpn1 (Alpha Diagnostics) was then performed for 45 min at R/T, followed by washes with 0,5% BSA in PBS and incubation with mix of secondary antibodies (goat anti-mouse IgG Alexa^{568} and goat anti-rabbit IgG Alexa^{488}) diluted in blocking solution for 45 min at R/T and in the dark. Finally, cells were washed with 0,5% BSA in PBS and mounted.

5.7. Immunophenotyping and flow cytometry analysis

After incubation with and without PIPLC (0,5 U/mL, 1 h, 37ºC), huPBMC (treated and untreated) were collected, washed and then resuspended in staining buffer (0,2% fetal calf serum, 0,09% NaN_3 in PBS, pH 7,4). Cells were then plated in 96-well round-bottomed microtiter plates (Nunclon) at 5×10^5 cells/well and incubated for 15 min at 4ºC with AB-human serum solution (1/10 in staining buffer), blocking the Fc-receptor binding sites for reduction of non-specific reactions. Afterwards, cells were stained for Cp using the rabbit anti-human Cp (KOMA Biotech) diluted in staining buffer for 45 min at 4ºC, washed once with staining buffer and centrifuged at 250 *g* for 5 min at 4ºC. Subsequently the cells were incubated for 45 min at 4ºC with the secondary antibody: goat F(ab′)2 anti-rabbit FITC-conjugated (Rockland) diluted in staining buffer. For huPBMn gating, in addition to the secondary antibody referred above, the following antibodies were added: monoclonal anti-CD45 PerCP-conjugated (BD Pharmigen) and anti-CD14 APC-conjugated (Miltenyi Biotec). Unstained cells of each condition were used as negative control in order to determine autofluorescence of cells. After staining, cells were washed, centrifuged at 250 *g* for 5 min at 4ºC and resuspended in the staining buffer, transferred to cytometer tubes and immediately analyzed in a FACSCalibur Flow Cytometer (BD Biosciences). CellQuest (BD Biosciences) was used for data acquisition, and measurement of Cp expression was performed using Weasel v.2.7.4 software. Statistical analysis was performed using paired *t* student test for comparison of Cp expression level at cell surface of untreated and PIPLC-treated huPBMn. Primary and secondary antibodies used and the respective dilutions are indicated in Tables 2, 3 and 4.

6. Oil Red O staining

Cells were fixed in paraformaldehyde 4% for 20 min at R/T, washed and stored in PBS until staining. Cells were quickly rinsed in 60% isopropanol, stained in Oil Red O (ORO) solution (0,25% ORO in 60% isopropanol, filtered) for 10 min at R/T, rinsed quickly in 60% isopropanol and then in water. After

counterstaining with hematoxylin (Mayer's solution, Sigma-Aldrich) for 4 min at R/T, cells were rinsed several times with water, incubated for 1 min at R/T in saturated sodium bicarbonate solution, and again rinsed several times in water. Coverslips were air-dried and mounted in glycerol mounting medium (Sigma-Aldrich). Slides were observed at Leica DM4000 B microscope with 20x and 40x objective.

7. Production of polyclonal antibodies against human ferroportin-1

For the production of the rabbit polyclonal anti-human Fpn1 antibody, three different epitopes were selected: Fpn1' (intracellular loop), Fpn2' (extracellular epitope) and Fpn3' (C-terminus). The nucleotidic sequence of the different epitopes was cloned in-frame with glutathione-*S*-transferase (GST) in pGEX vectors. The respective fusion proteins GST-Fpn1', 2' and 3' were expressed in large scale and affinity purified as described (see section 12.1). New Zealand White rabbits were injected with purified GST-Fpn1'/2'/3' fusion proteins (800 µg/injection) in different time points (day 0, 14, 28, 42 and 56). Blood collection was performed before and during the immunization process (days 28, 49 and 63) before sacrifice and final blood collection. Two rabbits were immunized for each epitope, but one of the GST-Fpn3' immunized hosts died during manipulation. For affinity purification of the anti-serum, the same nucleotidic sequence of the Fpn1 epitopes (Fpn1', 2' or 3') was fused to dihydrofolate reductase (DHFR) with a histidine tag. The respective fusion proteins ((6xHis)-DHFR-Fpn1', 2' or 3') were used for the affinity purification of the different anti-sera using a preparative immunoblot protocol (see section 12.2).

7.1. Expression and purification of ferroportin-1 fusion proteins

The nucleotidic sequence of the three different epitopes (Fpn1', 2' and 3') of human Fpn1 was cloned in pGEX and pQ40 vectors (IMAGIF, Gif-sur-Yvette, France), creating a total of 6 different plasmids (pGEX-Fpn1'/2'/3' and pQ40-Fpn1'/2'/3'). Bacteria were transformed with the different plasmids and recombinant cells were seeded in 50 ml of Terrific Broth (TB) medium supplemented with ampicillin and incubated O/N at 37ºC with agitation. The culture was then diluted to OD_{600} = 0,6 with TB medium supplemented with ampicillin, and synthesis of fusion protein was induced by IPTG (0,5 mM) for 4 h at 37ºC with agitation. Cells were then centrifuged at 5500 *g* for 10 min at 4ºC (SLA-3000 rotor, Sorvall) and the cell pellet medium was stored at -20ºC until purification procedure.

For purification of GST-Fpn1'/2'/3' fusion proteins, glutathione sepharose 4B beads (Amersham, GE Healthcare) were used according with the

manufactory's instructions. Briefly, each cell pellet was resuspended in ice-cold PBS solution supplemented with PI's and PMSF (pH 7,3), followed by sonication for complete cell lysis. Triton-X100 was then added to the lysate at final concentration of 1%, followed by incubation for 30 min at 4ºC with gentle agitation. The lysate was centrifuged, followed by supernatant recovery (cleared lysate). Glutathione sepharose 4B beads (pre-washed according to instructions) were then added to each cleared lysate and incubated for binding of beads to GST-Fpn1'/2'/3' fusion proteins. Purification of GST-Fpn1'/2'/3' fusion proteins was performed according to the gravity flow column purification method, using a solution of 50 mM Tris-HCl, 10 mM reduced glutathione (pH 8.0) as elution buffer. A total of eight elution fractions were collected per lysate and stored at -80ºC.

For purification of (6xHis)-DHFR-Fpn1'/2'/3' fusion proteins, Ni-NTA agarose beads (QIAGEN) were used according with the manufactory's instructions. Briefly, each cell pellet was lysed in denaturating conditions using guanidine hydrochloride 6 M buffer. The lysate was then centrifuged, followed by supernatant recovery (cleared lysate). Imidazole solution was added to the cleared lysate to a final concentration of 20 mM, followed by incubation with Ni-NTA agarose beads (pre-washed according to instructions). Purification of (His)-DHFR-Fpn1'/2'/3' fusion proteins was performed according to the gravity flow column purification method, using a solution of 250 mM Imidazole as elution buffer (native conditions). A total of six elution fractions were collected per lysate and stored at -80ºC. All elution fractions of GST-Fpn1'/2'/3' and (6xHis)-DHFR-Fpn1'/2'/3' fusion proteins were dosed using Bradford Reagent and analyzed by SDS-PAGE.

7.2. Antibody purification from crude serum

One aliquot of 250 µg of purified fusion protein was prepared in Laemmli buffer for each (6xHis)-DHFR-Fpn1 (1', 2' and 3'), followed by denaturation for 5 min at 99ºC. Each aliquot was loaded on a 12% acrylamide gel with a single well and separated by regular SDS-PAGE electrophoresis. Electrotransfer to a PVDF membrane was performed at 30 V for 18 h at 4ºC. Each membrane was stained in Red Ponceau solution and the band identified as the 6xHis-DHFR-Fpn1'/2'/3' was then excised and cut in pieces into a tube. The membrane pieces were unstained by washes in 0,1% Tween-PBS (5 min, R/T) and blocked in 0,1% Tween-PBS with 7% skim milk for 2 h at R/T with agitation. After blocking, the membrane pieces were washed twice in 0,1% Tween-PBS and then incubated with 3 ml of anti-serum diluted in PBS (1:1) O/N at 4ºC with agitation. After incubation, the supernatant was removed and the membrane pieces underwent 4 washes in PBS, 1 wash in 0,1% Tween-PBS and 3 washes in PBS (5 min, R/T). The purified antibody bound to the respective fusion protein was eluted from the PVDF pieces by addition of 0,5-0,75 ml of 0,2 M

glycine elution buffer (pH 2,2) and incubation for 3 min at R/T with agitation. The supernatant containing the eluted purified antibody was then recovered to a new tube, immediately followed by pH neutralization with 1 M Tris solution (pH 8,0) and addition of glycerol and BSA to a final concentration of 50% (v/v) and 0,1% (w/v), respectively. The affinity-purified antibodies (anti-huFpn1'/2'/3') were stored at -20ºC.

Table 1 - Sequence of primers used in quantitative PCR.

Specie	Protein	Gene	Sequence	Primer sense
Mouse	HPRT	*Hprt*	CTGGTTAAGCAGTACAGCCCCAA	forward
			CAGGAGGTCCTTTTCACCAGC	reverse
	Fpn1	*Fpn1, also known as Scl40a1*	CATTGCTGCTAGAATCGGTCTT	forward
			GCAATCGTGTCACCGTCAAAT	reverse
	H-Ft	*Fth1*	GAGGTGGCCGAATCTTCCTG	forward
			GCTCTCCCAGTCATCACGGTC	reverse
	Cp	*Cp*	ACACTGTACACTTCCACGGCC	forward
			AGAACTGTATACTCCCCTGTGCTTG	reverse
	sCp	*Cp*	ACAGATGGACAGAGCAACAGACTG	forward
			CCCAGCGAACAAATGCATG	reverse
	GPI-Cp	*Cp*	AGGACCACAGACGCCAAATC	forward
			AACTATGGCAGAGAGCGTTGC	reverse
	HO-1	*Hmox1*	GGTGACAGAAGAGGCTAAGAC	forward
			GCTCCTCAAACAGCTCAATG	reverse
	APP	*App*	TGTGCCAGCCAATACCGAA	forward
			CAGAACCTGGTCGAGTGGTCA	reverse
	Hepc	*Hamp1*	AAGCAGGGCAGACATTGCGAT	forward
			CAGGATGTGGCTCTAGGCTATGT	reverse
	VEGF	*Vegf*	CCTGGTGGACATCTTCCAGGAGTACC	forward
			GAAGCTCATCTCTCCTATGTGCTGGC	reverse
Human	HPRT	*HPRT*	AAGCTTGCGACCTTGACCAT	forward
			TGCTTTCCTTGGTCAGGCAG	reverse
	Fpn1	*FPN1, also known as SLC40A1*	GCTGCTAGAATCGGTCTTTGGT	forward
			TCTTGCAGCAACTGTGTCACAG	reverse
	H-Ft	*FTH1*	AAATGACCCCCATTTGTGTGAC	forward
			AGAGATATTCCGCCAAGCCAG	reverse
	Cp	*CP*	ATGGGTAATGAAGTTGATGTGCAC	forward
			CAGGGTAGCAGGAAAGAGGTTG	reverse
	HO-1	*HMOX1*	GCCAGCAACAAAGTGCAAGATT	forward
			TGAGTGTAAGGACCCATCGGAG	reverse
	APP	*APP*	ACACCGTCGCCAAAGAGACAT	forward
			CACACAAACTCTACCCCTCGGA	reverse
	Hepc	*HAMP*	CTCTGTTTTCCCACAACAGAC	forward
			TAGGGGAAGTGGGTGTCTC	reverse

Table 2 - List of unconjugated primary antibodies and respective use dilutions. WB: Western blot; IF: imunofluorescense; ICW: In-Cell Western blot; FC: flow cytometry.

Antibody	Source	IF	WB	ICW	FC
Polyclonal Goat anti-human Cp	Koma BioTECH	-	1:100 to 1/1000	-	1/50
Monoclonal mouse anti-mouse Cp	BD Bioscience	1/25 (double labeling w/ Fpn1); 1/50 (single labeling)	1/100 to 1/250	1/50	-
Monoclonal mouse anti-human APP (22C11)	Chemicon, Millipore	-	1/500 to 1/1000	1/50 to 1/100	-
Polyclonal rabbit anti-human HO-1	Stressgen	1/500 to 1/1000	-	1/500 to 1/1000	-
Monoclonal rat anti-mouse CD11b IgG	Developmental Studies Hybridoma Bank (DHSB), University of Iowa	1/50	-	-	-
Polyclonal mouse anti-TfR1	Zymed Laboratories	-	1/1000 to 1/10000	-	-
Monoclonal mouse anti-mouse Flot-1	BD Bioscience	-	1/1000 to 1/5000	-	-
Polyclonal rabbit anti-human Cav-1	Tebu-Bio	-	1/200	-	-
Polyclonal rabbit anti-human Cav-1	Santa Cruz Biotecnology	-	1/1000	-	-

Table 3 - List of unconjugated primary antibodies against ferroportin-1 and respective use dilutions**.** WB: Western blot; IF: immunofluorescense; ICW: In-Cell Western blot.

Antibody	Source		IF	WB	ICW
Polyclonal rabbit anti-mouse Fpn1	Alpha Diagnostics	Ab#3	-	1/1000 to 1/2000	-
Polyclonal rabbit anti-mouse Fpn1	Non-commercial, produced by F Canonne-Hergaux *et al* [269]	Ab#6	1/100	1/200 to 1/1000	1/100 to 1/200
Polyclonal rabbit anti-human Fpn1	Non-commercial, gift from another laboratory	Ab#1	-	1/400	-
Polyclonal rabbit anti-human Fpn1	Non-commercial, gift from another laboratory	Ab#4	-	1/1000	-
Polyclonal mouse anti-human Fpn1	Novus Biologicals (H00030061-B01)	Ab#2	-	1/200	-
Polyclonal rabbit anti-human Fpn1	Novus Biologicals (NBP1-21502SS)	Ab#5	-	1/1500	-
Polyclonal rabbit anti-human Fpn1	Lifespan Biosciences	Ab#7	-	1/100	-
Polyclonal rabbit anti-human Fpn1	Non-commercial, developed by our laboratory		-	1/500	-
Polyclonal rabbit anti-human Fpn2	Non-commercial, developed by our laboratory		-	1/500	-
Polyclonal rabbit anti-human Fpn3	Non-commercial, developed by our laboratory		-	1/500 to 1/100	-

Table 4 - List of conjugated primary and secondary antibodies and respective use dilutions**.** WB: Western blot; IF: immunofluorescense; ICW: In-Cell Western blot; FC: flow cytometry.

Conjugated antibody	Source	IF	WB	ICW	FC
Polyclonal sheep anti-human Cp FITC	BioTREND GmbH	1/50 (single labeling); 1/800 (double labeling w/ CD14)	-	-	-
Polyclonal anti-mouse IgG Cy3-conjugated	Jackson Immunoresearch Laboratories	1/200	-	-	-
Alexa^{488} goat anti-rabbit IgG	Invitrogen	1/200	-	-	-
Alexa^{568} goat anti-mouse IgG	Invitrogen	1/200	-	-	-
Alexa^{568} goat anti-rat IgG	Invitrogen	1/200	-	-	-
Alexa^{488} goat anti-mouse IgG	Invitrogen	1/200	-	-	-
Polyclonal Goat Anti-Mouse IgG, HRP-conjugated	Dako	-	1/20000	-	-
Polyclonal Goat Anti-Rabbit IgG, HRP-conjugated	Dako	-	1/20000	-	-
Polyclonal Rabbit Anti-Goat IgG, HRP-conjugated	Dako	-	1/20000	-	-
IRDye 800CW Goat anti-Rabbit Secondary Antibody	Li-COR Biosciences	-	-	1/800	-
Polyclonal rabbit anti-IgG Goat, F(ab)'$_2$, FITC-conjugated	Rockland	-	-	-	1/50
Monoclonal mouse anti-human CD45 PerCP-conjugated	BD Biosciences	-	-	-	1/10
Monoclonal mouse anti- human CD14 APC-conjugated	Miltenyi Biotec	-	-	-	1/10

III. Results

Chapter 1

Study of ceruloplasmin isoforms and ferroportin-1 in human lymphocytes and monocytes

1. Introduction

Cp is a multicopper oxidase able to oxidize Fe^{2+} to Fe^{3+}, a reaction that has been shown to participate in cellular iron export by Fpn1 and subsequent iron distribution associated with Tf [51,133,270]. This ferroxidase activity has also been associated with an anti-oxidant effect, by preventing Fe^{2+} participation in Fenton reactions and subsequent formation of ROS [132,133]. However, Cp capacity to oxidize other substracts such as lipids has been associated with a pro-oxidant activity and has been associated to the physiopathology of some diseases, including ATH [271,272]. Despite previous studies of Cp expression in immune cells, the characterization of the specific Cp isoforms expressed by human peripheral blood mononuclear cells (huPBMC) is poorly documented and only sCp isoform was previously reported in lymphocytes, monocytes and macrophages [273-275]. Our previous results showed that human peripheral blood lymphocytes (huPBL) constitutively express the transcripts for the two distinct Cp isoforms, confirming Cp detection at huPBL cell surface by flow cytometry and immunofluorescence [276].

2. Aims

The goal of this study was to characterize the expression of both Cp isoforms in distinct human immune cells (lymphocytes and monocytes). For this, the human hepatocarcinoma cell line HepG2 was used as a positive control for Cp expression and as a hepatocyte model.

3. Results

3.1. Membrane and soluble ceruloplasmin isoforms are expressed in human peripheral blood lymphocytes and hepatocytes

Cp expression was investigated by immunofluorescence on permeabilized and non-permeabilized HepG2 cells and huPBL, showing that Cp is detected at cell surface (non-permeabilized cells) as well as intracellularly (permeabilized cells), which suggests the existence of a membrane Cp isoform in addition to the soluble isoform already reported in these cells (Figure III.1A). Noteworthy, Cp detection in permeabilized cells was stronger than in non-permeabilized cells. In contrast with huPBL, Cp detection at the surface of HepG2 cells is characterized by a distinct dotted pattern suggestive of Cp accumulation in specific membrane domains at cell surface (Figure III.1A). Immunoblotting of subcellular fractions isolated from both huPBL and HepG2 showed that Cp is detected in both cytosolic and crude membrane fractions (Figure III.1B), confirming the existence of a soluble isoform as well as a membrane-associated

isoform of Cp in these cells. The specificity of the anti-Cp antibody was controlled using a human serum-purified Cp and protein extracts from transfected CHO expressing the membrane-associated human GPI-Cp (Figure III.1B). The pattern of detection of the human serum-purified Cp suggests that the lowest molecular weight specie of Cp in huPBL likely corresponds to a proteolytical cleavage fragment frequently observed in Cp detection [271,277].

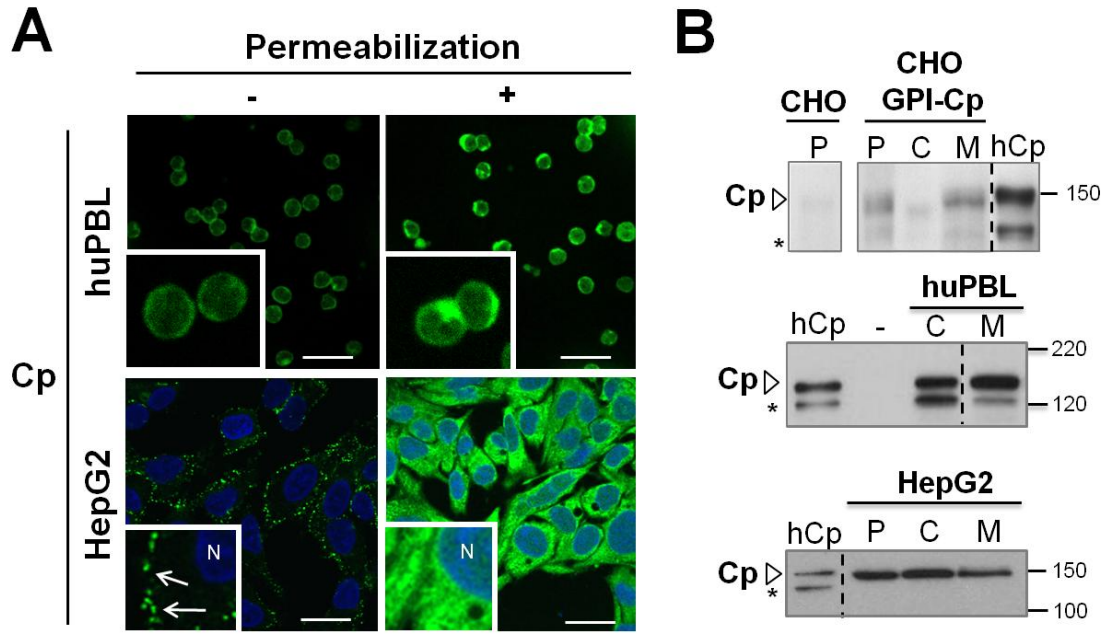

Figure III.1 - Ceruloplasmin expression in human peripheral blood lymphocytes and HepG2 cell line. (A) Immunostaining of Cp in permeabilized (right; +) and non-permeabilized (left; -) huPBL and HepG2 cells. Insets at the left bottom corners correspond to high magnification of individual cells. Cp staining is shown in green, while nuclei (N) are stained in blue (DAPI). The white bars represent 25 µm. **(B)** Immunoblotting detection of Cp in post-nuclear supernatants (P), cytosolic fractions (C) and crude membrane fractions (M) isolated from huPBL and HepG2. Purified human Cp (hCp) was used as a positive control as well as transfected CHO expressing GPI-Cp. The position and size in kilodaltons (kDa) of the molecular weight markers are indicated on the right. Vertical dashed lines indicate repositioned gel lanes. * Cp proteolitic cleavage product.

To test the hypothesis that Cp detected in membrane extracts from huPBL and HepG2 corresponds to the GPI-Cp isoform, cells were treated with the enzyme PIPLC – which specifically cleaves GPI-anchored proteins from cell surface to the extracellular medium – prior to Cp immunostaining. The results obtained (Figure III.2A and III.2B) showed a significant decrease of 34% and 50% on Cp staining in PIPLC-treated huPBL and HepG2 cells compared with untreated cells ($p<0.001$, T-student test, Figure III.2B), which demonstrate that the membrane-associated Cp detected at cell surface of these cells corresponds, at least in part, to the GPI-Cp isoform.

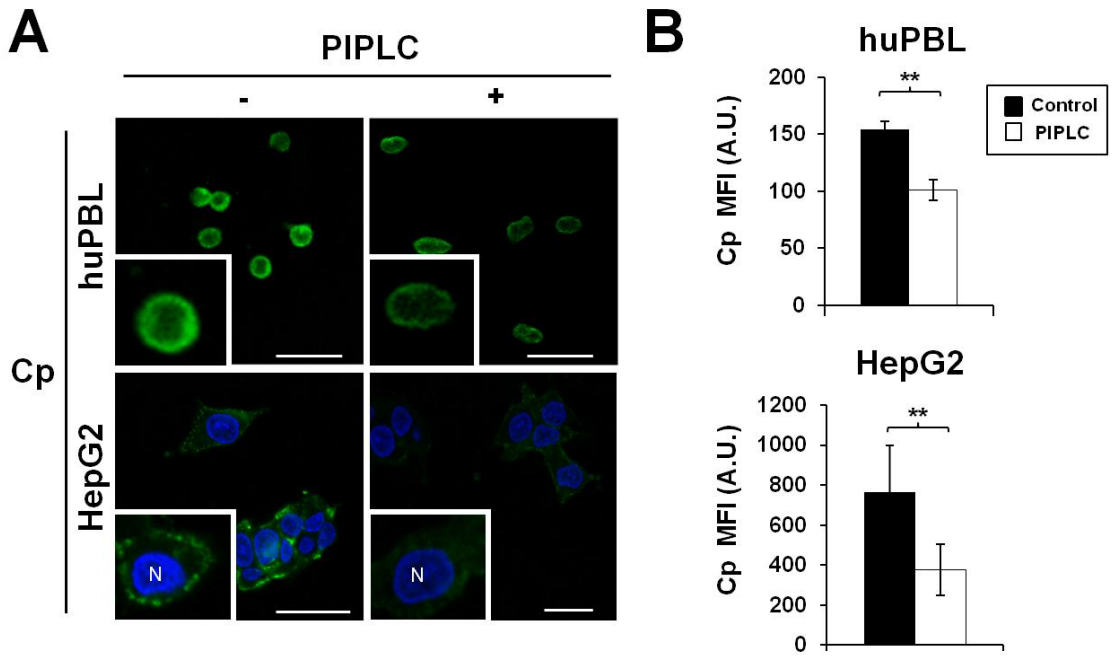

Figure III.2 - Effect of PIPLC on ceruloplasmin expression in human peripheral blood lymphocytes and HepG2 cell line. (A) Confocal analysis of PIPLC enzyme effect on Cp membrane expression in non-permeabilized huPBL and HepG2 cells. Insets at the left bottom corners correspond to high magnification of individual cells. Cp staining is shown in green, while nuclei (N) are stained in blue (DAPI). The white bars represent 25 µm. **(B)** Graphics of Cp mean fluorescence intensity (MFI) in untreated (control) and PIPLC-treated huPBL and HepG2 cells. MFI analysis is indicated in arbitrary units (A.U.). ** Statistically significant differences on Cp surface expression between untreated and PIPLC-treated cells (p<0,01), Student's *t* test.

To evaluate the efficiency of PIPLC activity, the expression of CD14 (a known GPI-protein) in human peripheral blood monocytes (huPBMn) treated or untreated with PIPLC was analyzed by flow cytometry. The results obtained revealed a significant (p<0,01), but also partial decrease of 64% of CD14 staining in PIPLC-treated cells compared with control. Analysis of CD45 expression, a non-GPI-protein, remained unchanged by PIPLC treatment, confirming the enzyme specificity (Figure III.3).

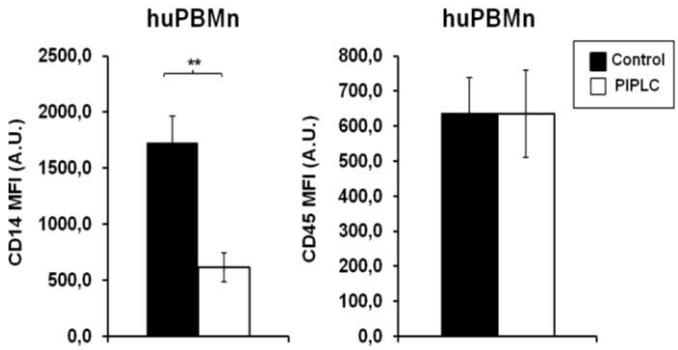

Figure III.3 - Effect of PIPLC on CD14 and CD45 expression in human peripheral blood monocytes. Graphics of CD14 (GPI-protein) and CD45 (non-GPI-protein) mean fluorescence intensity (MFI) in untreated (control) and PIPLC-treated huPBMn analyzed by flow cytometry. MFI is indicated in arbitrary units (A.U.). **Statistically significant differences on CD14 or CD45 surface expression between untreated and PIPLC-treated cells (p<0,01), using paired Student's t test.

As a ferroxidase reported to promote iron export through interaction with Fpn1, the effect of iron on the expression of both Cp isoforms was investigated in huPBL. However, no effect was observed in huPBL treated with iron complex (FeNTA) or Tf-bound iron (apo/holo-Tf) in the conditions tested (Figure III.4A,D). In addition, no effect was observed upon Hepc stimulation (Figure III.4B,D), known to downregulate Fpn1 levels at cell surface. Considering that Cp is an acute phase protein, the modulation of Cp isoforms expression in huPBL by cytokines was also tested. However, no significant modulation of Cp was observed as result of the pro-inflammatory cytokines tested in total huPBL (Figure III.4C,D), with exception of IFNγ which upregulated sCp detected in concentrated extracellular culture medium (Figure III.4D), but only slightly in the cytosolic fraction (Figure III.4C).

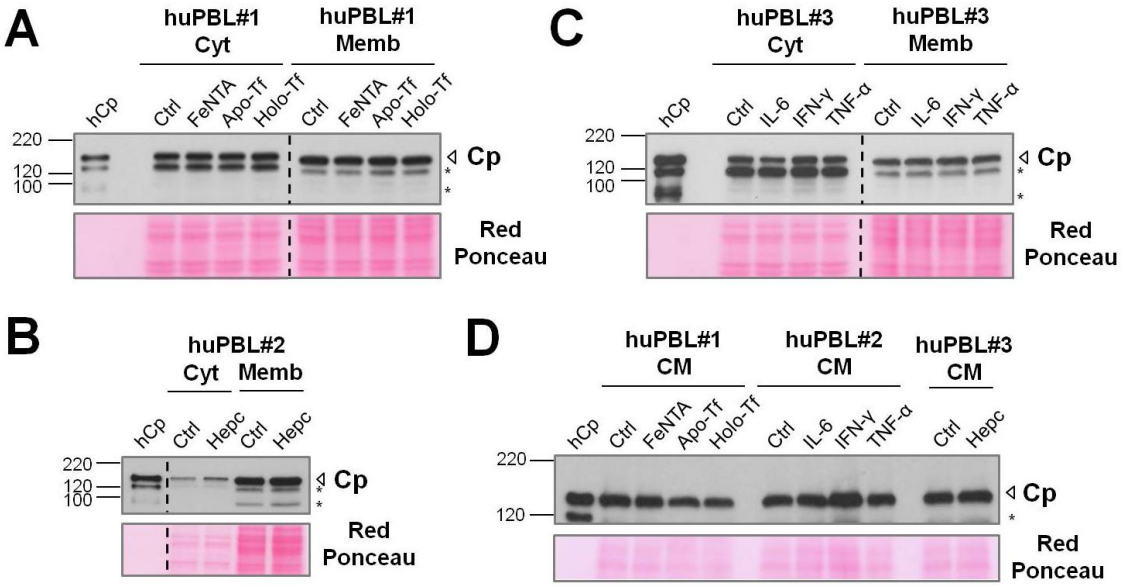

Figure III.4 - Effect of different stimuli on ceruloplasmin expression in human peripheral blood lymphocytes. (A-C) Immunoblotting detection of Cp in cytosolic (Cyt) and crude membrane (Memb) fractions isolated from huPBL untreated (ctrl) and treated with different stimuli: **(A)** free iron (FeNTA, 100 µM, 18 h) and apo-Tf/holo-Tf (3 mg/ml, 18 h); **(B)** Hepc (700 nM, 3 h); **(C)** cytokines IL-6, IFNγ, and TNFα (20 ng/ml, 18 h). **(D)** Immunoblotting of concentrated extracellular culture medium (CM) of the huPBL cultures analyzed in (A-C). Purified human Cp (hCp) was used as a positive control. Red Ponceau staining was used for control of equal protein loading of samples. The position and size in kilodaltons (kDa) of the molecular weight markers are indicated on the left. Vertical dashed lines indicate repositioned gel lanes. *Cp proteolitic cleavage product**.**

3.2. Human Peripheral Blood Monocytes express both soluble and membrane-associated ceruloplasmin isoforms

Cp expression was studied by immunofluorescence in non-permeabilized huPBMC, including both lymphocytes and monocytes. Two distinct patterns of Cp staining were observed, with cells expressing low Cp levels (arrowhead, Figure III.5A) or high Cp levels (arrow, Figure III.5A). Considering the cell size, the nucleus shape and the frequency of these cells in huPBMC, the cells expressing high levels of Cp at cell surface were likely to be huPBMn whereas the cells expressing low levels of Cp could correspond to huPBL.

To test this hypothesis, double labeling of Cp and CD14 (surface monocyte marker) was performed in non-permeabilized huPBMC. The cells expressing high level of Cp (acquired at low laser intensity; Figure III.5B) were all positive for CD14, which confirmed that these cells correspond to huPBMn (Figure III.5B). In addition, co-localization of Cp/CD14 (arrows in Figure III.5B) also confirmed that Cp is expressed at the cell surface of huPBMn. Such observation was reinforced by immunofluorescence studies realized with non-permeabilized huPBMn isolated by cell adherence (Figure III.5C), which showed Cp accumulation at specific areas of the cell membrane (Figure III.5C, arrows), suggesting that this form of Cp could be concentrated in particular cell membrane domains.

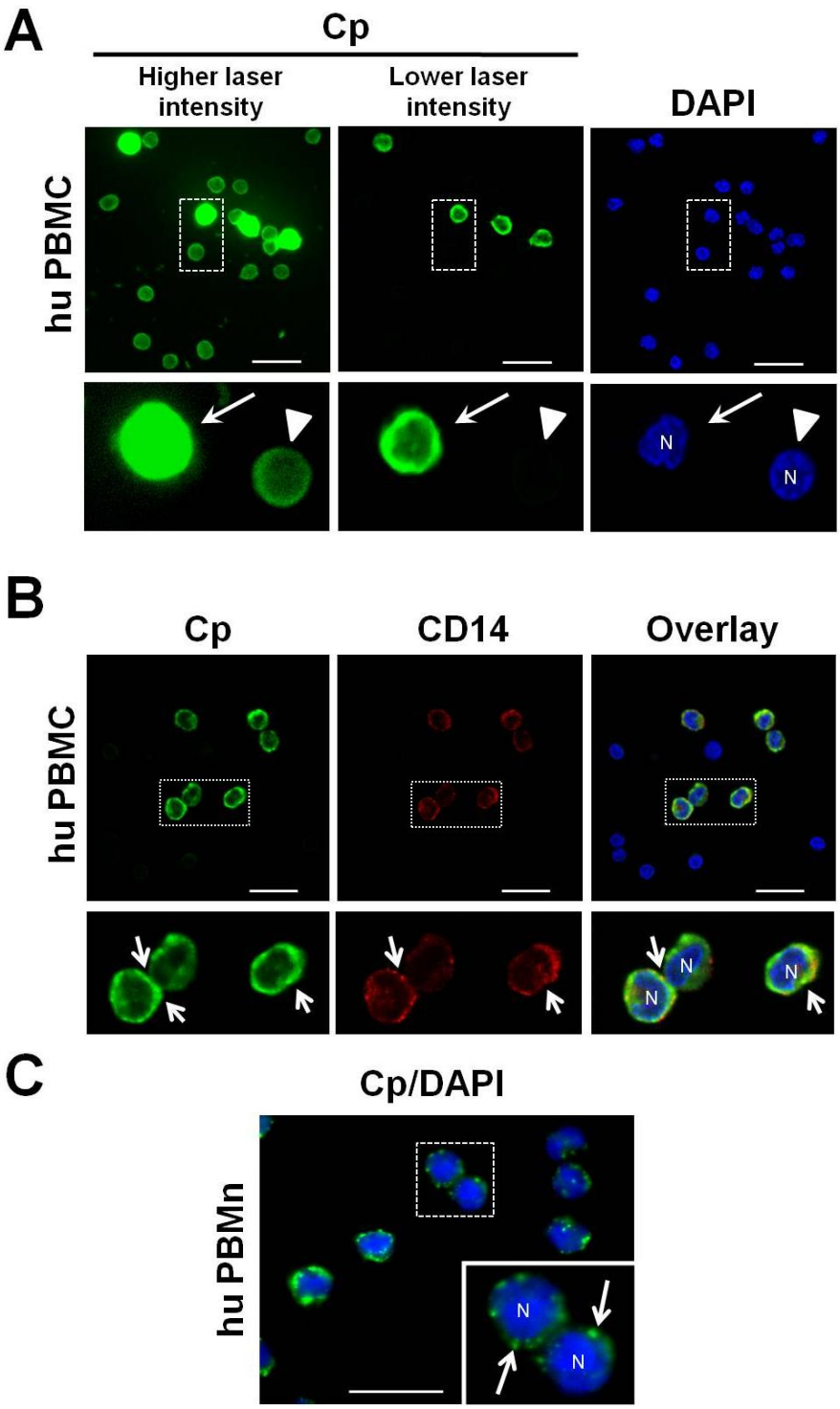

Figure III.5 - Ceruloplasmin expression in human peripheral blood mononuclear cells. (A) Confocal analysis of Cp staining in non-permeabilized huPBMC. Depending of the intensity of the laser lamp of the confocal microscope, two different staining patterns were observed, one intense (arrows) and one faint (arrowheads). **(B)** Confocal analysis of Cp (low laser intensity) and CD14 (monocyte marker) staining in huPBMC. Morphological features and co-localization of Cp and CD14 identified the Cp positive (bright cells) as human monocytes. **(C)** Cp staining in human monocytes (huPBMn) by immunofluorescence indicates accumulation of Cp in specific membrane domains (arrows) at the cell surface. Insets in **(A-C)** correspond to high magnification of individual cells. Cp staining is shown in green, CD14 in red and nuclei (N) are in blue (DAPI). The white bars represent 25 µm.

In addition, immunoblotting analysis of Cp expression in cytosolic and crude membrane extracts of huPBMn confirmed that, besides sCp, these cells also express a membrane form of Cp, which may correspond to GPI-Cp (Figure III.6A). Treatment of huPBMn cells with the enzyme PIPLC lead to a decrease of approximately 30% of Cp staining at their cell surface (Figure III.6B), which suggests that at least part of the membrane-associated Cp in huPBMn corresponds to GPI-Cp isoform.

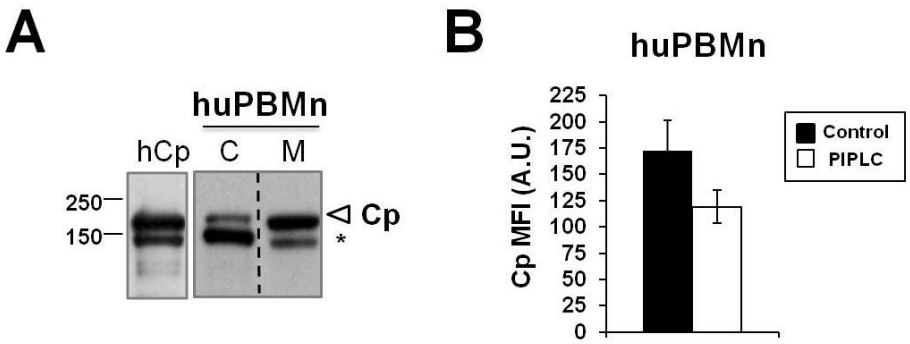

Figure III.6 - Ceruloplasmin expression in human peripheral blood monocytes. (A) Immunoblotting detection of Cp in cytosolic (C) and crude membrane (M) protein extracts of huPBMn, using purified human sCp as a positive control. The position and size in kilodaltons (kDa) of the molecular weight markers are indicated on the left. Vertical dashed lines indicate repositioned gel lanes. *Cp proteolitic cleavage product. **(B)** Graphic of Cp mean fluorescence intensity (MFI) in untreated and PIPLC-treated huPBMn analyzed by flow cytometry, with a decrease of 30% not statistically significant by paired Student's *t* test (p=0,1191). MFI analysis is indicated in arbitrary units (A.U.).

3.3. Study of ferroportin-1 expression in human cells

The endogenous expression of fpn1 in huPBL was investigated considering it is a key protein in iron metabolism and that it was previously reported to interact with Cp in other cells. As a positive control for Fpn1 detection, different cell lines were tested in order to determine the specificity of the different antibodies tested (Table 3).

3.3.1. THP-1 cell line as a macrophage model

The human monocytic cell line THP-1 was cultured in the presence of the activator phorbol myristate acetate (PMA) for differentiation into macrophages (20nM PMA, 48h), followed by Hepc addition to culture medium (1µM, 4h) as described elsewhere [85,278]. According to these authors, Hepc induced Fpn1 downregulation in THP-1 macrophages in such conditions. Four different antibodies raised against human Fpn1 (Ab#1, Ab#2, Ab#4 and Ab#5) as well as one antibody raised against murine Fpn1 (Ab#3, same antibody used by the authors in [85,278]) were tested by Western blot using membrane extracts of THP-1 macrophages treated or not with Hepc. Multiples bands were detected in each antibody with no common band within all the antibodies tested. In addition, none of the bands detected with a molecular weight compatible with Fpn1 was

decreased in Hepc-treated THP-1 macrophages (Figure III.7). Therefore, none of the antibodies tested was validated for human Fpn1 detection in this THP-1 macrophage model.

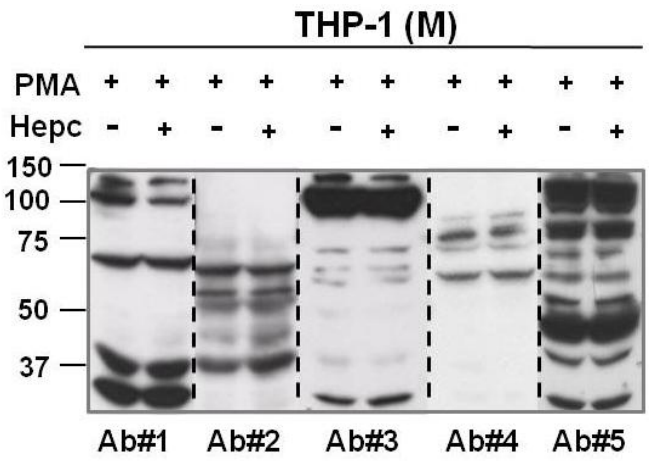

Figure III.7 - Immunoblotting analysis of ferroportin-1 detection in THP-1 macrophages. Human THP-1 derived macrophages were differentiated in the presence of the activator PMA (20ng/ml, 48h), followed by Hepc stimulation (1µM, 4h). Crude membrane extracts (M) were analyzed using four different antibodies raised against human Fpn1 (Ab#1, 2, 4, 5) and murine Fpn1 (Ab#3). The position and size in kilodaltons (kDa) of the molecular weight markers are indicated on the left. Vertical dashed lines indicate repositioned gel lanes.

3.3.2. HepG2 cell line as an hepatocyte model

Recently, Fpn1 was reported to be expressed in murine hepatocytes, being upregulated by serum starvation and downregulated by Hepc [55]. HepG2 was chosen as a cellular model for human hepatocyte Fpn1 detection. A commercial antibody raised against murine Fpn1 (Ab#3) detected a band with the expected molecular weight (Figure III.8A-C), exclusive of membrane protein extract (Figure III.8A). This potential human Fpn1 band was detected at the same level as murine Fpn1 in iron-treated murine macrophage cell line J774 (Figure III.8A-C) and was also detected in huPBL membrane extracts (Figure III.8D). However, unlike murine Fpn1 in J774 macrophages, this band was not modulated by increasing concentrations of iron, Hepc or serum starvation in HepG2 cells (Figure III.8B-C), indicating that this band may not correspond to human Fpn1. Moreover, TNFα, inorganic iron (FeNTA) and holo-Tf, which were reported to induce Hepc expression and subsequent internalization of the overexpressed human GFP-Fpn1 in huPBL [74], had no effect on the intensity of the putative Fpn1 band detected by Ab#3 in huPBL (Figure III.8D).

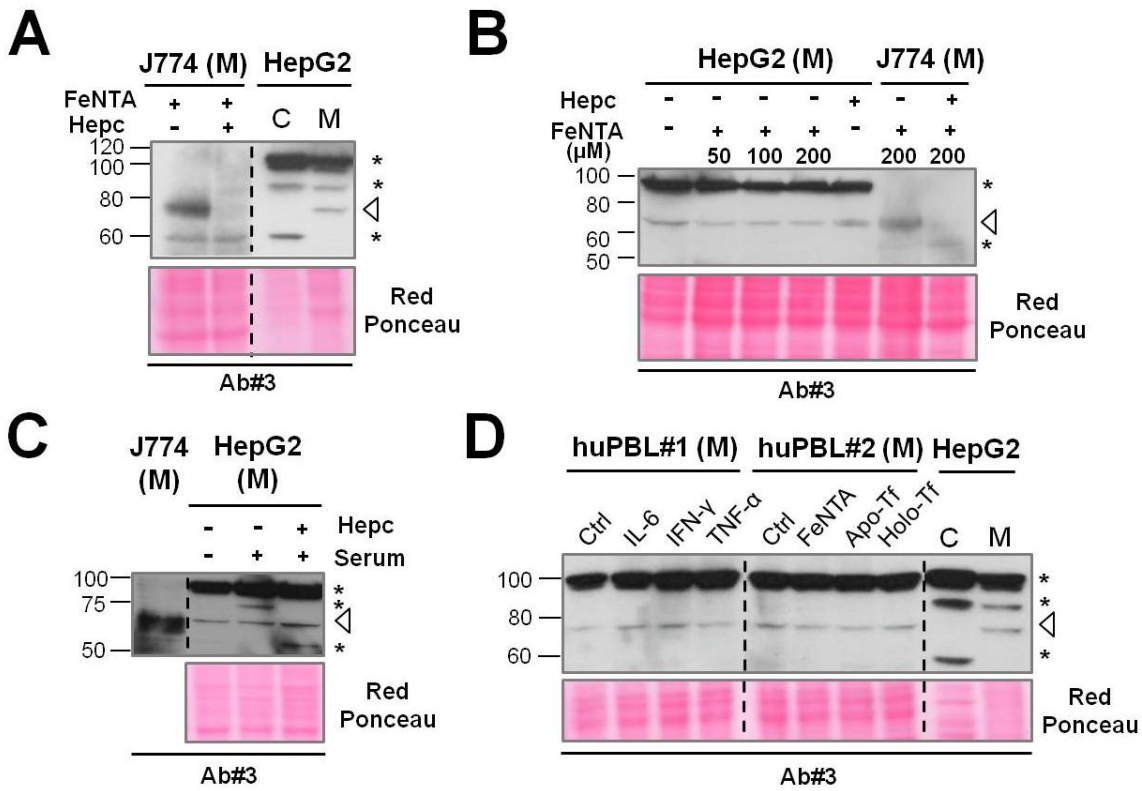

Figure III.8 - Immunoblotting analysis of ferroportin-1 detection in HepG2 cell line and human lymphocytes. (A-D) Immunoblotting analysis of Fpn1 on cytosolic (C) and crude membrane extracts (M) of HepG2 cell line, murine macrophagic cell line J774 (positive control for mFpn1) and human lymphocytes (huPBL) using a commercial anti-murine Fpn1 antibody (Ab#3). Red Ponceau staining was used as control of equal protein loading of samples. The position and size in kilodaltons (kDa) of the molecular weight markers are indicated on the left. Vertical dashed lines indicate repositioned gel lanes. The potential human Fpn1 band in HepG2 membrane extract is indicated by the arrowhead while "*" indicates unspecific bands. **(A-B)** Comparison of the Ab#3 detection between HepG2 and J774 subcellular extracts. J774 cells were pre-treated with iron (200 µM FeNTA, 18h), followed or not by Hepc treatment stimulation (700nM, 3h). HepG2 were untreated or treated with different concentrations of iron (FeNTA 50-200µM, 18h) or Hepc (700nM, 3h). **(C)** Membrane extracts of HepG2 cells treated with 0% (-, lane 2), 10% serum (+, lane 3) for 36h, or treated with 10% serum for 24 h followed by treatment with Hepc (700nM, 18h) in the presence of 10% serum (lane 4). Membrane extract of iron-treated J774 macrohages was used as Fpn1 detection positive control. **(D)** Membrane extracts isolated from huPBL untreated (ctrl) and treated with different stimuli: free iron (100µM FeNTA, 18h); apo-Tf/holo-Tf (3mg/ml, 18h); cytokines IL-6, IFNγ, TNFα (20ng/ml, 18h). HepG2 extracts were used as a potential positive control for human Fpn1 (arrowhead).

Nonetheless, the lack of Hepc effect on the potential Fpn1 band detected by Ab#3 in both huPBL and HepG2 could also be explained by a "Hepc resistance" due to the Hepc autocrine production by these cells. As Hepc main producers, hepatocytes could be expected not to present significant levels of Fpn1 at cell surface. In such conditions, despite the putative low level of Fpn1 expression at cell surface, Fpn1 could still be detected in crude membrane extracts as these extracts contain the plasma membrane as well as intracellular endomembranes. To test this hypothesis, HepG2 were cultured in the absence

or presence of a non-commercial antibody against Hepc, in order to sequester any Hepc that could exist in culture medium as a result of endogenous production and secretion by HepG2 cells. Crude membrane extracts were then analyzed by immunoblotting using Ab#3, but no effect was observed on the potential human Fpn1 band detected on HepG2 treated with anti-Hepc antibody (Figure III.9A). However, although the antibody against Hepc was used in the conditions indicated by its producer, we cannot conclude about the antibody efficiency in the sequestration of external Hepc.

At last, a highly specific antibody raised against murine Fpn1 (Ab#6, [119]) as well as a recently reported commercial antibody raised against human Fpn1 (Ab#7, [139]) were tested in crude membrane extracts of HepG2 treated or not with Hepc. Again, multiple bands were detected but none of the potential Fpn1 bands with compatible molecular weight was modulated by incubation with Hepc (Figure III.9B).

Altogether, no conclusive and consistent detection of human Fpn1 was obtained using the different models, conditions and antibodies tested. As a result, Fpn1 detection in human cells was not validated and the study of Fpn1 in human cells, and in particular huPBL, was not further investigated in this chapter.

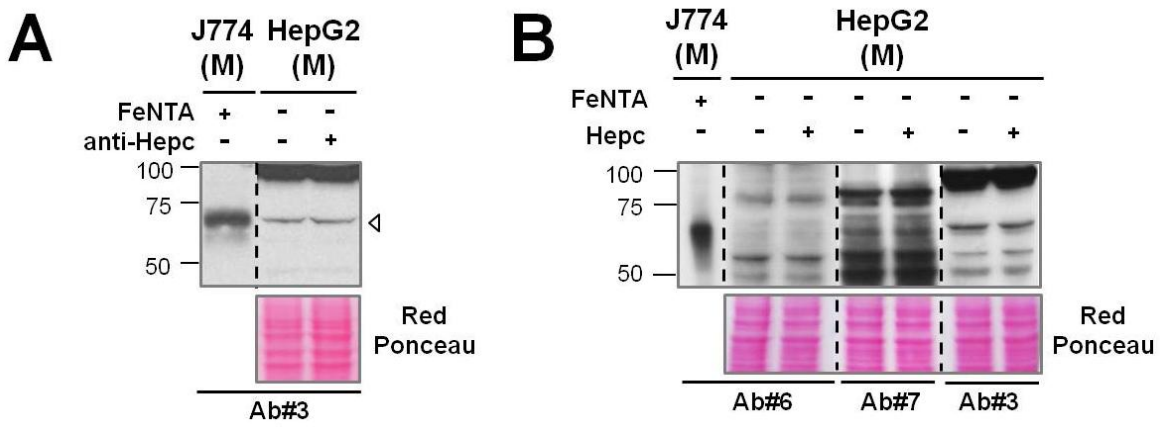

Figure III.9 - Immunoblotting analysis of Fpn1 detection in HepG2 cell line using different antibodies. (A) Immunoblotting analysis of membrane extracts of HepG2 cell line, cultured in the absence or presence of an antibody raised against Hepc (0,6µg/ml, 18h), was performed using Ab#3. Membrane extract of iron pre-treated J774 was using as a positive control for Fpn1 detection. The potential human Fpn1 band is indicated by the arrowhead while "*" indicates unspecific bands. **(B)** Immunoblotting analysis of crude membrane extracts of HepG2 cells untreated and treated with Hepc (700nM, 3h) using one antibody raised against human Fpn1 (Ab#7) and two antibodies raised against murine Fpn1 (Ab#3 and 6). Iron treated J774 membrane extract was used as positive control for Fpn1 detection. Red Ponceau staining was used for control of equal protein loading of samples. The position and size in kilodaltons (kDa) of the molecular weight markers are indicated on the left. Vertical dashed lines indicate repositioned gel lanes.

4. Discussion

The current concept about Cp expression in mammals describes that Cp is mainly synthesized as a soluble protein secreted by hepatocytes into plasma, whereas the membrane GPI-Cp isoform is predominantly expressed in cells of the brain and of the testis [134,279,280]. The results presented in this work revealed a more ubiquitous expression of the GPI-Cp isoform than the one described previously in the literature and gives further support for a recent study showing GPI-Cp detection in purified membranes of multiple organs of rats and mice [281].

Herein, we demonstrated that immune cells as well as hepatocytes express the GPI-Cp isoform in addition to the secreted form of Cp. Indeed, expression of both Cp isoforms was demonstrated by immunofluorescence and Western blot analysis in human lymphocytes, monocytes, and in HepG2 cells. Treatment with PIPLC induced a partial decrease of Cp staining at cell surface in all the cells studied, indicating that at least part of membrane-Cp corresponds to the GPI-Cp isoform. The partial decrease could be due to incomplete efficiency of the enzyme as observed on CD14 (Figure III.3). In addition, a Cp receptor was reported previously in immune cells, including lymphocytes and monocytes [282]. It is therefore possible that part of Cp staining detected by immunofluorescence and FACS could be due to sCp bound to its receptor. Furthermore, immunofluorescence analysis of Cp staining showed that Cp levels at cell surface of huPBL is significantly lower compared with huPBMn (Figure III.5). Interestingly, contrasting with the diffuse and homogenous Cp staining at huPBL membrane, the dotted pattern of Cp expression exhibited in huPBMn and HepG2 membranes was highly suggestive of Cp localization in specific cell membrane domains such as lipids rafts. Noteworthy, results presented in Supplemental Data (section V), confirmed that GPI-Cp expressed in HepG2 is indeed localized in lipid raft microdomains.

The expression of sCp and GPI-Cp in immune cells, namely lymphocytes and monocytes, suggests a close functional relationship among immune system, oxidative stress and iron metabolism. In fact, Cp is an acute-phase protein with its plasma concentration increasing in many diseases such as hepatitis, ATH, polyarthritis, cancer and many other inflammatory and infectious diseases [271,283,284]. Inflammatory processes that occur in these diseases are associated with strong local recruitment of immune cells, including lymphocytes and monocytes. In such context, lymphocytes and monocytes-derived Cp could play an important local role in host protective function against the potential toxicity of iron and its deposition in tissues. For instance, Cp secretion or shedding of membrane Cp by immune cells would rapidly promote iron loading onto Tf and Lf molecules, thus contributing for iron withhold from pathogens. Simultaneously, iron loading on Tf and Lf molecules would prevent dissociated iron from participating in Fenton reactions and thus contribute to decrease ROS

generation and protection of host cells. Accordingly, it was recently reported that Cp forms a complex with Lf and MPO enzyme [285], which supports the hypothesis that Cp plays an important role in host immune response that is closely associated with free iron availability.

Alternatively, expression of GPI-Cp by immune cells, and in particular higher expression at cell surface of innate immune system cells like monocytes (Figure III.5A-B) and NK cells [276], could be regarded as a self-protection mechanism against oxidative stress. These cells produce and secrete high amounts of toxic compounds during their killing activity that could harm its own cellular integrity. Expressing high levels of Cp at cell surface could therefore constitute a defense mechanism against oxidative stress by immune cells.

In striking contrast, several reports have shown that Cp possess pro-oxidant activity depending on the microenvironment [271]. For instance, the oxidation of other substracts (e.g. lipoproteins) by Cp in conditions of chronic inflammation would have a harmful effect at both local and systemic level and could be involved in the etiology of inflammatory pathologies involving oxidative stress such as ATH.

In addition to the delivery of high amounts of Cp at site of inflammation, leukocytes could also participate into the systemic acute-phase response, an observation that is so far only attributed to hepatocytes in regard to their ability to secret high amounts of sCp. The dramatic increase of circulating leukocytes, in particular lymphocytes, observed during inflammatory and/or infectious status [286] could contribute to the raise in plasma Cp, either through the synthesis of sCp and/or through cell surface shedding of the GPI-Cp as previously observed for other GPI-proteins expressed in immune cells [287]. Supporting this hypothesis, it was previously proposed that the serum concentration of Cp during inflammation reflects not only hepatic but also extra-hepatic synthesis [283]. Indeed, IFNγ was reported to induce sCp expression in human monocytes [274]. Herein, our immunoblotting analysis detected IFNγ-induced mild upregulation of sCp at the cytosolic fraction and culture medium (Figure III.4C-D) of human PBL, giving further support to this hypothesis.

Effect of different stimuli on GPI-Cp in human monocytes and lymphocytes was investigated in our lab using flow cytometry [288]. GPI-Cp higher expression in monocytes vs. total lymphocytes and in non-T cells (B and NK cells) vs. T cells was confirmed. Interestingly, both naturally activated monocytes and lymphocytes presented higher levels of GPI-Cp compared with non-activated cells. However, PMA-induced activation of these cells significantly upregulated GPI-Cp in human monocytes, while significantly downregulating GPI-Cp in total and activated human lymphocytes. Similar results were obtained by LPS-induced activation of human monocytes and lymphocytes [288]. Such opposite effects of activation on human monocytes and lymphocytes activation suggest a

cell-specific regulation of GPI-Cp expression. Cp upregulation in human activated monocytes is in agreement with the general immune response strategy of sequestration of free iron by promoting its oxidation and loading in iron-binding proteins such Tf, Lf, and Ft [289].

On the other hand, regarding GPI-Cp downregulation in activated lymphocytes, it was recently reported that either activated or iron-stimulated lymphocytes expressed increased levels of Hepc, downregulating GFP-Fpn1 at lymphocyte cell surface and promoting intracellular iron retention. This mechanism was demonstrated to be essential for proliferation of human activated lymphocytes [74]. Considering that both Cp isoforms have been reported to promote iron export by Fpn1 in other cells [51,254,270], GPI-Cp downregulation in activated lymphocytes could be regarded as a strategy to promote intracellular iron retention and subsequent cell proliferation. Supporting this hypothesis, stimulation of human lymphocytes with IL-2, a cytokine known to activate and induce lymphocyte proliferation, downregulated GPI-Cp in total and activated lymphocytes [288].

Lymphocyte Cp expression gives further support to the original postulate from de Sousa *et al* addressing an important role for lymphocytes circulation in the regulation of iron metabolism [147,190]. Herein, no iron effect on Cp expression was observed when immunoblotting membrane and cytosolic fractions of human lymphocytes in the conditions tested (Figure III.2A). However, it is possible that a mild effect in total lymphocytes or a strong effect in only a fraction of total lymphocytes could fail to be detected by such technique. Interestingly, unpublished data by our group showed that the number of huPBL expressing Cp at cell surface (GPI-Cp) was increased in iron deficiency anemia patients in agreement with increased circulating levels of Cp compared with appropriate controls. Accordingly, in HH patients with systemic iron overload, the number of huPBL expressing Cp at cell surface as well as the level of circulating Cp was downregulated. These results suggest that hypoxia/iron deficiency conditions might be more relevant for the putative role of Cp in promoting huPBL iron export than the iron overload conditions investigated in this study.

Ultimately, GPI-Cp expressed in human monocytes and lymphocytes could be playing a role in iron export along with Fpn1. However, as observed in Figure III.7-9, despite our effort to demonstrate the endogenous expression of human Fpn1, we could not anticipate any conclusion regarding the specific detection of endogenous Fpn1 in the models and conditions tested using different antibodies. The contribution of GPI-Cp and sCp as well as its possible interaction with Fpn1 on iron export from human lymphocytes, monocytes and hepatocytes remains thus to be further clarified. Noteworthy, while writing the manuscript of this thesis, recent work by Pinto *et al* characterizes the

expression of endogenous Fpn1 and iron export in human lymphocytes using a commercial antibody [290].

Nonetheless, during the course of the work presented in this manuscript, our limitation in detecting endogenous human Fpn1 in immune cells lead us to change the initial plan of studying the key proteins involved in iron export in human macrophages. Given the features and specificity of antibodies available for murine Fpn1, including one developed by one of the co-supervisors of this work (Doctor François Canonne-Hergaux), murine macrophages were the selected model for the subsequent studies presented in Chapters 2 and 3. In addition, aiming to overcome the antibody limitation, a project to produce a specific antibody against human Fpn1 was initiated during the course of this work. The design, production, validation and current status of this project are presented in Chapter 4.

5. Conclusion

In summary, we demonstrated that both Cp isoforms are expressed in all the cell types analyzed. The cell surface Cp was identified as a membrane GPI-anchored isoform. Due to the importance of lymphocytes and monocytes in the immune response, the role of both secreted and GPI-Cp isoforms in these cells is likely cell-specific and needs to be further explored. Therefore, further research in the different cell types is needed in order to clarify the specific function of each Cp isoform on the molecular mechanisms underlying the iron transport as well as the cellular protection against iron-mediated oxidative stress and the cellular damage mediated through oxidative reactions. Deciphering the role of sCp and GPI-Cp isoforms in immune cells and hepatocytes may likely contribute to clarify the importance of this ferroxidase in many diseases related to iron metabolism, inflammation and oxidative biology, including ATH.

6. Authorship

The results presented in this chapter were produced by the author of the thesis, by Alexandra Willemetz who contributed to the Fpn1 antibody tests, and by João Banha, Bruno Silva and Cláudia Bispo that contributed to the HepG2 Cp immunofluorescence detection and Cp MFI analysis by flow cytometry in huPBMn.

The majority of the results presented in this chapter were published in:

L. Marques*, A. Auriac*, A. Willemetz, J. Banha, B. Silva, F. Canonne-Hergaux** and L. Costa**, "*Immune cells and hepatocytes express glycosylphosphatidylinositol-anchored ceruloplasmin at their cell surface".* Blood Cells Mol Dis, 2012. 48(2): p. 110-20. (*co-first authors; ** co-senior authors)

Chapter 2

Ceruloplasmin and β-amyloid precursor protein as potential functional partners of ferroportin-1 in murine macrophages

1. Introduction

The macrophage is the cell responsible for erythrophagocytosis and erythrocytes iron recycling, a key event for daily iron supply for erythropoiesis. The iron recycled by this cell can be either stored or exported by Fpn1 to extracellular medium coupled with the activity of a ferroxidase partner [35,122,270]. Cp has been proposed as the ferroxidase interacting with Fpn1 in macrophages [254]. Indeed, *Cp*$^{-/-}$ mice show significant iron accumulation in the liver, particularly in Kupffer cells (tissue macrophages) [51]. However, the only isoform of Cp previously reported in macrophages was sCp, being upregulated and secreted in macrophages upon stimulation with pro-inflammatory and infectious conditions [274,275]. We showed in chapter 1 that human monocytes express high levels of Cp at cell surface, likely to correspond to the GPI-Cp isoform, which suggest that this isoform may also be detected in macrophages. In addition to Cp, other ferroxidases were shown to interact with Fpn1 in other cells, namely Heph and APP [25,139]. Noteworthy, APP was previously shown to be expressed in human monocytes and macrophages [262].

2. Aims

In this study, we investigated if GPI-Cp is expressed in murine macrophages and if GPI-Cp, APP or both co-localize with Fpn1 in these cells. Murine bone marrow-derived macrophages (BMDM) were the model selected to the study due to the lack of specific antibody against human Fpn1 at the time of investigation.

3. Results

3.1. Murine macrophages express both ceruloplasmin isoforms

The results obtained through immunofluorescence in non-permeabilized and permeabilized BMDM showed that these cells express Cp at their cell surface as well as in the cytosol (Figure III.10A). Moreover, immunoblotting of Cp in cytosolic and crude membrane extracts confirmed the existence of a soluble and a membrane-anchored isoform of Cp (Figure III.10C). Interestingly, the pattern of Cp staining in non-permeabilized BMDM (Figure III.10B) showed Cp accumulation in plasma membrane domains, resembling GPI-Cp staining in HepG2 cell line (chapter 1) and suggesting that this membrane-associated Cp could be localized in lipid rafts.

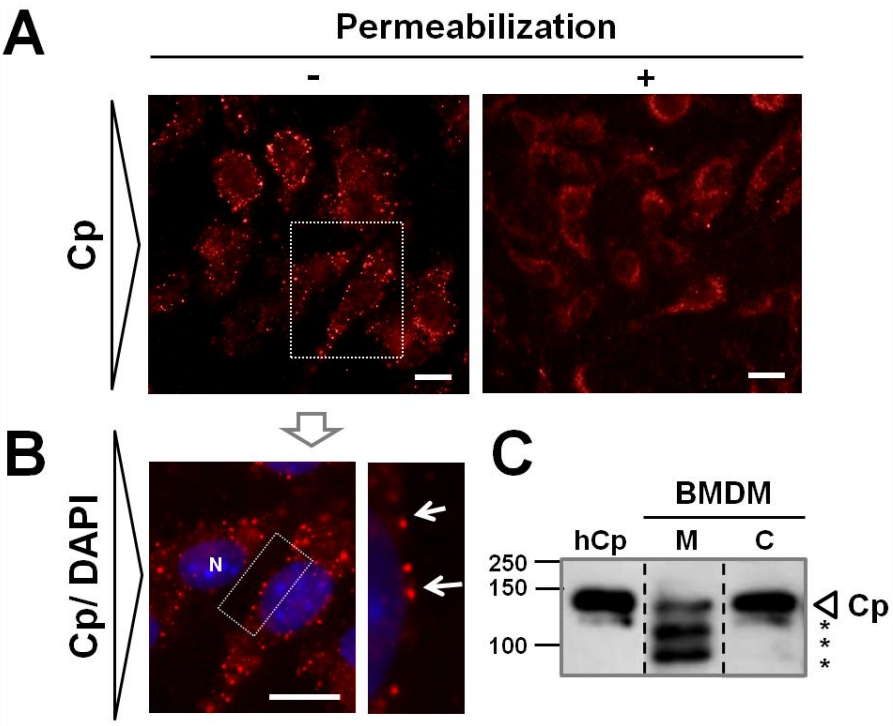

Figure III.10 - Subcellular localization of ceruloplasmin in murine macrophages. (A) Cp immunostaining in non-permeabilized (left; -) and permeabilized (right; +) bone marrow-derived macrophages (BMDM), showing Cp positive staining at both cell surface and intracellular level. **(B)** High magnifications of Cp immunostaining in non-permeabilized BMDM show Cp concentration in discrete membrane microdomains at the cell surface. Cp staining is shown in red and nuclei (N) are stained in blue (DAPI). The white bars in panels represent 20 µm. Insets in **(B)** show enlargement of individual cells staining. **(C)** Immunoblotting detection of Cp in untreated BMDM subcellular fractions: cytosol (C) and crude membrane extracts (M). Human serum-purified Cp (hCp) was used as a positive control. The position and size in kilodaltons (kDa) of the molecular weight markers are indicated on the left. Vertical dashed lines indicate repositioned gel lanes. *Cp proteolitic cleavage product.

Cp immunostaining in non-permeabilized BMDM untreated or treated with PIPLC (0,5 U/ml, 1h at 37ºC) showed a significant decrease of Cp signal at cell surface, showing that this membrane-associated Cp likely correspond to the GPI-cp isoform (Figure III.11).

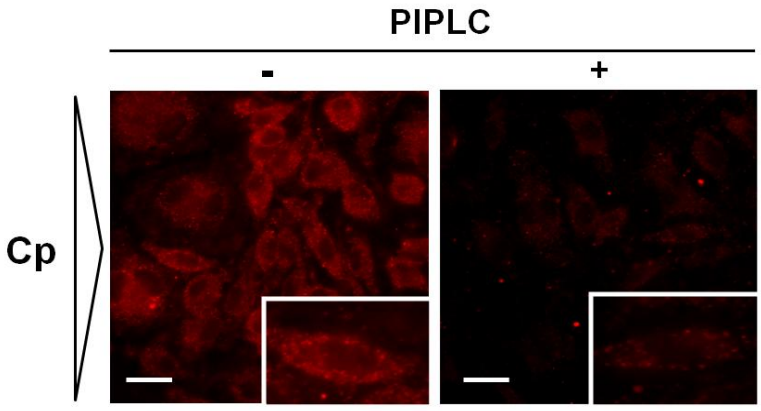

Figure III.11 - GPI-anchored ceruloplasmin at the cell surface of in murine macrophages. The effect of the enzyme PIPLC on Cp expression was analyzed in non-permeabilized BMDM and a significant decrease of Cp staining is observed in PIPLC-treated BMDM (right, +). Insets show enlargement of individual cells staining. The white bars in panels represent 20 µm.

3.2. Ceruloplasmin and ferroportin-1 partially co-localize in lipid rafts in iron-treated murine macrophages

The pattern of GPI-Cp staining at cell surface of iron-treated BMDM (Figure III.10B) was suggestive of its accumulation in membrane domains. To test if this ferroxidase could be localized in lipid rafts, GPI-Cp immunostaining was investigated in iron-treated BMDM. The results obtained showed a partial co-localization with CD11b, a cell surface marker and a lipid raft-associated antigen (Figure III.12A) [291]. Noteworthy, co-localization of Fpn1 and CD11b at cell surface was previously reported to be significantly enhanced upon iron stimulation in BMDM [119]. Also, in order to test if GPI-Cp and Fpn1 could co-localize in the same lipid rafts at the plasma membrane of murine BMDM upon iron stimulation, co-staining of both Cp and Fpn1 was investigated in iron-treated BMDM (Figure III.12B). As observed, both proteins were localized at the cell surface with some overlay of the Fpn1 and GPI-Cp staining (see arrows in Fig III.12B). However, only a partial co-localization of GPI-Cp and Fpn1 was observed.

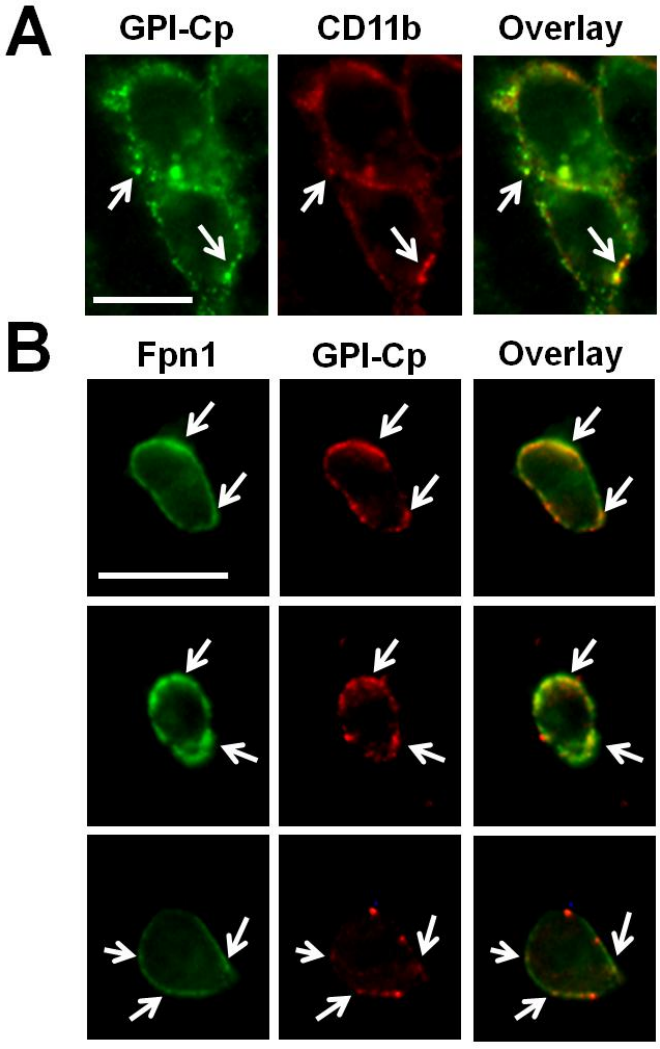

Figure III.12 - GPI-anchored ceruloplasmin is partially co-localized with CD11b and ferroportin-1 in lipid rafts on iron-treated murine macrophages. (A) Co-staining of GPI-Cp (green) with CD11b (red, cell surface marker and raft-associated antigen) in iron-treated BMDM. **(B)** Co-staining of GPI-Cp (red) and Fpn1 (green) in iron-treated BMDM. The white bars represent 20 µm. Arrows indicate the co-localization sites of the two labeled proteins (yellow) in some areas at cell surface.

For further confirmation, lipid rafts from untreated and iron-treated BMDM were isolated as detergent (Triton X-100) resistant membranes (DRM) as previously described [118], followed by immunoblotting analysis (Fig III.13). According to the principle of this technique, proteins localized in lipid rafts are expected not to be solubilized by detergent and to float associated with phospholipids to the lighter fractions of the density gradient (DRM). Caveolin forms oligomers and associates with cholesterol and sphingolipids in lipid rafts, leading to the formation of caveolae, a specific subset of lipid rafts [292]. Therefore, caveolin-1 (Cav-1) was used as a lipid raft marker and its distribution in the gradient was used as a guide to define the DRM fractions. Accordingly, the top six lower density fractions were defined as DRM, whereas the non-DRM (NDRM) was defined as the denser material in fractions 7 to 11(Figure III.13). Interestingly, Fpn1 was only detected in DRM fractions, with its expression being significantly enhanced by iron treatment and its distribution mostly enriched in fractions 1 to 3. On the other hand, Cp was mostly detected in fractions 8 to 10 in untreated cells. Upon iron treatment, Cp expression was increased and distributed in fractions 5 to 11. Moreover, in both untreated and iron-treated BMDM, Cp was strongly detected in NDRM fractions (9 to 11), and likely correspond to sCp isoform in these cells (Figure III.13). Indeed, NDRM fractions typically correspond to solubilized membrane proteins as well as cytosolic proteins and broken membrane/cells. Nonetheless, an overlap between Fpn1 and Cp distribution in the iodixanol gradient was observed in fractions 5 and 6, supporting immunofluorescence studies in which only a partial co-localization of Fpn1 and GPI-Cp was observed in iron-treated BMDM.

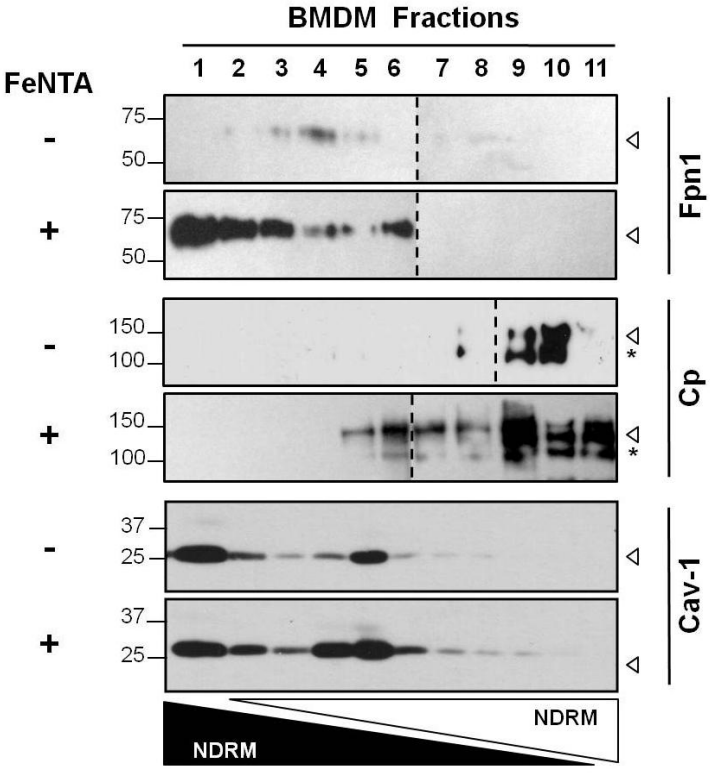

Figure III.13 - Ceruloplasmin partially co-localizes with ferroportin-1 in lipid rafts fractions in iron-treated murine macrophages. Immunoblotting detection of Fpn1, Cp and cav-1 (raft marker) in detergent resistant membrane (DRM) and non-detergent resistant membrane (NDRM) fractions of BMDM untreated and iron-treated (FeNTA, 100 µM). The positions and sizes in kilodaltons (kDa) of the molecular weight markers are indicated on the left. Vertical dashed lines indicate repositioned gel lanes. *Cp proteolitic cleavage product.

3.3. Effect of iron on ceruloplasmin expression in murine macrophages

Our previous results with the iodixanol gradient showed an upregulation of Cp in iron-treated BMDM (Figure III.13). To confirm this result, we investigated the effect of iron on Cp protein levels using different technical approaches. The results obtained by immunofluorescence (Figure III.14A), In-Cell Western blot (Figure III.14B), and conventional Western blot of BMDM subcellular fractions (Figure III.14C) confirmed the upregulation of Cp in response to iron treatment. Moreover, analysis of Cp labeling in permeabilized and non-permeabilized BMDM showed that iron loading in these cells increased both membrane-associated Cp and intracellular Cp (Figure III.14A). The increased Cp detection in both cytosolic and crude membrane fractions of iron-treated BMDM further confirmed these results. In addition to Cp upregulation, Fpn1 was also strongly induced by iron (Figure III.14A and III.14C) as previously reported [119]

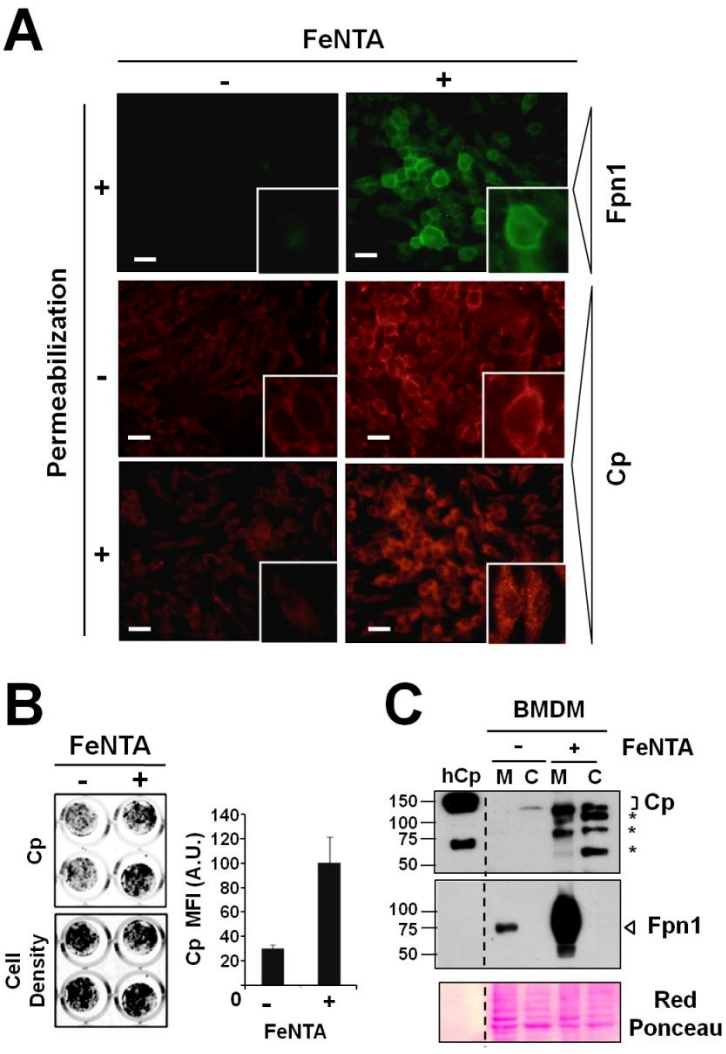

Figure III.14 – Regulation of ceruloplasmin by iron in murine macrophages. (A) Immunofluorescence staining of Fpn1 (green) and Cp (red) in non-permeabilized and permeabilized BMDM untreated or treated with iron (FeNTA). **(B)** In-Cell Western blot detection (left panel) and quantification (histogram, right panel) of Cp expression in iron treated (+) and untreated (-) BMDM. For correction of variation in cell numbers from well to well, Cp intensity signals in histogram were normalized to cell density (left panel). **(C)** Immunoblotting of Cp and Fpn1 in crude membrane (M) and cytosolic (C) extracts isolated from untreated or iron-treated BMDM (FeNTA, 100 µM). Red Ponceau staining was used for total protein loading control. Vertical dashed lines indicate repositioned gel lanes. The positions and sizes in kilodaltons (kDa) of the molecular weight markers are indicated on the left. Vertical dashed lines indicate repositioned gel lanes. *Cp proteolitic cleavage product.

The effect of iron on total *Cp* mRNA levels was also investigated and no difference was observed between untreated and iron-treated BMDM for short time point (Figure III.15A), suggesting a post-transcriptional regulation of Cp by iron. However, posterior qPCR experiments in which iron-treated BMDM were used as a positive control, revealed a progressive decrease of *Cp* mRNA levels (total Cp and both isoforms: GPI-Cp and sCp) directly proportional to time of culture in the presence of iron (Figure III.15B).

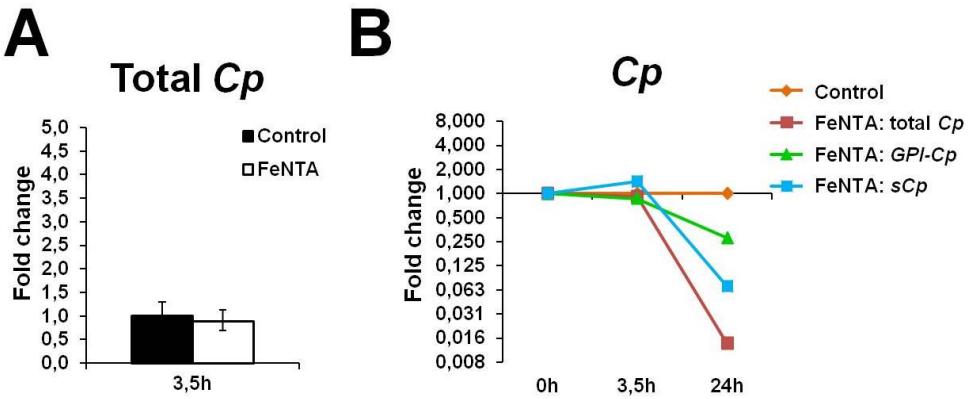

Figure III.15 - Iron effect on ceruloplasmin transcriptional expression in murine macrophages. (A) qPCR analysis of total *Cp* mRNA levels in untreated (control) and iron-treated BMDM (FeNTA, 100 µM) for 3,5 h. Graphic representative of one experiment with biological and technical duplicates, with fold change data presented as mean ± confidence interval (95%). **(B)** Kinetics of total *Cp* and its isoforms *GPI-Cp* and *sCp* mRNA levels in BMDM untreated (control) and iron-treated BMDM (FeNTA, 100 µM) at different time points. Graphic represents data obtained in three independent experiments, each with biological and technical duplicates. Data in **(A-B)** are shown in mean fold change calculated as $2^{-\Delta\Delta Ct}$ using *Hprt* as the reference gene and then normalized against the respective experimental control condition at each time point.

3.4. β-amyloid precursor protein is upregulated by iron and co-localizes with ferroportin-1 in lipid rafts microdomains in murine macrophages

Considering the partial co-localization of GPI-Cp and Fpn1, we investigated if another ferroxidase could be also interacting with Fpn1 in iron-treated BMDM. Besides Cp, of the three other proteins reported to interact with Fpn1 in different cells and tissues, only APP was previously described to be expressed in human monocytes and macrophages [262]. In order to test this hypothesis, we first analyzed APP expression in crude membrane extracts of untreated and iron-treated BMDM. We observed a significant upregulation of both immature (≈110 kDa, *N*-glycosylated form) and mature APP (≈130 kDa, *N*- and *O*-glycosylated form) along with Fpn1 upregulation in iron-treated cells (Figure III.16A). A higher molecular weight band (*) was also observed in iron-treated BMDM membrane extract, but its identification was uncertain. Noteworthy, other authors have reported a spectrum of bands of mature APP corresponding to both fully glycosylated and phosphorilated mature APP [293].

Analysis of *App* mRNA levels revealed that, unlike Fpn1, APP upregulation was not observed at the mRNA level (Figure III.16B), indicating that APP upregulation occurs exclusively through a post-transcriptional mechanism.

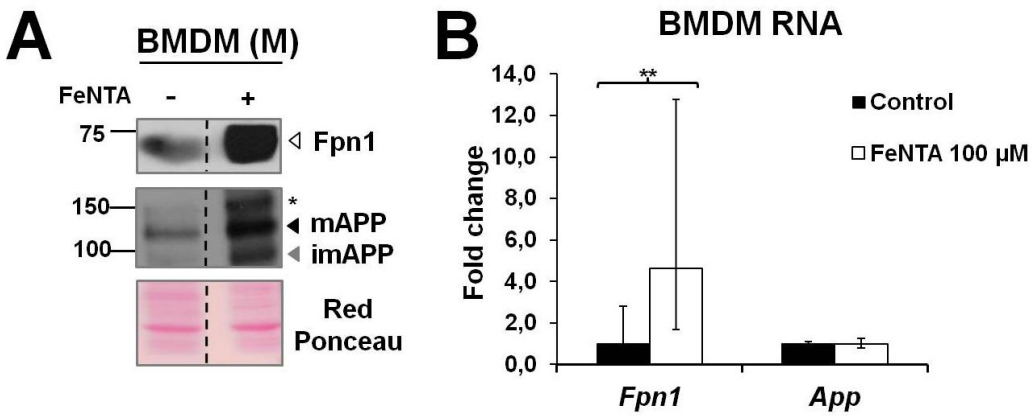

Figure III.16 - β-amyloid precursor protein is upregulated by iron in murine macrophages. **(A)** Immunoblotting detection of Fpn1 and APP on crude membrane extracts (M) of untreated and iron-treated BMDM. The position and size in kilodaltons (kDa) of the molecular weight marker are indicated on the left. The black arrowhead indicates mature APP protein (mAPP) while the gray arrowhead indicates immature APP protein (imAPP). *Unknown protein positively detected by antibody raised against APP. Red Ponceau staining was used for control of total protein loading. **(B)** Quantification of *App* and *Fpn1* mRNA levels by qPCR in untreated and iron-treated BMDM (FeNTA, 100 µM). Fold change data are represented as mean ± confidence interval (95%), in which fold change data were calculated as $2^{-\Delta\Delta Ct}$ using *Hprt* as the reference gene and then normalized against the respective experimental control condition at 3,5 h. Statistical analysis was performed on the ΔCt values obtained during three independent experiments, using Student's *t* test. Statistically significant differences on *Fpn1* and *App* mRNA mean expression between untreated and iron-treated (FeNTA) BMDM at 3,5 h time point are indicated as **(p<0,01).

Fpn1 was previously reported to localize in lipid rafts at cell surface of iron-treated BMDM [118]. In order to test if APP would co-localize with Fpn1, lipid rafts of untreated and iron-treated BMDM were isolated as described before and analyzed by immunoblotting (Figure III.17A). Distribution of the raft marker Cav-1 through the gradient fractions showed that DRM proteins were mostly enriched in fractions 1 to 6. Analysis of Fpn1 and APP detection confirmed that iron stimulation upregulates both APP and Fpn1, with Fpn1 being distributed in DRM fractions, but mainly enriched in fractions 1 to 5. On the other hand, in untreated BMDM, APP was detected in fractions 5 to 11 being enriched in fractions 10 and 11. Upon iron stimulation, APP was significantly upregulated, being detected in almost all fractions of the gradient. Despite the significant detection of APP in fractions 5 to 11, its mature form (130 kDa) was detected in the top four DRM fractions where it overlaps with Fpn1 distribution, pointing to a co-localization of these two proteins in DRM fractions.

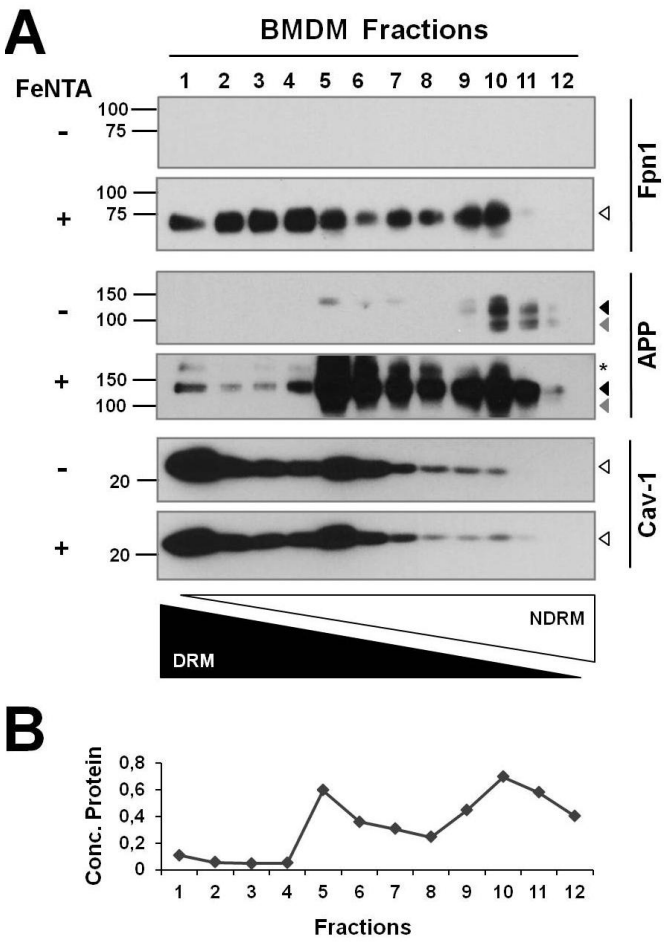

Figure III.17 - β-amyloid precursor protein co-localizes with ferroportin-1 in lipid rafts microdomains in iron-treated murine macrophages. (A) Immunoblotting detection of Fpn1, APP and caveolin-1 (cav-1; raft marker) in detergent resistant membrane (DRM) and non-detergent resistant membrane (NDRM) fractions isolated from untreated and iron-treated BMDM (FeNTA, 100 µM). The position and size in kilodaltons (kDa) of the molecular weight marker are indicated on the left. Black arrowheads indicate mature APP protein (mAPP) while gray arrowheads indicate immature APP protein (imAPP). *Unknown protein positively detected by antibody raised against APP. **(B)** Typical protein distribution in BMDM iodixanol gradient. The low protein concentration in DRM fractions 1-4 compared with NDRM-enriched fractions 9-12, show that fractions 1-4 are highly enriched in DRM proteins despite the minimal protein content.

Immunofluorescence studies were also attempted to demonstrate APP and Fpn1 co-localization in the same lipid rafts. However, the detection of APP by immunofluorescence was not validated (Figure III.18). The staining of APP observed was not typical of a membrane protein as expected and its detection was not modulated by iron (a known inducer of APP expression [263,264]) and as previously observed in Western blot (Figure III.16A. and III.17A). One possibility is that the antibody used for APP detection (22C11, Millipore) may have higher affinity for the denaturated APP protein in Western blot conditions than for the native form of APP, failing to detect APP in immunofluorescence experiments.

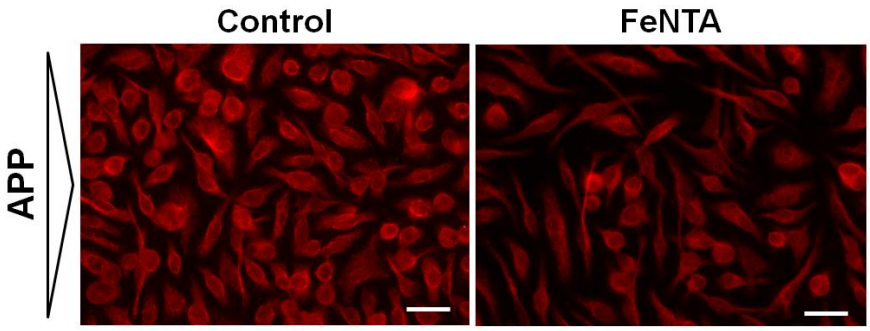

Figure III.18 - Immunofluorescence study of β-amyloid precursor protein in murine macrophages. Staining of BMDM untreated and treated with iron (FeNTA, 100 µM) overnight using an antibody against APP protein. The white bars represent 25 µm.

Co-immunoprecipitation (Co-IP) studies were also attempted as an alternative approach, but the results obtained were inconclusive. The antibody used for APP precipitation (22C11, Millipore) often contaminated the immunoprecipitated protein extracts, being detected when probed with secondary antibody during Western blot. As the IgG heavy chain dimers of the anti-APP antibody used for the immunoprecipitation possess a molecular weight close to APP, the strong detection of the antibody in the eluted protein extracts chains masked the results. As an alternative to overcome this technical limitation, a biotinilated conjugate of the antibody against APP was tested for the Western blot detection. In such conditions, the antibody used for precipitation would not be detected in the Western blot. However, the biotinilated antibody failed to detect APP in total extracts as well as eluted extracts of iron-treated BMDM (data not shown).

4. Discussion

In the present study, we showed that murine macrophages (BMDM) express a membrane-associated Cp in addition to the soluble form already reported in macrophages [274,275]. Decrease of Cp membrane staining upon incubation with PIPLC, an enzyme that specifically cleaves GPI-anchored proteins, demonstrated that this form of Cp corresponds, at least in part, to GPI-Cp as we have reported in human lymphocytes, monocytes and hepatocytes. In addition, we confirmed previous observations describing increased Fpn1 expression at BMDM cell membrane in response to iron overload conditions, being enriched in lipid raft microdomains [118,119].

In this study, we also demonstrated an upregulation of Cp protein in iron-treated BMDM using different technical approaches. However, the upregulation was observed exclusively at protein level, which suggested a post-transcriptional mechanism mediated by iron regulating Cp levels in BMDM. Surprisingly, posterior studies consistently revealed a progressive decrease of *Cp* mRNA level directly proportional to time in culture in the presence of free iron. For such reason, the upregulation of Cp protein induced by iron in BMDM

is currently under investigation in our group in order to clarify the opposite effects of iron observed on Cp expression (mRNA and protein). Noteworthy, a study in the C6 glioma cells reported Cp upregulation by iron deficiency and downregulation by iron overload conditions [294]. Accordingly, circulating Cp was reported to be downregulated in HH patients [295], hepcidin-deficient murine models presenting systemic iron overload [84], and further confirmed in HH patients by our group (unpublished results). On the contrary, increased circulating Cp was reported in iron deficient rats [296] and iron deficiency anemia patients [297], which is in agreement with unpublished results by our group in these patients. Nonetheless, regulation of Cp expression by iron in a specific cell such as the macrophage could differ from circulating Cp or glial cells and, for that reason, our previous results concerning iron regulation of macrophagic Cp need to be further investigated and clarified.

Considering the reported localization of Fpn1 in lipid raft microdomains in iron-treated BMDM, the expression and distribution of Cp in DRM and NDRM fractions of iron-treated BMDM was also investigated. Indeed, a partial co-localization of GPI-Cp with Fpn1 was found in lipid raft fractions of iron-treated BMDM. As previously proposed, GPI-Cp ferroxidase activity could promote iron efflux by Fpn1 in a situation whenever iron recycling is more demanding in order to maintain iron homeostasis [254,270]. Accordingly, iron efflux assays after challenging the reticuloendothelial system, revealed that both hepatocytes and tissue macrophages had impaired iron release in $Cp^{-/-}$ mice compared with $Cp^{+/+}$ mice. Such impairment was not observed when $Cp^{-/-}$ mice were injected with holo-Cp, showing that Cp indeed plays a role on iron export in both hepatocytes and tissue macrophages [51].

However, in our study, only a partial co-localization of Fpn1 and GPI-Cp was observed in iron-treated BMDM. Indeed, Fpn1 was strongly enriched in lipid rafts fractions that did not express any GPI-Cp, showing that a significant amount of Fpn1 located at cell surface is not co-localized with GPI-Cp in the conditions tested. This suggests that iron export by Fpn1 may not be exclusively dependent on GPI-Cp activity in iron-treated BMDM. In fact, the participation of the soluble Cp isoform also expressed and secreted by macrophages may also contribute to Fpn1 transport activity. Additionally, it is possible that another ferroxidase besides Cp could be also expressed in our murine macrophage model. Interestingly, despite the progressive iron accumulation in different tissues, $Cp^{-/-}$ mice and aceruloplasminemia patients only develop anemia at early adult life [51]. This fact suggests that despite the lack of Cp, recycling macrophages are still exporting enough iron to sustain the erythropoietic demand during the first years of life. Although non-enzymatic iron oxidation was proposed to be responsible for the Tf iron loading in this condition [51], the existence of another ferroxidase in recycling macrophages should not be disregarded. Indeed, the expression of different ferroxidases in the same tissue

has been previously reported. For instance, in rats, Heph and Cp were reported to be co-expressed with Fpn1 in the heart, being differently regulated by iron and indicating that both could interact with Fpn1 under different conditions [125]. On the other hand, APP and Cp were reported to be co-expressed in liver of mice, more specifically in hepatocytes, both contributing equally to the ferroxidase activity presented by this organ [139].

Our results showed that APP is expressed in murine BMDM, being upregulated by iron through a post-transcriptional mechanism likely associated with the IRE on the 5´-UTR sequence of its mRNA reported elsewhere [263]. Additionally, we demonstrated that, in response to iron, both mature APP and Fpn1 detection overlapped in DRM/lipid rafts fractions indicating that these two proteins could co-localize in such microdomains under iron overload conditions. Previous studies reported that APP is present in two different pools in neurons, following different processing destinations according to its localization in or out of lipid raft microdomains [298,299]. It is therefore not surprising to find APP not exclusively enriched in DRM fractions where Fpn1 is also enriched in iron-stimulated BMDM. However, only the mature form of APP was detected in such fractions, suggesting that APP localization in lipid rafts could be essential to its function. The fact that both APP and Fpn1 are upregulated by iron likely through an IRE element, co-localizing in the lightest DRM fractions suggests that these two proteins could be interacting in order to promote iron release from macrophage in conditions of cellular iron overload.

Interestingly, the expression of both Cp and APP in BMDM could indicate overlapping, but also complementary roles as potential ferroxidase partners of Fpn1 in macrophages. For instance, as APP and Fpn1 are upregulated by iron overload conditions likely through an IRE element in their mRNA, also Fpn1 and Cp were reported to be transcriptionally upregulated by hypoxia (condition often associated with anemia) through the HRE element in their mRNA [65,108,254,300]. One may propose that APP could be the main ferroxidase partner of Fpn1 under normoxic and iron overload conditions, while Cp could be the main partner under hypoxic conditions in which the stored iron would be mobilized from Ft and exported to respond to the increased erythropoietic demand. Under such conditions, despite the increased intracellular iron levels derived from Ft degradation, the observed progressive *Cp* mRNA decay mechanism triggered by intracellular iron could be counteracted by the transcriptional upregulation of Cp induced by hypoxia. Accordingly, extracellular Cp activity was shown to promote macrophage iron export in a hypoxia-dependent mechanism. However, our results in this chapter did not investigate the Cp/Fpn1/APP interaction nor its modulation in hypoxia, demonstrating only partial co-localization of GPI-Cp/Fpn1 and Fpn1/APP in normoxic conditions combined with iron overload. Noteworthy, it is possible that co-localization of GPI-Cp and Fpn1 could be differently modulated by hypoxia and thus further research on this topic is

necessary in order to clarify the ferroxidase partner(s) of Fpn1 and their regulation by iron in murine macrophages.

Additionally, the ferroxidase activity of domain E2 in APP reported by Duce *et al* [139] was recently challenged by another group that pointed technical limitations in the ferroxidase experiments in Duce *et al* and concluded that APP has no ferroxidase activity [140,141]. Nonetheless, $APP^{-/-}$ mice present increased iron accumulation in the cells where APP is endogenously expressed (neurons, hepatocytes and others) [139] and a very recent publication by a third group showed that sAPP modulates iron export in brain microvascular endothelial cells by stabilizing Fpn1 at cell surface, despite no iron oxidation promoted by sAPP was observed [142]. Thus, even if APP ferroxidase activity is currently discussed, different publications support that APP or its soluble form sAPP interact with Fpn1 and influence iron export. In such scenario, the ferroxidase activity of sCp secreted by macrophages could play a major role promoting iron export through Fpn1.

Ultimately, one should not neglect the important anti-oxidant role played by Cp not only at systemic level, but also at site of inflammation/infection [275,283,284]. The significant upregulation of Cp under inflammatory and infectious conditions, that simultaneously downregulate Fpn1, emphasize how Cp function in immune cells is not limited to the partnership with Fpn1 on iron export. In fact, it was recently reported that macrophage-derived Cp contributes significantly towards protection against inflammation and tissue injury in acute and chronic experimental colitis [179], supporting the relevance of Cp anti-oxidant function. However, the significant upregulation of Cp in conditions of chronic inflammation might lead to a deleterious effect due to its pro-oxidant activity and subsequent oxidative modification of other substracts besides iron. An example of such role of Cp is the high values of plasma Cp associated with increased risk of developing VD events in ATH [258,259,271], most likely associated with Cp capacity to oxidize LDL particles in circulation and at the site of lesion.

5. Conclusion

In this study, we focused on the expression and subcellular localization of two possible ferroxidase partners of Fpn1 in murine macrophages. Herein, we reported the expression of GPI-Cp in addition to the soluble isoform of Cp in BMDM, demonstrating a partial co-localization between GPI-Cp and Fpn1 in lipid raft microdomains after iron challenge. Given the partial co-localization, we proposed that another protein besides GPI-Cp and sCp could be also interacting with Fpn1 in these cells. APP, which was recently reported as a ferroxidase interacting with Fpn1 in neurons, was as a likely candidate. Our results confirmed that APP is significantly upregulated by iron in BMDM, and demonstrated that part of mature APP is co-localized with Fpn1 in lipid raft

fractions and could therefore correspond to an additional ferroxidase partner for Fpn1 in iron-treated macrophages. Alternatively, given the recent controversy on APP ferroxidase activity, it is possible that APP would interact with Fpn1 promoting Fpn1 stabilization while a ferroxidase, possibly sCp, could promote iron oxidation in addition to iron non-enzymatic oxidation (Figure III.19).

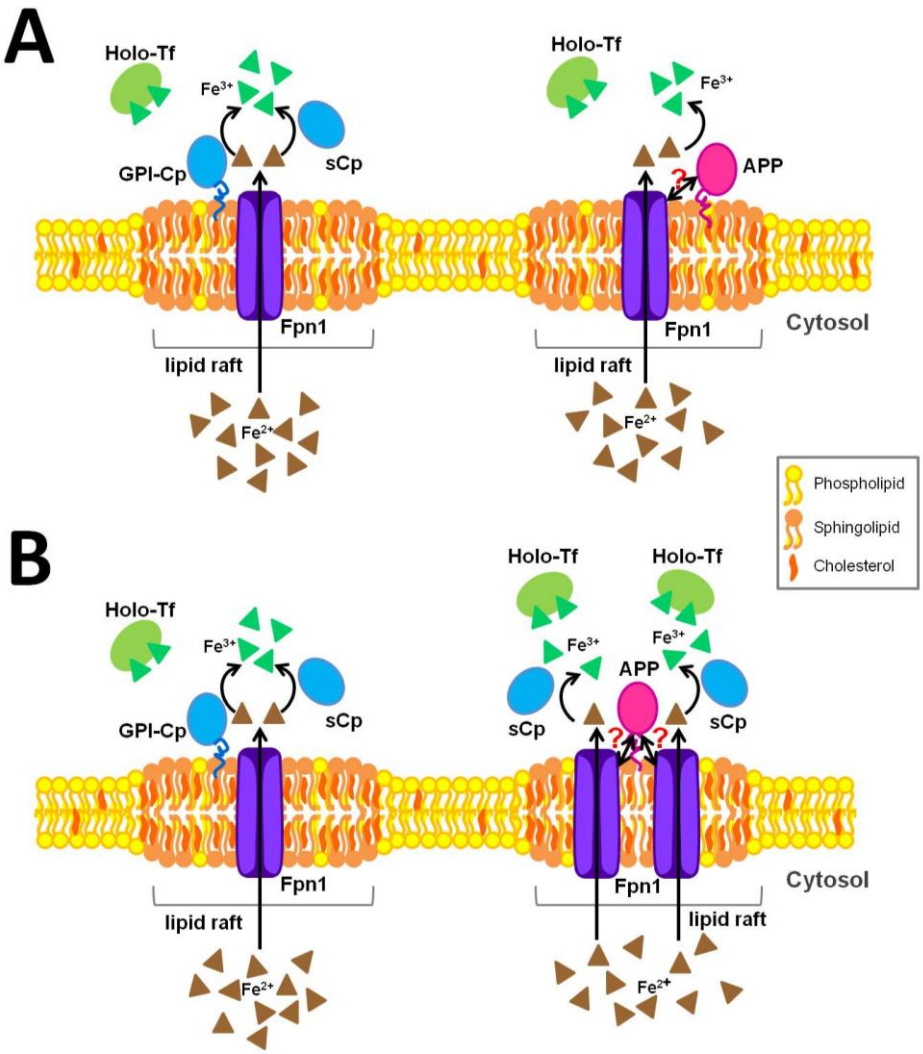

Figure III.19 - Scheme of possible interactions between ferroportin-1, ceruloplasmin and β-amyloid precursor protein in lipid rafts microdomains in murine macrophages. At macrophage cell surface, lipid rafts constitute microdomains enriched in sphingolipids and cholesterol as well as GPI-anchored proteins. In BMDM, Fpn1, GPI-Cp and APP are localized in lipid rafts microdomains. Iron export by Fpn1 is dependent on interaction with a ferroxidase that oxidizes Fe^{2+} to Fe^{3+}, maintaining an iron gradient while facilitating iron load onto Tf (holo-Tf). In **(A)**, one possible model of macrophage iron export proposes that Fpn1 interacts with GPI-Cp, sCp and APP in lipid rafts, which oxidize the exported Fe^{2+} to Fe^{3+}. This interaction with different membrane ferroxidases (GPI-Cp and APP) is likely to occur in different lipid rafts microdomains given the partial co-localization of GPI-Cp/Fpn1. Alternatively, in **(B)** APP presents no ferroxidase activity, but enhances Fpn1 levels at cell surface through physical interaction with the iron exporter. In this model, iron oxidation associated with Fpn1 iron export would be dependent on a multicopper oxidase, herein represented by sCp.

6. Authorship

The results presented in this chapter were produced by the author of the thesis, Anne Auriac and Alexandra Willemetz who contributed to part of the results concerning Cp protein detection in BMDM.

Part of the results presented in this chapter was published in:

L. Marques*, A. Auriac*, A. Willemetz, J. Banha, B. Silva, F. Canonne-Hergaux** and L. Costa**, "*Immune cells and hepatocytes express glycosylphosphatidylinositol-anchored ceruloplasmin at their cell surface".* Blood Cells Mol Dis, 2012. 48(2): p. 110-20. (*co-first authors; ** co-senior authors)

Chapter 3

Modification of macrophage iron metabolism in pro-atherogenic conditions

1. Introduction

ATH is characterized by the formation of plaques in the vessel wall triggered by the accumulation and modification of LDL and subsequent recruitment of immune cells, namely monocytes and lymphocytes. Once in the lesion, monocyte-derived macrophages uptake and accumulate modified LDL, differentiating into lipid-laden cells named foam cells [198]. Iron accumulation in atherosclerotic plaques was previously reported, in particular associated with macrophage-derived foam cells [220,301-303], and was proposed to be a modifiable risk factor in atherogenesis [214,218]. The iron accumulation in foam cells could be the consequence of iron export impairment in the intraplaque macrophages and we decided to test this hypothesis. Different macrophages phenotypes have been described in the atherosclerotic lesion [243], including the classically activated M1 macrophages in which the iron export is impaired [111]. Recently, a new macrophage phenotype (Mox) was reported to result from exposure to oxidized phospholipids (oxPAPC, also a product of LDL oxidation) and the transcriptional factor Nrf2 was shown to be involved in their polarization [249]. However, apart from HO-1, the expression of iron metabolism proteins is poorly described in Mox macrophages [249].

2. Aims

In this study, we proposed to investigate the modulation of some key iron metabolism proteins expression in the Mox phenotype, with particular interest on the iron exporter Fpn1 and its potential partners Cp and APP. Moreover, in order to mimick the complex intraplaque microenvironment, we investigated the effect of simultaneous stimulation with activators of M1 and Mox polarization on these proteins expression.

Given the difficulties expressed in chapter 1 in studying human Fpn1 due to lack of a specific antibody at the time of investigation, murine BMDM were the main macrophage model selected to the study.

3. Results

3.1. Effect of modified LDL on the transcriptional expression of iron metabolism proteins in murine macrophages

BMDM were incubated in the absence (control) or presence of native LDL (nLDL), oxidized LDL (oxLDL) or acetylated LDL (acLDL). Staining with Red Oil O revealed significant lipid accumulation in both oxLDL and acLDL-treated BMDM, but not with nLDL or untreated cells (Figure III.20), showing that both sources of modified LDL can be uptaken by BMDM and promote foam cell differentiation. Noteworthy, oxLDL-derived foam cells presented higher lipid

accumulation than acLDL-derived foam cells, while these latter ones showed larger lipid droplets.

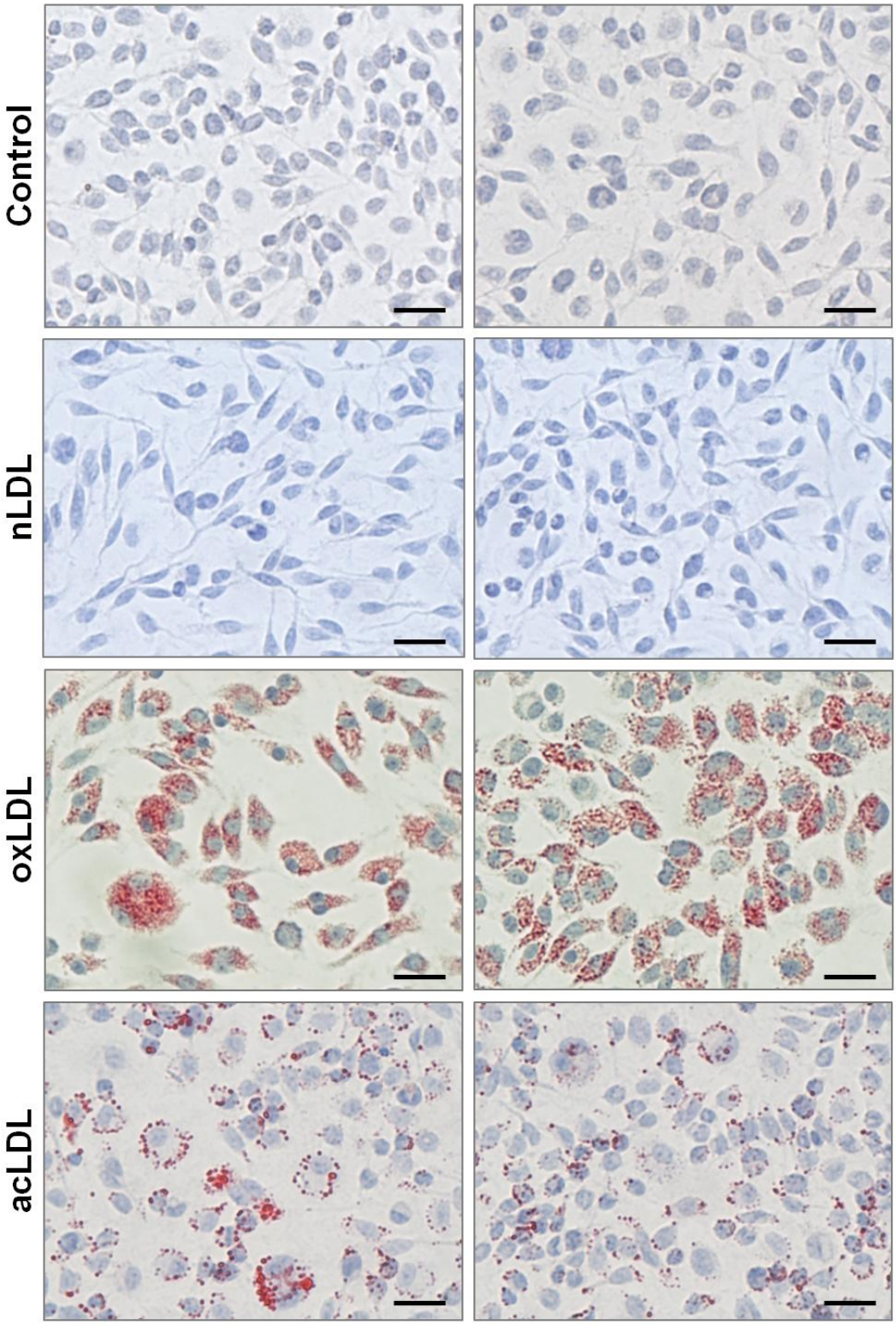

Figure III.20 - Effect of native and modified LDL on foam cell differentiation from murine macrophages. BMDM were incubated for 24 h in complete medium and in the absence (control) or presence of nLDL, oxLDL or acLDL, followed by fixation and Oil Red O staining (lipid specific dye, red) with hematoxylin counterstain. Images were acquired using a Leica DM4000 B microscope with a 40x objective. The black bars represent 20 µm.

As can be observed in table 5, no significant mortality was associated with nLDL, oxLDL or acLDL treated cells and assay with MTT indicated increased cell viability in all conditions studied compared with untreated BMDM (control). Other authors have reported a dual effect of oxLDL, protecting against apoptosis at low concentrations while promoting cellular death at high and toxic concentrations [304]. In particular, one study in murine BMDM reported an anti-apoptotic effect of oxLDL (concentrations up to with 50 g/mL) [305], which is in agreement with our own observations.

Table 5 - Effect of native and modified LDL on murine macrophages viability. The results are expressed as percentage and were normalized against the viability of untreated BMDM (control).

	Control	**nLDL 50 µg/ml**	**nLDL 100 µg/ml**	**oxLDL 50 µg/ml**	**oxLDL 100 µg/ml**	**acLDL 50 µg/ml**	**acLDL 100 µg/ml**
Viability	100%	151%	158%	189%	142%	171%	185%

On the other side, the effect of oxLDL on the transcriptional expression of iron metabolism proteins in BMDM was analyzed by qPCR at different time points. A high and transient upregulation of *Hmox1* (HO-1 gene) and *Fpn1* mRNA level was observed on BMDM in response to oxLDL. This upregulation occurred at early time point and in a dose dependent-manner, followed by a decrease to basal expression level after 24 h of culture with oxLDL (Figure III.21A).

Both nLDL and acLDL had no significant effect on *Hmox1* and *Fpn1* mRNA level when compared with oxLDL (Figure III.21B), which indicates that the oxidative modification of LDL is important for the mechanism underlying the transcriptional upregulation of these genes. Moreover, the upregulation induced by oxLDL was directly proportional to the degree of LDL oxidation (Figure III.21C).

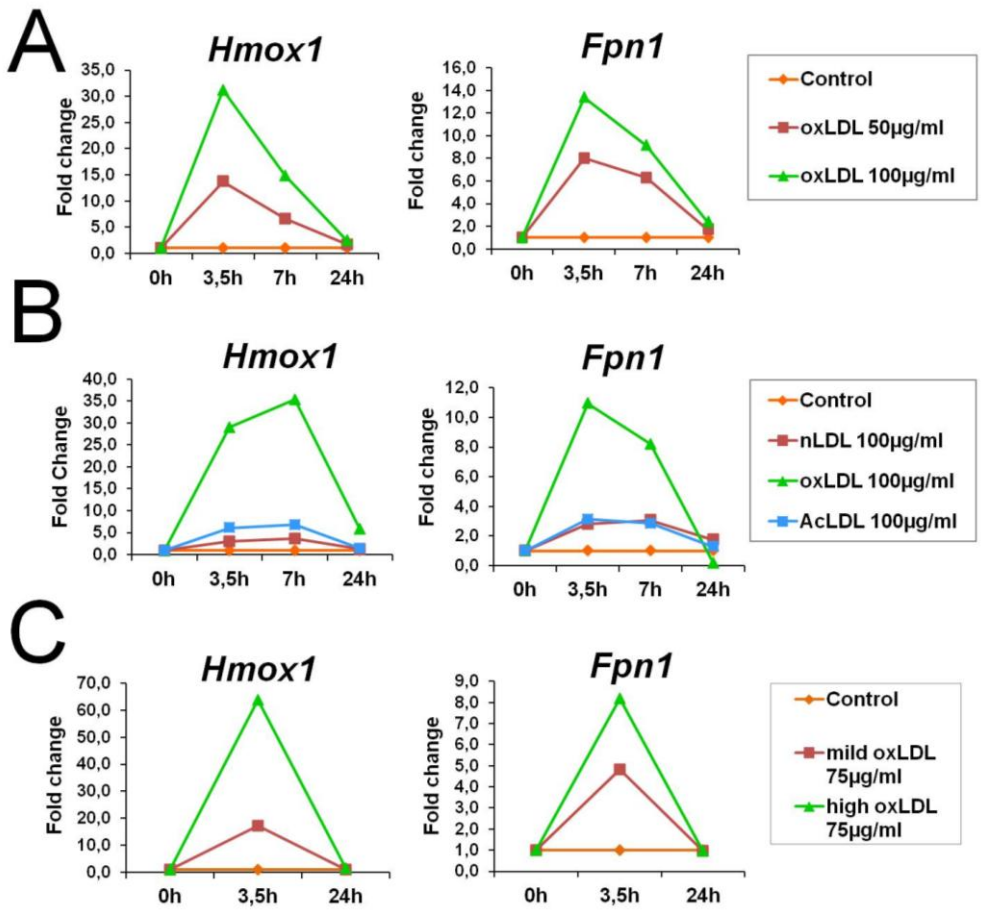

Figure III.21 - Effect of modified LDL on heme oxygenase-1 and ferroportin-1 transcriptional expression. (A-C) qPCR analysis of *Hmox1* and *Fpn1* expression levels, at different time points, in BMDM untreated (control) or treated with: **(A)** different concentrations of oxLDL; **(B)** different sources of LDL (nLDL, oxLDL, or acLDL); **(C)** different degree of LDL oxidation. Fold change data were calculated as $2^{-\Delta\Delta Ct}$ using *Hprt* as the reference gene and then normalized against the respective experimental control condition at each time point. Mean of Ct values in the experiments analyzed: *Hmox1* (Ct=19,1), *Fpn1* (Ct=21,1).

An upregulation of *Fth1* (H-Ft gene) mRNA level was also observed in response to oxLDL, while no significant effect was observed on *App* mRNA level (Figure III.22). Total *Cp* mRNA level were significantly downregulated by oxLDL, reaching a minimum at 24 h of culture. This transcriptional downregulation of *Cp* was also confirmed on both *sCp* and *GPI-Cp* isoforms (Figure III.22). An upregulation of *Hamp1* (Hepc gene) mRNA level was also observed on BMDM in response to oxLDL (Figure III.22). However, *Hamp1* basal expression levels (Mean Ct=31) indicates that no significant effect of oxLDL is expected on Hepc protein level. Other iron metabolism proteins such as DMT1 and TfR1 were also analyzed, but no significant and consistent effect of oxLDL was observed in Mox macrophages (data not shown).

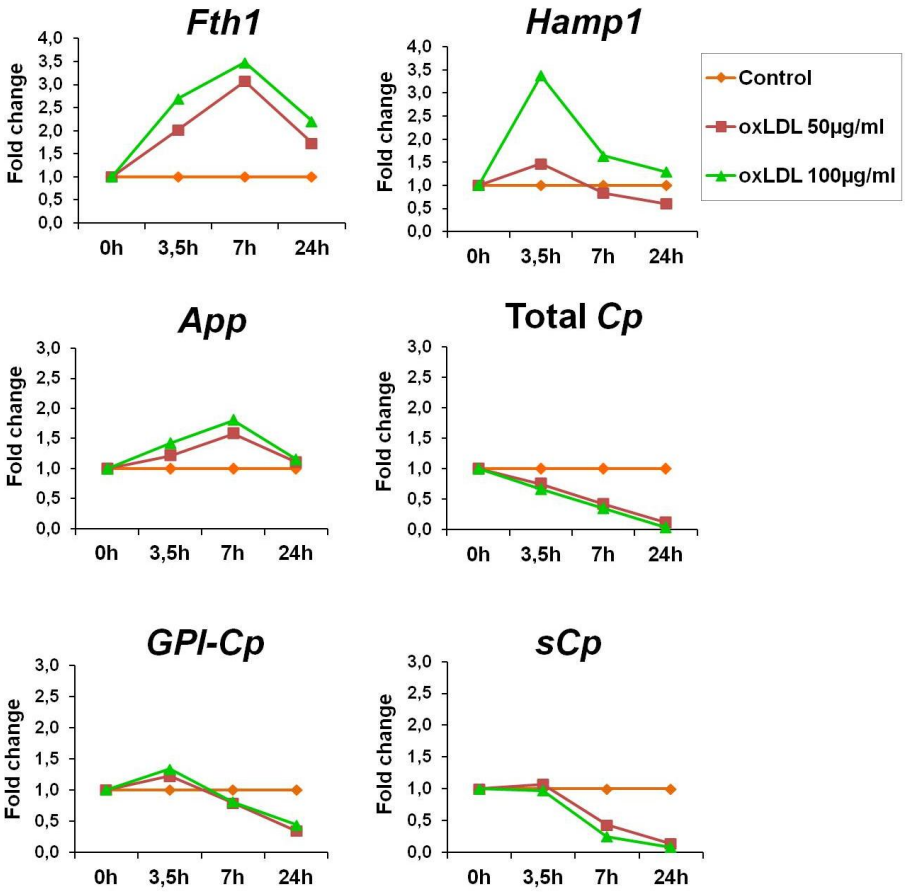

Figure III.22 - Effect of oxidized LDL on the expression of iron metabolism proteins. qPCR analysis of *Fth1*, *App*, *Hamp1* and *Cp* mRNA level in BMDM untreated (control) or treated with different concentrations of oxLDL at different time points. Fold change data were calculated as $2^{-\Delta\Delta Ct}$ using *Hprt* as the reference gene and then normalized against the respective experimental control condition at each time point. Mean of Ct values in the experiments analyzed: *Fth1* (Ct=13,3), *Hamp1* (Ct=31,4), *App* (Ct=20,7), total *Cp* (Ct=23,2), *GPI-Cp* (Ct=27,3), *sCp* (Ct=24,6).

3.2. Transcriptional upregulation of heme oxygenase-1 and ferroportin-1 by oxidized LDL is Nrf2-dependent in murine macrophages

In order to test the hypothesis that Fpn1 upregulation in Mox macrophage model is Nrf2-mediated, BMDM were prepared from wild type ($Nrf2^{+/+}$) and Nrf2 null mice ($Nrf2^{-/-}$), and treated or not with oxLDL or iron (FeNTA) for 3,5 h before RNA extraction and analysis by qPCR. As observed in Figure III.23, upregulation of *Hmox1* mRNA by both oxLDL and FeNTA was significantly inhibited in $Nrf2^{-/-}$ BMDM compared with $Nrf2^{+/+}$ BMDM ($p<0,0001$). However, while the upregulation of *Hmox1* mRNA by FeNTA was almost abrogated in $Nrf2^{-/-}$ BMDM, *Hmox1* mRNA was still significantly upregulated by oxLDL in these cells. A significant difference was also observed on *Fpn1* mRNA level on $Nrf2^{-/-}$ BMDM and $Nrf2^{+/+}$ BMDM in response to oxLDL or FeNTA challenge (Figure III.23, $p<0,0001$). Noteworthy, *Fpn1* mRNA level in $Nrf2^{-/-}$ BMDM is

severely downregulated compared with *Nrf2*$^{+/+}$ BMDM (Figure III.23). In fact, *Fpn1* mRNA level in *Nrf2*$^{-/-}$ BMDM untreated and treated with oxLDL or iron is bellow the basal expression level of *Fpn1* in untreated *Nrf2*$^{+/+}$ cells.

As a control for the experiment, *Vegf* expression was also analyzed as it was reported to be upregulated by oxPAPC in Mox macrophages in an Nrf2-independent manner [249]. Accordingly, the upregulation of *Vegf* mRNA in response to oxLDL was not inhibited in *Nrf2*$^{-/-}$ BMDM compared with *Nrf2*$^{+/+}$ BMDM in our model of Mox macrophages (Figure III.23). In fact, *Vegf* mRNA level in *Nrf2*$^{-/-}$ BMDM was even upregulated when compared with *Nrf2*$^{+/+}$ BMDM, as observed in Kadl *et al* [249].

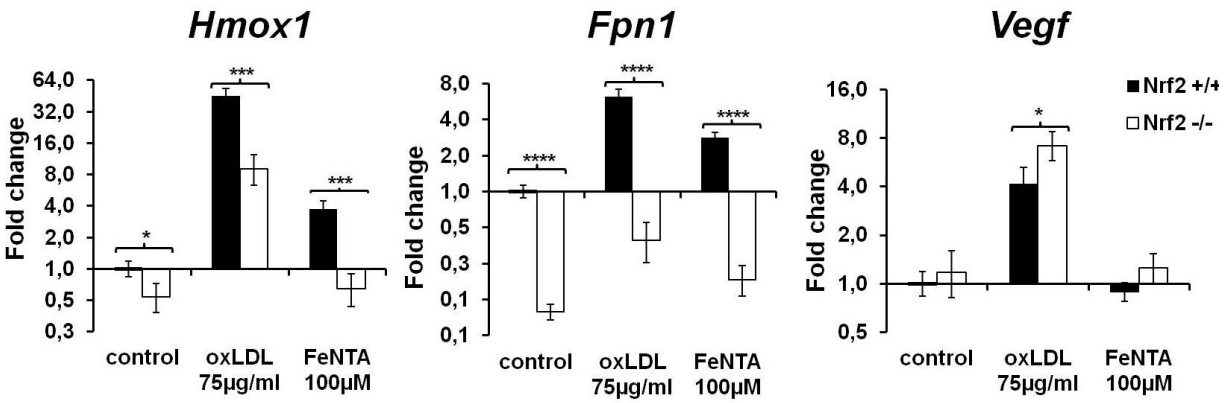

Figure III.23 - Effect of oxidized LDL and iron on heme oxygenase-1 and ferroportin-1 expression is Nrf2-dependent in murine macrophages. qPCR analysis of *Hmox1* and *Fpn1* mRNA level in BMDM of *Nrf2*$^{+/+}$ (black) and *Nrf2*$^{-/-}$ (white) mice, untreated (control) or treated with oxLDL or iron (FeNTA) for 3,5 h. *Vegf* mRNA expression was analyzed as a control. Fold change data were calculated as $2^{-\Delta\Delta Ct}$ using *Hprt* as the reference gene and then normalized against the respective *Nrf2*$^{+/+}$ experimental control condition. Data are presented as mean ± confidence interval (95%), in which fold change (*Nrf2*$^{+/+}$ control)=1. Statistical analysis was performed on the ΔCt values obtained during three independent experiments, using 2-way repeated measures-ANOVA followed by Bonferroni's post-hoc test for multiple comparisons. Statistically significant differences on *Hmox1*, *Fpn1* or *Vegf* mean expression between *Nrf2*$^{+/+}$ and *Nrf2*$^{-/-}$ BMDM at a specific condition are indicated by: *(p<0,05); **(p<0,01); ***(p<0,001), and ****(p<0,0001). Interaction between Nrf2 genotype and *in vitro* treatment was also analyzed and was statistically significant for both *Hmox1* (p<0,01) and *Fpn1* (p<0,05). Mean of Ct values for each gene in the experiments analyzed: *Nrf2*$^{+/+}$ *Hmox1* (Ct=19,3) vs. *Nrf2*$^{-/-}$ *Hmox1* (Ct=20,8), *Nrf2*$^{+/+}$ *Fpn1* (Ct=19,5) vs. *Nrf2*$^{-/-}$ *Fpn1* (Ct=22,9), *Nrf2*$^{+/+}$ *Vegf* (Ct=22,4) vs. *Nrf2*$^{-/-}$ *Vegf* (Ct=22,0).

3.3. Heme oxygenase-1, but not ferroportin-1, is highly upregulated by oxidized LDL at protein level

The significant upregulation of *Hmox1* and *Fpn1* mRNA level by oxLDL was subsequently studied at protein level. Iron-treated BMDM were used as a positive control since both HO-1 and Fpn1 were reported to be significantly upregulated at transcriptional and protein level in response to iron [107]. In addition, both *Hmox1* and *Fpn1* mRNA level presented a similar kinetics when

challenged by oxLDL or iron, showing a highly but transient upregulation at early time point (Figure III.24A).

In-Cell Western blot was used for analysis and quantification of protein levels of HO-1 and Fpn1 in BMDM untreated and treated with oxLDL or iron during 24 h. The results obtained showed that HO-1 is significantly upregulated by both oxLDL ($p<0,05$) and iron ($p<0,01$) (Figure III.24B). Noteworthy, contrary to the effect in mRNA levels shown in Figure III.24A, the induction of HO-1 protein was significantly higher in response to iron than to oxLDL (Figure III.24B). On the other hand, despite the oxLDL-induced significant upregulation at transcriptional level, Fpn1 upregulation was only slightly reflected at protein level in BMDM while iron induced a significant upregulation of Fpn1 at both transcriptional and protein level ($p<0,01$)(Figure III.24B).

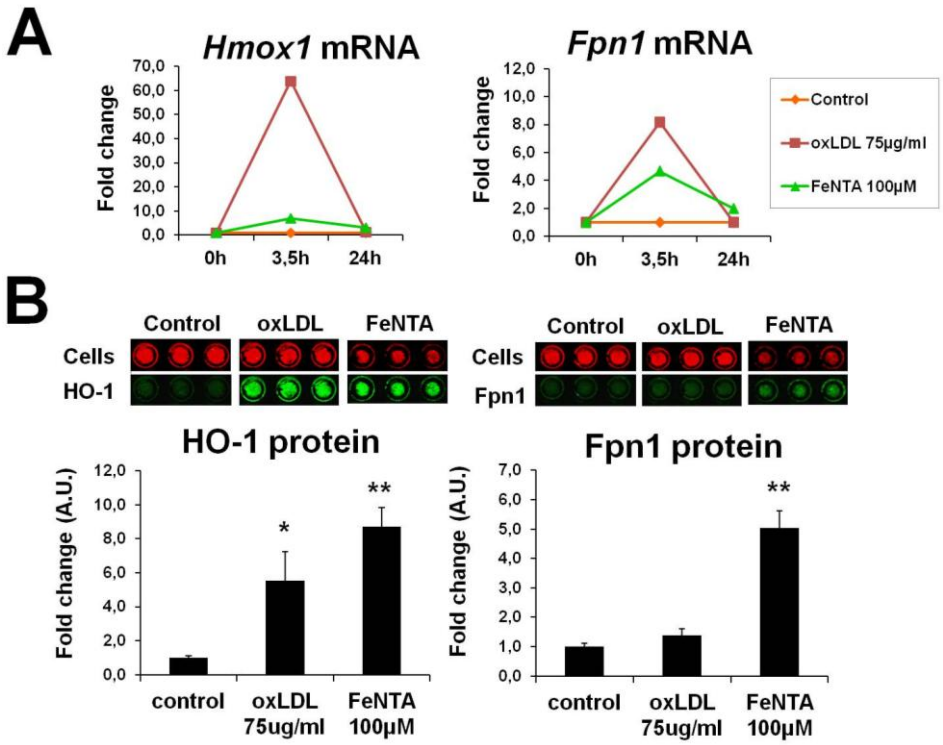

Figure III.24 - Effect of iron and oxidized LDL on heme oxygenase-1 and ferroportin-1 expression in murine macrophages. (A) qPCR analysis of *Hmox1* and *Fpn1* mRNA expression in BMDM untreated (control) or treated with either iron (FeNTA, 100 µM) or oxLDL (75 µg/ml) in different time points (n=3). Fold change data were calculated as $2^{-\Delta\Delta Ct}$ using *Hprt* as the reference gene and then normalized against the respective experimental control condition at each time point. Mean of Ct values for each gene in the experiments analyzed: *Hmox1* (Ct=19) and *Fpn1* (Ct=21). (**B)** In-Cell Western blot analysis of HO-1 and Fpn1 protein expression in BMDM untreated or treated with iron or oxLDL for 24 h. In-Cell Western blot images correspond to one experiment representative of the three independent experiments analyzed. Cell density (red) was used for normalization of protein expression (green) between wells. Fold change data were normalized against control (arbitrary units) and are presented as mean ± standard deviation (n=3). Statistical analysis was performed by Student's *t* test and statistically significant differences on HO-1 or Fpn1 expression levels between treated and untreated cells are indicated by *($p<0,05$) and **($p<0,01$).

Immunofluorescence analysis of both HO-1 and Fpn1 further confirmed the results obtained by In-Cell Western blot. BMDM showed an intracellular staining of HO-1 in response to oxLDL or iron (Figure III.25, top panel). Fpn1 staining was detected at intracellular as well as at cell surface level in both untreated (control) and oxLDL-treated BMDM (Figure III.25, bottom panel). However, upon iron treatment, Fpn1 protein levels were highly upregulated and mostly detected at the cell surface as previously reported [119]. In addition, these observations are further supported by its significant downregulation after Hepc treatment (data not shown).

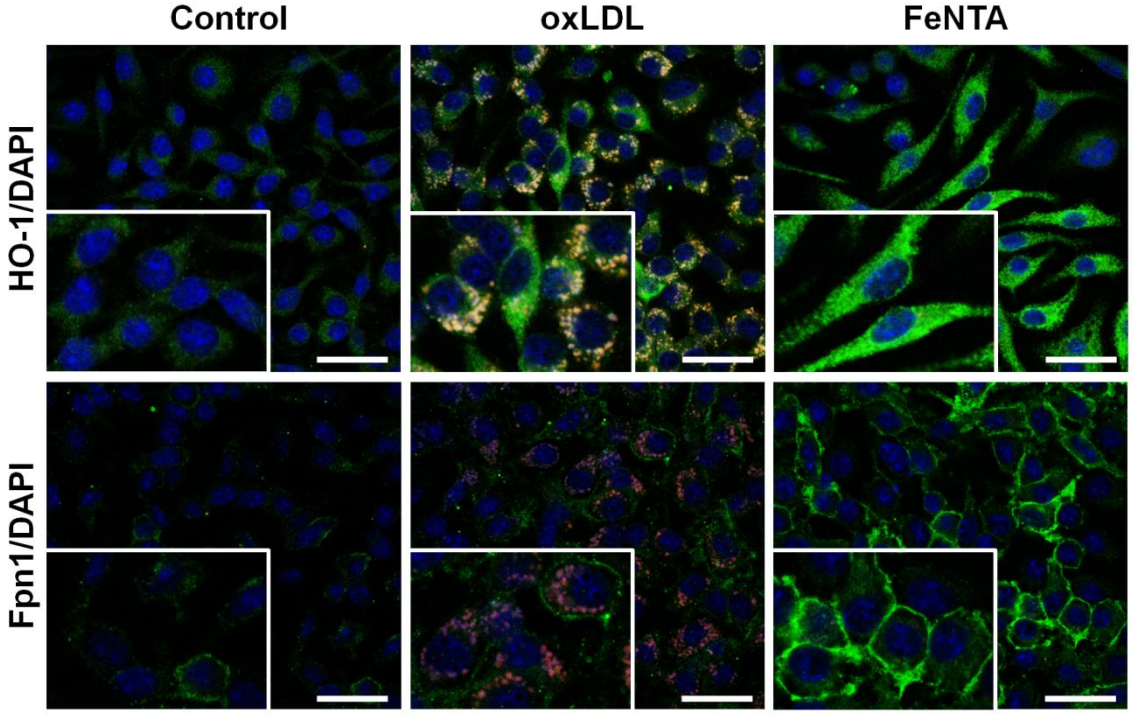

Figure III.25 - Immunofluorescence study of iron and oxidized LDL effect on heme oxygenase-1 and ferroportin-1 expression in murine macrophages. Immunofluorescence analysis of HO-1 and Fpn1 protein in BMDM untreated (control) and treated with oxLDL (75 µg/ml) or iron (FeNTA, 100 µM) for 24 h. HO-1 and Fpn1 staining is indicated in green, nuclei in blue (DAPI staining) and intracellular lipid droplets in red or yellow (autofluorescence of oxLDL). Yellow staining indicates overlay between HO-1 or Fpn1 staining (green) and intracellular lipid droplets (red) in BMDM. Insets at the lower left corner of each image represent high magnification of cells. The white bars represent 25 µm.

3.4. Transient upregulation of heme oxygenase-1 and ferroportin-1 mRNA triggered by oxidized LDL is inhibited by LPS/IFNγ

Kadl *et al* reported that upon stimulation with oxPAPC, resting macrophages (M0) and polarized M1 or M2 macrophages would differentiate into Mox macrophages [249]. However, in these assays, macrophages would be firstly polarized and then exposed only to oxPAPC for Mox polarization. Herein, we investigated the effect of simultaneous stimulation with M1 activator (LPS/IFNγ) and Mox activator (oxLDL) on macrophage polarization and

expression of some iron metabolism proteins. BMDM were untreated (control, M0) or treated with oxLDL (Mox), LPS/IFNγ (M1) or both oxLDL and LPS/IFNγ (Mox/M1) for different time points. Oil Red O confirmed the differentiation of foam cells in both conditions in which oxLDL was added to culture medium (Figure III.26).

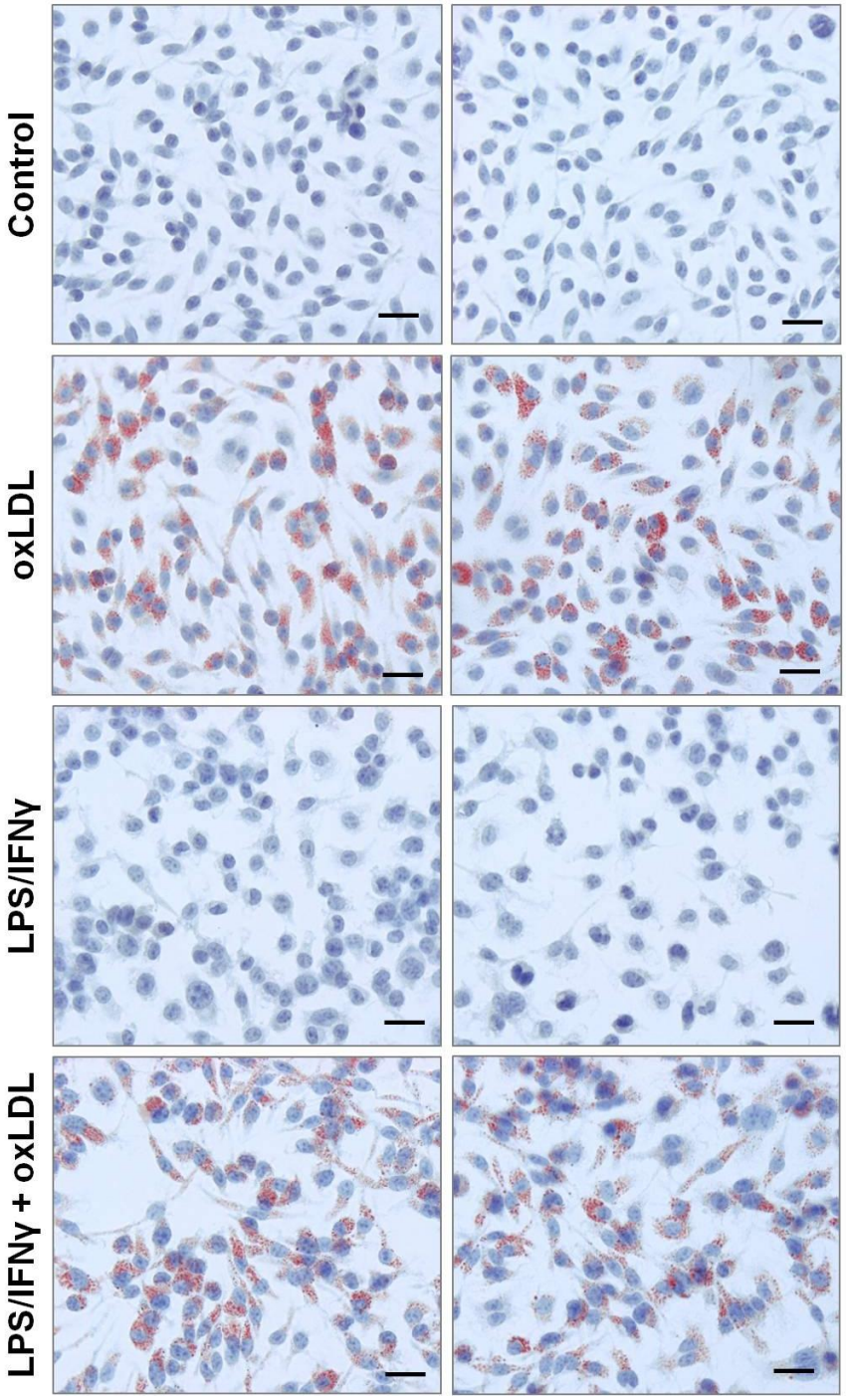

Figure III.26 - Effect of oxidized LDL and pro-inflammatory conditions on foam cell differentiation from murine macrophages. BMDM were incubated for 24 h in complete medium and in the absence (control) or presence of oxLDL (Mox), LPS/IFNγ (M1) or both (Mox/M1). After incubation, cells were fixed and stained with Oil Red O (lipid specific dye, red) with hematoxylin counterstain. Images were acquired using a Leica DM4000 B microscope with a 40x objective. The black bars represent 20 µm.

Mox and M1 phenotypes were confirmed by the early upregulation (3,5 h) of *Vegf* and *Hmox1* mRNA in Mox and *Il6* (IL-6 gene) mRNA in M1 macrophages. Mox/M1 phenotype presented a combination of Mox and M1 features, with early high upregulation of *Il6* mRNA and late upregulation of *Vegf* mRNA as observed in M1 macrophages (Figure III.27).

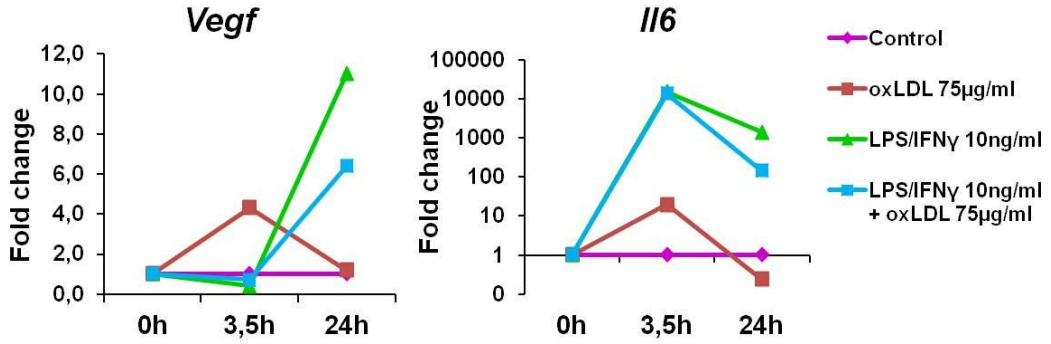

Figure III.27 - Gene expression analysis of specific markers in M1, Mox and Mox/M1 macrophages. Graphic representation of *Vegf* and *Il6* mRNA kinetics. Data are presented in fold change calculated as $2^{-\Delta\Delta Ct}$ using *Hprt* as the reference gene and then normalized against the respective experimental control condition at each time point. BMDM were untreated (control, M0) or treated with oxLDL (Mox), LPS/IFNγ (M1) or both stimuli in different time points (Mox/M1). The results presented are the mean of three independent experiments, each with biological and technical duplicates.

HO-1 is a Mox phenotype marker, reported to be transcriptionally upregulated by Mox activator and downregulated by M1 activator after 3h stimulation [249]. In our studies, *Hmox1* mRNA is highly upregulated at 3,5 h, returning to basal levels at 24 h in Mox macrophages, whereas in M1 macrophages, *Hmox1* mRNA is firstly downregulated at 3,5 h, followed by an upregulation at late time point (24 h) (Figure III.28A-B). In Mox/M1, the early downregulation of *Hmox1* mRNA level typically induced by LPS/IFNγ is counteracted by oxLDL. However, the induction of *Hmox1* mRNA at 3,5 h in Mox/M1 macrophages is milder than in Mox macrophages ($p<0,01$). Moreover, while *Hmox1* transcriptional upregulation in Mox macrophages is transient, in Mox/M1 macrophages the induction of *Hmox1* mRNA level is stable at early and late time points (Figure III.28A-B).

Fpn1 mRNA is highly upregulated by oxLDL in Mox macrophages, while LPS/IFNγ significantly downregulates *Fpn1* mRNA at early and late time points in M1 macrophages (Figure III.28A-B). In Mox/M1, no induction or significant downregulation of *Fpn1* mRNA was observed at early time point, but at 24 h, *Fpn1* mRNA level was significantly downregulated compared with control (M0) and Mox ($p<0,01$), although to a less extent than in M1 macrophages ($p<0,05$) (Figure III.28A-B).

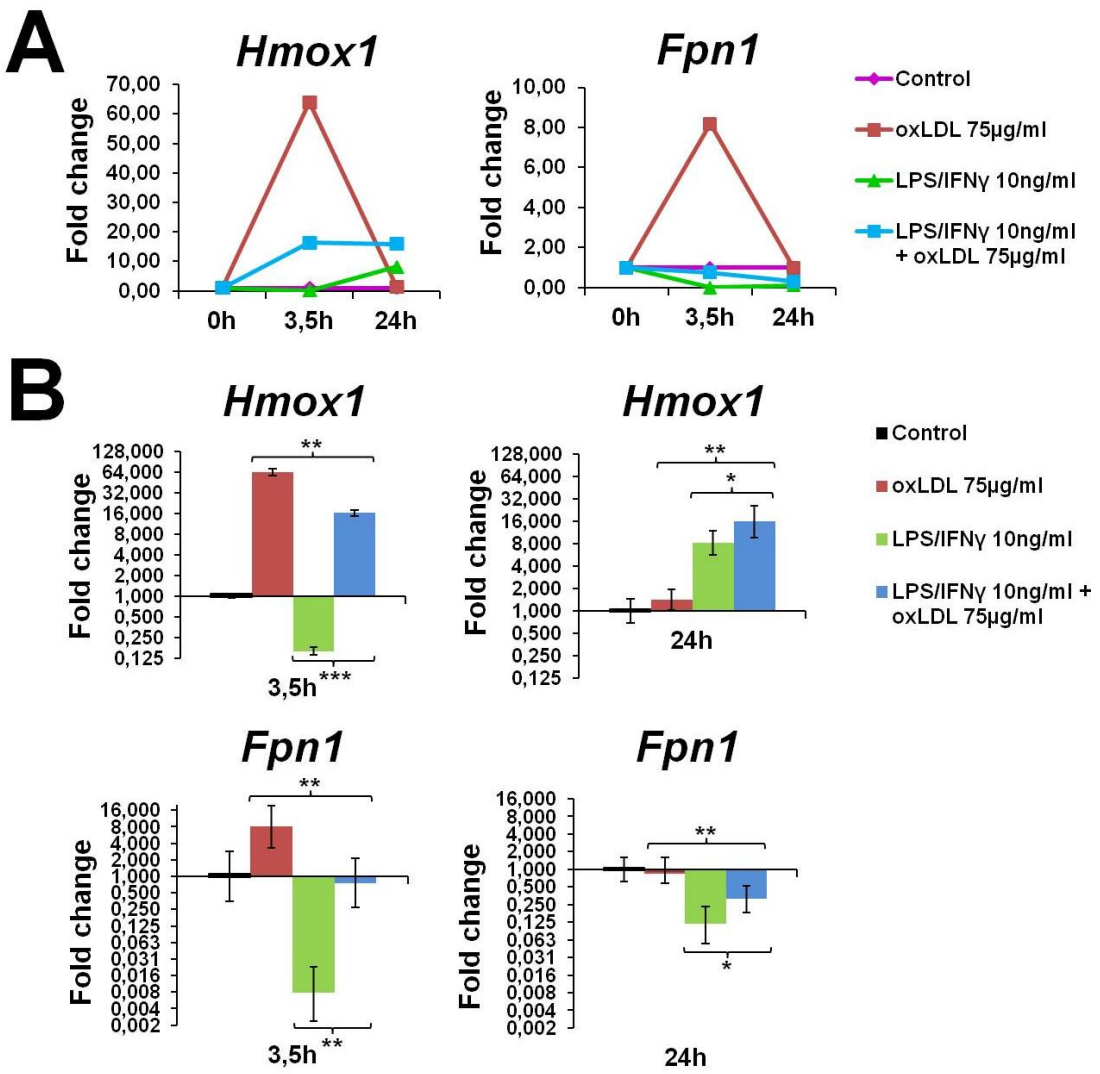

Figure III.28 - Effect of oxidized LDL and pro-inflammatory stimuli on heme oxygenase-1 and ferroportin-1 expression in murine macrophages. BMDM were untreated (control, M0 macrophages) or treated with oxLDL (Mox macrophages), LPS/IFNγ (M1 macrophages) or both stimuli (Mox/M1 macrophages) in different time points, followed by qPCR analysis. **(A)** Kinetics of *Hmox1* and *Fpn1* expression levels. Fold change data were calculated as $2^{-\Delta\Delta Ct}$ using *Hprt* as the reference gene and then normalized against the respective experimental control condition at each time point. Mean of Ct values in the experiments analyzed: *Hmox1* (Ct=19,8) and *Fpn1* (Ct=21,9). **(B)** Statistical analysis of the *Hmox1* and *Fpn1* expression levels shown in (A) at 3,5 h and 24 h. Data are presented in a logarithmic scale and as mean ± confidence interval (95%). Statistical analysis was performed on the ΔCt values obtained during three independent experiments using Student's *t* test. Statistically significant differences on *Hmox1* and *Fpn1* expression levels between oxLDL vs. oxLDL+LPS/IFNγ and LPS/IFNγ vs. oxLDL+LPS/IFNγ treated BMDM are indicated by * (p<0,05), ** (p<0,01), and *** (p<0,001).

On the other hand, *Fth1* mRNA level was transiently upregulated in Mox macrophages with a maximum of 5-fold induction at 3,5 h, while in M1 macrophages *Fth1* mRNA was upregulated at later time point (9-fold at 24 h). In Mox/M1, *Fth1* mRNA was progressively upregulated through time, reaching the maximum of 11-fold at late time point (Figure III.29). Total *Cp* mRNA level was highly upregulated in M1 macrophages (18-fold at 3,5 h) while a progressive downregulation was observed in Mox macrophages (0,1-fold at 24 h). In

Mox/M1, total *Cp* mRNA level was upregulated, but to a less extent than in M1 macrophages (7-fold) (Figure III.29). Interestingly, while the regulation of the *sCp* mRNA was fairly represented by the total *Cp* mRNA level, the *GPI-Cp* isoform was modulated differently in M1 and Mox/M1 macrophages. In such polarized phenotypes, inflammatory conditions did not significantly upregulate *GPI-Cp* mRNA level as observed for *sCp* mRNA in M1 and Mox/M1 phenotypes. Finally, the other potential ferroxidase *App* mRNA was mildly upregulated in Mox/M1 in a similar way as observed in M1 macrophages, whereas no significant effect was induced in Mox macrophages (Figure III.29).

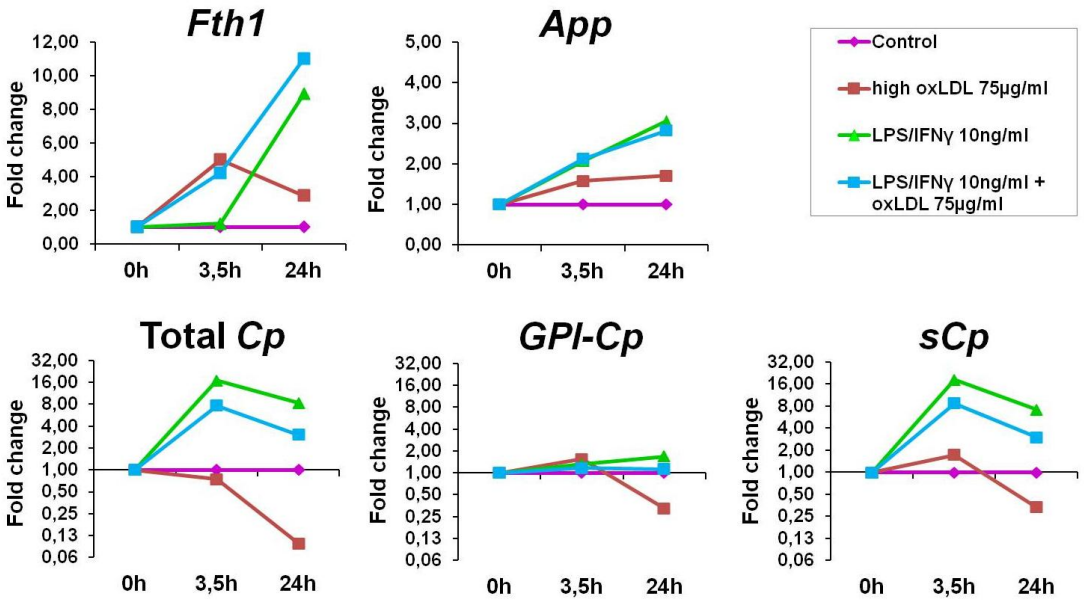

Figure III.29 - Kinetics of ferritin, β-amyloid precursor protein and ceruloplasmin expression after oxLDL and inflammatory stimuli in murine macrophages. BMDM were untreated (control, M0 macrophages) or treated with oxLDL (Mox macrophages), LPS/IFNγ (M1 macrophages) or both stimuli (Mox/M1 macrophages) in different time points, followed by qPCR analysis. Fold change data were calculated as $2^{-\Delta\Delta Ct}$ using *Hprt* as the reference gene and then normalized against the respective experimental control condition at each time point. Mean of Ct values in the experiments analyzed: *App* (Ct=24,0), *Fth1* (Ct=13,7), total *Cp* (Ct=26,9), *GPI-Cp* (Ct=28,4), and *sCp* (Ct=27,0).

3.5. Effect of oxidized LDL on transcriptional expression of iron metabolism proteins in human macrophages

In order to test if oxLDL would also induce a similar Mox phenotype in human macrophages, a preliminary assay was performed. In this context, primary human macrophages were fully differentiated from peripheral blood monocytes in the presence of M-CSF and then untreated (control) or treated with nLDL, oxLDL or iron during different time points.

Staining with Oil Red O confirmed the uptake of oxLDL and differentiation of foam cells with high lipid accumulation. Noteworthy, unlike murine macrophages (BMDM), human macrophages untreated or treated with nLDL already showed a significant lipid accumulation (Figure III.30). This effect of

nLDL was also previously reported to result from macropinocytosis in human macrophages differentiated with M-CSF [306].

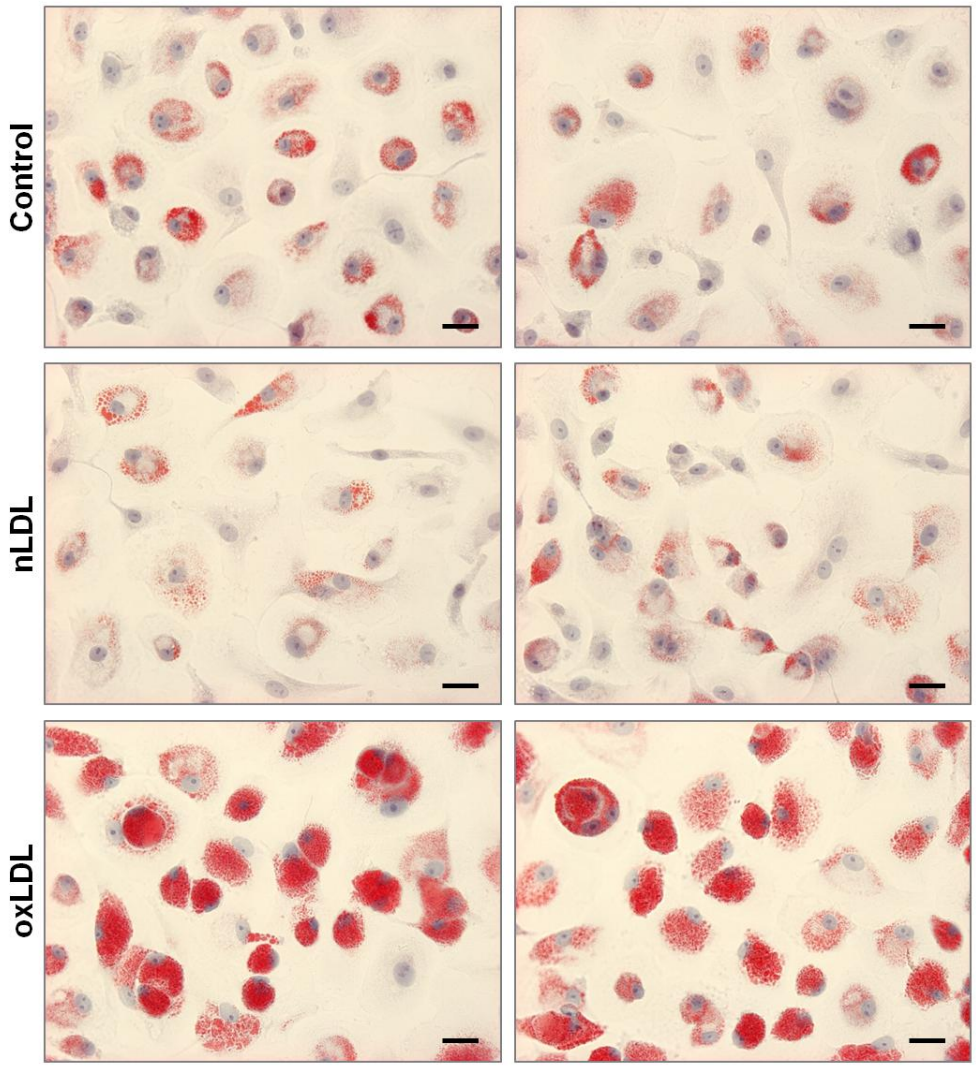

Figure III.30 – Effect of native and oxidized LDL on foam cell differentiation from human macrophages. Mature human macrophages were untreated (control) or treated with nLDL or oxLDL for 24 h, followed by fixation and Oil Red O staining (lipid specific dye, red) with hematoxylin counterstain. Images were acquired using a Leica DM4000 B microscope with a 40x objective. The black bars represent 20 µm.

Transcriptional expression of iron metabolism proteins in human macrophages was analyzed by qPCR. The Mox marker *HMOX1* mRNA level was transiently upregulated at 3,5 h (8-fold) by oxLDL as observed in murine macrophages, while iron induced *HMOX1* mRNA to a less extent and at a later time point (Figure III.31). In addition, both the iron exporter *FPN1* and the iron storage *FTH1* mRNA levels were also upregulated in a synchronized manner in response to iron and oxLDL at 24 h (2,5-fold, Figure III.31). No significant effect was observed on *APP* or *CP* mRNA level in response to nLDL, oxLDL or iron (Figure III.31). However, unlike BMDM, not only a downregulation was not observed in response to oxLDL, but a slight upregulation was noticed on *CP* mRNA level at 24 h, in a pattern similar to the one observed in *FTH1* and *FPN1*.

An upregulation of *HAMP* mRNA mediated by oxLDL (3,5-fold) was observed in human Mox macrophages, similar to murine Mox macrophages. However, the mRNA basal level of *HAMP* was significantly higher in human macrophages than the homologous *Hamp1* in murine macrophages (Mean Ct=24,3 in human macrophages vs. Mean Ct=31,4 in BMDM), thus suggesting that Hepc may be upregulated at protein level in human Mox macrophages.

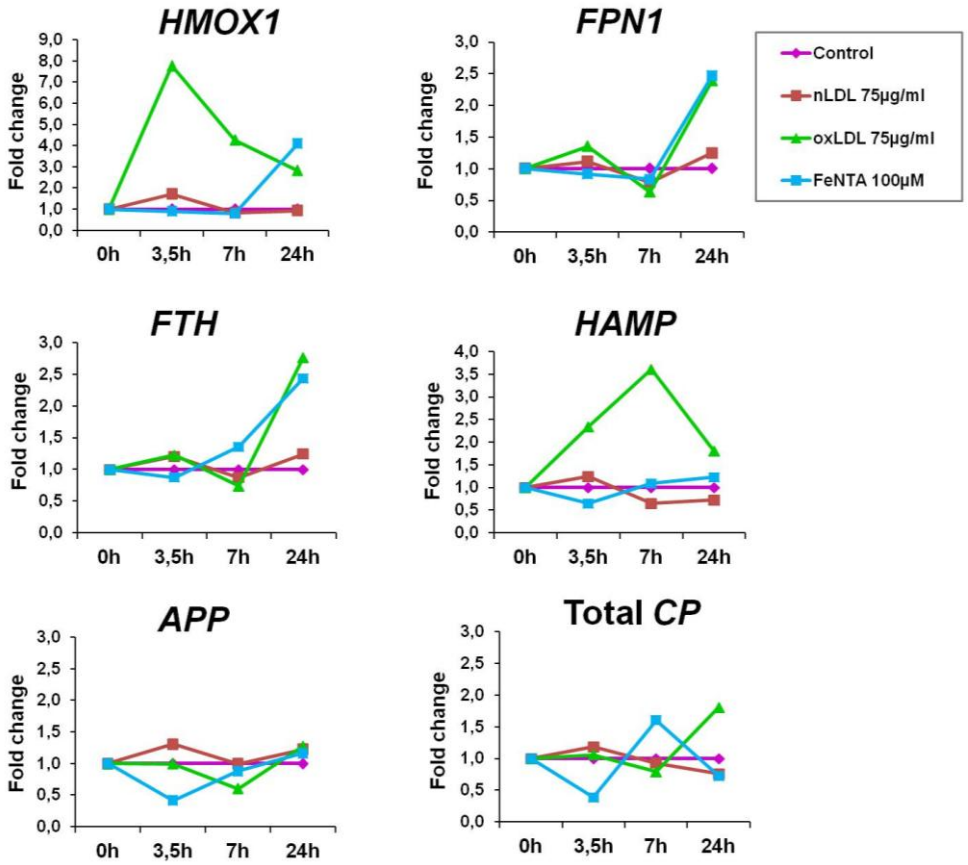

Figure III.31 - Effect of iron, native and oxidized LDL on iron metabolism proteins in human macrophages. Human macrophages were untreated (control) or treated with nLDL, oxLDL or iron (FeNTA) during different time points, followed by qPCR analysis of *HMOX1*, *FPN1*, *APP*, *CP*, *FTH1* and *HAMP*. Fold change data were calculated as $2^{-\Delta\Delta Ct}$ using *HPRT* as the reference gene and then normalized against the respective experimental control condition at each time point. Mean of Ct values in the experiment analyzed: *HMOX1* (Ct=20,2), *FPN1* (Ct=27,6), *CP* (Ct=29,2), *APP* (Ct=23,6), *FTH1* (Ct=13,7), and *HAMP* (Ct=24,3).

4. Discussion

4.1. Expression of iron metabolism proteins in Mox macrophages phenotype

In atherogenesis, the macrophage plays a key role in which the uptake of modified LDL and differentiation of foam cells constitute early features in atherosclerotic lesions development and progression [307]. Recently, a new macrophage phenotype named Mox was described as the result from exposure to oxidized phospholipids and to correspond to a significant part of the macrophage population in atherosclerotic lesions [249]. Herein, we characterized the expression of some key iron metabolism proteins in murine and human Mox macrophages. As oxidized phospholipids are components of oxLDL, a model of oxLDL-derived Mox macrophage was used in this study. Upregulation of *Vegf* and *Hmox1* at early time point in oxLDL-treated BMDM confirmed that our model corresponded to Mox phenotype.

Gene expression analysis showed that, in addition to *Hmox1*, oxLDL also strongly upregulated *Fpn1* mRNA level and, to a less extent, *Fth1*. The ferroxidase *Cp* mRNA was progressively downregulated while no significant effect was observed on *App* mRNA. The significant upregulation of *Hmox1* and *Fpn1* was shown to be specific of oxLDL, not being reproduced by nLDL or by another source of modified LDL (acLDL), which reinforces the concept that oxidative modification of LDL is important to trigger the differentiation of Mox phenotype. Accordingly, the upregulation of *Hmox1* and *Fpn1* was also directly proportional to the concentration and, most importantly, to the degree of oxidation of oxLDL. Interestingly, unlike nLDL, exposure of BMDM to acLDL lead to the differentiation of lipid-laden foam cells which confirmed the acLDL uptake. However, acLDL-derived foam cells presented minor lipid burden than in oxLDL-derived foam cells, which may indicate a differential uptake between acLDL and oxLDL that could also contribute in part to the different effect of acLDL and oxLDL on *Hmox1* and *Fpn1* expression.

Moreover, *Hmox1* and *Fpn1* upregulation triggered by oxLDL was significantly decreased in *Nrf2*$^{-/-}$ BMDM compared with *Nrf2*$^{+/+}$ BMDM, which indicates that this transcription factor is involved in the upregulation of both genes in response to oxLDL. Noteworthy, despite the significant decrease, *Hmox1* mRNA level was still significantly upregulated in oxLDL-treated BMDM compared to *Nrf2*$^{-/-}$ and *Nrf2*$^{+/+}$ untreated BMDM. This observation is indicative that other mechanisms Nrf2-independent must also be involved in the massive *Hmox1* upregulation by oxLDL in BMDM. Indeed, *Hmox1* expression was previously reported to be upregulated by multiple transcription factors including Nrf2, AP-1, Sp-1, Ets, CREB and NF-κB [308], of which some are also known to be triggered by oxLDL uptake in macrophages [309].

Remarkably, when comparing murine and human Mox macrophages, the kinetics of *Hmox1/HMOX1* and *Fpn1/FPN1* transcription in response to oxLDL and iron were not perfectly synchronized as previously observed in murine Mox macrophages. Indeed, in human Mox phenotype, *HMOX1* was significant and transiently upregulated at early time point (3,5h) in response to oxLDL like observed in murine Mox macrophages. On the other hand, *FPN1* seemed to be significantly upregulated only at late time point (24h) by oxLDL. Iron treatment lead to a parallel increase at 24h of *HMOX1*, *FPN1* and *FTH*, suggesting a common regulatory mechanism in human macrophages in response to iron. Interestingly, Harada *et al* [318] showed a positive regulation of *FPN1* in human macrophages in response to an Nrf2 activator, an upregulation which resembles the kinetics observed after iron or oxLDL treatment in our human macrophage model. One can hypothesize that Nrf2 could play a role in *FPN1, FTH and HMOX1* upregulation by iron. Nrf2 could be also involved in the regulation of *FPN1* and *FTH* by oxLDL. On the other hand, the regulation of *HMOX1* by oxLDL likely occurs through distinct molecular mechanisms.

Analysis of protein expression by both In-Cell Western blot and immunofluorescence in murine macrophages showed that, unlike HO-1, Fpn1 significant transcriptional upregulation triggered by oxLDL was only slightly reflected at protein level, which suggests that a post-transcriptional mechanism must be limitating Fpn1 translation in these cells. On the other hand, upon stimulation with iron, both *Hmox1* and *Fpn1* mRNA levels were significantly upregulated in Nrf2-dependent mechanism as observed for oxLDL. However, unlike Mox macrophages, HO-1 and Fpn1 were significantly upregulated at protein level in iron-treated macrophages. This result indicates that iron might be the limitating factor regulating the post-transcriptional mechanism involved in Fpn1 translation in Mox macrophages.

In addition, contrary to the effect observed on mRNA, the induction of HO-1 protein was significantly higher in response to iron than to oxLDL, which suggests that a post-transcriptional mechanism mediated by iron could also enhance HO-1 synthesis. Recently, several microRNA's were reported to modulate HO-1 translation in a direct (miR-217, miR-377, and miR-378) [310,311] or indirect manner (miR-155 and miR122) [312,313] and could constitute possible pathways for the iron-mediated enhancement of HO-1 translation.

Concerning Fpn1 limitated translation in murine Mox macrophages, one post-transcriptional mechanism involved in the regulation of many iron metabolism proteins and which is sensitive to iron levels is the IRE/IRP system. Indeed, *Fpn1* mRNA has an IRE element in its 5'-UTR sequence to which the IRP1 protein binds in conditions of low intracellular iron, blocking Fpn1 translation [314]. In iron-treated cells, the higher level of intracellular iron lead to a conformational change on IRP1 and subsequent dissociation from the IRE,

unblocking Fpn1 translation and leading to the upregulation of Fpn1 protein. In our study, exposure to oxLDL activated *Fpn1* transcriptional upregulation as part of the response to oxidative stress in macrophages, but without an iron source, the intracellular iron level likely remains unchanged. In such case, the majority of IRP1 would not dissociate from the IRE, impairing Fpn1 translation and synthesis despite its significant transcriptional upregulation (Figure III.32). Additionally, *Fpn1* mRNA level quickly returned to the basal level of expression which indicates a short time window for Fpn1 translation.

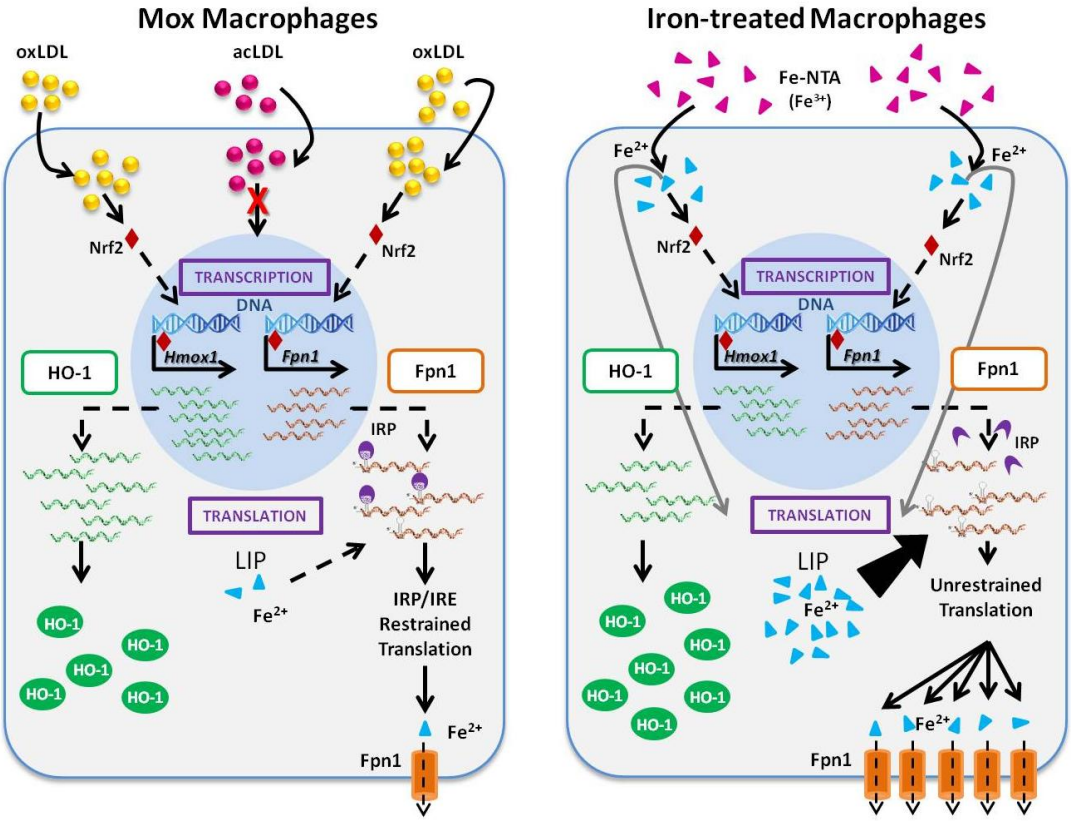

Figure III.32 - Schematic illustration of heme oxygenase-1 and ferroportin-1 regulation in Mox macrophages and iron-treated macrophages. Uptake of oxLDL (but not acLDL) in Mox macrophages as well as uptake of iron by non-polarized macrophages activates the transcription factor Nrf2, which subsequently triggers a significant upregulation of both *Hmox1* and *Fpn1* (also known as *Slc40a1*) mRNA. However, unlike *Hmox1*, *Fpn1* transcriptional upregulation is only slightly reflected at protein level in Mox macrophages. On the other hand, in iron-treated macrophages, both HO-1 and Fpn1 are significantly upregulated at mRNA and protein level, indicating that the IRP/IRE system might be involved in the limited Fpn1 translation in Mox macrophages. Iron transport in Mox macrophages is most likely unchanged whereas, in iron-treated macrophages, the high Fpn1 levels at cell surface indicate enhanced iron export in these cells. In addition, HO-1 translation is enhanced in iron-treated macrophages compared to Mox phenotype.

Accordingly, considering the limited synthesis of Fpn1 in Mox macrophages, *Fth1* transcriptional upregulation is also not expected to be

reflected at protein level as its translation is also controlled by the IRE/IRP system [70]. The upregulation of *Fpn1* and *Fth1* together with *Hmox1* and other genes associated to with anti-oxidant properties would constitute part of a complex cellular response against oxidative stress triggered by oxLDL in Mox macrophages, in which the iron storage and export could play an important role in reducing ROS formation.

Another possible mechanism for cellular protection against oxidative stress triggered by oxLDL uptake could be the downregulation of both Cp isoforms in murine Mox macrophages. Indeed, a mechanism of *Cp* mRNA decay induced by extracellular and intracellular oxidative stress was recently reported, which supports this hypothesis [315]. Despite its anti-oxidant "label" often associated with iron oxidation, Cp is a potent oxidase that acts on many substracts such as amines, lipids and lipoproteins [136]. In fact, Cp has been associated with increased cardiovascular risk due to its pro-oxidant capacity, in which Cp promotes LDL oxidation [256]. Nonetheless, downregulation of *Cp* induced by oxLDL could also have a potential deleterious effect on Fpn1 expression and compromise on iron efflux. Indeed, Cp ferroxidase activity was reported to be essential for Fpn1 stabilization at cell surface [121,122]. Although the co-localization of GPI-Cp and Fpn1 observed in our studies (chapter 2) was only partial in iron-treated macrophages, we could not dismiss the contribution of sCp on macrophage iron export nor evaluate the role of both Cp isoforms under other conditions such as hypoxia, often observed at the plaque. Therefore, lack of Cp ferroxidase activity in intraplaque macrophages triggered by oxLDL could contribute to higher Fpn1 degradation and possible impairment of iron export, which would lead to increased ROS formation and intracellular oxidative stress. However, this mechanism of *Cp* mRNA downregulation triggered by oxLDL was not observed in human Mox macrophages.

In addition, our results showed that oxLDL also induced a mild but significant upregulation of *Il6* (20-fold, Figure III.13) in BMDM, which may explain the observed upregulation of *Hamp1* in response to oxLDL. An upregulation of IL-1β (20-fold) in Mox macrophages was reported by Kadl *et al* [249] which, combined with our results, show that Mox macrophages express pro-inflammatory cytokines, although to a lesser extent than M1 macrophages. Accordingly, we showed that oxLDL induced *Hamp1/HAMP* transcription in both murine and human Mox macrophages, which could be associated with the upregulation of *Il6* induced by oxLDL. Although the low level of *Hamp1* mRNA in murine BMDM indicates that this upregulation is likely to have no significant effect at protein level in these cells, the higher basal expression of *HAMP* in human Mox macrophages suggests that an upregulation of Hepc peptide should not be disregarded. In fact, Li *et al* reported that culture of J774 murine macrophages with oxLDL upregulated Hepc peptide along with increased production of pro-inflammatory cytokines and ROS, promoting cell apoptosis [240].

Induction of Hepc in response to oxLDL uptake could therefore constitute an atherogenic mechanism, promoting Fpn1 degradation and iron sequestration in macrophages.

Overall, macrophage exposure to oxLDL triggers the polarization of a specific phenotype (Mox) characterized by enhanced transcriptional expression of genes associated with anti-oxidant properties in order to resolve the oxidative stress induced by oxLDL uptake, including *Hmox1*, *Fpn1* and *Fth1*. However, Fpn1 was surprisingly not significantly upregulated at protein level despite the significant transcriptional induction by oxLDL, showing that iron export in Mox macrophages is not enhanced. In addition, the possible Cp downregulation in murine macrophages as well as Hepc upregulation in both murine and human macrophages in response to oxLDL could contribute to Fpn1 degradation and subsequent impairment of iron export in Mox macrophages.

4.2. Expression of iron metabolism proteins in the combined Mox/M1 macrophages phenotype

Another objective of this study was to investigate the effect of simultaneous exposure of macrophages to the activators of Mox (oxLDL) and M1 (LPS/IFNγ) phenotypes. M1 macrophages have been associated with plaque instability and are characterized by increased production of pro-inflammatory cytokines and ROS as well as increased iron retention due to Fpn1 downregulation at both mRNA and protein level.

Previous authors reported that exposure of macrophages to oxLDL inhibited the inflammatory response driven by LPS [316,317]. Moreover, Kadl *et al* reported that fully polarized M1 and M2 macrophages would switch to Mox phenotype once exposed to oxLDL [249]. However, in none of these studies the macrophages were simultaneous stimulated with oxLDL and M1 activators. However, Harada *et al* reported that simultaneous stimulation with LPS and Nrf2 specific activators counteracted LPS-induced downregulation of Fpn1 in murine and human macrophages, supporting the previous data that Nrf2 activation would inhibit the LPS-driven inflammatory response [318].

In this study, we showed that oxLDL significantly upregulates *Fpn1* at transcriptional level through an Nrf2-dependent mechanism. According to the literature, it was expected that co-stimulation of murine macrophages with both oxLDL and LPS/IFNγ would lead to a Mox-like phenotype with normal or enhanced *Fpn1* expression. Surprisingly, a mixed Mox/M1 phenotype was observed with early upregulation of *Hmox1* (Mox marker) along with massive *Il6* upregulation (M1 marker). Additionally, *Hmox1* upregulation was significantly lower than in Mox macrophages, but stable remaining high up to 24 h. Unlike previous reports, NF-κB activation by LPS remained unaffected by oxLDL as

can be observed in *App*, *Fth1* and *Hmox1* expression, all NF-κB target genes that are significantly upregulated in Mox/M1 compared with murine Mox macrophages at 24 h.

Moreover, the transcriptional upregulation of the iron exporter *Fpn1* triggered by oxLDL was inhibited in Mox/M1 macrophages and even downregulated at 24 h, showing that LPS/IFNγ counteracts the Nrf2-dependent upregulation of *Fpn1* normally induced by oxLDL, which is contrary to previous studies [318]. Nonetheless, in our model, we used oxLDL which activates Nrf2, but also other transcription factors, while Harada *et al* used electrophilic compounds (DEM and SFN) that are known to be specific Nrf2 activators [318]. Indeed, the upregulation of *Fpn1* mRNA by DEM in murine macrophages was stable and remained high at 24 h, while *Fpn1* upregulation in our murine Mox macrophage model was transient, presenting basal mRNA levels at 24 h. Additionally, Harada *et al* used LPS in their experimental model while we used LPS combined with IFNγ, both stimuli reported to downregulate *Fpn1* mRNA expression. However, in the context of atherogenesis, the complex intraplaque microenvironment is rich in oxidized lipids and lipoproteins as well as pro-inflammatory cytokines such as IFNγ. It is therefore relevant to observe that *Fpn1* downregulation induced by LPS/IFNγ is mostly unaffected by oxLDL uptake. Additionally, the known Hepc inducer *Il6* was highly upregulated in Mox/M1 macrophages, which suggests that in addition to *Fpn1* transcriptional downregulation, Fpn1 levels at cell surface could also be decreased in a Hepc-dependent manner (Figure III.33).

Cp mRNA was also significantly upregulated in Mox/M1, but to a less extent than in M1 macrophages. Considering the distinct regulation of *Cp* mRNA level in M1 and Mox macrophages, it is possible that the lower *Cp* mRNA level observed in Mox/M1 when compared with M1 macrophages could be due to simultaneous increased *Cp* transcription (LPS/IFNγ) and increased *Cp* mRNA degradation (oxLDL) through distinct molecular mechanisms. Surprisingly, *Cp* isoforms were differently modulated in both M1 and Mox/M1 macrophages, with a significant upregulation of sCp mRNA triggered by inflammatory conditions, either combined or not with oxLDL, whereas *GPI-Cp* mRNA level remained mostly unaffected compared with untreated macrophages (M0). This differential modulation of Cp isoforms suggests a major role for sCp in inflammation compared with the membrane GPI-Cp.

Altogether, macrophages stimulated with both oxLDL and LPS/IFNγ present a mixed expression profile of Mox and M1 phenotypes, in which the expression of the iron metabolism genes analyzed was closer to the expression profile in M1 phenotype than Mox. Noteworthy, *Fpn1* expression was downregulated in Mox/M1, which indicates that iron export is likely impaired in

these cells leading to a progressive iron accumulation, which could be relevant to the pathogenesis of the atherogenic process (Figure III.33).

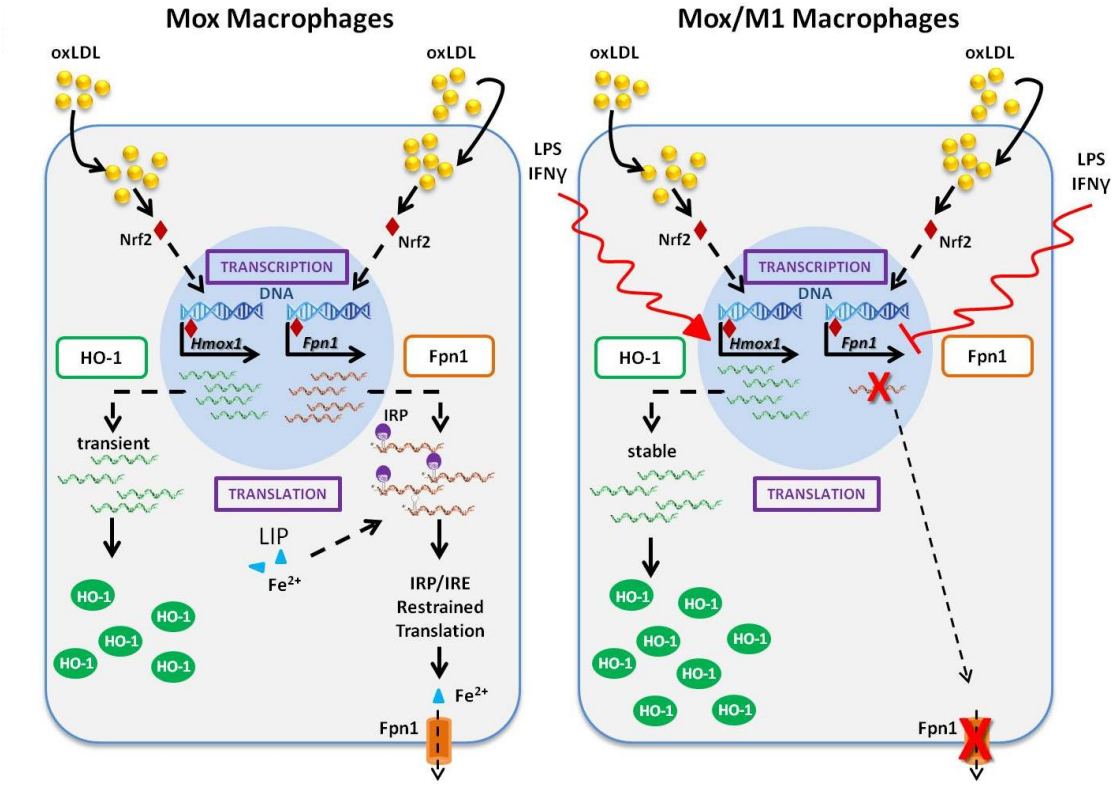

Figure III.33 - Schematic illustration of heme oxygenase-1 and ferroportin-1 regulation in Mox macrophages and combined Mox/M1 macrophages. Uptake of oxLDL in Mox macrophages triggers a significant upregulation of *Hmox1* and *Fpn1* (also known as *Slc40a1*) mRNA dependent on Nrf2 activation. In Mox macrophages, unlike HO-1 which is highly upregulated at protein level, Fpn1 translation is limited by a post-transcriptional mechanism most likely involving the IRP/IRE system. Co-stimulation with both oxLDL (Mox) and LPS/IFNγ (M1) leads to a mixed phenotype Mox/M1 in which *Hmox1* is stably upregulated at mRNA and protein level, while *Fpn1* is transcriptionally downregulated, likely leading to impaired iron export and promoting iron retention in these cells.

5. Conclusion

The uptake of oxLDL by BMDM drives the differentiation of the Mox phenotype, in which oxLDL and not acLDL specifically upregulated *Fpn1* and *Hmox1* transcription through an Nrf2-dependent mechanism. The Mox phenotype is also associated with an upregulation of *Fth1* and downregulation of *Cp* mRNA, while no significant changes on *App* expression were observed. However, unlike HO-1, Fpn1 upregulation by oxLDL was only slightly reflected at the protein level. On the other hand, iron induced a significant and Nrf2-dependent upregulation of *Fpn1* mRNA that was also observed at protein level, suggesting that basal intracellular iron level could be the factor restraining Fpn1 translation in Mox macrophages, likely associated with the IRE/IRP system (Figure III.32).

Additionally, the co-stimulation of LPS/IFNγ (M1 activators) and oxLDL (Mox activator) that tends to mimic the Mox/M1 mixed phenotype observed in atherosclerotic lesions [249], promotes the upregulation of *Hmox1* and *Fth1* mRNA combined with downregulation of *Fpn1* mRNA at 24 h (Figure III.33). Thus, low expression of Fpn1 and subsequent decrease of iron export in response to both oxLDL and pro-inflammatory conditions could lead to increased macrophage intracellular iron and storage in Ft, a possible mechanism for iron accumulation in the atherosclerotic plaque and promotion of plaque progression and destabilization.

6. Authorship

The results presented in this chapter were produced by the author of the thesis. A manuscript with these results is currently in preparation and will be submitted shortly.

L. Marques, F. Canonne-Hergaux** and L. Costa**, *"Ferroportin-1 is transcriptionally upregulated by oxLDL through Nrf2 and is counteracted by LPS/IFNγ in murine macrophages"*. **co-senior authors (in preparation)

Chapter 4

Production of an antibody against human ferroportin-1

1. Introduction

Fpn1 is a key protein in iron metabolism, being the only iron exporter in mammals. On chapter III, we investigated the expression of human Fpn1 in different cell types (PBL, THP-1 macrophages, and HepG2) using different commercial and non-commercial antibodies. The results obtained were inconclusive since none of the antibodies was considered specific in the cell models and conditions tested. Given the relevance of this protein in our study, we decided to produce our own antibody raised against human Fpn1. The project was designed and orchestrated by Doctor François Canonne-Hergaux, who has already developed a specific antibody against murine Fpn1 [269].

2. Aims

In this study, we aimed to produce and characterize a specific antibody against human Fpn1. Herein, we present the specificity and validation results available at the moment.

3. Results

Based on the hypothetical structural model of human Fpn1 [100], three different epitopes were selected for the production of the rabbit polyclonal antibody raised against this protein: Fpn1' (intracellular loop), Fpn2' (extracellular epitope) and Fpn3' (C-terminus) (Figure III.34).

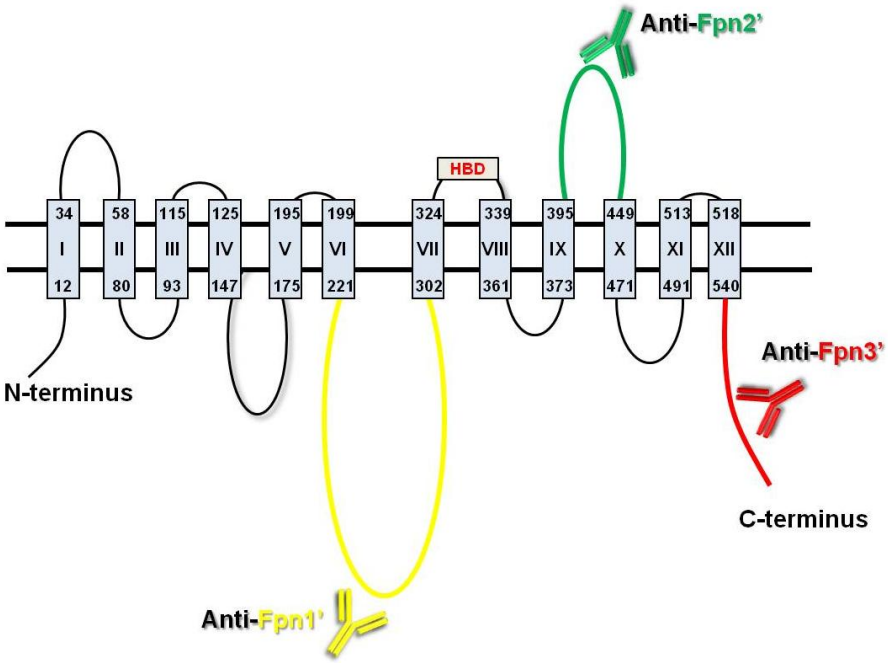

Figure III.34 - Illustration of the epitopes selected for the antibody production against human Ferroportin-1. Scheme of human Fpn1 structure reported by Rice *et al* [100]. The three different epitopes selected for antibody production are indicated in color: intracellular loop Fpn1' (yellow), extracellular loop Fpn2' (green) and intracellular C-terminus Fpn3' (red).

The strategy used as well as the part that each person and group/institution had in this project is described in Figure III.35.

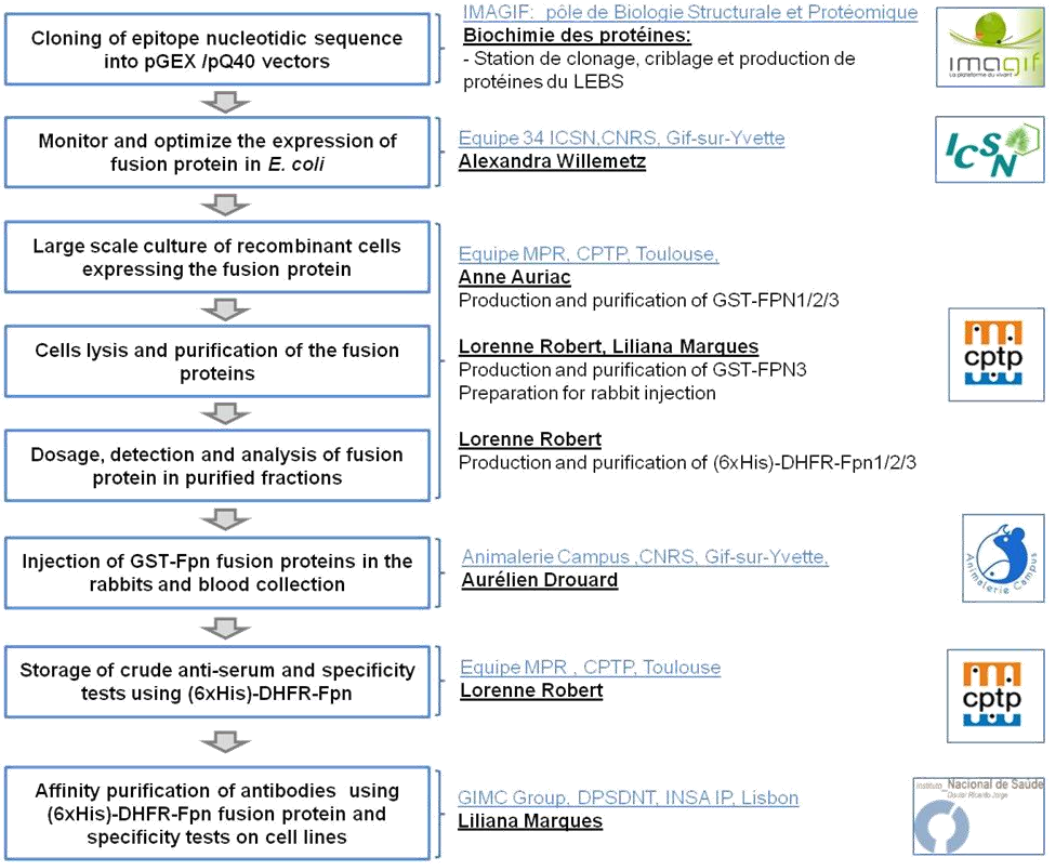

Figure III.35 - Scheme of the overall strategy for the production of antibody against human ferroportin-1. All institutions involved in the project are indicated, as well as the part that each person had in the production and validation of the antibodies.

Briefly, for each epitope of interest, the nucleotidic sequence was cloned in frame to generate two different fusion proteins per epitope: one fused with glutathione-*S*-transferase (GST) originating the peptides GST-Fpn1', 2' and 3'; one fused with dihydrofolate reductase (DHFR) with a histidine tag, originating the peptides (6xHis)-DHFR-Fpn1', 2' and 3.' The GST-Fpn1 fusion proteins were used for immunization of two New Zealand rabbits per epitope through a total of five injections. Blood was collected from each animal before and during the immunization process for title and specificity analysis of antibody production previous to the final bleeding and animal sacrifice. At last, the anti-serum of the final bleeding was affinity-purified using the (6xHis)-DHFR-Fpn1 fusion proteins and then tested on different cell lines overexpressing human Fpn1.

Preliminary specificity tests were performed by immunoblotting, using fusion protein DHFR-Fpn1'/2'/3' mixed with total extract of BMDM and testing crude anti-serum of the blood collected during the immunization process at different time points. As can be observed on Figure III.36, each antibody tested recognized the respective fusion-protein. Also, the title of antibody in the crude

anti-serum increased during the immunization process as expected. The antibody produced against epitope huFpn2' (anti-huFpn2') appears to have the strongest title whereas the one raised against huFpn3 (anti-huFpn3') has the lowest, reacting also unspecifically with other proteins.

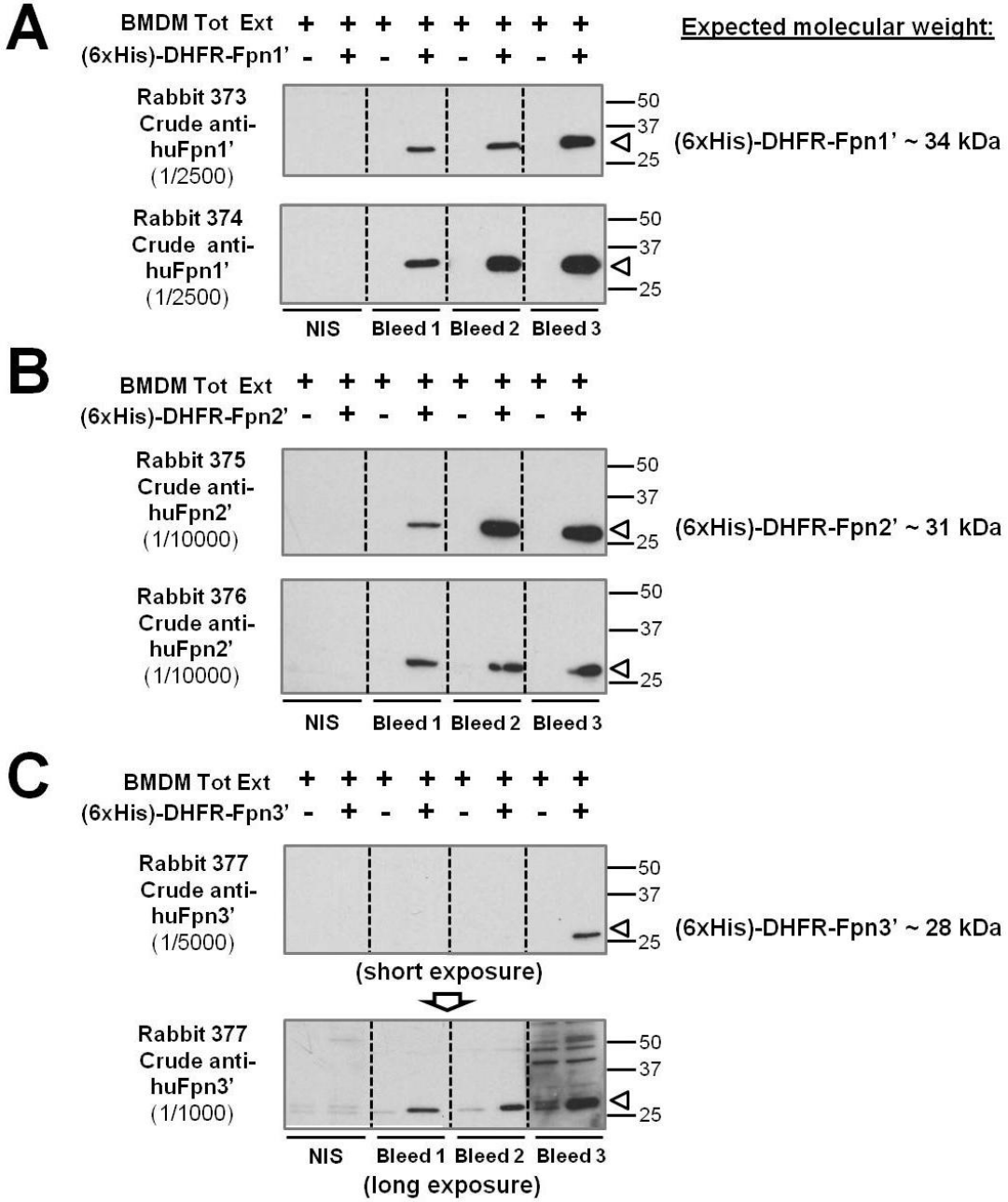

Figure III.36 - Specificity tests of crude antibodies raised against human ferroportin-1 using fusion protein. Immunoblotting analysis to evaluate the title and specificity of the crude anti-serum during the immunization process. Purified fusion protein (6xHis)-DHFR-Fpn1' (**A**, 10ng), (6xHis)-DHFR-Fpn2' (**B**, 10ng) or (6xHis)-DHFR-Fpn3' (**C**, 10ng) were mixed with total extract of murine BMDM (15µg), separated by SDS-PAGE and then immunoblotted using crude serum of rabbit before immunization (non-immunized serum, NIS) and after immunization in different time points: bleed 1(day 28), bleed 2 (day 49) and bleed 3 (day 63). The position and size in kilodaltons (kDa) of the molecular weight markers are indicated on the right. Vertical dashed lines indicate repositioned gel lanes.

In order to test if the antibodies would recognize the whole human Fpn1 protein, membrane extracts were prepared from transfected CHO cell line overexpressing human Fpn1 cDNA coding the full-length protein. On Figure III.37A, we can observe that only the crude anti-huFpn1' recognized a protein with a molecular weight compatible with the one predicted for human Fpn1. As a positive control, the affinity purified antibody raised against murine Fpn1 (anti-mFpn1') was also tested on CHO extracts. This antibody was raised against the same epitope as anti-huFpn1' and was characterized extensively [269], recognizing specifically murine Fpn1 and also cross-reacting with the human protein when overexpressed. Both anti-huFpn1' and anti-mFpn1' recognized the same band, providing further support to the specificity of anti-huFpn1'.

After affinity purification, all three antibodies raised against human Fpn1 recognized the same protein as the anti-mFpn1', supporting the specificity of reaction (Figure III.37B). The different intensity of reaction as well as time of exposure showed that anti-huFpn1' has the highest title whereas anti-huFpn3' presents the lowest title. Noteworthy, anti-huFpn3' reacted with an unspecific protein with higher molecular weight (indicated by "*") than human Fpn1. Comparison between affinity purified anti-huFpn1' and anti-mFpn1' shows that, despite similar specificity in this overexpression model, the antibody raised against the human epitope has the highest title as expected (FigureIII.37C).

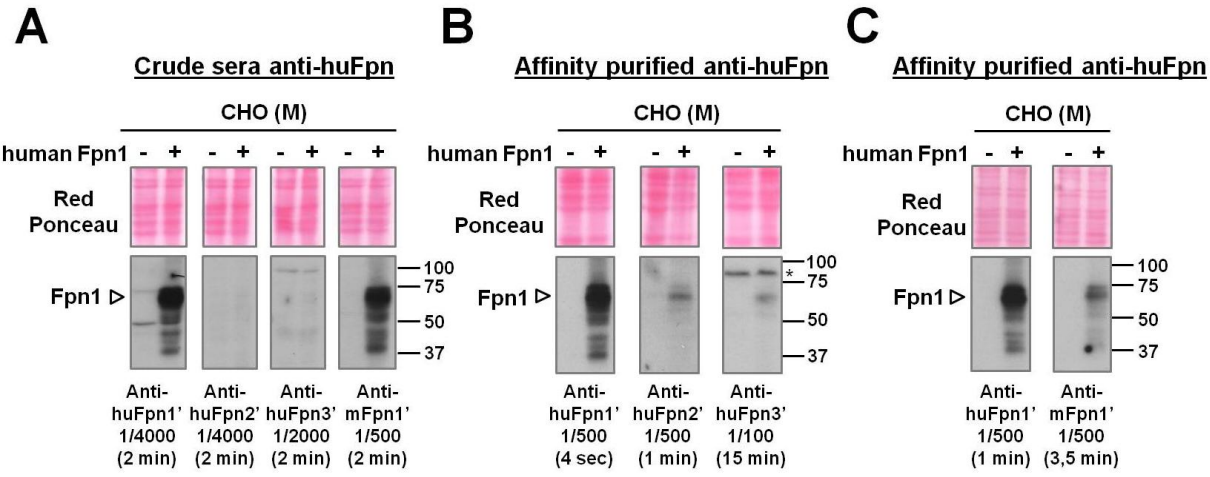

Figure III.37 - Specificity tests of antibodies raised against human ferroportin-1 using CHO cell line. CHO cells were transfected with a plasmid containing full-length human Fpn1 cDNA and incubated 18h for protein expression before protein extraction. Crude membrane extracts (M) were then prepared and analyzed by Western blot using different antibodies **(A-B)** Comparison between crude antibodies (A) or affinity-purified antibodies raised against huFpn1', 2' and 3' epitopes (B) on membrane extracts of CHO cells overexpressing or not human Fpn1 protein. The purified antibody raised against murine Fpn1' (mFpn1') epitope (equivalent to huFpn1') was used as a positive control. **(C)** Comparison between affinity purified antibodies raised against huFpn1' and mFpn1' epitopes, using CHO membrane extracts overexpressing or not human Fpn1. The position and size in kilodaltons (kDa) of the molecular weight markers are indicated on the right. Vertical dashed lines indicate repositioned gel lanes. Antibodies tested, dilutions and exposure time of films are indicated at the bottom. Red Ponceau staining was used as a control for total protein loading between samples. *Unspecific band.

For further confirmation of the specificity of antibodies raised against human Fpn1, HUH7 cell line was used as a human hepatocyte model which, unlike CHO, was previously reported to express endogenous human Fpn1 [319]. In such model, the intracellular trafficking of overexpressed human Fpn1 was expected to be normal and basal levels of endogenous human Fpn1 would also be expected. Nonetheless, in order to increase the expression of human Fpn1, HuH7 cells were also transfected with the plasmid coding the full-length human Fpn1 cDNA previous to analysis by immunoblotting. As observed in Figure III.38, the affinity purified anti-huFpn1' recognized the overexpressed human Fpn1 in transfected HuH7 cells. However, the lower transfection efficiency in HuH7 cell line lead to a diminished expression of human Fpn1 in these cells when compared with transfected CHO cell line. The affinity purified anti-huFpn2' and anti-huFpn3' antibodies failed to detect human Fpn1 in HuH7 cells (data not shown), likely due to the lower title of the antibody combined with the lower transfection efficiency.

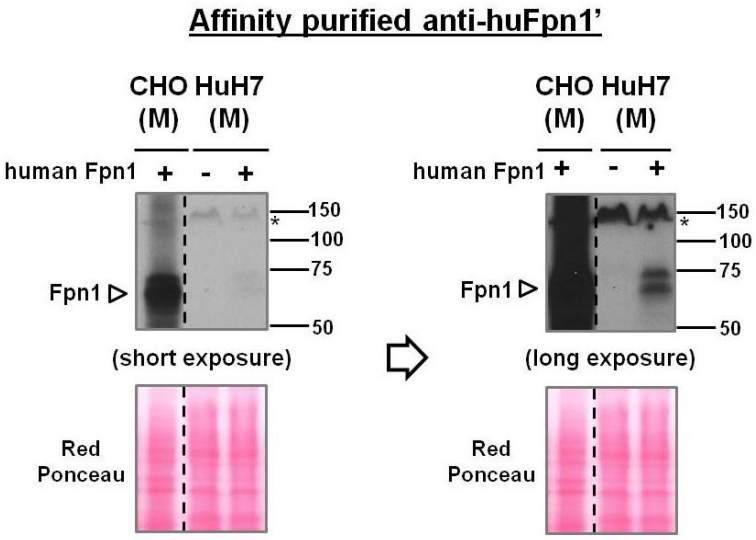

Figure III.38 - Specificity tests of an antibody raised against human ferroportin-1 using HuH7 cell line. HuH7 cells were transfected with a plasmid containing full-length human *Fpn1* cDNA and incubated 18h for protein expression before protein extraction. Crude membrane extracts (M) were analyzed by immunoblotting using the affinity purified anti-huFpn1'. Crude membrane extract of CHO cells overexpressing human Fpn1 was used as a positive control. The position and size in kilodaltons (kDa) of the molecular weight markers are indicated on the right. Vertical dashed lines indicate repositioned gel lanes. Red Ponceau staining was used as a control for total protein loading between samples. *Unspecific band.

For confirmation of the specificity of the band detected by the different antibodies, both CHO and HuH7 cells overexpressing human Fpn1 were treated or not with Hepc (700nm, 3h), followed by immunoblotting analysis using anti-huFpn1' antibody. The activity of Hepc was tested on iron-treated murine macrophages (J774A1) and confirmed by immunoblotting using the anti-mFpn1' antibody (data not shown). Additionally, the anti-huFpn1' antibody cross-reacted with murine Fpn1 in these same samples, detecting the same band as the anti-

mFpn1' antibody. However, the anti-huFpn1' antibody presented less avidity as well as less specificity, providing higher background in the detection (data not shown). As can be observed on Figure III.39, Hepc induced a downregulation of the protein detected by the anti-huFpn1' antibody in both CHO and HuH7 cells overexpressing human Fpn1, confirming that this protein corresponds to human Fpn1. Noteworthy, this antibody detected an unspecific band in HuH7 membrane extracts with higher molecular weight than human Fpn1.

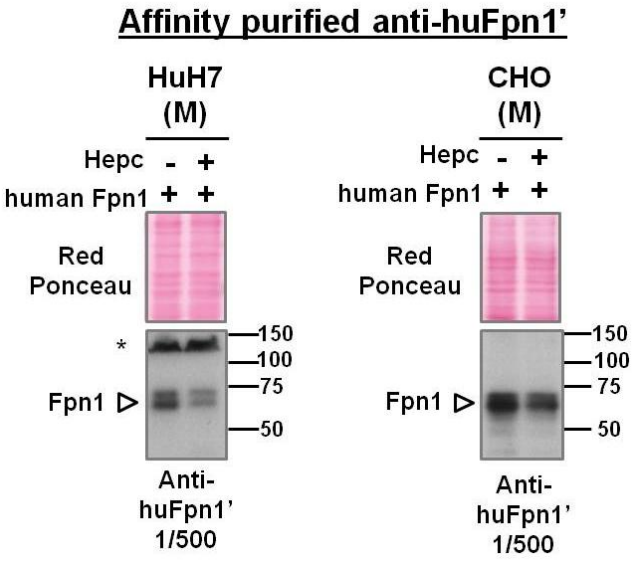

Figure III.39 - Hepcidin effect on human ferroportin-1 expression in transfected CHO and HuH7 cell lines. Cell line CHO and HuH7 were transfected with plasmid containing full-length human Fpn1 cDNA, incubated 18h for protein expression and then untreated or treated with Hepc (Hepc, 700nM, 3h). Crude membrane extracts (M) of HuH7 (left) and CHO (right) were then analyzed by immunoblotting using the affinity purified anti-huFpn1' antibody. The position and size in kilodaltons (kDa) of the molecular weight markers are indicated on the right. Vertical dashed lines indicate repositioned gel lanes. *Unspecific band.

Despite the results obtained in CHO and HuH7 cells, the final specificity test for antibody validation is to detect endogenous expression in non-transfected cells. Human THP-1 monocytic cells were differentiated into macrophages using the activator PMA, followed by treatment or not with iron (described to increase Fpn1 expression, as a positive control) and Hepc. All three affinity purified antibodies raised against human Fpn1 were tested on membrane extracts of THP-1 macrophages. Unlike the tests on CHO cell line, different detection patterns were generated by each antibody displaying different unspecific bands (indicated by "*"). The gray arrowhead indicates one band detected by the anti-huFpn1' antibody that has a molecular weight compatible with human Fpn1 and seems to increase with iron and decrease upon Hepc treatment as expected (Figure III.40). However, the detection was weak and may reflect low human Fpn1 protein level in these cells despite PMA activation and iron treatment. Indeed, a posterior and unrelated experiment confirmed using qPCR that the basal level of human *Fpn1* mRNA was low in THP-1 derived macrophages (Mean Ct = 28,5). Therefore, further tests on

endogenous human Fpn1 detection using a different cell model are necessary to complete the validation of the antibodies produced.

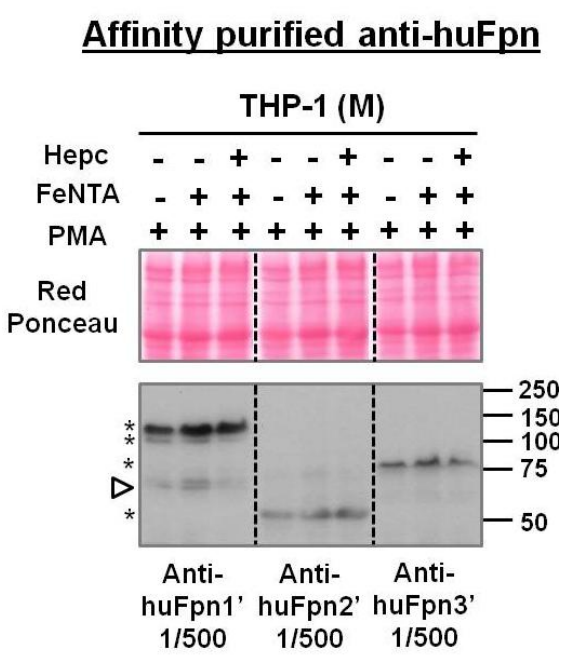

Figure III.40 - Specificity tests of antibodies raised against human ferroportin-1 THP-1 macrophages. Comparison between affinity purified antibodies raised against huFpn1', 2' and 3' epitopes using membrane extracts of PMA-induced THP-1 macrophages stimulated or not with iron (FeNTA, 100µM, 18h) and Hepc (700nM, 3h). The arrowhead indicates a possible band for endogenous expression of human Fpn1 in THP-1 macrophages. The (*) indicates unspecific bands. The position and size in kilodaltons (kDa) of the molecular weight markers are indicated on the right. Vertical dashed lines indicate repositioned gel lanes. Antibodies tested and respective dilutions used are indicated at the bottom. Red Ponceau staining was used as a control for total protein loading between samples.

4. Discussion and conclusion

In this study, three different antibodies were produced against human Fpn1, recognizing different epitopes. Specificity tests on cell lines overexpressing human Fpn1 show that, despite presenting different avidity and/or title, all three antibodies can recognize the same protein and with a molecular weight compatible with human Fpn1. Cross-reaction with the same protein by the antibody raised against mFpn1' epitope gives further support to the specificity of the band detected by the three antibodies raised against human Fpn1. Noteworthy, despite the cross-reaction of anti-mFpn1' antibody with human Fpn1, the power of detection of human Fpn1 by the anti-mFpn1' antibody was lower in comparison with the antibodies generated against human Fpn1 and were exclusive of transfected cells overexpressing human Fpn1.

The decrease of the putative human Fpn1 band intensity observed in Hepc-treated CHO and HuH7 cells overexpressing human Fpn1 provides further confirmation on the specificity of anti-huFpn1' antibody detection in this system. The incomplete degradation of human Fpn1 after Hepc treatment in these samples could be explained by the overexpression system itself, in which the concentration of Hepc used could have been insufficient to induce complete degradation of human Fpn1 protein levels. Additionally, the overexpression system may also lead to a significant amount of intracellular human Fpn1 (cellular trafficking) that would not be available for Hepc binding. As a

consequence, the intracellular human Fpn1 would not be degraded and would be detected in the crude membrane extracts.

Preliminary tests on THP-1 macrophages, which were reported elsewhere to endogenously express human Fpn1 [85,278], revealed unspecific reaction by the three antibodies tested, recognizing bands with higher or lower molecular weight than human Fpn1. Only the anti-huFpn1' antibody reacted against a protein with a molecular weight compatible to human Fpn1, increasing mildly with iron and decreasing upon Hepc treatment on iron-treated cells, which suggests that it could correspond to human Fpn1. However, the weak reaction and at the limit of detection indicate low expression of human Fpn1 in these cells, which could also explain the unspecific bands detected. Indeed, posterior experiments confirmed the low human *Fpn1* mRNA basal level in these cells. The low human Fpn1 expression in THP-1 derived macrophages may result from the fact that these are immortalized cells, which are therefore prone to store iron in order to promote their proliferation in culture. For this reason, we concluded that THP-1 macrophages are not a good model and further studies in primary cells such as human peripheral blood macrophages stimulated with different conditions know to modulated Fpn1 expression (iron overload, iron deficiency, hypoxia, erythrophagocytosis, Hepc) are thus necessary to complete the characterization of these antibodies and to conclude on their specificity on systems with endogenous expression of human Fpn1. In addition, given the fact that some antibodies against human Fpn1 were tested in THP-1 macrophages in chapter 1, it is possible that the lack of specific detection in those experiments could also be an artifact of the low expression of human Fpn1 in these cells and should also be re-tested in primary cells.

5. Authorship

The project of antibody production was designed and organized by Doctor François Canonne-Hergaux in a large network involving different participants, groups, and institutions as described in Figure III.35.

All the validation results presented in this chapter were produced by the author of the thesis, with exception to the ones shown in Figure III.36 which were performed by Lorenne Robert.

IV. General Discussion and Conclusion

1. Discussion

In atherogenesis, the infiltration of immune mononuclear cells is an early and continuous event associated with the development and progression of the atherosclerotic lesions. An association between iron and cardiovascular risk has been proposed, in which the iron status of the immune cells within the lesion, and particularly in macrophages, could be decisive for its development and progression into an unstable or stable atherosclerotic plaque [214,218,234].

In the present study, we focused on the expression of specific iron metabolism proteins on the three main immune cell types that are found in the atherosclerotic lesions: lymphocytes, monocytes and macrophages.

1.1. Ceruloplasmin and immune cells in atherosclerosis

We demonstrated that human lymphocytes and monocytes express both isoforms of Cp (GPI-Cp and sCp) [320], an acute phase protein with oxidase activity that is essential for iron export through Fpn1, but that also oxidizes other substracts such as LDL [51,256]. Additionally, the results obtained suggested that Cp expression and regulation in these cells is likely to be cell-specific, particularly in activated cells. Moreover, the expression of both Cp isoforms was also confirmed in murine macrophages.

In ATH, the accumulation and oxidative modification of LDL is believed to be the primordial factor in atherogenesis, activating ECs to produce chemokines and pro-inflammatory cytokines that will promote the recruitment of monocytes and lymphocytes to the site of lesion. The synthesis of Cp by the main immune cell types found in the atherosclerotic plaque may therefore constitute an additional mechanism contributing to LDL oxidation. As an acute phase protein, the production of pro-inflammatory cytokines by activated ECs and infiltrated immune cells will significantly upregulate local Cp expression. Indeed, in addition to the previous report of sCp upregulation by IFNγ in monocytes [274], we showed that IFNγ also promotes expression of sCp by lymphocytes. Moreover, our results confirmed previous reports by other authors in which M1 polarized macrophages significantly express Cp.

Interestingly, when analyzing the effect of M1 polarization on the different Cp isoforms, we observed that GPI-Cp mRNA remains mostly unchanged whereas sCp mRNA was significantly upregulated by the combined pro-inflammatory conditions LPS/IFNγ. The same differential upregulation was observed in the mixed phenotype Mox/M1, but not in the downregulation of Cp in Mox macrophages, thus indicating that it is exclusively induced by pro-inflammatory conditions. This differential regulation of GPI-Cp and sCp in murine macrophages points to a major role of sCp local expression at site of inflammation. This role is most likely linked to iron loading onto Tf and/or Lf

molecules instead of cellular iron export, considering the lack of GPI-Cp mRNA upregulation along with Fpn1 downregulation in pro-inflammatory conditions.

A previous study showed that monocyte-derived sCp can oxidize LDL [256], demonstrating how local Cp upregulation by inflammatory conditions can promote LDL oxidation and thus contribute to the progression of the plaque. Moreover, in addition to Cp-mediated LDL oxidation, Cp was also reported to enhance SMC- and EC-mediated LDL oxidation by a superoxide-dependent mechanism [261]. Accordingly, co-localization of Cp and oxLDL in the enlarged intima of pro-atherosclerotic areas was previously demonstrated [260], supporting the hypothesis that local Cp production by immune cells (lymphocytes, monocytes and macrophages) within the plaque might be associated with increased LDL oxidation and thus contribute to increased susceptibility to VD [260]. Interestingly, an association between high Cp activity and increased oxLDL levels was reported in patients with acromegaly, a pathology associated with increased mortality due to cardiovascular causes [258], which reinforces the hypothesis of increased Cp levels could constitute a risk factor for developing VD.

1.2. Ferroportin-1 and its partners in murine macrophages

Given the key role of macrophages in ATH progression and how iron accumulation in atherosclerotic lesions has been associated with macrophages and macrophage-derived foam cells, the study focused on the expression of iron metabolism proteins in murine macrophages and, in particular, on the ones involved in iron export.

As one of the main aims of this study, we studied the potential partners of Fpn1 in murine macrophages. The results obtained showed that, as observed in human lymphocytes and monocytes, murine macrophages also express both Cp isoforms. Moreover, we demonstrated that GPI-Cp partially co-localizes with Fpn1 in lipid rafts microdomains in iron-treated macrophages, which indicates that GPI-Cp is at least in part involved in iron export in these cells [320]. However, the partial co-localization also suggested indicated that another ferroxidase, including sCp, could be additionally interacting with Fpn1 in iron-treated BMDM. APP was recently reported to possess ferroxidase activity and to interact with Fpn1 promoting iron export in neurons [139] and its expression was previously reported in human monocytes and macrophages [262]. Herein, we showed that APP is expressed in murine macrophages, being strongly upregulated by iron and recruited to the DRM fractions enriched in lipid raft proteins, where its expression overlaps with Fpn1. A model of Fpn1 interaction with GPI-Cp, sCp and APP during iron export was therefore suggested in murine macrophages (Figure III.19), in which APP could influence iron export despite presenting or not ferroxidase activity.

Nonetheless, further studies are necessary in order to clarify the ferroxidase partners of Fpn1 in macrophages and how these proteins and iron export are modulated by different conditions, particularly iron deficiency and hypoxia that were not explored in this study.

1.3. Macrophage polarization and iron export in atherosclerosis

Iron export has been pointed out as a key event on the resistance to macrophage-derived foam cell formation [239,248]. Characterizing how the proteins involved in macrophage iron export are modulated under pro-atherogenic conditions is therefore essential to understand the role of iron in atherogenesis.

An association between macrophage iron overload and the development of an unrestrained pro-inflammatory M1 phenotype was recently reported [184]. M1 macrophages, which were previously reported to constitute the main macrophage subpopulation in advanced and unstable plaques [321], are characterized by increased iron retention and high production of pro-inflammatory cytokines, chemokines and ROS, which promote the recruitment of more immune cells in a vicious cycle that perpetuates the pro-inflammatory environment of the plaque [169]. On the other hand, the increased ROS production contributes to the oxidative intraplaque environment in which accumulation of oxLDL continuously induce the expression of adhesion molecules, chemokines and pro-inflammatory cytokines by ECs. Accordingly, recent observations point to an important role of Hepc-mediated macrophage iron overload in the progression of atherosclerotic lesions into vulnerable plaques. Noteworthy, in addition to macrophages, lymphocytes and monocytes were also reported to produce Hepc in response to pro-inflammatory conditions (TNFα and IL-6, respectively) [74,322] and may therefore contribute to Hepc local production in atherosclerotic lesions. Furthermore, increased serum Hepc and iron macrophage were associated to increased MCP-1 release and vascular damage in patients with metabolic syndrome [237], pointing to a role for circulating Hepc in addition to local Hepc in atherogenesis.

The present study showed that exposure of macrophages to oxLDL (Mox activator) upregulated *Il6* and *Hamp1* mRNA in Mox macrophages, indicating that intraplaque environment rich in oxLDL may contribute to the production of pro-inflammatory cytokines and Hepc promoting local inflammation and intracellular iron accumulation. Our results are supported by Li *et al* study showing that J774 macrophages exposed to oxLDL presented increased production of ROS and synthesis of pro-inflammatory cytokines and Hepc [240]. Remarkably, despite the transcriptional upregulation of *Fpn1*, we showed that murine Mox macrophages presented basal Fpn1 protein level. Although the upregulation of *Hamp1* mRNA induced by oxLDL in BMDM is unlikely to be reflected at protein level due to the low basal *Hamp1* mRNA level in these cells, this mechanism is preserved in other models and was also observed in primary

human macrophages. The higher level of expression of *HAMP* in these cells suggests that Hepc might be upregulated at protein level in human Mox macrophages, promoting Fpn1 downregulation at cell surface and impairing iron export. Considering this, it is plausible to consider that Mox macrophages *in vivo* may present Fpn1 downregulation and impaired iron export due to increased Hepc production. Additionally, we also showed that a combined environment of oxLDL and pro-inflammatory stimuli (LPS/IFNγ, M1 activators) induces a mixed Mox/M1 macrophage phenotype in which *Fpn1* in transcriptionally downregulated, suggesting impairment of iron export and subsequent iron accumulation in these cells. Moreover, significant *Il6* upregulation in Mox/M1 macrophages similar to the one observed in M1 phenotype further suggests increased Hepc production and Hepc-mediated Fpn1 downregulation in these cells.

According to Kadl *et al*, the following macrophage subpopulations were observed in *LdlR*$^{-/-}$ mice aortic lesions: 39.2% M1, 34.4% Mox, 21.8% M2, 9.6% Mox/M1 and 2.3% Mox/M2 of the total F4/80^{+}/CD11b^{+} aortic cells [249]. Considering that iron export is impaired in M1 and Mox/M1 macrophages (transcriptional Fpn1 downregulation) and likely to be impaired also in Mox macrophages (Hepc upregulation and basal levels of Fpn1 protein expression), a significant part of approximately 49% to 83% of the total macrophage population at the aortic lesions likely presents intracellular iron accumulation along with increased production of pro-inflammatory cytokines and Hepc. These results along with the recent publications on Hepc fundamental role in plaque progression are in agreement with the iron hypothesis proposed by Sullivan, in which macrophage iron accumulation likely induced by Hepc under pro-inflammatory conditions could contribute to plaque destabilization and disease progression [234].

However, the iron hypothesis was recently questioned by a study conducted by Kautz *et al* in which mice deficient for ApoE and heterozygous for the Fpn1 mutation *ffe* (*ApoE*$^{-/-}$*Fpn1*$^{+/ffe}$) that promotes macrophage iron overload were used in order to evaluate the possible effect of macrophage iron overload in ATH progression. In this study, no significant differences were observed on the lesions area when comparing *ApoE*$^{-/-}$*Fpn1*$^{+/ffe}$ and *ApoE*$^{-/-}$ mice, which lead the authors to conclude that there was no significant association of macrophage iron overload and ATH progression [323]. Interestingly, in another experimental model in which macrophage iron overload was induced by local overexpression of Hepc, no significant differences were observed concerning the area of lesions. However, analysis of plaque composition releaved increased macrophage infiltration along with decreased SMC and collagen content. In addition, the plaques also presented increased oxLDL content, but no difference in plaque total lipid content [240]. All these features indicated that Hepc overexpression and subsequent macrophage iron trapping promoted the

development of unstable atherosclerotic plaques that are more vulnerable to rupture, without necessarily correspond to larger lesions. It is therefore reasonable to question if such alterations in the composition of the atherosclerotic plaques would also have been found in the study conducted by Kautz *et al*, despite the lack of significant changes in the area of lesions.

1.4. Comparison between Mox and Mhem/M(Hb) macrophages

The recent polarized macrophage phenotypes of Mhem and M(Hb) characterized by low intracellular iron and resistance to foam cell formation are also in agreement with the iron hypothesis, in which macrophage iron depletion was proposed to protect against foam cell formation. Both Mhem and M(Hb) are found in intraplaque hemorrhage areas *in vivo* and can be reproduced *in vitro* by incubation of monocytes with Hb:Hp or heme during their differentiation into macrophages (6-7 days). These macrophages are characterized by high levels of HO-1, low intracellular ROS and increased expression of cholesterol exporters.

Although there are some differences in the molecular mechanisms described in Mhem and M(Hb) phenotypes, low intracellular ROS is a common feature essential for the increased cholesterol efflux and protection against foam cell formation. While in Mhem, HO-1 activity is essential for reducing intracellular ROS, in M(Hb) it is the upregulation of Fpn1 and increased iron export that is associated with reduced ROS production and subsequent protection against foam cell formation [246,248,324]. However, both HO-1 activity and increased iron export seem to be interconnected and the results herein presented support it.

In fact, exposure to heme or Hb:Hp activates a cellular response against “heme stress” in which Nrf2 plays a key role and, among other target genes, upregulates Hmox1, Fpn1 and Fth1 transcription. As observed in our results, while HO-1 upregulation is easily reflected at protein level in Mox macrophages, Fpn1 and H-Ft translation is regulated by the IRE/IRP system and kept at basal level by low intracellular iron levels. The HO-1 activity on heme catabolism in Mhem/M(Hb) macrophages generates higher intracellular iron levels to promote IRP1 dissociation from the IREs and subsequent significant induction of Fpn1 and H-Ft protein synthesis. Intracellular iron can then be stored in Ft molecules and/or be exported by Fpn1 out of the macrophage, reducing the intracellular LIP and preventing the formation of ROS, thus leading to LXR activation and subsequent upregulation of cholesterol exporters ABCA1/ABCG1.

Thus, one of the key differences between Mhem/M(Hb) and Mox phenotypes (Figure IV.1) is likely the lack of an abundant intracellular iron source during Mox differentiation that would promote the significant upregulation of Fpn1 protein and later on lead to LXR activation, triggering the

upregulation of cholesterol exporters and reducing intracellular lipid content. Noteworthy, LXR activation was recently associated with decreased Hepc expression [325], which could constitute an additional mechanism for protection against foam cell formation in Mhem/M(Hb).

In addition, in the absence of heme, the increased HO-1 levels found in Mox macrophages will not be translated in increased production of heme catabolism end-products such as biliverdin/bilirubin and CO that possess known anti-oxidant and anti-inflammatory properties. As a consequence, IL-10 induction will not be induced in Mox macrophages, which also contributes to the distinction between Mox and Mhem/M(Hb) macrophages.

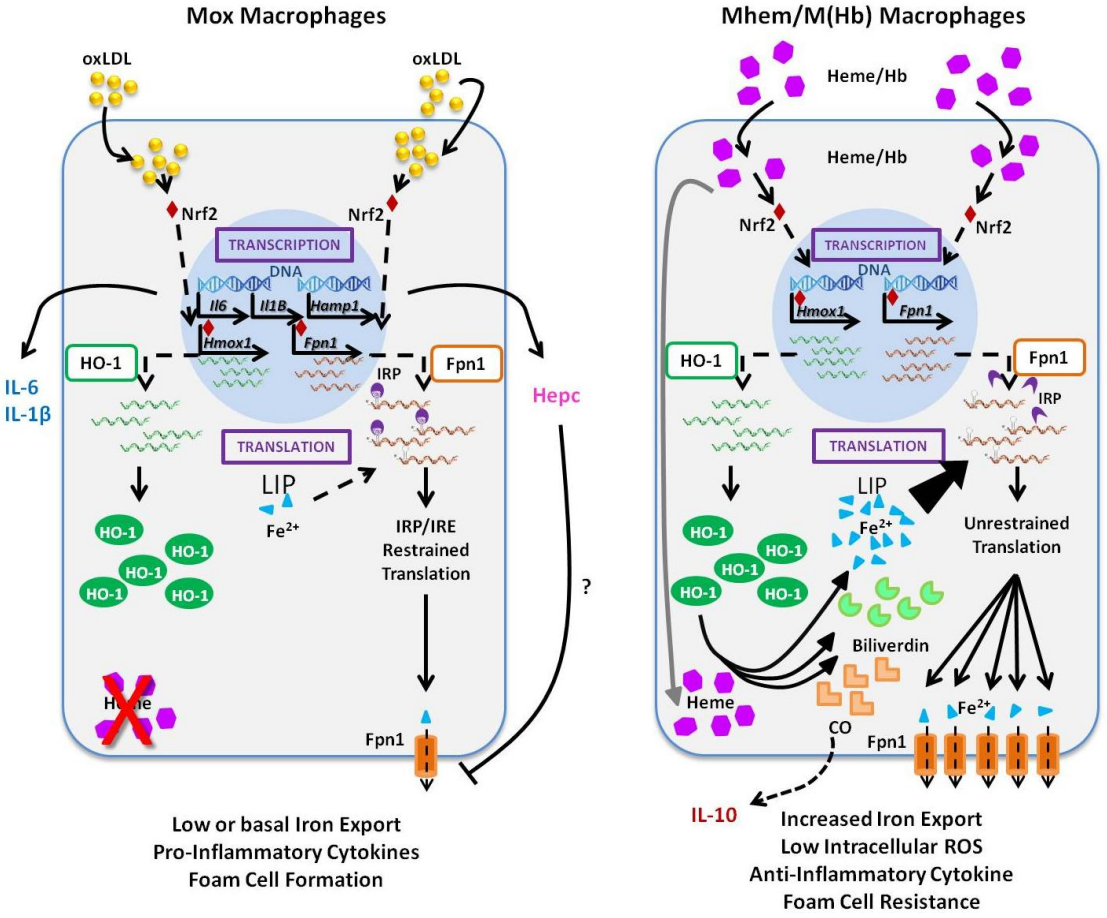

Figure IV.1 - Schematic illustration of the main differences between Mox and Mhem/M(Hb) macrophages. At early phase of polarization, both Mox and Mhem/M(Hb) activators trigger Nrf2 pathway, leading to significant mRNA upregulation of *Hmox1* and *Fpn1* (officially known as *Slc40a1*). Unlike Mhem/M(Hb) macrophages, despite the massive HO-1 upregulation, the absence of heme during Mox polarization leads to the lack of an abundant LIP in order to promote significant Fpn1 translation. As a consequence, iron export in Mox macrophages likely remains at basal levels and may even be impaired by Hepc upregulation. On the contrary, increased Fpn1 protein levels lead to increased iron export in Mhem/M(Hb), reducing ROS formation and triggering the LXR-mediated resistance against foam cells formation. In addition, heme catabolism by HO-1 in Mhem/M(Hb) macrophages leads to the formation of biliverdin and CO, which have known anti-oxidant and anti-inflammatory properties, such as triggering the production of IL-10, a cytokine essential for Mhem/M(Hb) polarization and resistance to foam cell formation.

2. Conclusion

In summary, in this study we characterized the expression of proteins involved in iron metabolism in immune cells with particular focus on the ones involved in iron export. We demonstrated that, in addition to sCp, lymphocytes, monocytes and macrophages also express the membrane isoform GPI-Cp that was previously detected mostly in CNS cells, where its activity was shown to be essential for cellular iron export mediated by Fpn1 [270]. In murine macrophages, we showed that GPI-Cp partially co-localizes with Fpn1 in lipid rafts microdomains and could participate in the Fpn1-mediated iron export. [254]. However, we proposed that besides Cp, APP could be also interacting with Fpn1 and contributing to iron export in macrophages under iron overload conditions. Further research is currently necessary to clarify the role of APP in macrophage iron export.

In the context of ATH, in addition to the serum circulating Cp, the three immune cell types (lymphocyte, monocytes and macrophages) present in atherosclerotic lesions express both Cp isoforms and likely contribute to local Cp accumulation in atherosclerotic lesions. Such Cp activity in the lesion could contribute to the local oxidation of LDL, providing a potential mechanism for the association between high Cp levels and increased cardiovascular risk [257-259].

The effect of oxLDL on iron metabolism proteins expression in macrophages was then investigated. We demonstrated that despite Nrf2 activation induced by oxLDL, Mox macrophages are not protected from foam cell formation as are Mhem/M(Hb) macrophages, showing lipid accumulation, basal levels of Fpn1 at cell surface along with upregulation of pro-inflammatory cytokines and Hepc. In addition, simultaneous exposure of macrophages to oxLDL and LPS/IFNγ showed that Mox polarization is not dominant over M1, and the resulting Mox/M1 phenotype was closer to M1 than Mox, with increased IL-6 expression, downregulated Fpn1 expression combined with increased H-Ft expression. These results suggests that macrophages exposed to an environment rich in oxLDL and pro-inflammatory cytokines are prone to accumulate both lipids and iron while secreting high levels of pro-inflammatory cytokines and Cp, which will further promote the local inflammation and LDL oxidation.

In general, the results presented in this study are in agreement with the iron hypothesis proposed initially by Sullivan [214,234], in which macrophage iron trapping induced by Fpn1 transcriptional and/or post-transcriptional downregulation induced by Hepc could promote the development of unstable atherosclerotic plaques and thus contribute to the progression of the disease.

3. Future perspectives

One fundamental aspect for many of the questions generated during this study relies on the validation of a specific antibody against human Fpn1. The results presented in chapter 4 about our home-made antibodies showed specific detection in overexpressed Fpn1 system, but low title and unspecific detection when tested on THP-1 macrophages, likely due to low Fpn1 expression in this cell model. Completing the validation tests on primary human cells that endogenously express Fpn1 under different experimental conditions is therefore essential for any further investigation involving Fpn1 expression in human cells. In addition, recent publications indicate that one commercial antibody previously tested in chapter 1 could be a specific tool for detecting human Fpn1 and should therefore be re-tested in an appropriate human primary cell model.

Another major priority would be to clarify the iron regulation of Cp in BMDM and to characterize GPI-Cp/Fpn1 and APP/Fpn1 co-localization in hypoxia/iron deficiency conditions. In addition, performing iron export studies combined with specific Cp isoforms or APP knockdown would be important in order to confirm their role in iron export in BMDM and extent those studies to human macrophages. Characterization of the role of Cp isoforms in iron export in human lymphocytes would also complete our own study as well as the recent work by Pinto *et al* [290].

One additional and interesting experiment would be to test if increasing macrophage LIP previous to oxLDL exposure would affect the level of Fpn1 protein expression in Mox macrophages as we proposed in this study. Also, further characterization of human Mox and Mox/M1 macrophages at both mRNA and protein level, including quantification of secreted cytokines and Hepc, would also be important to understand how the results obtained in this study would be confirmed in human cells.

Since macrophage characterization in human atherosclerotic plaques is mostly focused in M1 and M2 phenotypes, it would be interesting to characterize the different polarized macrophage populations (M1, M2, Mox, Mox/M1, Mox/M2, M4 and Mhem/M(Hb)) in human stable and unstable atherosclerotic lesions at different stages of development in order to understand how the different specific macrophage phenotypes could be associated with the plaque progression and destabilization. Additional characterization of Fpn1 expression in intraplaque macrophages and search for its correlation with iron and lipid accumulation associated with specific macrophage phenotype markers would also bring further insight on the iron hypothesis.

Finally, analysis of the effect of statins and other promising therapeutic agents such as Metformin (Mhem activator), LXR and Nrf2 activators on the

expression of Fpn1, Hepc and cholesterol exporters in macrophages would also be important for the identification of potential therapeutic strategies for ATH.

Overall, with these experiments, we would like to answer the questions generated in this study concerning Cp and APP role in Fpn1 iron export in immune cells. Furthermore, we would aim to complete the work on macrophage polarization and iron export in atherogenesis and thus contribute to understand the role of iron as a risk factor in ATH as well as possibly identify future therapeutical targets for this disease.

V. Supplemental Data

1. Introduction

Like macrophages, hepatocytes play a key role in iron homeostasis being the main iron storage cell in the human body. Previous reports had only reported the expression of the soluble isoform of Cp in hepatocytes. In the results of chapter 1, we used the hepatocarcinoma cell line HepG2 as a hepatocyte model and showed that these cells express both Cp isoforms. In addition, the immunostaining of GPI-Cp in non-permeabilized cells showed a pattern of detection very similar to the one observed on GPI-Cp staining in non-permeabilized murine macrophages (BMDM, chapter 2). Furthermore, we showed that GPI-Cp partially co-localizes with Fpn1 in lipid rafts microdomains in iron-treated BMDM.

2. Aims

In this study, we aimed to clarify if Cp expression in HepG2 would be modulated by iron as observed in murine macrophages. Additionally, we investigated the distribution of GPI-Cp in lipid rafts microdomains at cell surface of HepG2 cells.

3. Results

3.1. Ceruloplasmin is not modulated by iron in HepG2 cells

This observation was further confirmed by immunoblotting analysis of cytosolic and crude membrane extracts of HepG2 cells untreated and iron-treated with increasing concentrations of FeNTA (50-200µM), where no significant effect was observed on GPI-Cp (M) nor on sCp (C) isoforms expression level (Figure V.1A). A slight difference in electrophoretic migration was observed between the Cp specie detected in membrane-associated Cp (GPI-Cp) and the cytosolic Cp (sCp), indicating a slight molecular weight difference as previously reported [135]. Again, downregulation of TfR1 was observed in iron-treated HepG2 crude membrane extracts, confirming successful iron uptake by these cells (Figure V.1B).

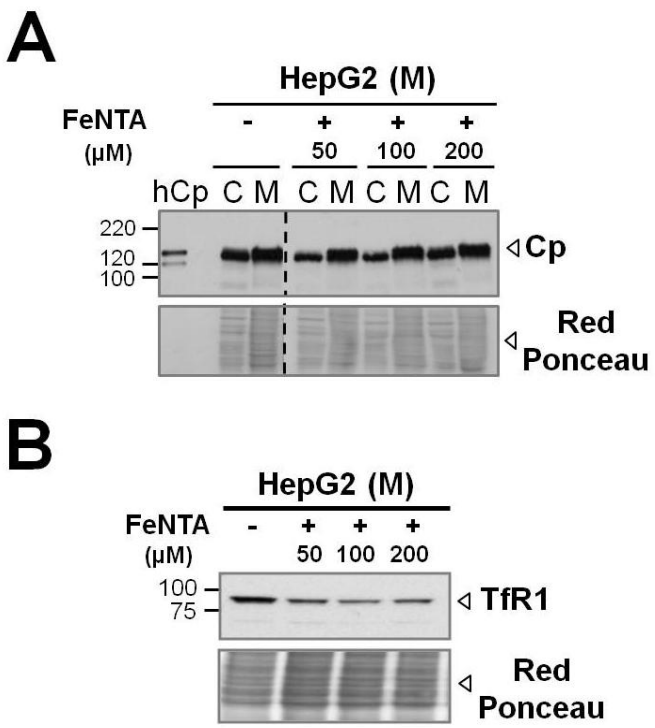

Figure V.1 - Effect of iron on ceruloplasmin expression in HepG2. (A) Immunoblotting of Cp in cytosolic (C) and crude membrane (M) extracts of HepG2 cells untreated and treated with increasing concentrations of iron (FeNTA, 50-200µM). **(B)** Immunoblotting of TfR1 in membrane extracts isolated from HepG2 cells untreated or treated with FeNTA (50-200µM). Downregulation of TfR1 in iron-treated HepG2 extracts confirms successful iron uptake by these cells, despite no observed effect of iron on Cp expression levels (A).

3.2. GPI-anchored Cp is localized in lipid rafts in HepG2 cells

As observed in figure V.2A, the dot-like pattern of Cp staining at cell surface of HepG2 cells suggested that this protein could be present in microdomains such as lipid rafts, known to be enriched in GPI-anchored proteins. To test this hypothesis, immunoblotting analysis of Cp was performed in iodixanol gradient fractions prepared from HepG2 cells untreated and iron-treated. In both conditions, as determined by the subcellular fractionation on iodixanol gradient, the localization of Cp and flotillin-1 (a marker for lipid rafts in hepatocytes) overlapped notably in the lightest fractions 1 and 5 (Figure V.2B). Such observation indicated the presence of some of the detected Cp in the fractions enriched in lipid raft-associated proteins (DRM). Non-rafts membranes (NDRM) containing TfR1 were mostly defined as the denser material (fractions 6 to 12) and were shown to contain high amount of Cp.

Analysis of Cp species detected in DRM and NDRM fractions, a slight difference in eletrophoretic migration is observed in figure V.2B. According to the nature of the fractions and to our previous observations in membrane versus cytosolic extracts (see Figure V.1A), we concluded that the GPI-Cp isoform is present in DRM (black arrowhead) whereas the cytosolic isoform is strongly detected in NDRM (gray arrowhead). After FeNTA treatment, a decrease of TfR1 expression was observed, confirming downregulation of this receptor by iron overload as expected. However, no effect was observed in Cp expression levels nor its localization, indicating that Cp expression and distribution is not modulated by iron overload conditions in human hepatocytes.

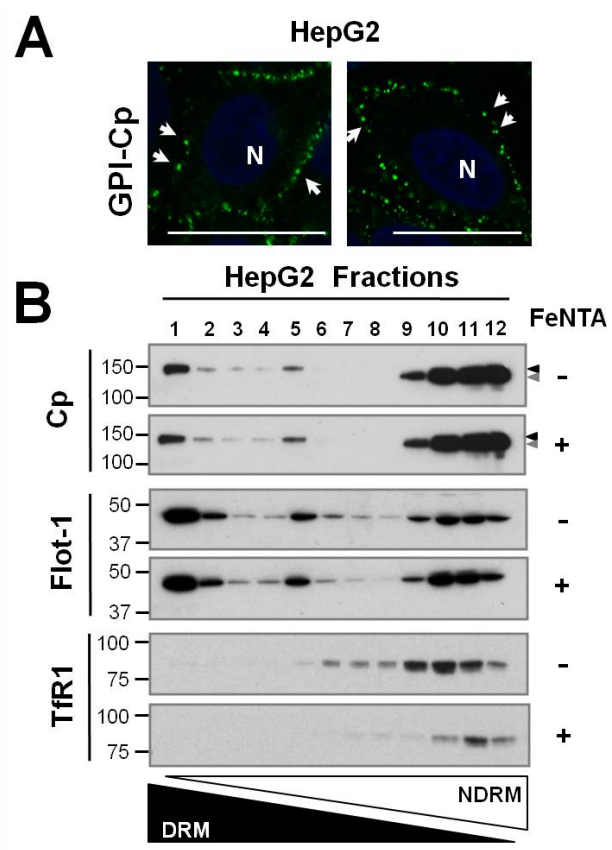

Figure V.2 - Ceruloplasmin localizes in lipid raft microdomains at cell surface of HepG2 cells. (A) Immunofluorescence staining of Cp (green) in non-permeabilized HepG2 cells. Nuclei are stained with DAPI (blue). The white bars represent 25 µm. **(B)** Immunoblotting detection of Cp, Flotillin1 (Flot-1; raft marker) and TfR1 (non-raft marker) in detergent resistant membrane (DRM) and non-detergent resistant membrane (NDRM) fractions isolated from iron-treated (FeNTA, 100 µM) and untreated HepG2 cells. Human serum-purified Cp (hCp) was used as a positive control for Cp detection. Red Ponceau (RP) staining was used for control of total protein loading. The positions and sizes in kilodaltons (kDa) of the molecular weight markers are indicated on the left. Vertical dashed lines indicate repositioned gel lanes.

4. Discussion and conclusion

The hepatocyte is a key cell in iron homeostasis, being the major iron store in the human body and also the main producer of some proteins important in iron metabolism. One of those proteins is Cp, which is an abundant plasma protein reported to be produced and secreted by hepatocytes. Our results in chapter 1 showed that HepG2 cells express GPI-Cp in addition to the soluble isoform of Cp. Herein, we investigated if GPI-Cp was indeed localized in lipid rafts microdomains as suggested by Cp surface staining in HepG2 cells. Our results confirmed that GPI-Cp and the hepatocytes raft marker Flot-1 are highly enriched in the lightest DRM fractions, indicating that GPI-Cp is localized in lipid rafts microdomains. This subcellular localization suggests that, in addition to sCp, GPI-Cp could also contribute to promote iron release through Fpn1 in hepatocytes. Despite the fact we were not able to clarify Fpn1 expression in HepG2 cells (Figure III.8-9), Fpn1 has been described at the cell surface of hepatocytes in hepcidin-deficient mice [55]. Moreover, lack of Cp activity in aceruloplasminemia patients or *Cp*$^{-/-}$ induces progressive and significant iron accumulation in several organs, in which the liver and, in particular, hepatocytes are highly affected [51,63]. However, neither Cp expression nor its distribution in DRM fractions were affected by iron overload conditions in HepG2 cells. Hepatocytes are cells committed mostly to iron storage, promoting unrestricted NTBI uptake and storage. The massive iron accumulation in the liver of HH or secondary iron overload patients shows that these cells favor iron uptake rather

than release. Therefore, it is not surprising that iron overload conditions would not modulate Cp expression in these cells. In addition, as mentioned before, other authors reported that APP is also expressed in liver, where it would equally contribute to liver ferroxidase activity along with Cp. In fact, *App*$^{-/-}$ mice presented iron accumulation in this organ, more specifically in hepatocytes [139]. However, further studies are needed in order to clarify the role of Cp and APP as ferroxidases promoting iron export in hepatocytes.

On the other hand, GPI-Cp expression in hepatocytes may not be limited to its putative role in iron export. Hepatocytes store significant amounts of intracellular iron, presenting therefore increased risk of oxidative stress. Indeed, the ROS production and oxidative damage originated by free hepatic iron were already reported as being highly mutagenic and carcinogenic [326]. In these cells, the expression of both Cp isoforms may also have an important anti-oxidant role in order to preserve membrane integrity and cellular function against iron-mediated oxidative stress. We observed a higher basal level of expression of both Cp isoforms in HepG2 compared with BMDM, which may reflect the higher risk of oxidative damage on hepatocytes compared with macrophages.

Finally, one should keep in mind that HepG2 is n hepatocarcinoma cell line and, in this context, cellular iron homeostasis in these cells could be regulated in order to favor the intracellular iron demands to promote cell proliferation. Studies of Fpn1 expression in breast cancer cells show that its expression is inversely correlated with cell proliferation [187]. In HepG2, the expression of proteins involved in iron release such as Cp or Fpn1 could be regulated in a different way compared with primary hepatocytes. Therefore, further research in primary hepatocytes in culture as well as in tissue hepatocytes using histological techniques are needed to clarify the role and the regulation of the proteins involved in iron export in hepatocytes.

5. Authorship

The results presented were produced by the author of the thesis and by João Banha, and were published in:

L. Marques*, A. Auriac*, A. Willemetz, J. Banha, B. Silva, F. Canonne-Hergaux** and L. Costa**, "*Immune cells and hepatocytes express glycosylphosphatidylinositol-anchored ceruloplasmin at their cell surface".* Blood Cells Mol Dis, 2012. 48(2): p. 110-20. (*co-first authors; ** co-senior authors)

VI. References

1. Papanikolaou G, Pantopoulos K. Iron metabolism and toxicity. Toxicol Appl Pharmacol 2005;202(2):199-211.
2. Finch C. Regulators of iron balance in humans. Blood 1994;84(6):1697-702.
3. Fairweather-Tait SJ. Iron nutrition in the UK: getting the balance right. Proc Nutr Soc 2004;63(4):519-28.
4. Zimmermann MB, Hurrell RF. Nutritional iron deficiency. Lancet 2007;370(9586):511-20.
5. Andrews NC. Disorders of iron metabolism. N Engl J Med 1999;341(26):1986-95.
6. Andrews NC. Forging a field: the golden age of iron biology. Blood 2008;112(2):219-30.
7. Ganz T. Systemic iron homeostasis. Physiol Rev 2013;93(4):1721-41.
8. Gunshin H, Mackenzie B, Berger UV, Gunshin Y, Romero MF, Boron WF, Nussberger S, Gollan JL, Hediger MA. Cloning and characterization of a mammalian proton-coupled metal-ion transporter. Nature 1997;388(6641):482-8.
9. Canonne-Hergaux F, Gruenheid S, Ponka P, Gros P. Cellular and subcellular localization of the Nramp2 iron transporter in the intestinal brush border and regulation by dietary iron. Blood 1999;93(12):4406-17.
10. Fleming MD, Romano MA, Su MA, Garrick LM, Garrick MD, Andrews NC. Nramp2 is mutated in the anemic Belgrade (b) rat: evidence of a role for Nramp2 in endosomal iron transport. Proc Natl Acad Sci U S A 1998;95(3):1148-53.
11. Iolascon A, De Falco L. Mutations in the gene encoding DMT1: clinical presentation and treatment. Semin Hematol 2009;46(4):358-70.
12. Gunshin H, Starr CN, Direnzo C, Fleming MD, Jin J, Greer EL, Sellers VM, Galica SM, Andrews NC. Cybrd1 (duodenal cytochrome b) is not necessary for dietary iron absorption in mice. Blood 2005;106(8):2879-83.
13. Frazer DM, Wilkins SJ, Vulpe CD, Anderson GJ. The role of duodenal cytochrome b in intestinal iron absorption remains unclear. Blood 2005;106(13):4413; author reply 4414.
14. McKie AT, Barrow D, Latunde-Dada GO, Rolfs A, Sager G, Mudaly E, Mudaly M, Richardson C, Barlow D, Bomford A and others. An iron-regulated ferric reductase associated with the absorption of dietary iron. Science 2001;291(5509):1755-9.
15. Wang D, Wang LH, Zhao Y, Lu YP, Zhu L. Hypoxia regulates the ferrous iron uptake and reactive oxygen species level via divalent metal transporter 1 (DMT1) Exon1B by hypoxia-inducible factor-1. IUBMB Life 2010;62(8):629-36.
16. Brasse-Lagnel C, Karim Z, Letteron P, Bekri S, Bado A, Beaumont C. Intestinal DMT1 cotransporter is down-regulated by hepcidin via proteasome internalization and degradation. Gastroenterology 2011;140(4):1261-1271.e1.
17. Shayeghi M, Latunde-Dada GO, Oakhill JS, Laftah AH, Takeuchi K, Halliday N, Khan Y, Warley A, McCann FE, Hider RC and others. Identification of an intestinal heme transporter. Cell 2005;122(5):789-801.
18. Yanatori I, Tabuchi M, Kawai Y, Yasui Y, Akagi R, Kishi F. Heme and non-heme iron transporters in non-polarized and polarized cells. BMC Cell Biol 2010;11:39.
19. Rajagopal A, Rao AU, Amigo J, Tian M, Upadhyay SK, Hall C, Uhm S, Mathew MK, Fleming MD, Paw BH and others. Haem homeostasis is regulated by the conserved and concerted functions of HRG-1 proteins. Nature 2008;453(7198):1127-31.
20. Khan AA, Quigley JG. Control of intracellular heme levels: heme transporters and heme oxygenases. Biochim Biophys Acta 2011;1813(5):668-82.
21. Theil EC, Chen H, Miranda C, Janser H, Elsenhans B, Núñez MT, Pizarro F, Schümann K. Absorption of iron from ferritin is independent of heme iron and ferrous salts in women and rat intestinal segments. J Nutr 2012;142(3):478-83.
22. Abboud S, Haile DJ. A novel mammalian iron-regulated protein involved in intracellular iron metabolism. J Biol Chem 2000;275(26):19906-12.

23. Donovan A, Brownlie A, Zhou Y, Shepard J, Pratt SJ, Moynihan J, Paw BH, Drejer A, Barut B, Zapata A and others. Positional cloning of zebrafish ferroportin1 identifies a conserved vertebrate iron exporter. Nature 2000;403(6771):776-81.
24. McKie AT, Marciani P, Rolfs A, Brennan K, Wehr K, Barrow D, Miret S, Bomford A, Peters TJ, Farzaneh F and others. A novel duodenal iron-regulated transporter, IREG1, implicated in the basolateral transfer of iron to the circulation. Mol Cell 2000;5(2):299-309.
25. Vulpe CD, Kuo YM, Murphy TL, Cowley L, Askwith C, Libina N, Gitschier J, Anderson GJ. Hephaestin, a ceruloplasmin homologue implicated in intestinal iron transport, is defective in the sla mouse. Nat Genet 1999;21(2):195-9.
26. Cherukuri S, Potla R, Sarkar J, Nurko S, Harris Z, Fox P. Unexpected role of ceruloplasmin in intestinal iron absorption. Cell Metab 2005;2(5):309-19.
27. Ranganathan PN, Lu Y, Fuqua BK, Collins JF. Discovery of a cytosolic/soluble ferroxidase in rodent enterocytes. Proc Natl Acad Sci U S A 2012;109(9):3564-9.
28. Nemeth E, Tuttle M, Powelson J, Vaughn M, Donovan A, Ward D, Ganz T, Kaplan J. Hepcidin regulates cellular iron efflux by binding to ferroportin and inducing its internalization. Science 2004;306(5704):2090-3.
29. Schade AL, Caroline L. An iron-binding component in human blood plasma. Science 1946;104(2702):340.
30. Gao J, Chen J, Kramer M, Tsukamoto H, Zhang AS, Enns CA. Interaction of the hereditary hemochromatosis protein HFE with transferrin receptor 2 is required for transferrin-induced hepcidin expression. Cell Metab 2009;9(3):217-27.
31. Lawen A, Lane DJ. Mammalian iron homeostasis in health and disease: uptake, storage, transport, and molecular mechanisms of action. Antioxid Redox Signal 2013;18(18):2473-507.
32. Ponka P, Lok CN. The transferrin receptor: role in health and disease. Int J Biochem Cell Biol 1999;31(10):1111-37.
33. Ohgami RS, Campagna DR, Greer EL, Antiochos B, McDonald A, Chen J, Sharp JJ, Fujiwara Y, Barker JE, Fleming MD. Identification of a ferrireductase required for efficient transferrin-dependent iron uptake in erythroid cells. Nat Genet 2005;37(11):1264-9.
34. Brissot P, Ropert M, Le Lan C, Loréal O. Non-transferrin bound iron: a key role in iron overload and iron toxicity. Biochim Biophys Acta 2012;1820(3):403-10.
35. Ganz T. Macrophages and systemic iron homeostasis. J Innate Immun 2012;4(5-6):446-53.
36. Smith A, Morgan WT. Hemopexin-mediated transport of heme into isolated rat hepatocytes. J Biol Chem 1981;256(21):10902-9.
37. Hvidberg V, Maniecki MB, Jacobsen C, Højrup P, Møller HJ, Moestrup SK. Identification of the receptor scavenging hemopexin-heme complexes. Blood 2005;106(7):2572-9.
38. Kristiansen M, Graversen JH, Jacobsen C, Sonne O, Hoffman HJ, Law SK, Moestrup SK. Identification of the haemoglobin scavenger receptor. Nature 2001;409(6817):198-201.
39. Chiabrando D, Vinchi F, Fiorito V, Tolosano E. Haptoglobin and Hemopexin in Heme Detoxification and Iron Recycling, Acute Phase Proteins - Regulation and Functions of Acute Phase Proteins, Prof. Francisco Veas (Ed.), ISBN: 978-953-307-252-4, InTech, DOI: 10.5772/18241. 2011.
40. Fisher J, Devraj K, Ingram J, Slagle-Webb B, Madhankumar AB, Liu X, Klinger M, Simpson IA, Connor JR. Ferritin: a novel mechanism for delivery of iron to the brain and other organs. Am J Physiol Cell Physiol 2007;293(2):C641-9.
41. Han J, Seaman WE, Di X, Wang W, Willingham M, Torti FM, Torti SV. Iron uptake mediated by binding of H-ferritin to the TIM-2 receptor in mouse cells. PLoS One 2011;6(8):e23800.

42. Li L, Fang CJ, Ryan JC, Niemi EC, Lebrón JA, Björkman PJ, Arase H, Torti FM, Torti SV, Nakamura MC and others. Binding and uptake of H-ferritin are mediated by human transferrin receptor-1. Proc Natl Acad Sci U S A 2010;107(8):3505-10.
43. Shi H, Bencze KZ, Stemmler TL, Philpott CC. A cytosolic iron chaperone that delivers iron to ferritin. Science 2008;320(5880):1207-10.
44. Nandal A, Ruiz JC, Subramanian P, Ghimire-Rijal S, Sinnamon RA, Stemmler TL, Bruick RK, Philpott CC. Activation of the HIF prolyl hydroxylase by the iron chaperones PCBP1 and PCBP2. Cell Metab 2011;14(5):647-57.
45. Stemmler TL, Lesuisse E, Pain D, Dancis A. Frataxin and mitochondrial FeS cluster biogenesis. J Biol Chem 2010;285(35):26737-43.
46. Harrison PM, Arosio P. The ferritins: molecular properties, iron storage function and cellular regulation. Biochim Biophys Acta 1996;1275(3):161-203.
47. Tandara L, Salamunic I. Iron metabolism: current facts and future directions. Biochem Med (Zagreb) 2012;22(3):311-28.
48. Zhang Y, Mikhael M, Xu D, Li Y, Soe-Lin S, Ning B, Li W, Nie G, Zhao Y, Ponka P. Lysosomal proteolysis is the primary degradation pathway for cytosolic ferritin and cytosolic ferritin degradation is necessary for iron exit. Antioxid Redox Signal 2010;13(7):999-1009.
49. Kidane TZ, Sauble E, Linder MC. Release of iron from ferritin requires lysosomal activity. Am J Physiol Cell Physiol 2006;291(3):C445-55.
50. Cohen LA, Gutierrez L, Weiss A, Leichtmann-Bardoogo Y, Zhang DL, Crooks DR, Sougrat R, Morgenstern A, Galy B, Hentze MW and others. Serum ferritin is derived primarily from macrophages through a nonclassical secretory pathway. Blood 2010;116(9):1574-84.
51. Harris ZL, Durley AP, Man TK, Gitlin JD. Targeted gene disruption reveals an essential role for ceruloplasmin in cellular iron efflux. Proc Natl Acad Sci U S A 1999;96(19):10812-7.
52. Keel SB, Doty RT, Yang Z, Quigley JG, Chen J, Knoblaugh S, Kingsley PD, De Domenico I, Vaughn MB, Kaplan J and others. A heme export protein is required for red blood cell differentiation and iron homeostasis. Science 2008;319(5864):825-8.
53. Garcia-Santos D, Schranzhofer M, Horvathova M, Jaberi MM, Bogo Chies JA, Sheftel AD, Ponka P. Heme oxygenase 1 is expressed in murine erythroid cells where it controls the level of regulatory heme. Blood 2014;123(14):2269-77.
54. Bonkowsky HL, Sinclair PR, Sinclair JF. Hepatic heme metabolism and its control. Yale J Biol Med 1979;52(1):13-37.
55. Ramey G, Deschemin JC, Durel B, Canonne-Hergaux F, Nicolas G, Vaulont S. Hepcidin targets ferroportin for degradation in hepatocytes. Haematologica 2010;95(3):501-4.
56. Lescoat G, Hubert N, Moirand R, Jego P, Pasdeloup N, Brissot P. Iron load increases ferritin synthesis and secretion in adult human hepatocyte cultures. Liver 1991;11(1):24-9.
57. Ghosh S, Hevi S, Chuck SL. Regulated secretion of glycosylated human ferritin from hepatocytes. Blood 2004;103(6):2369-76.
58. ten Kate J, Wolthuis A, Westerhuis B, van Deursen C. The iron content of serum ferritin: physiological importance and diagnostic value. Eur J Clin Chem Clin Biochem 1997;35(1):53-6.
59. Bratosin D, Mazurier J, Tissier JP, Estaquier J, Huart JJ, Ameisen JC, Aminoff D, Montreuil J. Cellular and molecular mechanisms of senescent erythrocyte phagocytosis by macrophages. A review. Biochimie 1998;80(2):173-95.
60. Knutson M, Wessling-Resnick M. Iron metabolism in the reticuloendothelial system. Crit Rev Biochem Mol Biol 2003;38(1):61-88.

61. Delaby C, Rondeau C, Pouzet C, Willemetz A, Pilard N, Desjardins M, Canonne-Hergaux F. Subcellular localization of iron and heme metabolism related proteins at early stages of erythrophagocytosis. PLoS One 2012;7(7):e42199.
62. White C, Yuan X, Schmidt PJ, Bresciani E, Samuel TK, Campagna D, Hall C, Bishop K, Calicchio ML, Lapierre A and others. HRG1 is essential for heme transport from the phagolysosome of macrophages during erythrophagocytosis. Cell Metab 2013;17(2):261-70.
63. Gitlin JD. Aceruloplasminemia. Pediatr Res 1998;44(3):271-6.
64. Yang Z, Philips JD, Doty RT, Giraudi P, Ostrow JD, Tiribelli C, Smith A, Abkowitz JL. Kinetics and specificity of feline leukemia virus subgroup C receptor (FLVCR) export function and its dependence on hemopexin. J Biol Chem 2010;285(37):28874-82.
65. Peyssonnaux C, Zinkernagel A, Schuepbach R, Rankin E, Vaulont S, Haase V, Nizet V, Johnson R. Regulation of iron homeostasis by the hypoxia-inducible transcription factors (HIFs). J Clin Invest 2007;117(7):1926-32.
66. Ludwiczek S, Aigner E, Theurl I, Weiss G. Cytokine-mediated regulation of iron transport in human monocytic cells. Blood 2003;101(10):4148-54.
67. Wrighting DM, Andrews NC. Interleukin-6 induces hepcidin expression through STAT3. Blood 2006;108(9):3204-9.
68. Rouault TA. The role of iron regulatory proteins in mammalian iron homeostasis and disease. Nat Chem Biol 2006;2(8):406-14.
69. Gordeuk V, Caleffi A, Corradini E, Ferrara F, Jones R, Castro O, Onyekwere O, Kittles R, Pignatti E, Montosi G and others. Iron overload in Africans and African-Americans and a common mutation in the SCL40A1 (ferroportin 1) gene. Blood Cells Mol Dis;31(3):299-304.
70. Ricky S. Joshi EMaMS. Cellular Iron Metabolism – The IRP/IRE Regulatory Network, Iron Metabolism, Dr. Sarika Arora (Ed.). InTech; 2012.
71. Ganz T. Molecular control of iron transport. J Am Soc Nephrol 2007;18(2):394-400.
72. Kulaksiz H, Theilig F, Bachmann S, Gehrke SG, Rost D, Janetzko A, Cetin Y, Stremmel W. The iron-regulatory peptide hormone hepcidin: expression and cellular localization in the mammalian kidney. J Endocrinol 2005;184(2):361-70.
73. Merle U, Fein E, Gehrke SG, Stremmel W, Kulaksiz H. The iron regulatory peptide hepcidin is expressed in the heart and regulated by hypoxia and inflammation. Endocrinology 2007;148(6):2663-8.
74. Pinto JP, Dias V, Zoller H, Porto G, Carmo H, Carvalho F, de Sousa M. Hepcidin messenger RNA expression in human lymphocytes. Immunology 2010;130(2):217-30.
75. Theurl I, Theurl M, Seifert M, Mair S, Nairz M, Rumpold H, Zoller H, Bellmann-Weiler R, Niederegger H, Talasz H and others. Autocrine formation of hepcidin induces iron retention in human monocytes. Blood 2008;111(4):2392-9.
76. Sow FB, Florence WC, Satoskar AR, Schlesinger LS, Zwilling BS, Lafuse WP. Expression and localization of hepcidin in macrophages: a role in host defense against tuberculosis. J Leukoc Biol 2007;82(4):934-45.
77. Zumerle S, Mathieu JR, Delga S, Heinis M, Viatte L, Vaulont S, Peyssonnaux C. Targeted disruption of hepcidin in the liver recapitulates the hemochromatotic phenotype. Blood 2014;123(23):3646-50.
78. Valore EV, Ganz T. Posttranslational processing of hepcidin in human hepatocytes is mediated by the prohormone convertase furin. Blood Cells Mol Dis 2008;40(1):132-8.
79. Rivera S, Nemeth E, Gabayan V, Lopez MA, Farshidi D, Ganz T. Synthetic hepcidin causes rapid dose-dependent hypoferremia and is concentrated in ferroportin-containing organs. Blood 2005;106(6):2196-9.
80. Qiao B, Sugianto P, Fung E, Del-Castillo-Rueda A, Moran-Jimenez MJ, Ganz T, Nemeth E. Hepcidin-induced endocytosis of ferroportin is dependent on ferroportin ubiquitination. Cell Metab 2012;15(6):918-24.

81. Folgueras AR, de Lara FM, Pendás AM, Garabaya C, Rodríguez F, Astudillo A, Bernal T, Cabanillas R, López-Otín C, Velasco G. Membrane-bound serine protease matriptase-2 (Tmprss6) is an essential regulator of iron homeostasis. Blood 2008;112(6):2539-45.
82. Nicolas G, Bennoun M, Porteu A, Mativet S, Beaumont C, Grandchamp B, Sirito M, Sawadogo M, Kahn A, Vaulont S. Severe iron deficiency anemia in transgenic mice expressing liver hepcidin. Proc Natl Acad Sci U S A 2002;99(7):4596-601.
83. Nicolas G, Bennoun M, Devaux I, Beaumont C, Grandchamp B, Kahn A, Vaulont S. Lack of hepcidin gene expression and severe tissue iron overload in upstream stimulatory factor 2 (USF2) knockout mice. Proc Natl Acad Sci U S A 2001;98(15):8780-5.
84. Viatte L, Lesbordes-Brion JC, Lou DQ, Bennoun M, Nicolas G, Kahn A, Canonne-Hergaux F, Vaulont S. Deregulation of proteins involved in iron metabolism in hepcidin-deficient mice. Blood 2005;105(12):4861-4.
85. Chaston T, Chung B, Mascarenhas M, Marks J, Patel B, Srai S, Sharp P. Evidence for differential effects of hepcidin in macrophages and intestinal epithelial cells. Gut 2008;57(3):374-82.
86. Détivaud L, Nemeth E, Boudjema K, Turlin B, Troadec MB, Leroyer P, Ropert M, Jacquelinet S, Courselaud B, Ganz T and others. Hepcidin levels in humans are correlated with hepatic iron stores, hemoglobin levels, and hepatic function. Blood 2005;106(2):746-8.
87. Courselaud B, Pigeon C, Inoue Y, Inoue J, Gonzalez FJ, Leroyer P, Gilot D, Boudjema K, Guguen-Guillouzo C, Brissot P and others. C/EBPalpha regulates hepatic transcription of hepcidin, an antimicrobial peptide and regulator of iron metabolism. Cross-talk between C/EBP pathway and iron metabolism. J Biol Chem 2002;277(43):41163-70.
88. Camaschella C. Iron and hepcidin: a story of recycling and balance. Hematology Am Soc Hematol Educ Program 2013;2013:1-8.
89. Kautz L, Jung G, Valore EV, Rivella S, Nemeth E, Ganz T. Identification of erythroferrone as an erythroid regulator of iron metabolism. Nat Genet 2014;46(7):678-84.
90. Pak M, Lopez MA, Gabayan V, Ganz T, Rivera S. Suppression of hepcidin during anemia requires erythropoietic activity. Blood 2006;108(12):3730-5.
91. Besson-Fournier C, Latour C, Kautz L, Bertrand J, Ganz T, Roth MP, Coppin H. Induction of activin B by inflammatory stimuli up-regulates expression of the iron-regulatory peptide hepcidin through Smad1/5/8 signaling. Blood 2012;120(2):431-9.
92. Kemna E, Pickkers P, Nemeth E, van der Hoeven H, Swinkels D. Time-course analysis of hepcidin, serum iron, and plasma cytokine levels in humans injected with LPS. Blood 2005;106(5):1864-6.
93. Nemeth E, Rivera S, Gabayan V, Keller C, Taudorf S, Pedersen BK, Ganz T. IL-6 mediates hypoferremia of inflammation by inducing the synthesis of the iron regulatory hormone hepcidin. J Clin Invest 2004;113(9):1271-6.
94. Theurl I, Schroll A, Nairz M, Seifert M, Theurl M, Sonnweber T, Kulaksiz H, Weiss G. Pathways for the regulation of hepcidin expression in anemia of chronic disease and iron deficiency anemia in vivo. Haematologica 2011;96(12):1761-9.
95. Abboud S, Haile D. A novel mammalian iron-regulated protein involved in intracellular iron metabolism. J Biol Chem 2000;275(26):19906-12.
96. Donovan A, Brownlie A, Zhou Y, Shepard J, Pratt S, Moynihan J, Paw B, Drejer A, Barut B, Zapata A and others. Positional cloning of zebrafish ferroportin1 identifies a conserved vertebrate iron exporter. Nature 2000;403(6771):776-81.
97. Ganz T. Cellular iron: ferroportin is the only way out. Cell Metab 2005;1(3):155-7.
98. Donovan A, Lima C, Pinkus J, Pinkus G, Zon L, Robine S, Andrews N. The iron exporter ferroportin/Slc40a1 is essential for iron homeostasis. Cell Metab 2005;1(3):191-200.
99. Canonne-Hergaux F, Donovan A, Delaby C, Wang HJ, Gros P. Comparative studies of duodenal and macrophage ferroportin proteins. Am J Physiol Gastrointest Liver Physiol 2006;290(1):G156-63.

100. Rice A, Mendez M, Hokanson C, Rees D, Björkman P. Investigation of the biophysical and cell biological properties of ferroportin, a multipass integral membrane protein iron exporter. J Mol Biol 2009;386(3):717-32.
101. Schimanski L, Drakesmith H, Talbott C, Horne K, James J, Davis S, Sweetland E, Bastin J, Cowley D, Townsend A. Ferroportin: lack of evidence for multimers. Blood Cells Mol Dis;40(3):360-9.
102. Gonçalves A, Muzeau F, Blaybel R, Hetet G, Driss F, Delaby C, Canonne-Hergaux F, Beaumont C. Wild-type and mutant ferroportins do not form oligomers in transfected cells. Biochem J 2006;396(2):265-75.
103. De Domenico I, Ward D, Musci G, Kaplan J. Evidence for the multimeric structure of ferroportin. Blood 2007;109(5):2205-9.
104. Ward DM, Kaplan J. Ferroportin-mediated iron transport: expression and regulation. Biochim Biophys Acta 2012;1823(9):1426-33.
105. Zohn I, De Domenico I, Pollock A, Ward D, Goodman J, Liang X, Sanchez A, Niswander L, Kaplan J. The flatiron mutation in mouse ferroportin acts as a dominant negative to cause ferroportin disease. Blood 2007;109(10):4174-80.
106. Wallace DF, Harris JM, Subramaniam VN. Functional analysis and theoretical modeling of ferroportin reveals clustering of mutations according to phenotype. Am J Physiol Cell Physiol 2010;298(1):C75-84.
107. Delaby C, Pilard N, Puy H, Canonne-Hergaux F. Sequential regulation of ferroportin expression after erythrophagocytosis in murine macrophages: early mRNA induction by haem, followed by iron-dependent protein expression. Biochem J 2008;411(1):123-31.
108. Taylor M, Qu A, Anderson ER, Matsubara T, Martin A, Gonzalez FJ, Shah YM. Hypoxia-inducible factor-2α mediates the adaptive increase of intestinal ferroportin during iron deficiency in mice. Gastroenterology 2011;140(7):2044-55.
109. Marro S, Chiabrando D, Messana E, Stolte J, Turco E, Tolosano E, Muckenthaler MU. Heme controls ferroportin1 (FPN1) transcription involving Bach1, Nrf2 and a MARE/ARE sequence motif at position -7007 of the FPN1 promoter. Haematologica 2010;95(8):1261-8.
110. Sheikh N, Dudas J, Ramadori G. Changes of gene expression of iron regulatory proteins during turpentine oil-induced acute-phase response in the rat. Lab Invest 2007;87(7):713-25.
111. Recalcati S, Locati M, Marini A, Santambrogio P, Zaninotto F, De Pizzol M, Zammataro L, Girelli D, Cairo G. Differential regulation of iron homeostasis during human macrophage polarized activation. Eur J Immunol 2010;40(3):824-35.
112. Peyssonnaux C, Zinkernagel A, Datta V, Lauth X, Johnson R, Nizet V. TLR4-dependent hepcidin expression by myeloid cells in response to bacterial pathogens. Blood 2006;107(9):3727-32.
113. Deschemin JC, Vaulont S. Role of hepcidin in the setting of hypoferremia during acute inflammation. PLoS One 2013;8(4):e61050.
114. Nairz M, Fritsche G, Crouch M, Barton H, Fang F, Weiss G. Slc11a1 limits intracellular growth of Salmonella enterica sv. Typhimurium by promoting macrophage immune effector functions and impairing bacterial iron acquisition. Cell Microbiol 2009.
115. Nairz M, Fritsche G, Brunner P, Talasz H, Hantke K, Weiss G. Interferon-gamma limits the availability of iron for intramacrophage Salmonella typhimurium. Eur J Immunol 2008;38(7):1923-36.
116. Sangokoya C, Doss JF, Chi JT. Iron-responsive miR-485-3p regulates cellular iron homeostasis by targeting ferroportin. PLoS Genet 2013;9(4):e1003408.
117. Zhang D, Hughes R, Ollivierre-Wilson H, Ghosh M, Rouault T. A ferroportin transcript that lacks an iron-responsive element enables duodenal and erythroid precursor cells to evade translational repression. Cell Metab 2009;9(5):461-73.

118. Auriac A, Willemetz A, Canonne-Hergaux F. Lipid raft-dependent endocytosis: a new route for hepcidin-mediated regulation of ferroportin in macrophages. Haematologica 2010;95(8):1269-77.
119. Delaby C, Pilard N, Goncalves AS, Beaumont C, Canonne-Hergaux F. Presence of the iron exporter ferroportin at the plasma membrane of macrophages is enhanced by iron loading and down-regulated by hepcidin. Blood 2005;106(12):3979-84.
120. De Domenico I, Ward DM, di Patti MC, Jeong SY, David S, Musci G, Kaplan J. Ferroxidase activity is required for the stability of cell surface ferroportin in cells expressing GPI-ceruloplasmin. Embo J 2007;26(12):2823-31.
121. di Patti M, Maio N, Rizzo G, De Francesco G, Persichini T, Colasanti M, Polticelli F, Musci G. Dominant mutants of ceruloplasmin impair the copper loading machinery in aceruloplasminemia. J Biol Chem 2009;284(7):4545-54.
122. Kono S, Yoshida K, Tomosugi N, Terada T, Hamaya Y, Kanaoka S, Miyajima H. Biological effects of mutant ceruloplasmin on hepcidin-mediated internalization of ferroportin. Biochim Biophys Acta 2010;1802(11):968-75.
123. McCormack W, Dorsky R, Wright S, Rainier J, Davis D, Skliar M. University of Utah Consolidated Hearing Committee Report on DeDomenico. 2013 (http://retractionwatch.files.wordpress.com/2013/08/utah-report.pdf).
124. Vashchenko G, MacGillivray RT. Multi-copper oxidases and human iron metabolism. Nutrients 2013;5(7):2289-313.
125. Qian Z, Chang Y, Leung G, Du J, Zhu L, Wang Q, Niu L, Xu Y, Yang L, Ho K and others. Expression of ferroportin1, hephaestin and ceruloplasmin in rat heart. Biochim Biophys Acta 2007;1772(5):527-32.
126. Wang J, Jiang H, Xie J. Ferroportin1 and hephaestin are involved in the nigral iron accumulation of 6-OHDA-lesioned rats. Eur J Neurosci 2007;25(9):2766-72.
127. Hahn P, Qian Y, Dentchev T, Chen L, Beard J, Harris ZL, Dunaief JL. Disruption of ceruloplasmin and hephaestin in mice causes retinal iron overload and retinal degeneration with features of age-related macular degeneration. Proc Natl Acad Sci U S A 2004;101(38):13850-5.
128. Chen H, Attieh ZK, Syed BA, Kuo YM, Stevens V, Fuqua BK, Andersen HS, Naylor CE, Evans RW, Gambling L and others. Identification of zyklopen, a new member of the vertebrate multicopper ferroxidase family, and characterization in rodents and human cells. J Nutr 2010;140(10):1728-35.
129. Danzeisen R, Fosset C, Chariana Z, Page K, David S, McArdle HJ. Placental ceruloplasmin homolog is regulated by iron and copper and is implicated in iron metabolism. Am J Physiol Cell Physiol 2002;282(3):C472-8.
130. Danzeisen R, Ponnambalam S, Lea RG, Page K, Gambling L, McArdle HJ. The effect of ceruloplasmin on iron release from placental (BeWo) cells; evidence for an endogenous Cu oxidase. Placenta 2000;21(8):805-12.
131. Holmberg CG, Laurell CB. Investigations in serum copper. II. Isolation of copper containing protein, and a description of some of its properties.: Acta Chem. Scand.; 1948. p 2, 550–556.
132. Osaki S. Kinetic studies of ferrous ion oxidation with crystalline human ferroxidase (ceruloplasmin). J Biol Chem 1966;241(21):5053-9.
133. Osaki S, Johnson DA, Frieden E. The possible significance of the ferrous oxidase activity of ceruloplasmin in normal human serum. J Biol Chem 1966;241(12):2746-51.
134. Patel BN, Dunn RJ, David S. Alternative RNA splicing generates a glycosylphosphatidylinositol-anchored form of ceruloplasmin in mammalian brain. J Biol Chem 2000;275(6):4305-10.
135. Hellman NE, Kono S, Miyajima H, Gitlin JD. Biochemical analysis of a missense mutation in aceruloplasminemia. J Biol Chem 2002;277(2):1375-80.

136. Hellman NE, Gitlin JD. Ceruloplasmin metabolism and function. Annu Rev Nutr 2002;22:439-58.
137. Patel BN, Dunn RJ, Jeong SY, Zhu Q, Julien JP, David S. Ceruloplasmin regulates iron levels in the CNS and prevents free radical injury. J Neurosci 2002;22(15):6578-86.
138. Nittis T, Gitlin JD. The copper-iron connection: hereditary aceruloplasminemia. Semin Hematol 2002;39(4):282-9.
139. Duce JA, Tsatsanis A, Cater MA, James SA, Robb E, Wikhe K, Leong SL, Perez K, Johanssen T, Greenough MA and others. Iron-export ferroxidase activity of beta-amyloid precursor protein is inhibited by zinc in Alzheimer's disease. Cell 2010;142(6):857-67.
140. Ebrahimi KH, Hagedoorn PL, Hagen WR. A synthetic peptide with the putative iron binding motif of amyloid precursor protein (APP) does not catalytically oxidize iron. PLoS One 2012;7(8):e40287.
141. Honarmand Ebrahimi K, Dienemann C, Hoefgen S, Than ME, Hagedoorn PL, Hagen WR. The amyloid precursor protein (APP) does not have a ferroxidase site in its E2 domain. PLoS One 2013;8(8):e72177.
142. McCarthy RC, Park YH, Kosman DJ. sAPP modulates iron efflux from brain microvascular endothelial cells by stabilizing the ferrous iron exporter ferroportin. EMBO Rep 2014;15(7):809-15.
143. Parkin J, Cohen B. An overview of the immune system. Lancet 2001;357(9270):1777-89.
144. Cherayil BJ. Iron and immunity: immunological consequences of iron deficiency and overload. Arch Immunol Ther Exp (Warsz) 2010;58(6):407-15.
145. Oppenheimer SJ. Iron and its relation to immunity and infectious disease. J Nutr 2001;131(2S-2):616S-633S; discussion 633S-635S.
146. Scrimshaw NS, SanGiovanni JP. Synergism of nutrition, infection, and immunity: an overview. Am J Clin Nutr 1997;66(2):464S-477S.
147. De Sousa M. Immune cell functions in iron overload. Clin Exp Immunol 1989;75(1):1-6.
148. Porto G, De Sousa M. Iron overload and immunity. World J Gastroenterol 2007;13(35):4707-15.
149. Olakanmi O, Schlesinger LS, Britigan BE. Hereditary hemochromatosis results in decreased iron acquisition and growth by Mycobacterium tuberculosis within human macrophages. J Leukoc Biol 2007;81(1):195-204.
150. Bullen JJ, Spalding PB, Ward CG, Gutteridge JM. Hemochromatosis, iron and septicemia caused by Vibrio vulnificus. Arch Intern Med 1991;151(8):1606-9.
151. Bergmann TK, Vinding K, Hey H. Multiple hepatic abscesses due to Yersinia enterocolitica infection secondary to primary haemochromatosis. Scand J Gastroenterol 2001;36(8):891-5.
152. Wang L, Johnson E, Shi H, Walker W, Wessling-Resnick M, Cherayil B. Attenuated inflammatory responses in hemochromatosis reveal a role for iron in the regulation of macrophage cytokine translation. J Immunol 2008;181(4):2723-31.
153. Reimão R, Porto G, de Sousa M. Stability of CD4/CD8 ratios in man: new correlation between CD4/CD8 profiles and iron overload in idiopathic haemochromatosis patients. C R Acad Sci III 1991;313(11):481-7.
154. Porto G, Vicente C, Teixeira MA, Martins O, Cabeda JM, Lacerda R, Goncalves C, Fraga J, Macedo G, Silva BM and others. Relative impact of HLA phenotype and CD4-CD8 ratios on the clinical expression of hemochromatosis. Hepatology 1997;25(2):397-402.
155. Porto G, Cardoso CS, Gordeuk V, Cruz E, Fraga J, Areias J, Oliveira JC, Bravo F, Gangaidzo IT, MacPhail AP and others. Clinical and genetic heterogeneity in hereditary haemochromatosis: association between lymphocyte counts and expression of iron overload. Eur J Haematol 2001;67(2):110-8.

156. Cardoso EM, Hagen K, de Sousa M, Hultcrantz R. Hepatic damage in C282Y homozygotes relates to low numbers of CD8+ cells in the liver lobuli. Eur J Clin Invest 2001;31(1):45-53.
157. Barton JC, Wiener HW, Acton RT, Go RC. Total blood lymphocyte counts in hemochromatosis probands with HFE C282Y homozygosity: relationship to severity of iron overload and HLA-A and -B alleles and haplotypes. BMC Blood Disord 2005;5:5.
158. Ganz T, Nemeth E. Iron sequestration and anemia of inflammation. Semin Hematol 2009;46(4):387-93.
159. Cassat JE, Skaar EP. Iron in infection and immunity. Cell Host Microbe 2013;13(5):509-19.
160. Masson PL, Heremans JF, Schonne E. Lactoferrin, an iron-binding protein in neutrophilic leukocytes. J Exp Med 1969;130(3):643-58.
161. Baker HM, Baker EN. A structural perspective on lactoferrin function. Biochem Cell Biol 2012;90(3):320-8.
162. Dooley H, Buckingham EB, Criscitiello MF, Flajnik MF. Emergence of the acute-phase protein hemopexin in jawed vertebrates. Mol Immunol 2010;48(1-3):147-52.
163. Quaye IK. Haptoglobin, inflammation and disease. Trans R Soc Trop Med Hyg 2008;102(8):735-42.
164. Ganz T. Iron in innate immunity: starve the invaders. Curr Opin Immunol 2009;21(1):63-7.
165. Wandersman C, Delepelaire P. Bacterial iron sources: from siderophores to hemophores. Annu Rev Microbiol 2004;58:611-47.
166. Flo TH, Smith KD, Sato S, Rodriguez DJ, Holmes MA, Strong RK, Akira S, Aderem A. Lipocalin 2 mediates an innate immune response to bacterial infection by sequestrating iron. Nature 2004;432(7019):917-21.
167. Mosser DM, Edwards JP. Exploring the full spectrum of macrophage activation. Nat Rev Immunol 2008;8(12):958-69.
168. Cairo G, Recalcati S, Mantovani A, Locati M. Iron trafficking and metabolism in macrophages: contribution to the polarized phenotype. Trends Immunol 2011;32(6):241-7.
169. Martinez FO, Gordon S, Locati M, Mantovani A. Transcriptional profiling of the human monocyte-to-macrophage differentiation and polarization: new molecules and patterns of gene expression. J Immunol 2006;177(10):7303-11.
170. Delaby C, Pilard N, Hetet G, Driss F, Grandchamp B, Beaumont C, Canonne-Hergaux F. A physiological model to study iron recycling in macrophages. Exp Cell Res 2005;310(1):43-53.
171. Zhang Z, Zhang F, An P, Guo X, Shen Y, Tao Y, Wu Q, Zhang Y, Yu Y, Ning B and others. Ferroportin1 deficiency in mouse macrophages impairs iron homeostasis and inflammatory responses. Blood 2011;118(7):1912-22.
172. She H, Xiong S, Lin M, Zandi E, Giulivi C, Tsukamoto H. Iron activates NF-kappaB in Kupffer cells. Am J Physiol Gastrointest Liver Physiol 2002;283(3):G719-26.
173. Kim S, Ponka P. Effects of interferon-gamma and lipopolysaccharide on macrophage iron metabolism are mediated by nitric oxide-induced degradation of iron regulatory protein 2. J Biol Chem 2000;275(9):6220-6.
174. Schaer C, Vallelian F, Imhof A, Schoedon G, Schaer D. Heme carrier protein (HCP-1) spatially interacts with the CD163 hemoglobin uptake pathway and is a target of inflammatory macrophage activation. J Leukoc Biol 2008;83(2):325-33.
175. Nguyen NB, Callaghan KD, Ghio AJ, Haile DJ, Yang F. Hepcidin expression and iron transport in alveolar macrophages. Am J Physiol Lung Cell Mol Physiol 2006;291(3):L417-25.
176. Ludwiczek S, Aigner E, Theurl I, Weiss G. Cytokine-mediated regulation of iron transport in human monocytic cells. Blood 2003;101(10):4148-54.

177. Corna G, Campana L, Pignatti E, Castiglioni A, Tagliafico E, Bosurgi L, Campanella A, Brunelli S, Manfredi AA, Apostoli P and others. Polarization dictates iron handling by inflammatory and alternatively activated macrophages. Haematologica 2010;95(11):1814-22.
178. Cellier MF, Courville P, Campion C. Nramp1 phagocyte intracellular metal withdrawal defense. Microbes Infect 2007;9(14-15):1662-70.
179. Bakhautdin B, Febbraio M, Goksoy E, de la Motte CA, Gulen MF, Childers EP, Hazen SL, Li X, Fox PL. Protective role of macrophage-derived ceruloplasmin in inflammatory bowel disease. Gut 2013;62(2):209-19.
180. White C, Lee J, Kambe T, Fritsche K, Petris MJ. A role for the ATP7A copper-transporting ATPase in macrophage bactericidal activity. J Biol Chem 2009;284(49):33949-56.
181. Rushworth SA, Chen XL, Mackman N, Ogborne RM, O'Connell MA. Lipopolysaccharide-induced heme oxygenase-1 expression in human monocytic cells is mediated via Nrf2 and protein kinase C. J Immunol 2005;175(7):4408-15.
182. Song Y, Shi Y, Ao LH, Harken AH, Meng XZ. TLR4 mediates LPS-induced HO-1 expression in mouse liver: role of TNF-alpha and IL-1beta. World J Gastroenterol 2003;9(8):1799-803.
183. Sierra-Filardi E, Vega MA, Sánchez-Mateos P, Corbí AL, Puig-Kröger A. Heme Oxygenase-1 expression in M-CSF-polarized M2 macrophages contributes to LPS-induced IL-10 release. Immunobiology 2010;215(9-10):788-95.
184. Sindrilaru A, Peters T, Wieschalka S, Baican C, Baican A, Peter H, Hainzl A, Schatz S, Qi Y, Schlecht A and others. An unrestrained proinflammatory M1 macrophage population induced by iron impairs wound healing in humans and mice. J Clin Invest 2011;121(3):985-97.
185. Arnold L, Henry A, Poron F, Baba-Amer Y, van Rooijen N, Plonquet A, Gherardi RK, Chazaud B. Inflammatory monocytes recruited after skeletal muscle injury switch into antiinflammatory macrophages to support myogenesis. J Exp Med 2007;204(5):1057-69.
186. Biswas SK, Mantovani A. Macrophage plasticity and interaction with lymphocyte subsets: cancer as a paradigm. Nat Immunol 2010;11(10):889-96.
187. Pinnix ZK, Miller LD, Wang W, D'Agostino R, Jr., Kute T, Willingham MC, Hatcher H, Tesfay L, Sui G, Di X and others. Ferroportin and iron regulation in breast cancer progression and prognosis. Sci Transl Med 2010;2(43):43ra56.
188. Marques O, Porto G, Rêma A, Faria F, Pinto JP, da Silva BM, Lopes C. IRON (DE)REGULATION IN BREAST CANCER: A ROLE FOR STROMAL INFLAMMATORY CELLS IN THE TUMOR MICROENVIRONMENT. 2014; Brussels, Belgium. Annals of Oncology. p i17-i18.
189. De Sousa M. Lymphoid cell positioning: a new proposal for the mechanism of control of lymphoid cell migration. Symp Soc Exp Biol 1978;32:393-410.
190. De Sousa M, Smithyman A, Tan C. Suggested models of ecotaxopathy in lymphoreticular malignancy. A role for iron-binding proteins in the control of lymphoid cell migration. Am J Pathol 1978;90(2):497-520.
191. Neckers LM, Cossman J. Transferrin receptor induction in mitogen-stimulated human T lymphocytes is required for DNA synthesis and cell division and is regulated by interleukin 2. Proc Natl Acad Sci U S A 1983;80(11):3494-8.
192. Dorner MH, Silverstone A, Nishiya K, de Sostoa A, Munn G, de Sousa M. Ferritin synthesis by human T lymphocytes. Science 1980;209(4460):1019-21.
193. Torti SV, Kwak EL, Miller SC, Miller LL, Ringold GM, Myambo KB, Young AP, Torti FM. The molecular cloning and characterization of murine ferritin heavy chain, a tumor necrosis factor-inducible gene. J Biol Chem 1988;263(25):12638-44.

194. Arezes J, Costa M, Vieira I, Dias V, Kong XL, Fernandes R, Vos M, Carlsson A, Rikers Y, Porto G and others. Non-transferrin-bound iron (NTBI) uptake by T lymphocytes: evidence for the selective acquisition of oligomeric ferric citrate species. PLoS One 2013;8(11):e79870.
195. World Health Organization DoHSaIS. WHO methods and data sources for country-level causes of death 2000-2012. 2014.
196. Libby P. Current concepts of the pathogenesis of the acute coronary syndromes. Circulation 2001;104(3):365-72.
197. Breslow JL. Mouse models of atherosclerosis. Science 1996;272(5262):685-8.
198. Hansson GK, Robertson AK, Söderberg-Nauclér C. Inflammation and atherosclerosis. Annu Rev Pathol 2006;1:297-329.
199. Castelli WP. Lipids, risk factors and ischaemic heart disease. Atherosclerosis 1996;124 Suppl:S1-9.
200. Ross R, Glomset J, Harker L. Response to injury and atherogenesis. Am J Pathol 1977;86(3):675-84.
201. Skålén K, Gustafsson M, Rydberg EK, Hultén LM, Wiklund O, Innerarity TL, Borén J. Subendothelial retention of atherogenic lipoproteins in early atherosclerosis. Nature 2002;417(6890):750-4.
202. Kume N, Cybulsky MI, Gimbrone MA. Lysophosphatidylcholine, a component of atherogenic lipoproteins, induces mononuclear leukocyte adhesion molecules in cultured human and rabbit arterial endothelial cells. J Clin Invest 1992;90(3):1138-44.
203. Li AC, Glass CK. The macrophage foam cell as a target for therapeutic intervention. Nat Med 2002;8(11):1235-42.
204. Mietus-Snyder M, Gowri MS, Pitas RE. Class A scavenger receptor up-regulation in smooth muscle cells by oxidized low density lipoprotein. Enhancement by calcium flux and concurrent cyclooxygenase-2 up-regulation. J Biol Chem 2000;275(23):17661-70.
205. Rong JX, Shapiro M, Trogan E, Fisher EA. Transdifferentiation of mouse aortic smooth muscle cells to a macrophage-like state after cholesterol loading. Proc Natl Acad Sci U S A 2003;100(23):13531-6.
206. Virmani R, Burke AP, Kolodgie FD, Farb A. Vulnerable plaque: the pathology of unstable coronary lesions. J Interv Cardiol 2002;15(6):439-46.
207. Tabas I. Macrophage death and defective inflammation resolution in atherosclerosis. Nat Rev Immunol 2010;10(1):36-46.
208. Newby AC. Matrix metalloproteinases regulate migration, proliferation, and death of vascular smooth muscle cells by degrading matrix and non-matrix substrates. Cardiovasc Res 2006;69(3):614-24.
209. Faxon DP, Fuster V, Libby P, Beckman JA, Hiatt WR, Thompson RW, Topper JN, Annex BH, Rundback JH, Fabunmi RP and others. Atherosclerotic Vascular Disease Conference: Writing Group III: pathophysiology. Circulation 2004;109(21):2617-25.
210. van der Wal AC, Becker AE. Atherosclerotic plaque rupture--pathologic basis of plaque stability and instability. Cardiovasc Res 1999;41(2):334-44.
211. Burke AP, Kolodgie FD, Farb A, Weber DK, Malcom GT, Smialek J, Virmani R. Healed plaque ruptures and sudden coronary death: evidence that subclinical rupture has a role in plaque progression. Circulation 2001;103(7):934-40.
212. Virmani R, Kolodgie FD, Burke AP, Finn AV, Gold HK, Tulenko TN, Wrenn SP, Narula J. Atherosclerotic plaque progression and vulnerability to rupture: angiogenesis as a source of intraplaque hemorrhage. Arterioscler Thromb Vasc Biol 2005;25(10):2054-61.
213. Libby P. Inflammation in atherosclerosis. Nature 2002;420(6917):868-74.
214. Sullivan JL. Iron and the sex difference in heart disease risk. Lancet 1981;1(8233):1293-4.

215. Kannel WB, Hjortland MC, McNamara PM, Gordon T. Menopause and risk of cardiovascular disease: the Framingham study. Ann Intern Med 1976;85(4):447-52.
216. Sullivan JL. Are menstruating women protected from heart disease because of, or in spite of, estrogen? Relevance to the iron hypothesis. Am Heart J 2003;145(2):190-4.
217. Joint World Health Organization/Centers for Disease Control and Prevention Technical Consultation on the Assessment of Iron Status at the Population Level (2004 : Geneva S. Assessing the iron status of populations: including literature reviews: report of a Joint World Health Organization/Centers for Disease Control and Prevention Technical Consultation on the Assessment of Iron Status at the Population Level, Geneva, Switzerland, 6-8 April 2004. 2nd Edition ed: World Health Organization; 2007.
218. Sullivan JL. Iron in arterial plaque: modifiable risk factor for atherosclerosis. Biochim Biophys Acta 2009;1790(7):718-23.
219. Smith C, Mitchinson MJ, Aruoma OI, Halliwell B. Stimulation of lipid peroxidation and hydroxyl-radical generation by the contents of human atherosclerotic lesions. Biochem J 1992;286 (Pt 3):901-5.
220. Pang JH, Jiang MJ, Chen YL, Wang FW, Wang DL, Chu SH, Chau LY. Increased ferritin gene expression in atherosclerotic lesions. J Clin Invest 1996;97(10):2204-12.
221. Ponraj D, Makjanic J, Thong PS, Tan BK, Watt F. The onset of atherosclerotic lesion formation in hypercholesterolemic rabbits is delayed by iron depletion. FEBS Lett 1999;459(2):218-22.
222. Minqin R, Rajendran R, Pan N, Tan BK, Ong WY, Watt F, Halliwell B. The iron chelator desferrioxamine inhibits atherosclerotic lesion development and decreases lesion iron concentrations in the cholesterol-fed rabbit. Free Radic Biol Med 2005;38(9):1206-11.
223. Lee TS, Shiao MS, Pan CC, Chau LY. Iron-deficient diet reduces atherosclerotic lesions in apoE-deficient mice. Circulation 1999;99(9):1222-9.
224. Meyers DG, Strickland D, Maloley PA, Seburg JK, Wilson JE, McManus BF. Possible association of a reduction in cardiovascular events with blood donation. Heart 1997;78(2):188-93.
225. Salonen JT, Tuomainen TP, Salonen R, Lakka TA, Nyyssönen K. Donation of blood is associated with reduced risk of myocardial infarction. The Kuopio Ischaemic Heart Disease Risk Factor Study. Am J Epidemiol 1998;148(5):445-51.
226. Ascherio A, Rimm EB, Giovannucci E, Willett WC, Stampfer MJ. Blood donations and risk of coronary heart disease in men. Circulation 2001;103(1):52-7.
227. Zheng H, Cable R, Spencer B, Votto N, Katz SD. Iron stores and vascular function in voluntary blood donors. Arterioscler Thromb Vasc Biol 2005;25(8):1577-83.
228. Wang X, Li G, Zheng W. Efflux of iron from the cerebrospinal fluid to the blood at the blood-CSF barrier: effect of manganese exposure. Exp Biol Med (Maywood) 2008;233(12):1561-71.
229. Day SM, Duquaine D, Mundada LV, Menon RG, Khan BV, Rajagopalan S, Fay WP. Chronic iron administration increases vascular oxidative stress and accelerates arterial thrombosis. Circulation 2003;107(20):2601-6.
230. Araujo JA, Romano EL, Brito BE, Parthé V, Romano M, Bracho M, Montaño RF, Cardier J. Iron overload augments the development of atherosclerotic lesions in rabbits. Arterioscler Thromb Vasc Biol 1995;15(8):1172-80.
231. Dabbagh AJ, Shwaery GT, Keaney JF, Frei B. Effect of iron overload and iron deficiency on atherosclerosis in the hypercholesterolemic rabbit. Arterioscler Thromb Vasc Biol 1997;17(11):2638-45.
232. Makowski MR, Varma G, Wiethoff AJ, Smith A, Mattock K, Jansen CH, Warley A, Taupitz M, Schaeffter T, Botnar RM. Noninvasive assessment of atherosclerotic plaque progression in ApoE-/- mice using susceptibility gradient mapping. Circ Cardiovasc Imaging 2011;4(3):295-303.

233. Sempos CT. Do body iron stores increase the risk of developing coronary heart disease? Am J Clin Nutr 2002;76(3):501-3.
234. Sullivan JL. Macrophage iron, hepcidin, and atherosclerotic plaque stability. Exp Biol Med (Maywood) 2007;232(8):1014-20.
235. Sullivan JL. Misconceptions in the debate on the iron hypothesis. J Nutr Biochem 2001;12(1):33-37.
236. Kraml PJ, Klein RL, Huang Y, Nareika A, Lopes-Virella MF. Iron loading increases cholesterol accumulation and macrophage scavenger receptor I expression in THP-1 mononuclear phagocytes. Metabolism 2005;54(4):453-9.
237. Valenti L, Dongiovanni P, Motta BM, Swinkels DW, Bonara P, Rametta R, Burdick L, Frugoni C, Fracanzani AL, Fargion S. Serum hepcidin and macrophage iron correlate with MCP-1 release and vascular damage in patients with metabolic syndrome alterations. Arterioscler Thromb Vasc Biol 2011;31(3):683-90.
238. Abdel-Khalek MA, El-Barbary AM, Essa SA, Ghobashi AS. Serum hepcidin: a direct link between anemia of inflammation and coronary artery atherosclerosis in patients with rheumatoid arthritis. J Rheumatol 2011;38(10):2153-9.
239. Saeed O, Otsuka F, Polavarapu R, Karmali V, Weiss D, Davis T, Rostad B, Pachura K, Adams L, Elliott J and others. Pharmacological suppression of hepcidin increases macrophage cholesterol efflux and reduces foam cell formation and atherosclerosis. Arterioscler Thromb Vasc Biol 2012;32(2):299-307.
240. Li JJ, Meng X, Si HP, Zhang C, Lv HX, Zhao YX, Yang JM, Dong M, Zhang K, Liu SX and others. Hepcidin destabilizes atherosclerotic plaque via overactivating macrophages after erythrophagocytosis. Arterioscler Thromb Vasc Biol 2012;32(5):1158-66.
241. Vinchi F, Muckenthaler MU, Da Silva MC, Balla G, Balla J, Jeney V. Atherogenesis and iron: from epidemiology to cellular level. Front Pharmacol 2014;5:94.
242. Bouhlel MA, Derudas B, Rigamonti E, Dièvart R, Brozek J, Haulon S, Zawadzki C, Jude B, Torpier G, Marx N and others. PPARgamma activation primes human monocytes into alternative M2 macrophages with anti-inflammatory properties. Cell Metab 2007;6(2):137-43.
243. Waldo SW, Li Y, Buono C, Zhao B, Billings EM, Chang J, Kruth HS. Heterogeneity of human macrophages in culture and in atherosclerotic plaques. Am J Pathol 2008;172(4):1112-26.
244. Gleissner CA. Macrophage Phenotype Modulation by CXCL4 in Atherosclerosis. Front Physiol 2012;3:1.
245. Boyle JJ, Johns M, Lo J, Chiodini A, Ambrose N, Evans PC, Mason JC, Haskard DO. Heme induces heme oxygenase 1 via Nrf2: role in the homeostatic macrophage response to intraplaque hemorrhage. Arterioscler Thromb Vasc Biol 2011;31(11):2685-91.
246. Boyle JJ, Harrington HA, Piper E, Elderfield K, Stark J, Landis RC, Haskard DO. Coronary intraplaque hemorrhage evokes a novel atheroprotective macrophage phenotype. Am J Pathol 2009;174(3):1097-108.
247. Boyle JJ, Johns M, Kampfer T, Nguyen AT, Game L, Schaer DJ, Mason JC, Haskard DO. Activating transcription factor 1 directs Mhem atheroprotective macrophages through coordinated iron handling and foam cell protection. Circ Res 2012;110(1):20-33.
248. Finn AV, Nakano M, Polavarapu R, Karmali V, Saeed O, Zhao X, Yazdani S, Otsuka F, Davis T, Habib A and others. Hemoglobin directs macrophage differentiation and prevents foam cell formation in human atherosclerotic plaques. J Am Coll Cardiol 2012;59(2):166-77.
249. Kadl A, Meher AK, Sharma PR, Lee MY, Doran AC, Johnstone SR, Elliott MR, Gruber F, Han J, Chen W and others. Identification of a novel macrophage phenotype that develops in response to atherogenic phospholipids via Nrf2. Circ Res 2010;107(6):737-46.

250. Seneviratne AN, Cole JE, Goddard ME, Krams R, Monaco C. Macrophage heterogeneity in developing vulnerable atherosclerotic plaques modulated by shear stress. 2012; Birmingham, UK.
251. Recalcati S, Locati M, Gammella E, Invernizzi P, Cairo G. Iron levels in polarized macrophages: regulation of immunity and autoimmunity. Autoimmun Rev 2012;11(12):883-9.
252. Yang F, Liu XB, Quinones M, Melby PC, Ghio A, Haile DJ. Regulation of reticuloendothelial iron transporter MTP1 (Slc11a3) by inflammation. J Biol Chem 2002;277(42):39786-91.
253. Janabi M, Yamashita S, Hirano K, Sakai N, Hiraoka H, Matsumoto K, Zhang Z, Nozaki S, Matsuzawa Y. Oxidized LDL-induced NF-kappa B activation and subsequent expression of proinflammatory genes are defective in monocyte-derived macrophages from CD36-deficient patients. Arterioscler Thromb Vasc Biol 2000;20(8):1953-60.
254. Sarkar J, Seshadri V, Tripoulas NA, Ketterer ME, Fox PL. Role of ceruloplasmin in macrophage iron efflux during hypoxia. J Biol Chem 2003;278(45):44018-24.
255. Fox PL, Mazumder B, Ehrenwald E, Mukhopadhyay CK. Ceruloplasmin and cardiovascular disease. Free Radic Biol Med 2000;28(12):1735-44.
256. Ehrenwald E, Fox PL. Role of endogenous ceruloplasmin in low density lipoprotein oxidation by human U937 monocytic cells. J Clin Invest 1996;97(3):884-90.
257. Makedou KG, Mikhailidis DP, Makedou A, Iliadis S, Kourtis A, Vavatsi-Christaki N, Papageorgiou GE. Lipid profile, low-density lipoprotein oxidation and ceruloplasmin in the progeny of families with a positive history of cardiovascular diseases and/or hyperlipidemia. Angiology 2009;60(4):455-61.
258. Boero L, Cuniberti L, Magnani N, Manavela M, Yapur V, Bustos M, Gómez Rosso L, Meroño T, Marziali L, Viale L and others. Increased oxidized low density lipoprotein associated with high ceruloplasmin activity in patients with active acromegaly. Clin Endocrinol (Oxf) 2010;72(5):654-60.
259. Kennedy DJ, Fan Y, Wu Y, Pepoy M, Hazen SL, Tang WH. Plasma Ceruloplasmin, a Regulator of Nitric Oxide Activity, and Incident Cardiovascular Risk in Patients with CKD. Clin J Am Soc Nephrol 2014;9(3):462-7.
260. Stancu C, Constantinescu E, Sima A. Ceruloplasmin and oxidized LDL colocalize in atherosclerotic lesions of hamster. Volume 6: Central European Journal of Biology; 2011. p 22-31.
261. Mukhopadhyay CK, Ehrenwald E, Fox PL. Ceruloplasmin enhances smooth muscle cell- and endothelial cell-mediated low density lipoprotein oxidation by a superoxide-dependent mechanism. J Biol Chem 1996;271(25):14773-8.
262. Vehmas A, Lieu J, Pardo CA, McArthur JC, Gartner S. Amyloid precursor protein expression in circulating monocytes and brain macrophages from patients with HIV-associated cognitive impairment. J Neuroimmunol 2004;157(1-2):99-110.
263. Rogers JT, Randall JD, Cahill CM, Eder PS, Huang X, Gunshin H, Leiter L, McPhee J, Sarang SS, Utsuki T and others. An iron-responsive element type II in the 5'-untranslated region of the Alzheimer's amyloid precursor protein transcript. J Biol Chem 2002;277(47):45518-28.
264. Cho HH, Cahill CM, Vanderburg CR, Scherzer CR, Wang B, Huang X, Rogers JT. Selective translational control of the Alzheimer amyloid precursor protein transcript by iron regulatory protein-1. J Biol Chem 2010;285(41):31217-32.
265. Hofman A, Ott A, Breteler MM, Bots ML, Slooter AJ, van Harskamp F, van Duijn CN, Van Broeckhoven C, Grobbee DE. Atherosclerosis, apolipoprotein E, and prevalence of dementia and Alzheimer's disease in the Rotterdam Study. Lancet 1997;349(9046):151-4.
266. Tibolla G, Norata GD, Meda C, Arnaboldi L, Uboldi P, Piazza F, Ferrarese C, Corsini A, Maggi A, Vegeto E and others. Increased atherosclerosis and vascular inflammation in

APP transgenic mice with apolipoprotein E deficiency. Atherosclerosis 2010;210(1):78-87.
267. Vaulont S, Gascan H, Froger J; Antibodies specific for human hepcidin2008.
268. Livak KJ, Schmittgen TD. Analysis of relative gene expression data using real-time quantitative PCR and the 2(-Delta Delta C(T)) Method. Methods 2001;25(4):402-8.
269. Canonne-Hergaux F, Donovan A, Delaby C, Wang H, Gros P. Comparative studies of duodenal and macrophage ferroportin proteins. Am J Physiol Gastrointest Liver Physiol 2006;290(1):G156-63.
270. Jeong SY, David S. Glycosylphosphatidylinositol-anchored ceruloplasmin is required for iron efflux from cells in the central nervous system. J Biol Chem 2003;278(29):27144-8.
271. Fox PL, Mukhopadhyay C, Ehrenwald E. Structure, oxidant activity, and cardiovascular mechanisms of human ceruloplasmin. Life Sci 1995;56(21):1749-58.
272. Shukla N, Maher J, Masters J, Angelini GD, Jeremy JY. Does oxidative stress change ceruloplasmin from a protective to a vasculopathic factor? Atherosclerosis 2006;187(2):238-50.
273. Pan Y, Katula K, Failla ML. Expression of ceruloplasmin gene in human and rat lymphocytes. Biochim Biophys Acta 1996;1307(2):233-8.
274. Mazumder B, Mukhopadhyay CK, Prok A, Cathcart MK, Fox PL. Induction of ceruloplasmin synthesis by IFN-gamma in human monocytic cells. J Immunol 1997;159(4):1938-44.
275. Fleming RE, Whitman IP, Gitlin JD. Induction of ceruloplasmin gene expression in rat lung during inflammation and hyperoxia. Am J Physiol 1991;260(2 Pt 1):L68-74.
276. Banha J, Marques L, Oliveira R, Martins Mde F, Paixao E, Pereira D, Malho R, Penque D, Costa L. Ceruloplasmin expression by human peripheral blood lymphocytes: a new link between immunity and iron metabolism. Free Radic Biol Med 2008;44(3):483-92.
277. Sato M, Schilsky ML, Stockert RJ, Morell AG, Sternlieb I. Detection of multiple forms of human ceruloplasmin. A novel Mr 200,000 form. J Biol Chem 1990;265(5):2533-7.
278. Chung B, Chaston T, Marks J, Srai S, Sharp P. Hepcidin Decreases Iron Transporter Expression in Vivo in Mouse Duodenum and Spleen and in Vitro in THP-1 Macrophages and Intestinal Caco-2 Cells. J Nutr 2009.
279. Fortna RR, Watson HA, Nyquist SE. Glycosyl phosphatidylinositol-anchored ceruloplasmin is expressed by rat Sertoli cells and is concentrated in detergent-insoluble membrane fractions. Biol Reprod 1999;61(4):1042-9.
280. Salzer JL, Lovejoy L, Linder MC, Rosen C. Ran-2, a glial lineage marker, is a GPI-anchored form of ceruloplasmin. J Neurosci Res 1998;54(2):147-57.
281. Mostar EJ, Prohaska JR. Glycosylphosphatidylinositol-linked ceruloplasmin is expressed in multiple rodent organs and is lower following dietary copper deficiency. Experimental Biology and Medicine 2011;[Epub ahead of print].
282. Kataoka M, Tavassoli M. Identification of ceruloplasmin receptors on the surface of human blood monocytes, granulocytes, and lymphocytes. Exp Hematol 1985;13(8):806-10.
283. Gitlin JD. Transcriptional regulation of ceruloplasmin gene expression during inflammation. J Biol Chem 1988;263(13):6281-7.
284. Deshmukh VK, Raman PH, Dhuley JN, Naik SR. Role of ceruloplasmin in inflammation: increased serum ceruloplasmin levels during inflammatory conditions and its possible relationship with anti-inflammatory agents. Pharmacol Res Commun 1985;17(7):633-42.
285. Samygina VR, Sokolov AV, Bourenkov G, Petoukhov MV, Pulina MO, Zakharova ET, Vasilyev VB, Bartunik H, Svergun DI. Ceruloplasmin: macromolecular assemblies with iron-containing acute phase proteins. PLoS One 2013;8(7):e67145.
286. Ali H, Haribabu B, Richardson RM, Snyderman R. Mechanisms of inflammation and leukocyte activation. Med Clin North Am 1997;81(1):1-28.

287. Owen CA. Leukocyte cell surface proteinases: regulation of expression, functions, and mechanisms of surface localization. Int J Biochem Cell Biol 2008;40(6-7):1246-72.
288. Bispo C. The role of peripheral blood mononuclear cells in atherogenesis: University of Lisbon; 2011.
289. Ward RJ, Crichton RR, Taylor DL, Della Corte L, Srai SK, Dexter DT. Iron and the immune system. J Neural Transm 2011;118(3):315-28.
290. Pinto JP, Arezes J, Dias V, Oliveira S, Vieira I, Costa M, Vos M, Carlsson A, Rikers Y, Rangel M and others. Physiological implications of NTBI uptake by T lymphocytes. Front Pharmacol 2014;5:24.
291. Orso E, Werner T, Wolf Z, Bandulik S, Kramer W, Schmitz G. Ezetimib influences the expression of raft-associated antigens in human monocytes. Cytometry A 2006;69(3):206-8.
292. Quest AF, Leyton L, Párraga M. Caveolins, caveolae, and lipid rafts in cellular transport, signaling, and disease. Biochem Cell Biol 2004;82(1):129-44.
293. Sano Y, Nakaya T, Pedrini S, Takeda S, Iijima-Ando K, Iijima K, Mathews PM, Itohara S, Gandy S, Suzuki T. Physiological mouse brain Abeta levels are not related to the phosphorylation state of threonine-668 of Alzheimer's APP. PLoS One 2006;1:e51.
294. Chang YZ, Qian ZM, Du JR, Zhu L, Xu Y, Li LZ, Wang CY, Wang Q, Ge XH, Ho KP and others. Ceruloplasmin expression and its role in iron transport in C6 cells. Neurochem Int 2007;50(5):726-33.
295. Cairo G, Conte D, Bianchi L, Fraquelli M, Recalcati S. Reduced serum ceruloplasmin levels in hereditary haemochromatosis. Br J Haematol 2001;114(1):226-9.
296. Ranganathan PN, Lu Y, Jiang L, Kim C, Collins JF. Serum ceruloplasmin protein expression and activity increases in iron-deficient rats and is further enhanced by higher dietary copper intake. Blood 2011;118(11):3146-53.
297. Venakteshwara Rao M, Khanijo SK, Chande RD, Chouhan SS, Bisarya BN. Serum ceruloplasmin in iron deficiency anaemia. J Assoc Physicians India 1975;23(9):571-6.
298. Ehehalt R, Keller P, Haass C, Thiele C, Simons K. Amyloidogenic processing of the Alzheimer beta-amyloid precursor protein depends on lipid rafts. J Cell Biol 2003;160(1):113-23.
299. Parkin ET, Turner AJ, Hooper NM. Amyloid precursor protein, although partially detergent-insoluble in mouse cerebral cortex, behaves as an atypical lipid raft protein. Biochem J 1999;344 Pt 1:23-30.
300. Mukhopadhyay CK, Mazumder B, Fox PL. Role of hypoxia-inducible factor-1 in transcriptional activation of ceruloplasmin by iron deficiency. J Biol Chem 2000;275(28):21048-54.
301. Stadler N, Lindner RA, Davies MJ. Direct detection and quantification of transition metal ions in human atherosclerotic plaques: evidence for the presence of elevated levels of iron and copper. Arterioscler Thromb Vasc Biol 2004;24(5):949-54.
302. Yuan XM. Apoptotic macrophage-derived foam cells of human atheromas are rich in iron and ferritin, suggesting iron-catalysed reactions to be involved in apoptosis. Free Radic Res 1999;30(3):221-31.
303. Li W, Xu LH, Forssell C, Sullivan JL, Yuan XM. Overexpression of transferrin receptor and ferritin related to clinical symptoms and destabilization of human carotid plaques. Exp Biol Med (Maywood) 2008;233(7):818-26.
304. Galle J, Heinloth A, Wanner C, Heermeier K. Dual effect of oxidized LDL on cell cycle in human endothelial cells through oxidative stress. Kidney Int Suppl 2001;78:S120-3.
305. Riazy M, Chen JH, Yamamato Y, Yamamato H, Duronio V, Steinbrecher UP. OxLDL-mediated survival of macrophages does not require LDL internalization or signalling by major pattern recognition receptors. Biochem Cell Biol 2011;89(4):387-95.
306. Zhao B, Li Y, Buono C, Waldo SW, Jones NL, Mori M, Kruth HS. Constitutive receptor-independent low density lipoprotein uptake and cholesterol accumulation by

macrophages differentiated from human monocytes with macrophage-colony-stimulating factor (M-CSF). J Biol Chem 2006;281(23):15757-62.
307. Packard RR, Libby P. Inflammation in atherosclerosis: from vascular biology to biomarker discovery and risk prediction. Clin Chem 2008;54(1):24-38.
308. Ryter SW, Alam J, Choi AM. Heme oxygenase-1/carbon monoxide: from basic science to therapeutic applications. Physiol Rev 2006;86(2):583-650.
309. Mazière C, Mazière JC. Activation of transcription factors and gene expression by oxidized low-density lipoprotein. Free Radic Biol Med 2009;46(2):127-37.
310. Beckman JD, Chen C, Nguyen J, Thayanithy V, Subramanian S, Steer CJ, Vercellotti GM. Regulation of heme oxygenase-1 protein expression by miR-377 in combination with miR-217. J Biol Chem 2011;286(5):3194-202.
311. Skrzypek K, Tertil M, Golda S, Ciesla M, Weglarczyk K, Collet G, Guichard A, Kozakowska M, Boczkowski J, Was H and others. Interplay between heme oxygenase-1 and miR-378 affects non-small cell lung carcinoma growth, vascularization, and metastasis. Antioxid Redox Signal 2013;19(7):644-60.
312. Pulkkinen KH, Ylä-Herttuala S, Levonen AL. Heme oxygenase 1 is induced by miR-155 via reduced BACH1 translation in endothelial cells. Free Radic Biol Med 2011;51(11):2124-31.
313. Qiu L, Fan H, Jin W, Zhao B, Wang Y, Ju Y, Chen L, Chen Y, Duan Z, Meng S. miR-122-induced down-regulation of HO-1 negatively affects miR-122-mediated suppression of HBV. Biochem Biophys Res Commun 2010;398(4):771-7.
314. Beaumont C. Multiple regulatory mechanisms act in concert to control ferroportin expression and heme iron recycling by macrophages. Haematologica 2010;95(8):1233-6.
315. Tapryal N, Mukhopadhyay C, Das D, Fox PL, Mukhopadhyay CK. Reactive oxygen species regulate ceruloplasmin by a novel mRNA decay mechanism involving its 3'-untranslated region: implications in neurodegenerative diseases. J Biol Chem 2009;284(3):1873-83.
316. Kuhn AM, Tzieply N, Schmidt MV, von Knethen A, Namgaladze D, Yamamoto M, Brüne B. Antioxidant signaling via Nrf2 counteracts lipopolysaccharide-mediated inflammatory responses in foam cell macrophages. Free Radic Biol Med 2011;50(10):1382-91.
317. Min KJ, Cho KH, Kwon TK. The effect of oxidized low density lipoprotein (oxLDL)-induced heme oxygenase-1 on LPS-induced inflammation in RAW 264.7 macrophage cells. Cell Signal 2012;24(6):1215-21.
318. Harada N, Kanayama M, Maruyama A, Yoshida A, Tazumi K, Hosoya T, Mimura J, Toki T, Maher JM, Yamamoto M and others. Nrf2 regulates ferroportin 1-mediated iron efflux and counteracts lipopolysaccharide-induced ferroportin 1 mRNA suppression in macrophages. Arch Biochem Biophys 2011;508(1):101-9.
319. Fillebeen C, Muckenthaler M, Andriopoulos B, Bisaillon M, Mounir Z, Hentze MW, Koromilas AE, Pantopoulos K. Expression of the subgenomic hepatitis C virus replicon alters iron homeostasis in Huh7 cells. J Hepatol 2007;47(1):12-22.
320. Marques L, Auriac A, Willemetz A, Banha J, Silva B, Canonne-Hergaux F, Costa L. Immune cells and hepatocytes express glycosylphosphatidylinositol-anchored ceruloplasmin at their cell surface. Blood Cells Mol Dis 2012;48(2):110-20.
321. Stöger JL, Gijbels MJ, van der Velden S, Manca M, van der Loos CM, Biessen EA, Daemen MJ, Lutgens E, de Winther MP. Distribution of macrophage polarization markers in human atherosclerosis. Atherosclerosis 2012;225(2):461-8.
322. Theurl I, Theurl M, Seifert M, Mair S, Nairz M, Rumpold H, Zoller H, Bellmann-Weiler R, Niederegger H, Talasz H and others. Autocrine formation of hepcidin induces iron retention in human monocytes. Blood 2008;111(4):2392-9.

323. Kautz L, Gabayan V, Wang X, Wu J, Onwuzurike J, Jung G, Qiao B, Lusis AJ, Ganz T, Nemeth E. Testing the iron hypothesis in a mouse model of atherosclerosis. Cell Rep 2013;5(5):1436-42.
324. Boyle JJ. Heme and haemoglobin direct macrophage Mhem phenotype and counter foam cell formation in areas of intraplaque haemorrhage. Curr Opin Lipidol 2012;23(5):453-61.
325. Bories G, Colin S, Vanhoutte J, Derudas B, Copin C, Fanchon M, Daoudi M, Belloy L, Haulon S, Zawadzki C and others. Liver X receptor activation stimulates iron export in human alternative macrophages. Circ Res 2013;113(11):1196-205.
326. Asare GA, Mossanda KS, Kew MC, Paterson AC, Kahler-Venter CP, Siziba K. Hepatocellular carcinoma caused by iron overload: a possible mechanism of direct hepatocarcinogenicity. Toxicology 2006;219(1-3):41-52.